

Graviton modes in fractional quantum hall liquids

Wang, Yuzhu

2023

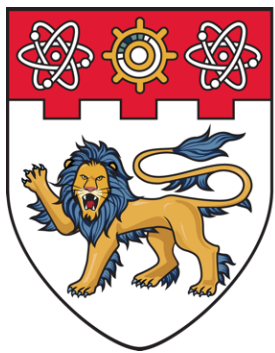
Wang, Y. (2023). Graviton modes in fractional quantum hall liquids. Doctoral thesis, Nanyang Technological University, Singapore. <https://hdl.handle.net/10356/165156>

<https://hdl.handle.net/10356/165156>

<https://doi.org/10.32657/10356/165156>

This work is licensed under a Creative Commons Attribution-NonCommercial 4.0 International License (CC BY-NC 4.0).

Downloaded on 04 Jun 2024 21:47:00 SGT



**NANYANG
TECHNOLOGICAL
UNIVERSITY**
SINGAPORE

**GRAVITON MODES IN FRACTIONAL
QUANTUM HALL LIQUIDS**

WANG YUZHU

School of Physical and Mathematical Sciences

A thesis submitted to the Nanyang Technological University
in partial fulfillment of the requirements for the degree of
Doctor of Philosophy

2023

Statement of Originality

I hereby certify that the work embodied in this thesis is the result of original research done by me except where otherwise stated in this thesis. The thesis work has not been submitted for a degree or professional qualification to any other university or institution. I declare that this thesis is written by myself and is free of plagiarism and of sufficient grammatical clarity to be examined. I confirm that the investigations were conducted in accord with the ethics policies and integrity standards of Nanyang Technological University and that the research data are presented honestly and without prejudice.

Oct 6th, 2022

.....
Date

2022
NTU NTU NTU NTU NTU NTU NTU NTU
NTU NTU NTU NTU NTU NTU NTU NTU NTU
NTU NTU NTU NTU NTU NTU NTU NTU NTU
NTU NTU NTU NTU NTU NTU NTU NTU NTU
.....
Wang Yuzhu

WANG YUZHU

Supervisor Declaration Statement

I have reviewed the content and presentation style of this thesis and declare it of sufficient grammatical clarity to be examined. To the best of my knowledge, the thesis is free of plagiarism and the research and writing are those of the candidate's except as acknowledged in the Author Attribution Statement. I confirm that the investigations were conducted in accord with the ethics policies and integrity standards of Nanyang Technological University and that the research data are presented honestly and without prejudice.

Oct 6th, 2022

.....

Date



NTU NTU NTU NTU NTU NTU NTU NTU
NTU NTU NTU NTU NTU NTU NTU NTU
NTU NTU NTU NTU NTU NTU NTU NTU
NTU NTU NTU NTU NTU NTU NTU NTU

.....

Prof. YANG BO

Authorship Attribution Statement

Please select one of the following; *delete as appropriate:

- (A) This thesis does not contain any materials from papers published in peer-reviewed journals or from papers accepted at conferences in which I am listed as an author.
- (B) This thesis contains material from 3 papers published in the following peer-reviewed journals / from papers accepted at conferences in which I am listed as an author.

Please amend the typical statements below to suit your circumstances if (B) is selected.

Part of Sec.3.4.3 and Chap.4 are published as Wang, Y., Yang, B.(2022). Analytic exposition of the graviton modes in fractional quantum Hall effects and its physical implications. *Physical Review B*, 105, 035144

The contributions of the co-authors are as follows:

- Prof Yang provided the initial project direction and edited the manuscript drafts.
- I prepared the manuscript drafts, including the analytical derivations and the numerical simulations.

Part of Sec.3.5 is published as Ha, Trung Q., Wang, Y., Yang, B.(2022). Spin-statistics relation and robustness of braiding phase for anyons in fractional quantum Hall effect. arXiv:2208.13786. (under review)

The contributions of the co-authors are as follows:

- Prof Yang provided the initial project direction and edited the manuscript drafts.
- Ha Quang Trung did most of the numerical work and prepared the manuscript drafts.
- I did the analytical derivations together with Trung and provided the theoretical part related to the composite fermionization.

Part of Chap.5 is posted online as Wang, Y., Yang, B.(2022). Geometric Fluctuation of Conformal Hilbert Spaces and Multiple Graviton Modes in Fractional Quantum Hall Effect. arXiv:2201.00020. (under review)

The contributions of the co-authors are as follows:

- Prof Yang suggested and edited the manuscript drafts.
- I prepared the manuscript drafts, including the analytical derivations and the numerical simulations.

Oct 6th, 2022

.....
Date


TU NTU NTU NTU NTU NTU NTU NTU
NTU NTU NTU NTU NTU NTU NTU NTU
NTU NTU NTU NTU NTU NTU NTU NTU
NTU NTU NTU NTU NTU NTU NTU NTU

WANG YUZHU

Acknowledgements

It is tough to believe that my career as a Ph.D. student is coming to an end because there have been so many precious memories along the journey. Reading the notes that I have written these years, it feels quite unrealistic - these things that look so natural to me nowadays took me tons of effort to understand back then. But maybe this is exactly the essence of getting a Ph.D., i.e. striving as much as possible to integrate a small portion of human knowledge into your own life and carry it forward.

The most valuable treasure I have got along the way must be all the great teachers and the lovely friends, who made my day even at the worst time when the formulas seemed desperate to be derived. I wish to express my greatest gratitude to my advisor, Prof. Yang Bo, who patiently taught me so many things about FQHE and relevant academic skills. Besides physics, I also benefited a lot from the freedom he gave, which allowed me to learn many things without worrying too much about the outcome. I also learned from him that it is a theoretical physicist's basic ability to write down explicit expressions to precisely explain the thinking to others. Prof Yang once told me that I should work hard from Monday to Saturday but go outside and wander around the island on Sunday, which I wish I can achieve in the next few years, considering at present Singapore is still approximately equal to Jurong West to me.

And I also want to thank Prof. Lee Ching Hua from NUS, who has been one of my guides in physics since I was an undergraduate. I still remember the high buildings Ching Hua took me to visit when I first came to Singapore in 2018, and the delicious Janggut Laksa and Otah he invited me to taste (I finally got to know the shop's exact location several months ago, which is in Alexandra.). Ching Hua is always passionate about physics and I learned incredible things about nodal systems, non-Hermitian physics, and topoelectric circuits from him. I am also grateful for the

suggestion of staying at theoretical physics from my undergraduate supervisor, Prof. Zhang Xiao, who led me into the world of research.

I am also indebted to many other professors for their help: Prof. Pinaki Sengupta for teaching me many things about condensed matter physics (and his terrific sense of humor); Prof. Justin Song for being my TAC member and offering me many comments on my work; Prof. Chong Yidong for teaching me quantum information and QED; Prof. Cheong Siew Ann for instructing me writing Monte Carlo algorithms; Prof. Yong Ee Hou for teaching me clustering expansion, RG group and other useful techniques in statistical mechanics; Prof. Zhang Baile for the delightful discussions on his research and experiences and Dr. Sujata S. Kathpalia for helping me with my academic writing.

It will be very frustrating due to the isolation from others during the pandemic if I did not meet so many good friends. Trung is definitely the one who I can always turn to, for help or maybe just a small chitchat. His wonderful FQH library saved so much time for me doing numerics. For a long while there were only two of us in PAP 04-24 so we can freely discuss lots of things. Trung also introduced me to Arifa, Jian Wei, Minjeong, and Farisan, and we had a short-term learning group where I learned many things about superfluid. I also want to thank other members in Prof. Yang's research group: Dr. Yang Chao for teaching me master equation hand by hand in prof's old office; Dr. Kristian Hauser Villegas for his nice tutorial about AdS/CMT duality and teaching me many things about superconductivity and the Higgs mechanism; Dr. Sun Hao for teaching me things about the Luttinger liquid and congratulations on his happy wedding; Dr. Chen Tianqi for teaching me things about quantum computation and leading me to explore the possible combination of FQHE and quantum computation; Dr. Yoshiki Fukusumi for revising my thesis carefully and offering me many constructive suggestions on the parts relevant to CFT

I also want to sincerely thank my family and especially my parents, who have been providing all the support I need since the first day of my life, to whom I owe too much because I did not have the chance to get back home since the pandemic spread. During this time my grandmother passed away and I did not have the chance to say goodbye to her, which is a significant regret for me and I really hope that I can live up to her expectations one day. I would like to thank my dear girlfriend Jiayi for coming to Singapore and creating so many good memories with

me. Besides, I would like to specifically thank my landlords, a kindly old couple for their always timely help.

Finally, I want to thank NTU and MOE for the scholarship over the past three years. It is a very enjoyable experience to study at NTU and I will choose it again if I have got the chance. The self-discipline and the scholarship spirit I learned from here will be cherished all the time.

“Aut inveniam viam aut faciam.”

—Hannibal Barca

To my dear family

Abstract

The fractional quantum Hall fluid is a two-dimensional quantum fluid of electrons subject to a strong magnetic field at low temperatures. Neutral excitations in a fractional quantum Hall droplet define the incompressibility gap of the topological phase. Among these states, there are some specific modes in the long-wavelength limit that can be understood as “spin-2 gravitons”. In this thesis, we will introduce a set of analytical results for the energy gap of the graviton modes for model Hamiltonians in the thermodynamic limit, which is governed by a well-defined and universal characteristic tensor. These results can help to construct model Hamiltonians for the graviton modes of different FQH phases and elucidate a hierarchical structure of conformal Hilbert spaces (null spaces of model Hamiltonians) containing the graviton modes and their corresponding ground states. An isomorphism can be defined for these conformal Hilbert spaces, and the mapping between them can be regarded as a more rigorous and general reinterpretation of the composite fermionization of FQH states, with naturally emergent composite fermions (each consisting of one electron and an even number of fluxes). The results from exact diagonalization will be shown, which confirm that for gapped phases, low-lying neutral excitations can undergo a phase transition even when the ground state remains in the same phase. Furthermore, the gaplessness of the Gaffnian state could be testified based on this formalism with further numerical experiments.

Recently there has been numerical evidence implying the signature of multiple graviton modes. We will introduce the microscopic theory for the emergence of multiple gravitons in fractional quantum Hall droplets based on composite fermionization and the well-defined particle-hole conjugate within a specific conformal Hilbert space. This reveals the dynamical nature of this phenomenon and provides theoretical insights into the chirality and the “merging and splitting” behaviors of the graviton modes. The experimental relevance of multiple graviton modes will be discussed. The microscopic theory of gravitons can also provide valuable insights into the field-theoretical approaches.

Contents

Acknowledgements	ix
Abstract	xv
List of Figures	xix
List of Tables	xxv
Symbols and Acronyms	xxvii
1 Introduction: the Chronicles of Fractional Quantum Hall Effect	1
1.1 Early stage: 1982 - 1984	2
1.2 Collective excitations: 1985-1988	5
1.3 Field theories and phenomenological theories: 1989 - 1992	8
1.4 Harvest time: 1993 - 2003	11
1.5 Topological models and new platforms: 2004 - 2007	13
1.6 Numerics, entanglement, and geometry: 2008 - now	14
1.7 What's next?	18
2 Microscopic Approaches to Fractional Quantum Hall Effect	21
2.1 Brief review on the experimental setup of QH systems	21
2.2 Basic model and energy scales	23
2.2.1 Minimal coupling	23
2.2.2 Full Hamiltonian	24
2.3 Gauge-independent approach	25
2.3.1 A case study: matrix elements of a single particle δ -potential on the LLL	29
2.4 Model Hamiltonians and model wave functions	31
2.4.1 Two-body case	32
2.4.2 Three-body case	35
3 Conformal Hilbert Space and Composite Fermionization	40
3.1 CFT: the theoretical minimum	40
3.2 CFT approach to FQHE	43

3.3	Conformal Hilbert spaces	48
3.4	Isomorphism of conformal Hilbert spaces	49
3.4.1	Partition	50
3.4.2	Restricted generating functions	53
3.4.3	Jack polynomials and generalized admissible rules	63
3.4.4	Isomorphic conformal Hilbert spaces	65
3.5	Composite fermionization	68
3.5.1	Brief review on the composite fermion theory	69
3.5.2	Composite fermionization as the mapping between isomorphic CHSs	70
3.5.3	Particle-hole conjugate within a CHS	73
3.6	Summary	74
4	Graviton Modes in Fractional Quantum Hall Liquids	79
4.1	Gravitons as quasiparticles	79
4.2	Single mode approximation	82
4.3	Structure factor	86
4.4	Analytic results of the graviton gap	89
4.4.1	Assumptions	89
4.4.2	Three-body interactions	91
4.4.3	Two-body interactions	104
4.5	Model Hamiltonian of graviton modes	105
4.5.1	Laughlin-1/3 graviton mode	106
4.5.2	Moore-Read graviton mode	108
4.5.3	Gaffnian graviton mode	109
4.6	Hierarchies within conformal Hilbert spaces	110
4.7	Transitions in low-lying excitations while the ground state is invariant	113
4.7.1	Laughlin-1/5 graviton mode	113
4.7.2	Gaffnian graviton mode	118
4.8	Experimental significance	119
4.9	Summary	121
5	Microscopic Theory of Multiple Graviton Modes	123
5.1	Gravitons as metric fluctuations	124
5.1.1	The cyclotron and guiding center metrics	126
5.1.2	Metrics within conformal Hilbert spaces	128
5.2	Emergence of multiple gravitons	130
5.2.1	Short-range two-body interaction	131
5.2.2	Effective few-body interactions	133
5.3	Chirality of gravitons	134
5.4	Spectral functions from exact diagonalization	136
5.5	Experimental relevance	139
5.6	Microscopic basis for the effective field theory	141

6 Conclusions	149
A Heisenberg algebra	152
A.1 Generic Heisenberg algebra	152
A.2 Physical implications	153
B W_∞-algebra and GMP algebra	155
B.1 w -algebra and W -algebra	155
B.2 SDiff(\mathbb{R}^2) in phase spaces and QH systems	156
B.3 GMP algebra and FFZ algebra	157
C Schrieffer-Wolff transformation	159
D Jacobi coordinates	160
E Generalized Laguerre polynomials	162
F Three-electron wave functions in a magnetic field	164
List of Author's Awards and Publications	167
Bibliography	169

List of Figures

1.1	Skipping orbits. The electrons circulate (gray orbit) in the magnetic field (the direction is denoted by the white circle) as in the classical limit, and bounce back when hitting on the boundary (red and blue orbits), which gives the chiral edge currents.	3
1.2	Calculating the entanglement spectrum. One can partition one system into two parts, A and B . Then by tracing out the degrees of freedom of one subsystem in the quantum state $ \psi\rangle$, one can get the reduced density matrix, the eigenvalues of which give the entanglement spectrum.	16
2.1	Haldane pseudopotential $V_1^{2\text{bdy}}$. This pseudopotential punishes any pair of electrons with the relative angular momentum 1 with the energy cost c^1	31
2.2	LL projection. To preserve the information from the higher LL, after the LL projection, effective many-body interactions have to be introduced.	35
3.1	Jack polynomials and the squeezing operation on the disk.	63
3.2	Relations between the generating function with restrictions and the degeneracy of L_z sectors within some CHS.	66
3.3	Isomorphism between the CHS of electrons and CFs. The electron CHS (left column) is defined by the model Hamiltonian $\hat{V}^{2\text{bdy}}$ and the CF one (right column) is the lowest CF level. All the eigenstates (k denotes the degeneracy) of the angular momentum operator can be expressed as the linear combination of the states on both sides, from which one can easily see the degeneracy of the highest-weight states.	75
3.4	Composite fermionization between electron and CF basis. On the left column, each state is a jack with the root configuration in the ket and on the right side, a monomial. One can clearly see the correspondence between the electronic Laughlin state at $\nu = 1/3$ /Gaffnian state at $\nu = 2/5$ and the CF IQH states.	76

3.5 The concept of CFs. A CF is given by attaching one electron with an even number of magnetic flux quanta (which is also called flux attachment). The simplest outcome is that one can eliminate the strong-coupling interactions between the electrons and makes the FQH phases of electrons degenerate into the IQH phases of CFs. Furthermore, one can also relate the FQH states at different filling factors by using the idea of flux attachment.	77
3.6 Commutative diagram of electronic states and CF states within different CHSs. Here we use particle ^{flux no.} _{filling factor} to denote the states and take the Laughlin state at $\nu = 1/7$ as an example, which can be described by three different CF states. U_{cf} denotes the unitary transformation or composite fermionization between isomorphic CHSs. One can find the corresponding particle-hole dual states (denoted by \mathcal{C}^{-1}) within \mathcal{H}_1 (null space of \hat{V}_1^{2bdy}), \mathcal{H}_3 (null space of $\hat{V}_1^{\text{2bdy}} + \hat{V}_3^{\text{2bdy}}$) or the LLL, and map them back to the electron basis. For the fully-filled CF level, we can also increase the LL index to get more Jain states, but the experimental signature could diminish with higher CF levels, as the fading color represents. The same formalism can be generalized to the Laughlin state with an arbitrary filling factor.	78
4.1 Illustration of the excitation spectrum of the Laughlin state. The graviton mode is the magneto-roton mode in the long-wavelength limit.	85
4.2 Illustration of the characteristic tensor $\tilde{\Gamma}$. This universal tensor can assemble the coefficients from the model Hamiltonian and the structure factor of the ground state to give the energy of the corresponding graviton mode.	103
4.3 Structure of the $\bar{d}_{n_1 n_2}$ coefficients of the Laughlin-1/3 state. Here, gray coefficients vanish due to the fermionic statistics. Bold coefficients are zero because of the vanishing ground state energy (different colors denote contributions from different three-body model Hamiltonians). Black coefficients are unknown and not necessarily zero. Note that here we omit the bars over the $\bar{d}_{n_1 n_2}$ coefficients for simplicity.	108
4.4 Hierarchy of the null spaces of different FQH states. The null space of different model Hamiltonians can be organized as a hierarchical structure in the full Hilbert space. Meanwhile, the density modes or, more precisely, the graviton modes (denoted by the stars with the corresponding colors) constructed from model ground states live in the next larger null space. For example, the graviton modes of the Laughlin-1/3 phase (orange star) live in the Haffnian null space (green circle), which contains the ground state and all the quasi-hole states of the Haffnian model Hamiltonian. It is efficient to verify this structure with the characteristic tensor formalism proposed in this thesis.	110

-
- 4.5 **Spectra of the toy Hamiltonian \hat{H}_L diagonalized in different Hilbert spaces.** The case with $\lambda = 0.05$ is shown in (a) and $\lambda = 0.95$ in (b). In the left panel, one can clearly observe the transition of the low-lying states when λ increases from 0.05 to 0.95. These states have different natures, as explained in Fig.4.7. In the right panel, we zoom in on the spectra to the range $E \in [0, 0.5]$ and mark the states living in the Haffnian null space with green squares and other states with blue dots. As expected, the CF picture shows that both the density and the hollow-core modes live in the Haffnian null space. Note that the lowest angular momentum of the hollow-core modes is $L_{\min} = 4$, as can be seen in (b). Furthermore, the quantized energy of the hollow-core modes (especially when $\lambda \rightarrow 0$) can be understood using the root configurations in Eq.(4.89). 112
- 4.6 **Spectrum of the toy Hamiltonian \hat{H}_L with respect to 6 electrons and 26 orbitals.** (a) As the color bar shows, the red dots depict the spectrum of the density modes, and the blue dots denote the hollow-core modes. The color of each dot is determined by calculating their collective overlap with all the density modes in the Laughlin-1/3 null space $\mathcal{H}_{L-1/3}$, or all the hollow-core modes in the complementary space $\bar{\mathcal{H}}_{L-1/3}$. As λ increases, though the ground state (denoted by dark red) stays invariant, the low-lying states show a clear cross-over behavior and transform from density modes to hollow-core modes. (b) illustrates the structure of the Hilbert space and the relationship between the states and the model Hamiltonians. The Laughlin-1/5 null space $\mathcal{H}_{L-1/5}$ (dark red circle) punished by neither $\hat{V}_1^{2\text{bdy}}$ nor $\hat{V}_3^{2\text{bdy}}$ is the sub-space of $\mathcal{H}_{L-1/3}$ (only punished by $\hat{V}_3^{2\text{bdy}}$). Meanwhile, there exist the hollow-core modes (blue circle) only punished by $\hat{V}_1^{2\text{bdy}}$ in $\bar{\mathcal{H}}_{L-1/3}$. All of the other states are punished by both $\hat{V}_1^{2\text{bdy}}$ and $\hat{V}_3^{2\text{bdy}}$, living in the remaining part of $\bar{\mathcal{H}}_{L-1/3}$ 114
- 4.7 **Nature of the low-lying states with different model Hamiltonian in the CF picture.** (a) The Laughlin-1/5 state of the electrons can be reinterpreted as the Laughlin-1/3 state of CFs consisting of one electron and two fluxes, which also follows from the Jain construction. (b) The graviton modes can be understood as the excitations of CFs in the lowest CF level. (c) The hollow-core modes are created by exciting CFs to the second CF level, which still live in the Gaffnian null space. 115

4.8	Spectrum of the toy Hamiltonian \hat{H}_G with respect to 10 electrons and 22 orbitals. (a) shows the spectra of the model Hamiltonian \hat{H}_G in Eq.(4.90). The low-lying states are density modes even when λ is quite large, and the absence of hollow-core modes is different from the Laughlin-1/5 state in Fig.4.6. (b) illustrates the structure of the Hilbert space and the relationship between the states and the model Hamiltonians. All the states in the complementary space of the Moore-Read null space are punished by both $\hat{V}_3^{3\text{body}}$ and $\hat{V}_5^{3\text{body}}$	117
4.9	Spectra of the toy Hamiltonian \hat{H}_G diagonalized in the full Hilbert spaces. The spectrum with $\lambda = 0.05$ is shown in the left panel and $\lambda = 0.95$ in the right panel. As expected, when $\lambda = 0.05$, all the low-lying states (density modes) live within the Moore-Read null space \mathcal{H}_{MR} . Meanwhile, when $\lambda = 0.95$, all the states except the ground state are in the complement of \mathcal{H}_{MR} within the LLL, denoted by $\bar{\mathcal{H}}_{\text{MR}}$	118
4.10	Finite size scaling of the structure factor coefficients of different states. (a) The structure factor expansion coefficients of the Laughlin-1/3 and the Laughlin-1/5 state. According to the orthogonality of Laguerre polynomials, d^m of the Laughlin-1/ m state is equal to the expectation value of the model Hamiltonian $\hat{V}_m^{2\text{bdy}}$ (thus $c^m = 1$) acting on this state. Thus the numerical results shown here provide the value of the corresponding dimensionless coefficients despite the dimension of energy, which is true for Fig.(b) as well. (b) The expectation value of $\hat{V}_7^{3\text{bdy}}$ with respect to the Gaffnian state (≈ 0.04 in the thermodynamic limit), denoted by $d_3^{7\text{bdy}}$, is significantly smaller than other coefficients in the plot, where the expectation value of $\hat{V}_5^{3\text{bdy}}$ with respect to the Moore-Read state is denoted by $d_3^{5\text{bdy}}$ (≈ 1.6 in the thermodynamic limit).	120
5.1	Intrinsic metrics in FQH states. The left panel shows that the fluctuations of the cyclotron metric \tilde{g}_{ab} originate from the LL mixing. The right panel shows the hierarchical structure of the CHSs (null spaces) of the corresponding model Hamiltonians (more details can be found in Table.4.1) in the LLL. Each of these spaces can have its own metric g_i^{ab} , the fluctuation around which can potentially lead to multiple graviton modes in a single LL.	128

5.2 (a) Illustration of the hierarchical structure of three CHSs and the ground state $ \psi_0\rangle$ within \mathcal{H}_{III} (red sphere) in the Hilbert space. The corresponding GMP mode $ \psi_g\rangle$ is outside \mathcal{H}_I so one can imagine the regularised guiding center density operator acting on the ground state goes through three CHSs, leading to three emergent gravitons because of the fluctuation around the metric of each of the CHSs. (b) PH conjugate of Laughlin states within different CHSs. Here \mathcal{C}_i denotes the PH conjugate within $\mathcal{H}_i^{\text{2bdy}}$, and \mathcal{C} denotes the PH conjugate within a single LL or a single CF level. Arrows represent magnetic fluxes, and the CFs denoted by $\text{cf}_{\nu^*}^n$, consist of one electron and n fluxes, form a CF FQH state at ν^* . Note that the red ($\text{cf}_{4/5}^2$) and the yellow ($\text{cf}_{2/3}^4$) CFs are anti-CFs with the fluxes opposite to the external field.	129
5.3 Spectral functions of the FQH states with the filling factor $\nu = 2/7, 4/13$ and $2/11$. The graviton mode of the FQH state with filling factor ν is called ν -graviton for simplicity. The blue, the turquoise, and the red region denote $\mathcal{H}_3^{\text{2bdy}}$, $\mathcal{H}_1^{\text{2bdy}}$ and its complement correspondingly, from which one can clearly see the gaps between different sectors. For the FQH states with $\nu = 2/7$ and $4/13$, model Hamiltonians show similar signatures of two peaks in the spectral functions as coulomb interactions (a small \hat{V}_5^{2bdy} is added in (b2) for stabilizing the proper ground state). The corresponding overlap between the model and ground states of the Coulomb interaction can be found in Table.5.1	143
5.4 Spectral functions of FQH states at $\nu = 2/9$ with 8 electrons. (a) shows two peaks within $\mathcal{H}_1^{\text{2bdy}}$ in the spectral function with respect to the model Hamiltonian, where the green sector denotes the null space of \hat{V}_9^{3bdy} . These peaks will merge after \hat{V}_9^{3bdy} is removed from the Hamiltonian as (b) shows. A slightly exaggerated ratio between different PPs is adopted to clearly show the signature of different CHSs. (c) shows the spectral function of Coulomb interaction, where two peaks can also be clearly observed. In experiments, one can tune \hat{V}_1^{2bdy} to increase (orange area) or decrease (blue area) the separation to get peaks resolved better. Note that the peaks with modified \hat{V}_1^{2bdy} have been smoothed by Gaussians.	144
5.5 Spectral functions of the Jain state at $\nu = 2/7$ with 8 electrons with respect to the Coulomb interaction on the LLL and the SLL is shown in the main figure, where we use different colors to distinguish the LLL gravitons with different chiralities, denoted as $\sigma = +$ or $-$. The overlap between the gravitons with respect to the coulomb interaction on the SLL (black peaks in the main plot) and those with different chiralities on the LLL can be found in the subplots, from which one can clearly observe that some of the peaks can be regarded as two gravitons of opposite chiralities at almost the same energy.	145

- 5.6 Spectral functions of the Anti-Pfaffian state at $\nu = 1/4$ with 8 electrons with respect to the Coulomb interaction on the LLL and the SLL is shown in the main figure, where we use different colors to distinguish the LLL gravitons with different chiralities, denoted as $\sigma = +$ or $-$. The overlap between the gravitons with respect to the coulomb interaction on the SLL (black peaks in the main plot) and those with different chiralities on the LLL can be found in the subplots, from which one can clearly observe a similar feature to the case of the Jain state at $2/7$ 146
- 5.7 Spectral functions of the Pfaffian state at $\nu = 1/4$ with 8 electrons. The turquoise, the orange and the pink region denote $\mathcal{H}_1^{2\text{bdy}}$, the null space of $\hat{\mathcal{V}}_8^{3\text{bdy}}$ and its complement correspondingly. When there is no two-body PP $\hat{\mathcal{V}}_1^{2\text{bdy}}$ in the Hamiltonian, one can clearly observe the merging of peaks from (a) to (b). Considering the coulomb interaction is $\hat{\mathcal{V}}_1^{2\text{bdy}}$ -dominated, we can also observe two peaks in (c), which also shows that one can significantly increase (orange area) or decrease (blue area, and both smoothed by using Gaussians) the separation between the peaks by properly tuning $\hat{\mathcal{V}}_1^{2\text{bdy}}$ in experiments. A slightly exaggerated ratio between different PPs is adopted to clearly show the signature of different CHSs. A small $\hat{\mathcal{V}}_5^{2\text{bdy}}$ is added in (c) for stabilizing the non-Abelian Pfaffian state. 147
- 5.8 Number of Haldane modes with different structures of CHSs. Laughlin states ($N = 1, \eta = 1$) are denoted by the white point in the corresponding CHS (blue circle). For the Jain states at $N/(2nN+\eta)$, (a) with $n = 1, N > 1, \eta = \pm 1$, (e.g., the FQH state at $2/3$ and $2/5$, etc.), because $\delta\hat{\rho}_{\mathbf{q}} = \delta\hat{\rho}_{\mathbf{q}}^*$, these states will show the same behavior as the Laughlin state at $1/3$, i.e., one peak with no Haldane mode required. When $n > 1$, (b) shows that a single Haldane mode is needed in the effective field theory despite two peaks observed in the spectral function, among which, given n , the states with $N = 2, \eta = -1$ can be regarded as the particle-hole conjugate partner of the corresponding Laughlin state within some specific CHS, and the states with $N > 1, \eta = 1$ are the states in higher CF levels as shown in Fig.5.2(b). (c) and (d) show more possibilities and conclude that the number of Haldane modes added to the effective theory cannot be easily reckoned from the number of peaks in the spectral function $I(E)$, which is closely related to the microscopic Hamiltonian used. 148
- D.1 Jacobi coordinates. 161

List of Tables

1.1	Some of the members in the great Hall effect family. The first column provides the time when the corresponding effect was proposed (T for theory) or observed (E for experiment). For the main topic of this report, FQHE, a more detailed timeline of the important methods can be found in the first chapter of this thesis. The main methods, preliminary explanation, or experimental platform of each effect can be found in the second column. This table may never be complete as new effects are being proposed every year.	15
3.1	Integer partition numbers $p(k)$ and $p(k i)$ (denoted by the corresponding integers in the first row for simplicity). Here i means that there are i parts in the partitions of integer k .	51
4.1	The CHSs and their model Hamiltonians. The CHSs are defined as the null spaces of the corresponding model Hamiltonians. Here λ_i can be any constant coefficient.	111
5.1	The overlap between the ground states with different filling factors (first row) of the corresponding model Hamiltonian and the Coulomb interaction. The corresponding electron numbers and the figure indices have been included.	132
F.1	The anti-symmetric three-body wave functions expanded in the basis of $n_1, n_2\rangle$. The values of α^{n_1, n_2} can be found easily by looking at the coefficient of the corresponding basis. For example, $\alpha^{5,0}$ is the coefficient of $ 5, 1\rangle$, i.e. $-\frac{\sqrt{5}}{4}$.	165

Symbols and Acronyms

Symbols

\mathbb{C}	complex field
\mathbb{R}	real number field
\mathbb{Q}	rational number field
\mathbb{Z}	integer ring
\mathbb{N}	natural number semiring
\mathcal{H}	Hilbert space
$ \cdot $	2-norm of a vector or matrix in Euclidean space
\wedge	wedge product
$\hat{\mathbf{e}}_\alpha$	unit vector along α -direction, $\alpha \in \{x, y, z\}$
$\hat{a}, \hat{a}^\dagger, \hat{b}_i^\dagger, \hat{b}_i$	ladder operators (of the i -th particle)
$\delta_{ij}, \delta_i^j, \delta^{ij}$	Kronecker delta
$\epsilon_{ab}, \epsilon_a^b, \epsilon^{ab}$	Levi-Civita symbols
\hbar	Planck constant
e	elementary charge
B	magnetic field
$\ell_B \equiv \sqrt{\hbar/eB}$	magnetic length
$\hat{\tilde{R}}_i^a$	cyclotron coordinate operator
$\hat{\tilde{R}}_i^a$	guiding center operator
$ \psi_0\rangle$	ground state
$\langle \hat{O} \rangle_0$	expectation value of the operator \hat{O} acting on the ground state
$\hat{\rho}_{\mathbf{q}}$	guiding center density operator
$\delta\hat{\rho}_{\mathbf{q}}$	regularized guiding center density operator
$V_{\mathbf{q}}$	effective potential

$S_{\mathbf{q}}$	static structure factor
$s_{\mathbf{q}}$	reduced structure factor
$L_k(q^2)$	Laguerre polynomials
$p(k)$	partition number of k
$p(k \mathcal{R})$	restricted partition number of k with the restrictions \mathcal{R}
$\mathcal{G}(q \mathcal{R})$	restricted generating function with \mathcal{R}
$(a)_n$	q-Pochhammer symbols
$\begin{bmatrix} n \\ m \end{bmatrix}_q$	q-Gaussian polynomials
$\hat{\Omega}_{\lambda}$	regularization operator
$\hat{\Lambda}_j^{(q)}$	extraction operator
J_{λ}^{α}	Jack polynomials
K_H	thermal Hall conductance
\cong	isomorphic to
\mathcal{P}_{LLL}	projection operator on the lowest Landau level
c^m	expansion coefficients of the effective potential
d^n	expansion coefficients of the reduced structure factor
$ \psi_{\mathbf{q}}\rangle$	single-mode approximation (SMA) model wave function
$\Gamma_{mn}^{\text{2bdy}}$	two-body characteristic matrix
$\hat{\rho}_{\mathbf{q}_1}^i$	guiding center density operator acting on the i -th electron $\hat{\rho}_{\mathbf{q}_1}^i = e^{iq_1 a} \hat{R}_i^a$
$\bar{S}_{\mathbf{q}_1, \mathbf{q}_2}$	reduced three-body structure factor
$\bar{S}_{\mathbf{p}_1, \mathbf{p}_2}$	Fourier pair of reduced three-body structure factor
$V_{\mathbf{q}_1 \mathbf{q}_2}$	three-body effective potential
$\tilde{\mathbf{q}}_i$	momentum components in Jacobi coordinates
$\tilde{\mathbf{p}}_i$	Fourier pair of $\tilde{\mathbf{q}}_i$
$\tilde{Q}_i \& \tilde{P}_i$	square of $\tilde{\mathbf{q}}_i$ & $\tilde{\mathbf{p}}_i$
$J_n(x)$	Bessel functions of the first kind
${}_0F_1(; n; x)$	hypergeometric functions
$L_k^{(\alpha)}(x)$	generalized Laguerre polynomials
$c^{m_1 m_2}$	expansion coefficients of three-body effective potential
$d_i^{m_1 m_2}$	expansion coefficients of reduced three-body structure factor

$\bar{d}^{n_1 n_2}$	redefined expansion coefficients of reduced three-body structure factor
$\alpha^{n_1 n_2}$	expansion coefficients of three-body anti-symmetric wave functions in the basis of $ n_1, n_2\rangle$
$\tilde{\Gamma}_{m_1 m_2 n_1 n_2}^{\text{3bdy}}$	three-body characteristic tensor
$\tilde{\Gamma}_{m_1 m_2 n_1 n_2}^{0/+-}$	diagonal/off-diagonal parts of the three-body characteristic tensor
\mathcal{N}_i	the index set of the neighbors of i

Acronyms

(I/F)QH(E)	(integer/fractional) quantum Hall (effect)
$n\text{D}$	n -dimensional
2DES	two-dimensional electron gas
MOSFET	metal–oxide–semiconductor field-effect transistor
GaAs	gallium arsenide
LL	Landau level
LLL	lowest Landau level
SLL	second Landau level
TT limit	thin-torus/Tao-Thouless limit
WC	Wigner crystal
GMP	Girvin-Macdonald-Platzman
ODLRO	off-diagonal long-range order
CF	composite fermion
CS	Chern-Simons
Pf	Pfaffian
MR	Moore-Read
FCI	fractional Chern insulator
ED	exact diagonalization
DMRG	density matrix renormalization group
MC	Monte Carlo
jack	Jack polynomial
BCS	Bardeen–Cooper–Schrieffer
MATBG	magic-angle twisted bilayer graphene
SW	Schrieffer-Wolff

CFT	conformal field theory
CHS	conformal Hilbert space
SMA	single-mode approximation
QFT	quantum field theory
GR	general relativity
AdS	anti-de Sitter

Chapter 1

Introduction: the Chronicles of Fractional Quantum Hall Effect

The interplay between charged particles and magnetic field has been discussed for more than one hundred years among physicists, which has also brought tons of applications to human society [1, 2]. However, with the rapid development of quantum mechanical formalism, the classical picture based on the Lorentz force was proved to be insufficient to describe the intrinsic physics anymore, which was confirmed by the discovery of the integer quantum Hall effect (IQHE) of two-dimensional electron gas (2DES) in a metal-oxide-semiconductor field-effect transistor (MOSFET) as discussed in details later [3]. The experimental measurements showed a very accurate quantized feature at integral values of the so-called Hall resistance R_{xy} . The Landau quantization of electronic kinetic energy perfectly explained this [4, 5]. Meanwhile, the role of dimension was found to be important in this phenomenon. That is, though we can have some other interesting magnetic-field-related effects such as the De Haas–van Alphen effect [6, 7] and the Shubnikov–de Haas effect [8, 9] in three-dimensional space (It is worth noticing that most of the effects related to the magnetic field show some periodic or oscillating behavior, which does remind us of the classical circular-motion picture from time to time), the quantum Hall effects are *essentially* restricted to 2D systems because additional dimensions could generate multiple sets of Landau levels (LLs) that mess up with the spectrum and destroy the plateaus [10]. However, the subsequent observation of the fractional quantum Hall effect (FQHE) under more extreme conditions raised new challenges to the coherent explanation of the plateaus at specific rational numbers,

which clearly cannot be explained by the Landau quantization[11]. In fact, it is one of the (strong-coupling) topological orders rarely found so far, and thus the core discussion is about properly resolving the interactions between particles.

In this introduction, we would like to provide a thorough historical review of the development of the FQHE. Although great progress has been made, a complete theory of FQHE remains a pendent problem in contemporary physics. Therefore, we will try separating the timeline by using several keywords, which are purely based on the author's own opinion and the topic of this thesis (so we will particularly mention the topic about geometric degrees of freedom in FQH phases) and can definitely be classified in other ways. Meanwhile, mathematical content will be suppressed to a minimum in this part - only those that are really important (or elegant) will be shown to tell a consistent story about concepts rather than techniques. In fact, every historical period is a mixture of studies on various topics, so here we only mean to focus on those first proposed or discovered in each period and make them more organized by following the chronological order. The key is, however, to learn from the trend and determine where the next step should be taken. More importantly, instead of using a separate section to present the main contribution in this thesis, we will add introductions or comments to the content in this thesis *at the proper place of the whole timeline of FQHE studies*, which could provide a big picture for the reader to see the relevance of this thesis to the related topics.

1.1 Early stage: 1982 - 1984

Unlike many other areas in physics where theoretical physicists are often able to make predictions that are later verified in experiments, the experimentalists have played the role of pioneers in the story of quantum Hall effects (they did not expect to see these phenomena themselves either, though). The era of quantum Hall started from the discovery of quantized Hall resistance at integers by Klitzing, Dorda, and Pepper in 1980 [3], followed by the remarkable experiments in GaAs systems by Tsui, Störmer and Gossard revealing richer structures with higher magnetic field and lower temperature two years later [11]. The fractionally-quantized Hall resistance, accompanied by the vanishing longitudinal resistance, drew attention from everyone working on condensed matter at that time. So the theories at

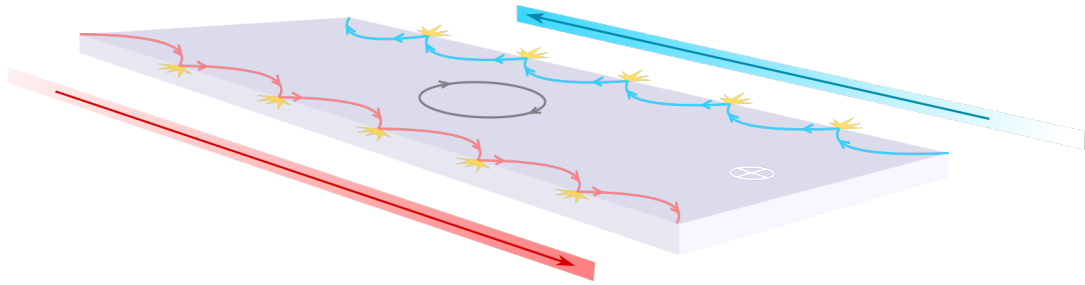


FIGURE 1.1: Skipping orbits. The electrons circulate (gray orbit) in the magnetic field (the direction is denoted by the white circle) as in the classical limit, and bounce back when hitting on the boundary (red and blue orbits), which gives the chiral edge currents.

this stage mainly focused on exploring the significance of specific fractional filling factors, debating the nature of the ground states, and establishing the relationship between different phases.

In 1982 Halperin proposed a nice and intuitive semi-classical explanation to the chiral and dissipationless edge current by using the picture of *skipping orbits* that have been commonly seen in textbooks nowadays, where the electrons circulate in the magnetic field as in the classical limit and bounce back when hitting on the boundary as shown in Fig.1.1 [12]. Meanwhile, Thouless, Kohmoto, Nightingale, den Nijs (and also Streda independently) derived the astonishing relationship between the Hall conductance and a topological invariant, the first Chern number, which was later found to be relevant to the geometric Berry phase and Berry curvature (they still called it “the Kubo formula” back then) [13–17]. Their discovery literally added *topology* to physicists’ toolbox and assigned explicit physical significance to the concepts in topology. Then in 1983, the acute physical instinct of Laughlin brought the community the first *model wave function* with a comprehensible “plasma analogy” based on his earlier closed-form solution to the Schrödinger equation of two and three electrons interacting with each other in a magnetic field (An interesting anecdote is that the term Laughlin used in the title, anomalous quantum Hall effect, to be distinguished from the integer quantum Hall, was used for totally different things afterward.), which describes the FQH state at the filling factor $1/m$ (and also the corresponding particle-hole conjugate partner at $1 - 1/m$)

where m is an odd integer, which is now known as the Laughlin states, and explained the quantized Hall resistance [18, 19]:

$$\psi_L(z) = \prod_{i < j} (z_i - z_j)^m e^{-\sum_{i=1}^n |z_i|^2 / 4\ell_B^2}. \quad (1.1)$$

Here z_i is the holomorphic coordinate of the i -th electron and $\ell_B = \sqrt{\hbar/eB}$ is the magnetic length. It is also from this time that writing down *first-quantized* model wave functions with complex coordinates to describe FQH states became some convention, unlike in many other areas, such as superconductivity, where second-quantized wave functions are preferred. Haldane attempted to generalize the FQH states to different geometries at the same time [20, 21], who considered a *hierarchy* of states on the sphere (and torus afterward with Rezayi [22]), and Tao and Thouless' construction by mapping the FQH ground states to a one-dimensional (1D) system, which is now called the thin-torus or Tao-Thouless limit [23–25]. More importantly, Haldane proposed the *model Hamiltonians* of the Laughlin model states, which are now called *Haldane pseudopotentials* as explained in the next chapter, and this was double-checked by Girvin and Jach's numerical study to the ground states of harmonic interactions ($\sim (\hat{r}_i - \hat{r}_j)^2$ where i, j are particle indices) [26, 27]. It is worth noticing that a favored choice of gauge typically accompanies a given geometry, but it is possible to study the FQH states in a *gauge-free* manner as introduced in Chap. 2. This will be more helpful for discussing the geometric aspects without any presumed geometry or symmetry, and by using the pseudopotentials one can either expand the Coulomb interaction or simply construct a model Hamiltonian to give the corresponding ground state.

The model wave functions proposed by Laughlin were also generalized to charged excitations, including *quasielectrons* and *quasiholes*, which are generally termed as *quasiparticles* [19]. These excitations were predicted to exhibit *anyonic* behaviors, i.e., *fractional charge* based on Laughlin's plasma analogy [19] and *fractional statistics* relevant to the filling factor of the state, by Arovas, Schrieffer, and Wilczek in 1984 [28, 29], accompanied by Halperin's study to the iterative construction of the FQH states by adding quasiparticles to a parent state (equivalent to the condensation of quasiparticles), which also confirmed the fractional statistics by using model wave functions [30]. The idea of looking for a possible hierarchy of FQH states was embedded into this field by Haldane and Halperin since then and proved very promising by the following theories.

In the same year, Tao and Wu started the discussion on the degeneracy of the FQH ground states based on the idea of gauge invariance [31], which was earlier adopted by Laughlin to explain the integer filling factors [15]. Numerical methods such as exact diagonalizations came into play as well, which has been able to provide the ground state energy and pair correlation functions of the Laughlin states back at that time [32]. Furthermore, even though the model wave function formalism works well for moderate filling factors, the discussion of the nature of the ground state with small filling factors remained controversial, and the mainstream point of view tended to support a Wigner crystal (WC) phase [33–35], which was actually one of the phenomena that Tsui *et al.* carried out their significant experiments to study in the first place. WCs are proposed to be a candidate with *long-range order* by Tao and Thouless in 1983, contrary to the Laughlin states, for the ground states corresponding to the quantized plateaus [23]. Their approach was afterward found helpful in the thin-torus limit but can not apply to the generic FQH states [36]. Later Lam and Girvin predicted a transition point between FQH liquids and WC by comparing their energy under different magnetic fields numerically and confirmed that the WC phase could finally take control as the ground state when the filling factor is smaller than $1/7$ [37–42]. Meanwhile, the role of the disorders (and thus the high mobility of electrons) was systematically studied by Paalanen *et al.*, who verified the critical role of high mobility in the observation and the stabilization (represented by temperature dependence) of plateaus for the Laughlin state at $1/3$ and its particle-hole conjugate partner [43–47].

1.2 Collective excitations: 1985-1988

The nontrivial properties of the quasiparticles foreshadowed that people's interests extended quickly to the excitations rather than just the ground states in FQH phases. At this stage, the main topics were the detailed discussion of the low-lying neutral and charged collective excitations, a more systematic understanding of the existing model wave functions, further experiments in more FQH states, and the attempts to unify the integer and the fractional quantum Hall effect. These proposals and ideas were like sparks that eventually ignited the explosion of FQH theories in the early 1990s.

Apart from the charged excitations, it is natural to consider the excitations of multiple quasiparticles with an equal number of quasiholes and quasielectrons that turned out to be neutral in effect. In a simultaneous development, the density-wave-like excitations, called the roton mode, had been found to be the low-lying neutral modes in *superfluids* [48–50]. Such insight from other areas was of great help to the discovery of the first model wave function describing the low-lying neutral excitations by Girvin, MacDonald, and Platzman (GMP) in 1985-1986, which are now called the GMP wave function [51, 52]. The key is the so-called *single-mode approximation (SMA)*, which allows one to predict a similar magneto-roton minimum in the spectrum and describe the neutral modes up to the magneto-roton minimum (thus also valid in the long-wavelength limit) as density fluctuations from the ground state and. The subsequent research further reveals the geometric features of the GMP modes, because they can be regarded as the excitations from the metric fluctuations in Hilbert spaces, which also serves as one of the main topics in this thesis. We shall introduce a rigorous way to define model Hamiltonians for these modes in the long wavelength limit, and the full story will be illustrated in Chapter 4, so we will leave it be for now.

At the same time, many details about the model wave functions have been investigated: The numerical study of the wave functions based on exact diagonalization had reached 7 electrons for the Laughlin state at $\nu = 1/3$ [53]; Fano, Ortolani, and Colombo found that the Laughlin wave function on the sphere and the disk are related by a stereographic mapping, which is now believed to be true for other wave functions as well [54]. They also derived the closed-form expression for the Haldane pseudopotential in the lowest Landau level (LLL) on the sphere, which became very valuable for numerics. Further studies in the systems with finite layer thickness confirmed the validity of both the Laughlin wave function as the proper description of the FQH state at 1/3 and GMP’s SMA description of the magneto-roton modes [55]; The role of spin has been taken into account since Chakraborty, Pietiläinen and Zhang’s numerical study, which found that spin-reversed states could be favored in some FQH phases [56]. The trial wave function, the density configuration, and spectra of collective excitations were also generalized to multi-component systems and brought more candidates to the ground state [53, 57–59].

Then in 1987, the first systematic textbook about the quantum Hall effect was published [60]. The progress of experimental conditions such as sample purity and

cryogenic method led to the first confirmed discovery of an FQH state with an *even-denominator* qt the filling factor, $\nu = 2+1/2$, by Willett *et al.* [61, 62]. This clearly challenged people's common point of view, that the fermionic FQH states should have odd denominators because of the statistics. Another important theoretical progress was made by Girvin and MacDonald, who found an off-diagonal long-range order (ODLRO) in the FQH ground states by calculating the singular-gauge density matrix of the Laughlin state at $\nu = 1/m$ [63–65]:

$$\tilde{\rho}(z, z') = (1/2\pi m)e^{-\beta\Delta f(z, z')} |z - z'|^{-\frac{m}{2}} \quad (1.2)$$

where $\Delta f(z, z')$ is the free energy difference between two impurities of charge $m/2$ and $\beta^{-1} \equiv m/2$ plays the role of temperature. This led to the later discovery that the FQH phases should be regarded as *topological orders*, which have become a hot topic in condensed matter theory nowadays, and also verified the possibility of using a field-theory approach to describe the FQH phases, which as introduced in the next stage, was found to be an elegant and powerful method.

Then in the next year, the deep consideration of Haldane to the essential requirements for realizing a quantum Hall phase or quantized Hall conductance provided a toy lattice model consisting of two sub-lattices that can generate QHE with no net magnetic flux through each unit cell (and thus no LLs) [66]:

$$H(\mathbf{k}) = 2t_2 \cos \phi \left[\sum_i \cos(\mathbf{k} \cdot \mathbf{b}_i) \right] \mathbb{I} + t_1 \left[\sum_i \cos(\mathbf{k} \cdot \mathbf{a}_i) \sigma^1 + \sin(\mathbf{k} \cdot \mathbf{a}_i) \sigma^2 \right] \\ + \left[M - 2t_2 \sin \phi \sum_i \sin(\mathbf{k} \cdot \mathbf{b}_i) \right] \sigma^3 \quad (1.3)$$

where \mathbf{a}_i is the unit vector pointing to neighboring sublattice, $\mathbf{b}_1 = \mathbf{a}_2 - \mathbf{a}_3$, $\mathbf{b}_2 = \mathbf{a}_3 - \mathbf{a}_1$, $\mathbf{b}_3 = \mathbf{a}_1 - \mathbf{a}_2$, and σ^i are Pauli matrices ($i \in \{1, 2, 3\}$), which showed it is the broken time-reversal symmetry (introduced by the last term in the Hamiltonian) that matters for the QHE rather than the magnetic field. Such a lattice model was considered highly unrealistic back then but was found to be extremely similar to graphene discovered afterward [67, 68]. Another controversy at that time was about the mechanism and the robustness of the edge current, and especially the evident absence of back-scattering in experiments [69, 70], the convincing explanation of which was given in the next few years by Wen.

1.3 Field theories and phenomenological theories: 1989 - 1992

The spiral of scientific progress was suddenly straightened by the God of physics - the theoretical studies of FQHE reached a remarkable climax by the end of its first decade, a veritable golden age. In this period, the application of new theoretical tools, such as effective field theories and conformal field theories, brought powerful approaches to the discussion on FQH phases and provided novel ways to get model wave functions for *non-Abelian* states and the phenomenological composite fermion theory, on the other hand, epitomized the idea of hierarchy. The rigorous derivation for the degeneracy of ground states further confirmed the FQH phases' topological nature. The controversy regarding the proper description of the gapless edge excitations of most FQH states was also temporarily put to an end by the Luttinger liquid theory. A prototype of the topological order theory was sketched, which became one of the most critical topics in contemporary condensed matter physics.

In 1989, Jain published his paper on a new formalism for organizing the FQH phases with the filling factor obeying some ordered pattern [71–76]. Even though experiments had not confirmed the existence of many states, this phenomenological picture still drew lots of attention due to the intuitive construction of the so-called composite fermion (CF). The basic idea is that if one thought about what is going on in the FQH experiment measuring Hall resistance, with the number of electrons fixed, increasing the magnetic field is equivalent to adding more flux quanta to the system. When the ratio ν between the number of electrons and fluxes reaches some specific value, the FQH phase will transform from one to another. The hierarchy idea proposed by Haldane and Halperin was essentially considering such a dynamic procedure as the condensation of quasiparticles generated by additional fluxes to relate different phases. Jain's idea was to consider the filling factor $\nu = p/(2mp \pm 1)$ with $p, m \in \mathbb{N}_+$ as indicating the ratio between electrons and fluxes within a *CF*, and if the accompanied flux number for each electron is even, this article will be fermionic. The advantages of this picture are that one can transform the strong-coupling FQH states of electrons to the effectively one-body IQH state of CFs, and the model wave function can be written down by following some well-defined steps termed as *composite fermionization*. However, the shortcoming is also

apparent: the formalism of why there can be emerging CFs formed by electrons and fluxes in a certain way is unclear. Also, when the magnetic field is strong enough, the interaction between CFs has to be taken into account, which complicates the problem. In Chapter 3, we will review the CF theory. More importantly, we will show another possible and more rigorous approach to the “flux-attachment” procedure and a generalized composite fermionization that can map states between sub-Hilbert spaces within a single LL.

The field-theoretical approaches were proposed first by Girvin and MacDonald [64], but their approach could not provide a satisfactory explanation for many observations in the experiments, such as the quantized values of plateaus and the incompressibility of ground states. It was the work of Zhang, Hansson, and Kivelsson in the same year that offered a reasonable low-energy effective field-theoretical description to the Laughlin phases [77, 78], who introduced a statistical gauge potential \mathbf{a} that couples s fluxes to the electrons, reminiscent of Wilczek’s explanation of the fractional charge of anyons, and the corresponding gauge field is given by:

$$b(\mathbf{r}) = -\epsilon^{ij} \partial_i a_j(\mathbf{r}) \equiv s \cdot \left(\frac{2\pi}{e} \right) \cdot |\phi(\mathbf{r})|^2 \quad (1.4)$$

Such a theory contains a Chern-Simons term of \mathbf{a} and thus also called a *topological* field theory considering this term does not include any metric tensor [79]. The field-theory approach to FQH phases has been proved valuable since 1989, e.g., the effective Chern-Simons theory based on the CF picture was proposed afterward [80]. More details about the Chern-Simons theory and especially its relation to another important theory describing the model wavefunctions and gapless edge modes in FQHE, called the conformal field theory (CFT), can be found in Sec. 3.2.

As might have been noticed by the reader, the word “topology” has appeared several times. This in fact implies the possibility to use several parameters to distinguish different FQH phases, because there are no local order parameters for these phases, such as the two integers p and q whose ratio gives the filling factor ν . In 1990, Wen and Niu further tested the dependence of the ground state degeneracy of FQH states to the topological structure of the background manifold [81], and derived the explicit expression based on Haldane’s former argument that the ground state degeneracy of the FQH phase at p/q on the torus is at least q [82]: the degeneracy on a manifold with genus g should be at least q^g . Another

impactful work by Wen at the same time is the discovery of the low-energy effective and solvable description to the edge modes called *chiral Luttinger liquid*, which is different from the ordinary Fermi liquids and exhibits novel features such as spin-charge separation [83–87]. Afterward, Wen found that the effective theories of both the bulk and the edge of an FQH phase are closely relevant to each other [87–89]. This idea was later well-illustrated in the study of the *bulk-edge correspondence* in topological systems [90]. Then in 1992, Wen and Zee derived another topological coefficient of FQH states, called the *topological shift* \mathcal{S} , which is a finite rational number depending on the topology of the space and influences the number of orbitals within a single LL [91].

Compared to the condensed matter community's enthusiasm for superconductivity, superfluidity, and quantum Hall effect at that time, the high-energy physicists were focusing on equally exciting topics like string theories and supersymmetry, which also brought vitality to many mathematical topics. In Witten's study of the Jones polynomials, he first noticed the close relation between CS theory and CFT under some conditions [92], which naturally drew people's attention to the newly-discovered phenomenon whose low-energy effective theory was exactly described by a CS action. In 1991, Moore (who is known as a great mathematical physicist) and Read proposed a model wave function for an FQH state with an even-denominator based on the similarities between the wave functions and conformal blocks in CFT, written as [93]:

$$\psi_{\text{MR}}(z) \propto \text{Pf} \left(\frac{1}{z_i - z_j} \right) \prod_{i < j} (z_i - z_j)^2 \quad (1.5)$$

which is now called the Moore-Read state or the Pfaffian (Pf) state (with the Gaussian factor dropped), and also similar to a BCS wave function in the real space [94, 95]. The model Hamiltonian was found to be a three-body pseudopotential [96]. Note that the model wave functions before this year were either written down from nowhere or adapted from the existing one, but since CFT is introduced to FQH, people have got more methods to formally write down model wave functions. Apart from these theoretical progresses, in 1992 two research groups generalized the experimental setup to more degrees of freedom and observed an FQH state at $\nu = 1/2$ in *double-layer* electronic systems [97, 98], the ground state of which is now conjectured to be the 331 state proposed by Halperin [99–102].

1.4 Harvest time: 1993 - 2003

In the next few years from the “golden age” of FQH theories, there were a lot of things to digest and test, with many significant discoveries on the experimental side and various applications to the existing theoretical formalism. The study of topological orders has been generalized to more cases and physicists were also abstracting the theories based on more serious mathematics such as algebraic topology. Here we will introduce some of the progress that is also important for the discussion in this thesis.

Richer algebraic structures in QH systems other than the Heisenberg algebra of the ladder operators were proposed by Cappelli, Trugenberger, and Zemba in 1993, who found that the product of ladder operators could form a W_∞ -algebra, and the similar algebra was generalized to FQH afterward [103–107]. In fact, the GMP algebra of density operators is isomorphic to a W_∞ -algebra as well, which reveals their nature as area-preserving deformations of the incompressible phase and partially explains why there can be analytic expressions of physical quantities for the SMA wave function including those derived in this thesis (more details can be found in Appendix.B). Meanwhile, the first explicit signature of neutral collective excitations was captured in the inelastic light scattering experiments carried out by Pinczuk, Dennis, Pfeiffer, and West, which verified the earlier predictions made by GMP for the low-lying collective excitation of the Laughlin state at $\nu = 1/3$ [108]. Even now scattering experiments still play an important role in probing the neutral excitations [109–114], such as the graviton mode (the magneto-roton mode in the long-wavelength limit) discussed in this thesis, we will discuss more the application of different particles in the scattering experiments for resolving various features such as the chirality in Chap.5.

Also, since the 1990s there have been several attempts to measure the fractional charge of the quasiparticles predicted by Laughlin, but none of the experiments, including measuring resistance fluctuations with the magnetic field, resonant tunneling through a quantum anti-dot and so on [115–120], have been fully convincing to the community until the results shown by two independent groups. The experiments were carried out with quantum shot-noise measurements to the 2DES in a GaAs-AlGaAs heterostructure, by de-Picciotto *et al.* in Israel [121], and Saminadayar *et al.* in France [122] (which also led to the first Nobel prize belonging to

the FQHE, shared by Störmer, Tsui and Laughlin in 1998). Such a method was proposed by Tsui firstly [60] and thanks to the comprehensive understanding of the edge of FQH droplet as a chiral Luttinger liquid (which was also confirmed by the power-law behavior of the tunneling conductance at the edge of the Laughlin state by Chang, Pfeiffer, and West in 1996 [123, 124]), the experimentalists successfully measured the noise power proportional to a fractional charge $e/3$ for the Laughlin state at $\nu = 1/3$. In comparison, the measurement to the fractional statistics of anyonic quasiparticles has recently got some preliminary results, but still under debate [120, 125–129].

Another important progress relevant to the Luttinger liquid nature of the edge was made by Kane and Fisher in 1997 [130], who found another topological invariant that can be used to distinguish different FQH phases (which can be regarded as one of the main tasks in the studies to FQHE as introduced above), called the thermal Hall conductance K_H , which shows the difference between the number of chiral edge currents and thus can be a positive or negative *integer*. But in 2000 Read and Green derived the thermal Hall conductance of the Moore-Read state when studying the pairing of CFs in this state (as in BCS paired states [95, 131, 132]), and found that it should be a *half-integer* due to the non-Abelian nature [94, 133, 134], which has been confirmed by experiments [135, 136]. Thus this quantity became an important index to distinguish the nature of non-Abelian states because Hall conductance experiments are incapable of detecting the signature of neutral non-Abelions, and was afterward found to be relevant to the central charge of the CFT describing the FQH phase as well [137]. Furthermore, they also studied the analogous FQH state of a d-wave paired state of spinless bosons in detail, which is now called the *Haffnian state* [138–140].

As introduced at the beginning, physicists are very interested in the phases with broken symmetries, such as the Wigner crystal (WC) phase in a magnetic field. There have been more symmetry-broken phases proposed by using Hartree-Fock methods in the 90s, such as bubble phases, stripe phases, crystalline phases, and nematic phases in higher LLs [141–145], which are believed to be related to the geometric degrees of freedom in FQH phases as well.

1.5 Topological models and new platforms: 2004 – 2007

The cumulative results about the topological order, both theoretical and experimental, originated from the discovery of FQHE and contributed to the establishment of the abstract paradigm describing topological orders, such as the toy models (Kitaev chain [146], toric code [147, 148], etc), the generalization to the Altland-Zirnbauer (AZ) ten-fold symmetry classification for fermions [149], the following application of the group cohomology and tensor categories in this field [150–153], and possible experimental realizations such as by using quantum wires [154–156]. Another topic started from then on is the widespread applications of the ideas in QHE to other systems, some of which have been listed in Table 1.1 for reference, among which the most successful one could be the prediction and the following realization of the quantum spin Hall effect, or *topological insulators* as its 3D generalization, considering their potential application in dissipationless circuits [90, 157–159].

As for the progress in FQH, the discovery of graphene in 2004 provides a new platform to study QH states with less extreme conditions at room temperature [160–164], and meanwhile simulating FQH phase with cold atoms in optical lattices was proposed [165–167], which could lead to the realization of bosonic FQH states in experiments with the rapid developments in manipulating atomic interactions and creating synthetic gauge potentials [168–170]. Furthermore, one important thing that brought FQHE to more physicists’ wishing lists is that people noticed the important role of non-Abelian excitations in realizing topological quantum computation [171], so the discussion on how to properly probe the quasiparticles with non-Abelian statistics became a hot topic [137, 172–175]. In 2005 Das Sarma, Freedman, and Nayak proposed an experimental approach to the measurement of the non-Abelian statistics of the Moore-Read state, and the braiding of the quasiparticles in this experiment was found to support robust topological qubits [176]. The corresponding experiment has not been carried out, while many following proposals about how to detect the non-Abelian quasiparticle statistics by using interferometric experiments have been put forward [134, 177], and it should only be a matter of time to see a concrete result. The fractional charge $e/4$ of the quasiparticles in the Moore-Read state, experimentally confirmed by Dolev *et al.*

in 2008 [178, 179], further convinced people of the promising applications of this state.

1.6 Numerics, entanglement, and geometry: 2008

- now

It is really hard (and also arrogant) to tell what are the most important questions at present, which can only be left for the future to distinguish. So here we will try introducing several main aspects in the recent research of FQHE.

Firstly, with the rapid development of information technology and engineer's endeavor to push the limit of Moore's Law, now the most economic and approachable way to simulate FQH phases is by using computers. Almost all the mainstream algorithms such as ED (as in this thesis), DMRG [180–182], Monte Carlo [128, 183–185], etc. have been adapted for studying the FQHE, but because of the strong-coupling nature of this problem, the largest system size available for numerical calculations is still far away from the usual experiments, *let alone* the thermodynamic limit. Recently, quantum computers have also been found to be an available platform for the simulation of FQH states and their dynamics, the difficulty of which, however, is that the construction of these states involves non-unitary operators, so only the simplest states like the Laughlin states have been realized on quantum computers so far [186, 187].

Besides the hardware and algorithm issues, physicists have found more *physical* ways to accelerate the simulation of FQH states. In 2007, Simon, Rezayi, and Cooper generalized Haldane's two-body pseudopotential to rotationally-invariant many-body pseudopotentials, which provides an efficient way to construct the model Hamiltonians numerically for simulating the effect of LL mixing [188], etc. They also formally constructed a group of wave functions defined by symmetric analytic function with the lowest degree that vanishes as at least p powers when q particles coincide [189]. Another non-Abelian model state at $\nu = 2/5$ was constructed from the nonunitary minimal model $M(5, 3)$ by Simon *et al.*, which is thus predicted to be *gapless* and named as the Gaffnian state [139, 190–194]. We will try analyzing the gaplessness of this state by combining analytical and numerical tools in Sec.4.8. Meanwhile, the experimental signature of this state remains elusive.

Year	Progress	Proposal (Discovery)
1879 (E)	Lorentz Force	(Classical) Hall effect
1880 (E)	Spontaneous magnetization, spin-orbit coupling	Anomalous Hall effect (AHE)
1980 (E) 1981 (T)	Landau quantization	Integer quantum Hall effect (IQHE)
1982 (E) 1983 (ψ_L) 1987 ($\psi_{\frac{5}{2}}$) 1989 (CF/TFT) 1991 (CFT)	Model wave functions, CFT, CS theory, composite Fermion, etc.	Fractional quantum Hall effect (FQHE)
1971 (T) 2004 (E)	Spin-orbit coupling	Spin Hall effect (SHE)
2005 (T) 2007 (E)	Spin-orbit coupling, BHZ model, Kane-Mele model, SPT order, etc.	Topological insulator (TI) /Quantum spin Hall effect (QSHE)
2005 (T&E)	Spin-phonon coupling, observed in $Tb_3Ga_5O_{12}$	Phonon Hall effect
2005 (T)	Orbital angular momentum decoupled with spin	Orbital Hall effect
2008 (T) 2013 (E)	Spontaneous magnetization; observed in $(Bi,Sb)_2Te_3$	Chern insulator (CI) /Quantum anomalous Hall effect (QAHE)
2010 (T)	Righi-Leduc effect	Thermal Hall effect (THE)
2011 (T) 2018 (E)	Flat Chern bands; observed in BLG/hBN and MATBG	Fractional Chern insulator (FCI)
2014 (E)	Observed in monolayer MoS_2	Valley Hall effect
2017 (E)	Observed in monolayer MoS_2	Exciton Hall effect

TABLE 1.1: **Some of the members in the great Hall effect family.** The first column provides the time when the corresponding effect was proposed (T for theory) or observed (E for experiment). For the main topic of this report, FQHE, a more detailed timeline of the important methods can be found in the first chapter of this thesis. The main methods, preliminary explanation, or experimental platform of each effect can be found in the second column. This table may never be complete as new effects are being proposed every year.

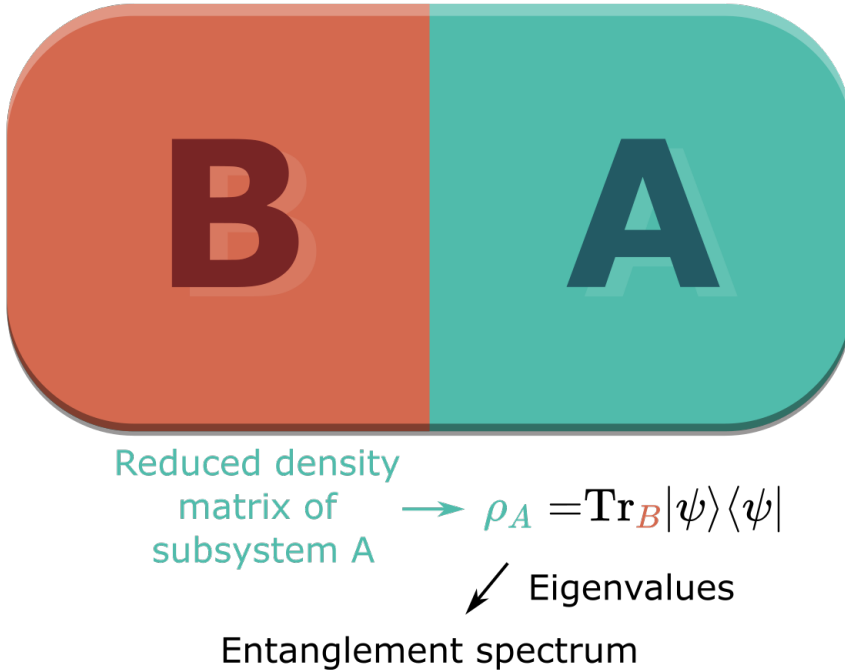


FIGURE 1.2: **Calculating the entanglement spectrum.** One can partition one system into two parts, A and B . Then by tracing out the degrees of freedom of one subsystem in the quantum state $|\psi\rangle$, one can get the reduced density matrix, the eigenvalues of which give the entanglement spectrum.

In 2008, Bernevig and Haldane found that many first-quantized model wave functions of FQH states [195–198], including the Laughlin state and Moore-Read state, can be written as a species of symmetric polynomials called the *Jack polynomials* (jacks), which will be introduced in Sec.3.4.3. The key point of this discovery is that one can construct these model wave functions following some well-defined patterns, and the states can be efficiently stored in computers. The binary representation of the basis brought huge convenience for the preparation of diagonalization as well. Following this approach, the numerical construction of the neutral modes was proposed by Yang *et al.* in 2012 [199], which can be used to simulate the magneto-roton mode accurately as explained in Sec.4.2. Then the model Hamiltonians were generalized to anisotropic systems [200–202], the case without Galilean invariance [203], etc. Classical constraints to the basis in a given FQH state were also proposed as the local exclusion conditions (LEC) by Yang in 2019, which also works for the states that jacks cannot describe [204, 205]. Thus the major question in physics is about how to universally and efficiently construct the states and the model Hamiltonians.

The lattice analog of FQHE was proposed by Regnault and Bernevig in 2011, which contains a flat Chern band similar to the LLs in FQH states and is named the fractional Chern insulators (FCI) [206]. Most of the so-derived formalisms working for FQH have been readily translated to these systems, such as the Laughlin-like states, three-body interactions that induce Moore-Read-like phases, and so on [207–210]. The experimental observation of FCI was first realized in the Bernal-stacked bilayer graphene aligned with hexagonal boron nitride with a large magnetic field in 2018 [211], and later it was also found in the magic-angle twisted bilayer graphene (MATBG) in 2021 [212], which can hold FCI phases even without a magnetic field. Also as a lattice model, FCI could be more tunable in practice. Thus the close relation between FCI and FQHE makes it tempting to consider them as supplements for each other, especially in experiments.

It has been realized that it is the entanglement rather than the correlations that govern the topological orders [213], so the quantum entanglement in topological orders has been systematically studied since 2000, mainly in the form of (topological) entanglement entropy [214–220]. Li and Haldane proposed another quantity that contains more information called the entanglement spectrum in 2008 [221], which is the spectrum of the reduced density matrix and can serve as another topological signature for distinguishing different FQH phases as introduced in Sec.3.2. Calculating the entanglement spectrum requires partitioning a system into parts, which can generate pseudo-edges in between, so it is natural for this spectrum to provide edge properties of the state as shown in Fig.1.2. The signature in the entanglement spectra also supports the bulk-edge correspondence in topological orders. Furthermore, in 2010, the proper definition of an entanglement gap for the Laughlin states and the Moore-Read state in the thermodynamic limit was given by Thomale *et al.* [175]. This requires pushing the system to the conformal limit by using unnormalized bases in the wave function, which can eliminate the effect of the length scale. Such an operation opens a stable gap between the low-lying model states and the high-energy Coulomb modes, and the behavior of the entanglement gap provides another method to distinguish the transition between different phases. Similar to the energy spectrum, two states are conjectured to share the same topological structure if one can deform their entanglement spectra from one to another without closing the entanglement gap [89, 222–226]. However, the proper definition of such a gap for more phases is pending. Further studies about the topological features

also lead to the matrix product state representation of some FQH phases [227–229], which is also helpful for the construction of FQH states on quantum computers.

The last thing we would like to introduce, also the main topic of this thesis, is the geometric degrees of freedom in FQH phases, which most physicists initially omitted because people cared more about the topological features. In 2011, Haldane summarized his results of the geometry in FQH phases by introducing the metrics of the kinetic energy (an effective mass tensor) and the interaction term (controlled by the medium) in the Hamiltonian, which were presumed to be identical until then [230]. Haldane argued that these two *independent* metrics do not have to be equal and if they are not, the guiding-center degrees of freedom (which is relevant to the physics within a single LL and thus crucial for discussing FQHE) will be governed by an intermediate metric between the two above, which effectively defines the shape of the FQH droplet and the intrinsic correlations. Thus the actual ground state should be the one with the metric giving the lowest energy rather than the isotropic one customarily considered. Now that we can define a “shape” for an FQH droplet, it is natural to consider its response to shear deformations, the quantitative description of which is captured by the Hall viscosity that contributes to the incompressibility as well [231–236]. The GMP modes were found to be closely related to the geometric aspects of FQH because of their emergent graviton signatures (as explained in Chap.4). In this thesis, we will call them *graviton modes* to understand them as the excitation from metric fluctuations in the Hilbert space. One can use effective gravitational field theory to describe these modes [237, 238], but instead, we will try establishing a *rigorous microscopic theory* for the graviton modes and the multi-graviton feature recently found in numerics as shown in Chap.4 and Chap. 5, which can be an excellent supplement to the field-theoretical approach.

1.7 What's next?

Forty years old is a blessed age in Chinese culture because it is believed that people should have no more perplexities about their lives or themselves at this age. In the case of the studies to FQHE, however, we might still be far away from such optimism. As we can see, an unusual point in the research on FQH is that almost all the important paradigms in this field have been proposed within 10 years since the

discovery of FQHE. Sadly, this is reflected in the fact that the research nowadays is mostly following the ways paved by the pioneers and tinkering with the existing formalism here and there. From this point of view, a unified theory about FQH phases, if there is one, might require some novel paradigms and new mathematics. Apart from the topics introduced in the last section, many basic and essential questions remain to be answered in FQHE. Here we will only list some of them echoing in the author's mind from time to time:

- *Is there a fractal nature in FQH states?* As we have seen in the various attempts to find hierarchies in the FQH states, and the discretized version of QH systems that show a Hofstadter's butterfly, there seems to exist some self-similarity structure among the FQH phases [239–241]. So how can we confirm it? What can we learn from such a feature?
- *What is the nature of CFs?* Although the CF theory has been quite successful and popular, they are still considered phenomenological because the reason why the electrons would combine with the fluxes in specific ways remained a conundrum, even if there has been evidence of observing CFs in experiments. Furthermore, the step of projecting the wave function to a single LL has not been rigorously proven to be valid as well. So again, there still exist interactions, although weak, between CFs, but how to adequately describe them?
- *Is it possible to realize an arbitrary model Hamiltonian? And how, if possible?* The model Hamiltonians provides rigorous definitions of the model states. It will be constructive to observe things like the transition of low-lying excitations in the experiments if we can tune the Hamiltonian freely as explained in Sec.4.7. The progress in quantum computers might bring a promising way to realize this.
- *How to numerically simulate FQH phases more efficiently?* This is not entirely a physical issue, but there could be some insights physicists can offer.
- *Does a gapless FQH phase exist in bulk or not?* The Gaffnian state at $\nu = 2/5$ constructed from the minimal model $M(5, 3)$ is believed to be a gapless state. But the Jain state at the same filling factor is still gapped [242, 243]. Another example is the CF-Fermi liquid [244, 245]. Such gapless phases, if exist, could

be the phase transition points between two phases, which requires further experiments to verify.

- *What is the correct description of the FQH state at $\nu = n + 1/2$?* There have been several candidates for this state, the Pfaffian (Moore-Read) state [93, 94], the anti-Pfaffian state [246, 247], and the PH Pfaffian state [248–250]. The study of the systems with LL mixing tends to support that the anti-Pfaffian state is favored [251–254], the thermal Hall signature of which, however, does not match the experiment without proper modifications [134–136]. There are also proposals of a bubble phase consisting of Pfaffian and anti-Pfaffian states, but no exact answer has been found [255, 256].
- *How to understand the role of LLs in forming FQH phases?* It has been noticed that some of the FQH phases with specific filling factors (here, by filling factors, we mean $\tilde{\nu} \equiv \nu \bmod N$, where N is the LL index) can only be observed in specific LLs, for example, the half-filling state.
- *How to extract more useful information from the excited states?* Just like the GMP modes constructed from the ground state can provide geometric information about the FQH phase, can we find more in other states?
- ...

Of course, this list can be expanded freely. But the ultimate question has not been answered, or maybe we have not even found the proper way to ask it:

- *What is the complete description of the FQH phases?* It should be able to explain and predict why the incompressibility gap only opens at specific filling factors with the corresponding signatures that can be observed in experiments, reveal why and when the quasiparticles can show non-Abelian statistics and combine the topology, the geometry, the entanglement, and all the other aspects into a coherent framework, etc.

The worst possible reason why we haven't got a unified formalism of FQHE could be that the states with different filling factors *have to be* described by various theories. But most physicists still believe that all the FQH phases can be described in the same manner, which might turn out to be a universal model wave function or some exotic pairing or binding formalism between electrons and fluxes. So we hope this thesis can contribute a bit to the approach to the final answer.

Chapter 2

Microscopic Approaches to Fractional Quantum Hall Effect

2.1 Brief review on the experimental setup of QH systems

One could expect it hard to realize a Quantum Hall (QH) liquid in experiments because of the relatively extreme conditions, i.e., a pretty low temperature ($T \rightarrow 0$ ideally in systems like MOSFETs [3]). On the other hand, integer quantum Hall effect can be realized at room-temperature in graphenes [160], but we will ignore this for now) and a very high magnetic field ($B \sim 10$ T, and to see how large it is, 1 T $\approx 4.836 \times 10^{14}$ magnetic flux quanta per square meter). Besides, a material with high purity is also required if one is expecting to see the plateaus in the Hall resistivity [257]. Here we would like to discuss the physical reasons and relations of these conditions considering the quantum Hall effects were initially discovered from experiments, which can also reveal the essential requirements for realizing an FQH liquid and constructing a proper theoretical model:

- Two dimensions: It is necessary for the formation of discrete LLs, which is the key to explaining the Integer Quantum Hall (IQH) effect and also the origin of the abundant physics in Fractional Quantum Hall (FQH) phases. Note that two-dimensional (2D) space here is effective because the “real” 2D space is pointless in our four-dimensional space-time, considering there is no

way to manipulate or probe anything within such an infinitely thin region. In practice, as long as the degree of freedom along z -direction (orthogonal to the 2D space considered) is completely independent (for comparison, the other two dimensions are not independent but coupled by the magnetic field) and strictly restricted, i.e., staying at one eigenstate with no transitions to other ones, we can regard the system as 2D.

- Electrons as the basic particles: The earliest realization of FQH phases was by using 2D electron gas [3]. However, the statistics of underlying particles is not crucial since it is also possible to study bosonic FQH phases (conceptually by using photons) [167, 258–260]. In this thesis, we will assume the particles are electrons, meaning only the Coulomb interaction is considered.
- Low temperature: The temperature gives an additional energy scale competing with the main one set up by the magnetic field. Thermal fluctuations can excite the low-lying states or even “unfreeze” the degrees of freedom along z -direction, introducing different sets of LLs to the spectrum. These could eventually destroy the discrete LLs when they accumulate to a specific density. Another reason to lower the temperature is to increase the mean free path ($\sim \sqrt{T}$) of the electrons for experimental measurements.
- Strong magnetic field: The magnetic field defines the unique length scale in the QH system, i.e., the magnetic length ℓ_B , invokes the non-commutative geometry (forms the LLs which relate two orthogonal directions to each other) [261], and results in the quenching of kinetic energy when it is strong enough. Meanwhile, it will inevitably break the time-reversal symmetry, which has physical implications such as the different energy costs of charged excitations, the Hall viscous force, etc. Still, it is not required for the existence of topological orders as verified by the Chern insulators [66, 206].
- Disorder: The disorders provide another energy scale that is unavoidable in experiments but is expected to be weak because it is irrelevant to the physics of FQH phases. However, suppose one expects to see clear plateaus in the Hall resistivity of some incompressible ground state. In that case, it is necessary to introduce a certain amount of disorders that can break the translational invariance and cause *Anderson localization* [262, 263]. Otherwise, the Hall resistivity can tell us nothing but the density of the electrons in the system, as can be derived concerning the Lorentzian or even the Galilean invariance.

The most significant feature in Quantum Hall experiments is the robustness of the quantized plateaus in the Hall resistivity, which inspired the idea of introducing topology into physics. Strictly speaking, all of the requirements above can find some corresponding substitutes, which can naturally give other topological phases because all these conditions are essentially adopted to realize a *nontrivial Chern number* in the bands [264]. We shall see how to construct a reasonable microscopic Hamiltonian based on our analysis of the experimental conditions in the next section.

2.2 Basic model and energy scales

2.2.1 Minimal coupling

Here we briefly introduce how to include the effect of the magnetic field in our discussion. Consider a generic action along the path γ :

$$S[\gamma] = \int_{\gamma} dt L(q(t), \dot{q}(t), t) \quad (2.1)$$

with the dynamic equation given by the Euler-Lagrange equation:

$$\frac{\partial L}{\partial q^i}(t, \mathbf{q}(t), \dot{\mathbf{q}}(t)) - \frac{d}{dt} \frac{\partial L}{\partial \dot{q}^i}(t, \mathbf{q}(t), \dot{\mathbf{q}}(t)) = 0, \quad i = 1, \dots, n \quad (2.2)$$

From the classical theory, we know that a velocity-dependent Lorentz force will act on the electrons, which bends the trajectory of the electrons. Thus the Lagrangian and the generalized force should be:

$$L = \frac{1}{2}m\dot{\mathbf{r}}^2 - U(\mathbf{r}, \dot{\mathbf{r}}), \quad \mathbf{F} = \left(-\frac{\partial}{\partial \mathbf{r}} + \frac{d}{dt} \frac{\partial}{\partial \dot{\mathbf{r}}} \right) U \quad (2.3)$$

where \mathbf{r} denotes the real-space coordinate. This approach is called *minimal coupling* because only q , the zeroth-moment of charge, is considered. From Maxwell's equations, the Lorentz force can be written as:

$$\mathbf{F} = -q(\mathbf{E} + \mathbf{v} \times \mathbf{B}) = \left(-\nabla + \frac{d}{dt} \frac{\partial}{\partial \dot{\mathbf{v}}} \right) [q\phi - q(\mathbf{v} \cdot \mathbf{A})] \quad (2.4)$$

where \mathbf{A} is the vector potential. Thus the canonical momentum is given by:

$$\mathbf{p} = \frac{\partial L}{\partial \mathbf{v}} = m\mathbf{v} - q\mathbf{A} \quad (2.5)$$

In conclusion, if one only takes the electric charge of a charged particle in the magnetic field into account, the covariant momentum should be defined as:

$$\hat{\pi} = \hat{\mathbf{p}} + q\mathbf{A} = -i\hbar\nabla + q\mathbf{A} \quad (2.6)$$

2.2.2 Full Hamiltonian

One can formally decompose the Hamiltonian of a QH liquid into:

$$\begin{aligned} \hat{H} &= \hat{H}_{\text{kinetic}} + \hat{H}_{\text{Coulomb}} + \hat{H}_{\text{Zeeman}} + \hat{H}_{\text{disorder}} + \hat{H}_{\text{thermal}} \\ &\equiv \hat{H}_k + \hat{H}_C + \hat{H}_s + \hat{H}_d + \hat{H}_t \end{aligned} \quad (2.7)$$

To discuss the physics of FQH phases, we need to simplify this Hamiltonian by making some assumptions. Firstly we assume that the system should be spin-polarised, which will be naturally fulfilled when the magnetic field is strong, so the third term about the Zeeman effect can be ignored. Secondly, as explained above, the disorders are unnecessary for the exciting physics of FQH phases (though unavoidable in reality). Thus in our theoretical model, we will set the system to be perfectly uniform. Finally, we can work in a zero-temperature system to suppress the last energy scale proportional to temperature (Note that generically the effects of temperature cannot be written as a single term in the Hamiltonian because it can influence the parameters in a complicated way. So here, we only use \hat{H}_t to denote these effects formally.). In short, we are constructing a theory for a *spin-polarised, homogeneous and zero-temperature* FQH liquid.

To write down the explicit form of the Hamiltonian, one will normally impose some auxiliary restrictions to the system, such as the geometry, the symmetries, and the boundary conditions of the 2D manifold, which can help to choose a proper gauge. Note that the physics should not depend on the gauge choice so that a gauge-free theory will be more generic, and no unnecessary details will be brought into our discussions. Furthermore, no specific symmetries should be assumed either, i.e., we will remove the non-generic Galilean invariance and isotropy from the system to

expose the geometric properties of QH phases so that only the metric-independent *inversion symmetry* is assumed to define the guiding center coordinates unambiguously.

2.3 Gauge-independent approach

Classical closed trajectories indicate the correlation between different directions, which can be expressed as the non-commutativity between the operators in the context of quantum mechanics. This is seen in the dynamics of 2D electrons moving in a magnetic field, where x -direction and y -direction are not independent. Hence, it is no longer inconvenient to write down the equations of motion along orthogonal directions. Instead, one can decompose the coordinate into two commutative parts, cyclotron coordinates and guiding center coordinates, which are given by [257]:

$$\hat{\tilde{R}}^a = \hat{r}^a + \epsilon^{ab}\hat{\pi}_b, \quad \hat{\tilde{R}}^a = -\epsilon^{ab}\hat{\pi}_b \quad (2.8)$$

where a and b denote spatial coordinates along x or y direction. \hat{r} and $\hat{\pi}$ are the real-space displacement and the covariant momentum, the commutation rule of which is given by:

$$[\hat{r}_j^a, \hat{\pi}_{jb}] = i\delta_b^a\delta_{ij}, \quad [\hat{\pi}_{ia}, \hat{\pi}_{jb}] = i \cdot eB \cdot \delta_{ij}\epsilon_{ab} \quad (2.9)$$

Here i and j denote the particle indices. For simplicity, we will set the magnetic length $\ell_B = 1/\sqrt{eB} = 1$. One can observe the Heisenberg algebra introduced in Appendix A. The cyclotron coordinates and guiding center coordinates are also the generators of the magnetic translation group:

$$\begin{aligned} \tilde{T} &= e^{iq_a\hat{\tilde{R}}^a} \implies \tilde{T}\hat{\tilde{R}}^a\tilde{T}^\dagger = \hat{\tilde{R}}^a + \epsilon^{ab}q_b \\ \bar{T} &= e^{iq_a\hat{\tilde{R}}^a} \implies \bar{T}\hat{\tilde{R}}^a\bar{T}^\dagger = \hat{\tilde{R}}^a - \epsilon^{ab}q_b \end{aligned} \quad (2.10)$$

The independence of cyclotron coordinates and guiding center coordinates can be seen from:

$$[\hat{\tilde{R}}^a, \hat{\tilde{R}}^b] = 0, \quad [\hat{\tilde{R}}^a, \hat{\tilde{R}}^b] = i\epsilon^{ab}\delta_{ij}, \quad [\hat{\tilde{R}}^a, \hat{\tilde{R}}^b] = -i\epsilon^{ab}\delta_{ij} \quad (2.11)$$

which clearly shows a broken time-reversal symmetry. These commutations also remind us of the Heisenberg algebra, so it is natural to define two sets of ladder operators as:

$$\hat{a} = \tilde{\omega}_a^* \hat{\bar{R}}^a, \quad \hat{a}^\dagger = \tilde{\omega}_a \hat{\bar{R}}^a; \quad \hat{b} = \bar{\omega}_a \hat{\bar{R}}^a, \quad \hat{b}^\dagger = \bar{\omega}_a^* \hat{\bar{R}}^a \quad (2.12)$$

Here both the complex structures should obey $\epsilon^{ab} \tilde{\omega}_a^* \tilde{\omega}_b = \epsilon_{ab} \bar{\omega}^{a*} \bar{\omega}^b = i$ corresponding to different metrics, which will reserve the commutation rules between the ladder operators, for example:

$$[\hat{b}, \hat{b}^\dagger] = [\bar{\omega}_a \hat{\bar{R}}^a, \bar{\omega}_b^* \hat{\bar{R}}^b] = -i\epsilon^{ab} \bar{\omega}_a \bar{\omega}_b^* = 1 \quad (2.13)$$

A special case is that when the system is rotationally invariant, the coefficients can be determined as $\tilde{\omega} = \bar{\omega}^* = \frac{1}{\sqrt{2}}(1, i)$ with isotropic metrics $\tilde{g}_{ab} = \bar{g}_{ab}$. Otherwise, one can write down the unimodular metric as:

$$\bar{g}_{ab} = \bar{\omega}_a^* \bar{\omega}_b + \omega_a \bar{\omega}_b^*; \quad \tilde{g}_{ab} = \tilde{\omega}_a^* \tilde{\omega}_b + \tilde{\omega}_a \tilde{\omega}_b^* \quad (2.14)$$

In the high-field limit ($\hbar\omega_B \gg U_C$), the low-lying states can be written as the tensor product of the cyclotron and the guiding center degrees of freedom $|\Psi_0, m\rangle = |\tilde{\psi}_0(\tilde{g})\rangle \otimes |\psi_m(\bar{g})\rangle$ [230]. Once equipped with these metrics, we can define the azimuthal angular momentum operator as:

$$\hat{L} = \epsilon_{ab} \cdot \hat{r}^a g^{bc} \hat{p}_c \quad (2.15)$$

which can be separated into the cyclotron and the guiding center angular momentum operators:

$$\hat{\tilde{L}} = \frac{1}{2} \tilde{g}_{ab} \hat{\tilde{\Lambda}}^{ab}; \quad \hat{\bar{L}} = \frac{1}{2} \bar{g}_{ab} \hat{\bar{\Lambda}}^{ab} \quad (2.16)$$

as the corresponding generators of rotation:

$$\begin{aligned} \tilde{\Theta} = e^{i\theta \hat{\tilde{L}}} &\implies \bar{\Theta} \hat{\bar{R}}^a \bar{\Theta}^\dagger = \cos \theta \cdot \hat{\bar{R}}^a + \sin \theta \cdot \epsilon^{ab} \tilde{g}_{bc} \hat{\tilde{R}}^c \\ \bar{\Theta} = e^{i\theta \hat{\bar{L}}} &\implies \bar{\Theta} \hat{\bar{R}}^a \bar{\Theta}^\dagger = \cos \theta \cdot \hat{\bar{R}}^a - \sin \theta \cdot \epsilon^{ab} \bar{g}_{bc} \hat{\bar{R}}^c \end{aligned} \quad (2.17)$$

where we have defined

$$\hat{\tilde{\Lambda}}^{ab} = \frac{1}{2} \left\{ \tilde{R}^a, \hat{\tilde{R}}^b \right\}; \quad \hat{\bar{\Lambda}}^{ab} = \frac{1}{2} \left\{ \hat{\bar{R}}^a, \hat{\bar{R}}^b \right\} \quad (2.18)$$

These operators are generators of linear area-preserving deformations, which form the $\mathfrak{sl}(2; \mathbb{R})$ Lie algebra [265]:

$$\begin{aligned} [\hat{\tilde{\Lambda}}^{ab}, \hat{\tilde{\Lambda}}^{cd}] &= i \left(\epsilon^{ac} \hat{\tilde{\Lambda}}^{bd} + \epsilon^{ad} \hat{\tilde{\Lambda}}^{bc} + \epsilon^{bd} \hat{\tilde{\Lambda}}^{ac} + \epsilon^{bc} \hat{\tilde{\Lambda}}^{ad} \right) \\ [\hat{\tilde{\Lambda}}^{ab}, \hat{\tilde{\Lambda}}^{cd}] &= -i \left(\epsilon^{ac} \hat{\tilde{\Lambda}}^{bd} + \epsilon^{ad} \hat{\tilde{\Lambda}}^{bc} + \epsilon^{bd} \hat{\tilde{\Lambda}}^{ac} + \epsilon^{bc} \hat{\tilde{\Lambda}}^{ad} \right) \end{aligned} \quad (2.19)$$

The metric \tilde{g}_{ab} and \bar{g}_{ab} originate from the complex structure required to define the ladder operators and the corresponding coherent states, which can be intuitively interpreted as describing the “shape” of Landau orbitals. Note that they are not the same as the quantum geometric tensors or Fubini-Study metrics \mathcal{G}_{ab} [266], which are induced by the Hermitian products defined on complex projective spaces and measure the “distance” between states on the quantum state manifold generated by some Lie group attached to a given state, even though \mathcal{G}_{ab} can be expressed as a function of g_{ab} and the orbital spin.

To describe the spatial distribution of particles, one can define the density operator in the real space as:

$$\hat{\rho}_{\mathbf{r}} \equiv \sum_{i=1}^N \delta^2(\mathbf{r}_i - \mathbf{r}) \quad (2.20)$$

where i is the particle index. It is more convenient to use the Fourier transform of the real-space density operator when writing down the interactions:

$$\hat{\rho}_{\mathbf{q}} = \int d^2\mathbf{r} \cdot e^{-i\mathbf{q} \cdot \mathbf{r}} \cdot \hat{\rho}_{\mathbf{r}} = \sum_{i=1}^N e^{iq_a \hat{r}_i^a} \quad (2.21)$$

which can be separated into the cyclotron and guiding center density operators defined by:

$$\hat{\rho}_{\mathbf{q}} = \sum_{i=1}^N e^{iq_a \hat{R}_i^a}; \quad \hat{\tilde{\rho}}_{\mathbf{q}} = \sum_{i=1}^N e^{iq_a \hat{R}_i^a} \quad (2.22)$$

These operators obeys the Girvin-Macdonald-Platzman (GMP) algebra (isomorphic to the W_∞ -algebra as introduced in Appendix.B) [51, 52]:

$$[\hat{\tilde{\rho}}_{\mathbf{q}_1}, \hat{\tilde{\rho}}_{\mathbf{q}_2}] = -2i \sin\left(\frac{1}{2}\mathbf{q}_1 \wedge \mathbf{q}_2\right) \hat{\tilde{\rho}}_{\mathbf{q}_1+\mathbf{q}_2}; \quad [\hat{\tilde{\rho}}_{\mathbf{q}_1}, \hat{\tilde{\rho}}_{\mathbf{q}_2}] = 2i \sin\left(\frac{1}{2}\mathbf{q}_1 \wedge \mathbf{q}_2\right) \hat{\tilde{\rho}}_{\mathbf{q}_1+\mathbf{q}_2} \quad (2.23)$$

where the wedge product $\mathbf{q}_1 \wedge \mathbf{q}_2 = \epsilon^{ab} q_{1a} q_{2b}$. Note that there is a sign difference in the commutation relations. This algebra shows highly nontrivial properties, as we

shall introduce in the following chapters. It is not hard to see that the regularised guiding center density operators also obey the same algebra:

$$\begin{aligned}\delta\hat{\rho}_{\mathbf{q}} &= \hat{\rho}_{\mathbf{q}} - \langle\hat{\rho}_{\mathbf{q}}\rangle_0 \\ [\delta\hat{\rho}_{\mathbf{q}_1}, \delta\hat{\rho}_{\mathbf{q}_2}] &= 2i \sin\left(\frac{1}{2}\mathbf{q}_1 \wedge \mathbf{q}_2\right) \delta\hat{\rho}_{\mathbf{q}_1+\mathbf{q}_2}\end{aligned}\quad (2.24)$$

where $\langle \cdot \rangle_0$ denotes the expectation value with respect to the ground state.

Because the Laplacian on a generic manifold is given by:

$$\nabla^2 = \nabla_a (\tilde{g}^{ab} \partial_b) = \frac{1}{\sqrt{\tilde{g}}} \partial_a \left(\sqrt{\tilde{g}} \tilde{g}^{ab} \partial_b \right) \quad (2.25)$$

we can write down the many-body kinetic energy Hamiltonian with a *constant and unimodular* cyclotron metric and thus equally-spaced LLs as:

$$\hat{H}_k = \frac{1}{2m} \sum_{i=1}^N \tilde{g}^{ab} \hat{\pi}_{ia} \hat{\pi}_{ib} \quad (2.26)$$

In this case, the effective mass tensor determines the energy scale. Note that in a crystalline system, the kinetic energy can be expanded as an infinite series of even-order terms of the cyclotron coordinates. All the physics of IQHE are embedded in this Hamiltonian, so essentially it is a one-body problem.

Once the magnetic field is strong enough to quench the kinetic energy, the Coulomb interaction between electrons will take effect and endow the system with a strong-coupling nature, given by:

$$\hat{H}_C = \sum_{i < j} \frac{e^2}{\epsilon |\hat{r}_i - \hat{r}_j|} \quad (2.27)$$

where ϵ is the permittivity that determines the Coulomb metric. One cannot precisely solve the system with more than two particles, let alone in the thermodynamic limit, even if the full Hamiltonian has been written down because of the exponentially increasing computation resources required to solve a strong-coupling system with more particle numbers. However, solving a relatively small system using exact diagonalization is still possible. If the system is rotationally invariant, we usually use the second-quantized form of the interaction term by labeling the orbitals with the angular momentum quantum number m , so the basis is given by:

$$|m_1, m_2, \dots, m_N\rangle \equiv \hat{c}_{m_1}^\dagger \hat{c}_{m_2}^\dagger \cdots \hat{c}_{m_N}^\dagger |\text{vac}\rangle \quad (2.28)$$

where c^\dagger denotes the fermionic creation operators and $|\text{vac}\rangle$ is the vacuum state. The genetic two-body interaction Hamiltonian \hat{H}_{int} can be written as:

$$\begin{aligned}\hat{H}_{\text{int}} &= \frac{1}{2} \sum_{m_1, m_2, m_3, m_4} \hat{c}_{m_1}^\dagger \hat{c}_{m_2}^\dagger \hat{c}_{m_3} \hat{c}_{m_4} \cdot \langle m_1, m_2 | \hat{V} | m_3, m_4 \rangle \\ &= \frac{1}{2} \sum_{m_1, m_2, m_3, m_4} V_{m_3 m_4}^{m_1 m_2} \cdot \hat{c}_{m_1}^\dagger \hat{c}_{m_2}^\dagger \hat{c}_{m_3} \hat{c}_{m_4}\end{aligned}\quad (2.29)$$

Thus the key is to solve the matrix elements of the potential $V_{m_3 m_4}^{m_1 m_2}$. On the other hand, one can also write down the microscopic form of the interaction in the momentum space. We shall see how this can help to deal with the interactions in the following section.

2.3.1 A case study: matrix elements of a single particle δ -potential on the LLL

Here we present an example of how to write down the matrix element of a given potential in an isotropic system, which means that we have the angular momentum as a good quantum number to label the single-particle orbits $|n\rangle$, so the density operator matrix element in this basis is given by [267]:

$$\langle m | \hat{\rho}_{\mathbf{q}} | n \rangle = \sqrt{\frac{m!}{n!}} (i \cdot \tilde{\mathbf{q}})^{n-m} L_m^{(n-m)}(\tilde{Q}) e^{-\frac{1}{2}\tilde{Q}} \quad (2.30)$$

and we can use the LLL form factor without loss of generality:

$$F_0(\mathbf{q}) = \langle M | \hat{\rho}_{\mathbf{q}} | N \rangle = \langle 0 | \hat{\rho}_{\mathbf{q}} | 0 \rangle = e^{-\frac{1}{2}\tilde{Q}} \quad (2.31)$$

where we have defined:

$$\tilde{\mathbf{q}} = \frac{1}{\sqrt{2}}(q_x - iq_y); \quad \tilde{Q} \equiv |\tilde{\mathbf{q}}|^2 = \frac{|\mathbf{q}|^2}{2} \quad (2.32)$$

For a single δ -potential at $(x_0, 0)$, the unitary Fourier transform with angular frequency in polar coordinates is given by the translation of $\tilde{V}_0(r_q, \theta_q)$:

$$V_{\mathbf{q}} = \tilde{V}_{x_0}(r_q, \theta_q) = e^{ix_0 \cdot q_x} = e^{ix_0 \sqrt{2\tilde{Q}} \cos(\theta_q)} \quad (2.33)$$

Then the matrix elements can be written as:

$$\begin{aligned} H_{mn}^{x_0} &= \int d^2\mathbf{q} \langle m | \hat{\rho}_{\mathbf{q}} | n \rangle F_0(\mathbf{q}) \cdot V_{\mathbf{q}} \\ &= \pi \sqrt{\frac{m!}{n!}} \cdot \int_0^\infty d\tilde{Q} \cdot i^{n-m} J_{n-m} \left(x_0 \sqrt{2\tilde{Q}} \right) \cdot \left(i \cdot \sqrt{\tilde{Q}} \right)^{n-m} L_m^{(n-m)}(\tilde{Q}) e^{-\tilde{Q}} \end{aligned} \quad (2.34)$$

where $J_\alpha(x)$ is the Bessel function of the first kind as introduced in Appendix E, which is related to the Laguerre polynomials as:

$$J_{n-m} \left(x_0 \sqrt{2\tilde{Q}} \right) = \left(\frac{x_0 \sqrt{\tilde{Q}}}{\sqrt{2}} \right)^{n-m} \cdot \frac{e^{-\frac{x_0^2}{2}}}{\Gamma(n-m+1)} \cdot \sum_{k=0}^{\infty} \frac{L_k^{(n-m)}(\tilde{Q})}{\binom{k+n-m}{k}} \frac{\left(\frac{x_0^2}{2} \right)^k}{k!} \quad (2.35)$$

substituting which into Eq.(2.34) gives:

$$H_{n \geq m}^{x_0} = \frac{(-1)^{n-m} \cdot \pi}{\sqrt{2^{m+n}} \cdot \sqrt{m! \cdot n!}} \cdot x_0^{m+n} e^{-\frac{x_0^2}{2}} \quad (2.36)$$

One can easily see the symmetry between x - and y -direction so for the δ -potential at (x_0, y_0) , the matrix elements of the Hamiltonian are given by:

$$H_{mn}(\mathbf{R}) = \frac{\pi}{\sqrt{m! \cdot n!}} \cdot \left(\frac{R}{\sqrt{2}} \right)^{m+n} e^{-\frac{R^2}{2}} e^{i(n-m) \cdot \theta_R} \quad (2.37)$$

where $\mathbf{R} \equiv R \cdot e^{i\theta_R} = x_0 + i \cdot y_0$.

In fact, the eigenstates and the eigenvalues of this Hamiltonian can be *rigorously* solved. However, V_q can be any function (commonly-used ones including $\nabla^2 \delta^{(2)}(\mathbf{r})$, cylindrical functions, Gaussian functions, etc.) so the corresponding Hamiltonian can be very complicated. Here we would like to mention a possible solution given by the δ -potential. By defining the differential operator:

$$\hat{\mathcal{G}}_{mn}^{-1} \equiv \int d^2\mathbf{q} \langle m | \hat{\rho}_{\mathbf{q}} | n \rangle F_0(\mathbf{q}) \quad (2.38)$$

one can see that what we have derived above gives the Green's function $H_{mn}(\mathbf{R})$ of this operator:

$$\hat{\mathcal{G}}_{mn} H_{mn}(\mathbf{R}) = \delta^{(2)}(\mathbf{R}) \quad (2.39)$$

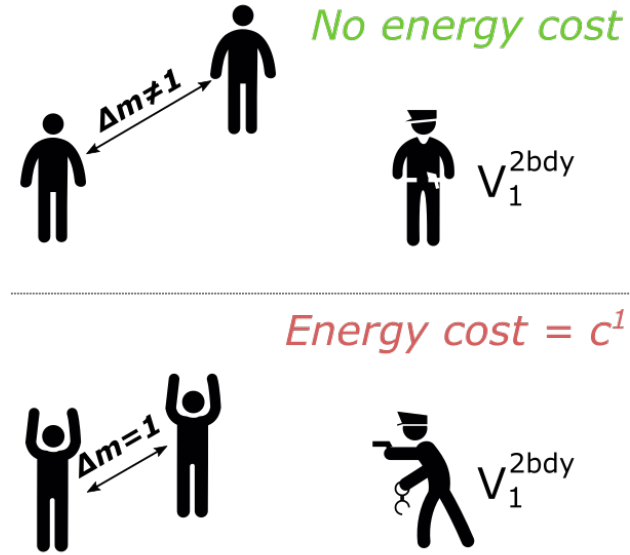


FIGURE 2.1: **Haldane pseudopotential $V_1^{2\text{bdy}}$.** This pseudopotential punishes any pair of electrons with the relative angular momentum 1 with the energy cost c^1 .

Thus in principle, one can use this solution to derive the matrix elements of any potential, the exact process of which will not be shown here.

2.4 Model Hamiltonians and model wave functions

Assuming the translational invariance, a generic two-body interaction in the momentum space can be written as:

$$\hat{H}^{2\text{bdy}} = \int \frac{d^2q}{(2\pi)^2} V_q \hat{\rho}_q \hat{\rho}_{-q} = \sum_{i < j} \int \frac{d^2q}{(2\pi)^2} V_q e^{iq_a(\hat{r}_i^a - \hat{r}_j^a)} \quad (2.40)$$

Thus one only needs to find the Fourier transform of the real-space potential. For the Coulomb interaction potential, $V_q \sim 1/q$. However, in practice, a second-quantized form is more effective because the exact forms of wave functions are extremely sensitive to the geometry and boundary conditions of the system. Numerical calculations normally require a second-quantized basis. Furthermore, the intrinsic physics of FQH phases are relevant to the electrons within a single LL, so it is reasonable to project everything to this specific LL. Note that usually,

this requires a high-field limit, which will restrict all the electrons to the lowest LL. But the mathematical procedure of mapping the Hilbert space to *any* single LL is still well-defined. This projection can significantly decrease the size of the Hilbert space, but to keep all the dynamical information, the infinite dimension of the Hilbert space will transform into the infinite number of effective many-body interactions, i.e.

$$\hat{H}(\hat{a}^\dagger, \hat{a}, \hat{b}^\dagger, \hat{b}) \implies \hat{H}_{\text{eff}}(\hat{b}^\dagger, \hat{b})$$

Infinitely large Hilbert space \implies Single LL

Coulomb interaction \implies Effective many-body interactions

Once a gauge is chosen with the corresponding boundary conditions, one can determine the single-particle orbitals and construct the second-quantized basis. In the following part, we will assume rotational invariance for the system and focus on the LLL to show how to deal with the two-body model Hamiltonians. Then we will use three-body interactions as an example to introduce how the effective many-body interactions arise from LL projection [203].

2.4.1 Two-body case

With rotational invariance, we can second-quantize the density operators as:

$$\hat{\rho}_q = \sum_{n_1 n_2, m_1 m_2} \langle n_1, m_1 | e^{i q_a \hat{r}^a} | n_2, m_2 \rangle \hat{c}_{n_1 m_1}^\dagger \hat{c}_{n_2 m_2} \quad (2.41)$$

where n_i denotes the LL indices, and m_i is the angular momentum quantum number. Here we shall introduce a formula that will be very commonly used in our discussions: Given two quantum numbers $A \geq B$, and the corresponding quantum states are denoted as $|A\rangle$ and $|B\rangle$. The matrix element of the corresponding ladder operators that fulfill $[\hat{a}, \hat{a}^\dagger] = 1$ is given by

$$P_{AB}(k) \equiv \left\langle A \left| e^{\frac{i}{\sqrt{2}} k \cdot \hat{a}^\dagger} \cdot e^{\frac{i}{\sqrt{2}} k^* \cdot \hat{a}} \right| B \right\rangle = \sqrt{\frac{A!}{B!}} \cdot \left(\frac{i}{\sqrt{2}} k \right)^{A-B} \cdot L_B^{(A-B)} \left(\frac{|k|^2}{2} \right) \quad (2.42)$$

where $L_n^{(\alpha)}(x)$ denotes the generalized Laguerre polynomials, defined by:

$$L_n^{(\alpha)}(x) = \sum_{i=0}^n (-1)^i \cdot \binom{n+\alpha}{n-i} \cdot \frac{x^i}{i!} \quad (2.43)$$

In fact, this result has been used in the former case study of calculating the matrix element of a δ -potential. Note that normal ordering has been assumed here. In the lowest LL, $n_1 = n_2 = 0$, only the guiding center degrees of freedom are relevant. The corresponding matrix element can be written as:

$$\begin{aligned} \langle 0, m_1 | e^{iq_a \hat{r}^a} | 0, m_2 \rangle &= \left\langle 0 \left| e^{iq_a \hat{\bar{R}}^a} \right| 0 \right\rangle \cdot \left\langle m_1 \left| e^{iq_a \hat{\bar{R}}^a} \right| m_2 \right\rangle \\ &= F_0(q) \cdot \left\langle m_1 \left| e^{iq_a \hat{\bar{R}}^a} \right| m_2 \right\rangle \end{aligned} \quad (2.44)$$

where we have defined the form factor $F_n(q) \equiv \left\langle n \left| e^{iq_a \hat{\bar{R}}^a} \right| n \right\rangle$, given by a Laguerre-Gaussian function of q in an isotropic system as shown in Eq.(2.42). Thus the density operators projected to the LLL are given by:

$$\hat{\rho}_q^{\text{LLL}} = F_0(q) \sum_{m_1 m_2} \left\langle m_1 \left| e^{iq_a \hat{\bar{R}}^a} \right| m_2 \right\rangle \hat{c}_{0m}^\dagger \hat{c}_{0n} = F_0(q) \cdot \hat{\rho}_q \quad (2.45)$$

so a generic two-body interaction in the LLL can be written as:

$$\hat{H}^{\text{2bdy}} = \int \frac{d^2 q}{(2\pi)^2} V_q^0 \hat{\rho}_q \hat{\rho}_{-q} = \sum_{i < j} \int \frac{d^2 q}{(2\pi)^2} V_q^0 e^{iq_a (\hat{\bar{R}}_i^a - \hat{\bar{R}}_j^a)} \quad (2.46)$$

where we have absorbed the form factor into the potential V_q^0 . We can further simplify this Hamiltonian by noticing that its only degree of freedom is the relative guiding center coordinate. Thus by defining the center of mass and the relative displacement of two guiding center coordinates:

$$\hat{R}_{i,j}^a = \frac{1}{\sqrt{2}} \left(\hat{\bar{R}}_i^a - \hat{\bar{R}}_j^a \right), \quad \hat{R}_{ij}^a = \frac{1}{\sqrt{2}} \left(\hat{\bar{R}}_i^a + \hat{\bar{R}}_j^a \right) \quad (2.47)$$

with the corresponding quantum number M and m , where the symmetric gauge has been used (the coefficients will change if a different gauge is adopted), we can rewrite the Hamiltonian as:

$$\hat{H}^{\text{2bdy}} = \sum_{M_1, M_2, m_1, m_2} \int \frac{d^2 q}{(2\pi)^2} V_q^0 \left\langle M_1, m_1 \left| e^{iq_a \hat{R}_{i,j}^a} \right| M_2, m_2 \right\rangle \hat{c}_{M_1, m_1}^\dagger \hat{c}_{M_2, m_2} \quad (2.48)$$

and define the ladder operators as:

$$\begin{cases} \hat{B}_{ij} = \frac{1}{\sqrt{2}} (\hat{b}_i + \hat{b}_j) \\ \hat{b}_{ij} = \frac{1}{\sqrt{2}} (\hat{b}_i - \hat{b}_j) \end{cases} \quad (2.49)$$

So the eigenstates can be expressed as:

$$|M, m\rangle = \frac{1}{\sqrt{M! \cdot m!}} (B_{ij}^\dagger)^M (\hat{b}_{ij}^\dagger)^m |\text{vac}\rangle \quad (2.50)$$

Thus the matrix element in the two-body Hamiltonian can be written as:

$$\langle M_1, m_1 | e^{iq_a \hat{R}_{i,j}^a} | M_2, m_2 \rangle = \delta_{M_1, M_2} \sqrt{\frac{m_1!}{m_2!}} \left(\frac{i}{\sqrt{2}} q \right)^{m_1 - m_2} L_{m_2}^{(m_1 - m_2)} \left(\frac{q^2}{2} \right) e^{-\frac{1}{2}q^2} \quad (2.51)$$

In a rotationally invariant system it will degenerate to $\delta_{M_1, M_2} \delta_{m_1, m_2} L_{m_1}(q^2) e^{-\frac{1}{2}q^2}$ because the angular momenta are conserved. In this case, considering the Laguerre-Gaussian functions make up a complete and orthogonal basis in the $L^2[0, \infty)$ space [268], we can expand the potential V_q^0 in the same basis as:

$$V_q^0 = c^m V_m^{\text{2bdy}} \quad (2.52)$$

where Einstein's summation has been adopted and we define $V_m^{\text{2bdy}} \equiv L_m(q^2) e^{-\frac{1}{2}q^2}$, so the coefficients c^m is given by:

$$c^m = \int d^2q V_q^0 L_m(q^2) e^{-\frac{1}{2}q^2} \quad (2.53)$$

which shows the physical significance of c^m as the energy cost of two particles with relative angular momentum m as illustrated in Fig.2.1. V_m^{2bdy} acts as projecting the states to the relative angular momentum m and it is also named as *Haldane pseudopotentials* [20].

Note that everything here can be generalized to higher LLs, different geometry, or topological manifolds, where a different form factor will be adopted, and the domain of angular momentum could be different. More importantly, these pseudopotentials bring enormous freedom for us to construct meaningful model Hamiltonians to study the FQH phases and define subspaces in the full Hilbert space (named as conformal Hilbert spaces as introduced in Chap.3). From this point of view, the

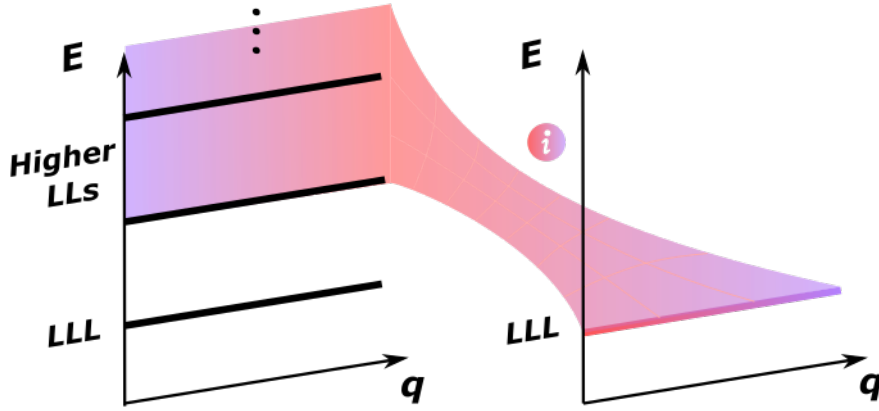


FIGURE 2.2: **LL projection.** To preserve the information from the higher LL, after the LL projection, effective many-body interactions have to be introduced.

Coulomb interaction can be regarded as nothing but a model Hamiltonian finely tuned by nature, whose coefficients are decreasing with m significantly so that we can numerically simulate the behavior of the Coulomb interaction with several leading pseudopotentials.

2.4.2 Three-body case

It is not hard to see *how* the two-body pseudopotentials can be appropriately generalized to many-body cases. But first, we need to understand *why* this is a meaningful generalization in physics. In other words, why does LL mixing induce effective many-body interactions in our Hamiltonian?

We can use the perturbation method to deal with the interactions. Thus the important quantity is the energy scale $\Delta = \frac{E_k}{E_{\text{int}}}$, which seemingly can always be fulfilled when the magnetic field is strong enough. However, in realistic materials, this could not be the case. A classical explanation is that when the magnetic field is stronger, the radii of the electron orbitals become smaller, so their decreasing distance will enhance the interactions between them. This process is proportional to the magnetic field as well. For example, in gallium arsenide (GaAs), $\Delta_{\text{GaAs}} \sim B$, so as long as the magnetic field is large enough, the perturbation method is reasonable to use. In comparison, for free-standing graphene $\Delta_{\text{graphene}} = \frac{e^2}{\varepsilon \hbar v_F} \sim 2.2$ thus irrelevant to the magnetic field, which is definitely too small to treat the interaction as perturbations [269, 270]. Note that the value of Δ_{graphene} can also

be influenced by the thickness (layer number) of the material, substrate variety, and suspension, so it usually takes some numerical simulations to get the results for graphene.

As a result, here we assume that Δ is sufficiently large for our theoretical discussion, which cannot be pushed to ∞ , though, because in that case, there will be no LL mixing at all. Considering that we are trying to project everything to a low-energy regime in the spectrum, the Schrieffer-Wolff (SW) transformation can serve the job (refer to Appendix.C for more details), which is a type of second-order perturbation operator method that acts as a rotation in the Hilbert space [203, 271, 272]. In practice, we are looking for an anti-Hermitian operator expanded as:

$$\hat{S} = \sum_{n=1}^{\infty} \hat{S}_n, \quad \hat{S}_n \sim O(\Delta^{-n}) \quad (2.54)$$

which gives the effective Hamiltonian in the low-energy regime (in our case, the lowest LL) as:

$$\hat{H}_{\text{eff}} = e^{\hat{S}} \hat{H} e^{-\hat{S}} = \hat{H} + [\hat{S}, \hat{H}] + \frac{1}{2} [\hat{S}, [\hat{S}, \hat{H}]] + \dots \quad (2.55)$$

After doing the perturbation order by order, one can see that effective many-body interactions arise. In other words, these interactions emerge to *compensate for the loss of information after LL projection* as shown in Fig.2.2. Based on the idea in the last section, now that we know how to derive the effective Hamiltonian from a given potential, it is also possible to construct three-body model Hamiltonians with exact physical significance. Here by assuming rotational invariance, we can reorganize the guiding center coordinates into commutative Jacobi coordinates (introduced in Appendix.D) to decrease degrees of freedom:

$$\begin{aligned} \hat{R}_{ij}^a &= \frac{1}{\sqrt{2}} \left(\hat{\bar{R}}_i^a - \hat{\bar{R}}_j^a \right) \\ \hat{R}_{ij,k}^a &= \frac{1}{\sqrt{6}} \left(\hat{\bar{R}}_i^a + \hat{\bar{R}}_j^a - 2\hat{\bar{R}}_k^a \right) \\ \hat{R}_{ijk}^a &= \frac{1}{\sqrt{3}} \left(\hat{\bar{R}}_i^a + \hat{\bar{R}}_j^a + \hat{\bar{R}}_k^a \right) \end{aligned} \quad (2.56)$$

Without loss of generality, we will set $\{i, j, k\} = \{1, 2, 3\}$ in the following discussions. Thus the ladder operators can be defined as:

$$\begin{cases} \hat{b}_1^\dagger = \frac{1}{\sqrt{2}} \left(\hat{R}_{12}^x + i\hat{R}_{12}^y \right) \\ \hat{b}_1 = \frac{1}{\sqrt{2}} \left(\hat{R}_{12}^x - i\hat{R}_{12}^y \right) \end{cases}, \quad \begin{cases} \hat{b}_2^\dagger = \frac{1}{\sqrt{2}} \left(\hat{R}_{12,3}^x + i\hat{R}_{12,3}^y \right) \\ \hat{b}_2 = \frac{1}{\sqrt{2}} \left(\hat{R}_{12,3}^x - i\hat{R}_{12,3}^y \right) \end{cases} \quad (2.57)$$

As usual, we have $[\hat{b}_1, \hat{b}_1^\dagger] = [\hat{b}_2, \hat{b}_2^\dagger] = 1$. The corresponding quantum numbers are denoted by m_1 and m_2 , with the differences

$$\Delta m_1 = m'_1 - m_1, \quad \Delta m_2 = m'_2 - m_2 \quad (2.58)$$

where the quantum number m_1 denotes the relative momentum between the first and the second electron, and m_2 represents the relative momentum between the center-of-mass of the first two electrons and the third one. Note that m_1 can only be odd due to the fermionic statistics. If there is a rotational invariance, we will always have $\Delta m_1 = -\Delta m_2$.

It is convenient to take a non-isometric basis transformation of the momenta to write down the Hamiltonian in a more compact way:

$$\tilde{\mathbf{q}}_1 = \frac{1}{\sqrt{2}} (\mathbf{q}_1 - \mathbf{q}_2), \quad \tilde{\mathbf{q}}_2 = \sqrt{\frac{3}{2}} (\mathbf{q}_1 + \mathbf{q}_2) \quad (2.59)$$

Thus:

$$\mathbf{q}_1 = \frac{1}{\sqrt{2}} \tilde{\mathbf{q}}_1 + \frac{1}{\sqrt{6}} \tilde{\mathbf{q}}_2, \quad \mathbf{q}_2 = -\frac{1}{\sqrt{2}} \tilde{\mathbf{q}}_1 + \frac{1}{\sqrt{6}} \tilde{\mathbf{q}}_2 \quad (2.60)$$

To turn the integral over \mathbf{q}_1 and \mathbf{q}_2 to the one over $\tilde{\mathbf{q}}_1$ and $\tilde{\mathbf{q}}_2$, we can work out the Jacobian as $J = \frac{1}{3}$, which transforms the three-body translationally invariant Hamiltonian into:

$$\hat{H}^{\text{3bdy}} = \int d^2 \tilde{q}_1 d^2 \tilde{q}_2 V_{q_1 q_2} e^{i\tilde{q}_1 a \hat{R}_{12}^a} e^{i\tilde{q}_2 a \hat{R}_{12,3}^a} \quad (2.61)$$

where we have absorbed the constant coefficients and the terms relevant to the center of mass into $V_{q_1 q_2}$. After mapping everything to \mathbb{C} , the regularized momentum can be defined as:

$$\mathbf{q} = \frac{1}{\sqrt{2}} |\tilde{\mathbf{q}}_1| \cdot e^{i\tilde{\theta}_1}, \quad \mathbf{q}' = \frac{1}{\sqrt{2}} |\tilde{\mathbf{q}}_2| \cdot e^{i\tilde{\theta}_2} \quad (2.62)$$

For a three-electron rotationally invariant state $|\psi_3\rangle$ with the conserved center of mass angular momentum in the magnetic field can be expanded with the complete basis $|m_1, m_2\rangle$:

$$|\psi_3\rangle = \sum_{m_1, m_2} \alpha^{m_1, m_2} |m_1, m_2\rangle \quad (2.63)$$

where the expansion coefficients α^{m_1, m_2} can be explicitly derived. Thus we can find the matrix element of the three-body Hamiltonian on this basis:

$$\begin{aligned} \langle m_1, m_2 | e^{i\tilde{q}_{1a}\hat{R}_{12}^a} e^{i\tilde{q}_{2a}\hat{R}_{12,3}^a} | m'_1, m'_2 \rangle &= \sqrt{\frac{m_1! \cdot m_2!}{m'_1! \cdot m'_2!}} (i\mathbf{q})^{\Delta m_1} (i\mathbf{q}')^{\Delta m_2} \\ &\cdot L_{m_1}^{(\Delta m_1)}(|\mathbf{q}|^2) L_{m_2}^{(\Delta m_2)}(|\mathbf{q}'|^2) e^{-\frac{1}{2}(|\mathbf{q}|^2 + |\mathbf{q}'|^2)} \end{aligned} \quad (2.64)$$

This inspires us to define the three-body model Hamiltonians by expanding $V_{q_1 q_2}$ in the complete and orthogonal generalized Laguerre-Gaussian basis:

$$V_{q_1 q_2} = c^{m_1 m_2 \Delta m_1 \Delta m_2} \cdot V_{m_1 m_2 \Delta m_1 \Delta m_2} \quad (2.65)$$

where we have defined $V_{m_1 m_2 \Delta m_1 \Delta m_2} \equiv L_{m_1}^{(\Delta m_1)}(|\mathbf{q}|^2) L_{m_2}^{(\Delta m_2)}(|\mathbf{q}'|^2) e^{-\frac{1}{2}(|\mathbf{q}|^2 + |\mathbf{q}'|^2)}$, and normally we only use the components with $\Delta m_1 = \Delta m_2 = 0$. In this case, we can write down the model Hamiltonian as follows:

$$V_{q_1 q_2} = c^{m_1 m_2} \cdot V_{m_1 m_2} = c^{m_1 m_2} L_{m_1}^{(0)}(|\mathbf{q}|^2) L_{m_2}^{(0)}(|\mathbf{q}'|^2) e^{-\frac{1}{2}(|\mathbf{q}|^2 + |\mathbf{q}'|^2)} \quad (2.66)$$

As for a given potential \tilde{V} , the expansion coefficients are given by the associated inner product defined in the Segal–Bargmann space [273]:

$$c^{m_1 m_2} = \int d\mathbf{q} d\mathbf{q}' \tilde{V} \cdot L_{m_1}^{(0)}(|\mathbf{q}|^2) L_{m_2}^{(0)}(|\mathbf{q}'|^2) e^{-\frac{1}{2}(|\mathbf{q}|^2 + |\mathbf{q}'|^2)} \quad (2.67)$$

In practice, it is also reasonable to label the three-body pseudopotentials with total relative angular momentum defined by $\alpha = m_1 + m_2$, which gives:

$$V_{q_1 q_2} = c^\alpha V_\alpha^{\text{3bdy}} \quad (2.68)$$

One can freely choose the coefficients c^α to construct different model Hamiltonians.

Generically speaking, we can mathematically generalize this to the interaction among an arbitrary number of particles. However, it is not very significant in

physics because (i) the many-body part in the Coulomb interaction expansion becomes less and less critical, and (ii) the many-body model Hamiltonians are hard to be realized in experiments. Therefore, in the following parts of this thesis, we will focus on the two-body and the three-body model Hamiltonians.

Chapter 3

Conformal Hilbert Space and Composite Fermionization

This chapter will introduce the relationship between the conformal field theory (CFT) and FQH phases. First, we will start with a very brief recap of CFT without proofs, especially those relevant to FQHE, and then discuss why two-dimensional CFT can be related to FQH phases, which also gives rise to the concept of conformal Hilbert space (CHS). Afterward, we will rigorously define the isomorphism between different CHSs with analytic number theory, leading to a rigorous interpretation of composite fermionization from unitary mappings between isomorphic CHSs.

3.1 CFT: the theoretical minimum

Instead of providing a thorough introduction to the concepts in CFT (which, in fact, can be written as a thesis itself), below, we will only mention the jargon we need for our later discussions on the application of CFT in FQHE. Further explanations can be found in Refs.[25, 274–276], which cover far more than the contents we discuss here.

CFT is a species of field theories with conformal symmetry, which means that they are invariant under conformal transformation given by:

$$g'_{\mu\nu}(x') = \Omega(x)g_{\mu\nu}(x) \quad (3.1)$$

where $\Omega(x)$ is the scale factor. Thus the metric $g_{\mu\nu}$ remains invariant up to a scale, which indicates that the angles between any two vectors on the (semi-Riemannian) manifold will not be changed by conformal transformations. Historically, conformal symmetry was found to exist in two-dimensional (2D) critical phenomena, such as the 2D Ising model, which can be solved by 2D CFT [277]. This is not surprising, though, because of the scale invariance at the critical point. One of the most exciting applications of CFT is in the string theory, where the Polyakov action that describes the time evolution of strings is found to be conformally invariant so that it can be studied using 2D CFT [278]. Furthermore, the duality between a gravitational theory and a conformal field theory was discovered by Maldacena, named AdS/CFT correspondence [279], which can also be generalized to condensed matter systems [280, 281].

The corresponding Lie group of global conformal transformations is naturally named a conformal group, which contains the Poincaré group as its proper subgroup (with $\Omega(x) = 1$). The associated Lie algebra of the generators is given by:

$$[J_{mn}, J_{pq}] = i(\eta_{mq}J_{np} + \eta_{np}J_{mq} - \eta_{mp}J_{nq} - \eta_{nq}J_{mp}) \quad (3.2)$$

where η_{mn} denotes the metric. We use $L_{\mu\nu}$, P_μ , K_μ and D to denote the generator of rotation, translation, special conformal transformation, and dilation respectively:

$$J_{\mu,\nu} \equiv L_{\mu\nu}, \quad J_{-1,\mu} \equiv \frac{1}{2}(P_\mu - K_\mu), \quad J_{0,\mu} \equiv \frac{1}{2}(P_\mu + K_\mu), \quad J_{-1,0} \equiv D \quad (3.3)$$

Things get intriguing in the 2D case because the algebra of (local) conformal transformations turns out to be infinite-dimensional [274]. Thus many correlation functions become solvable because of the infinite restrictions one can impose. Moreover, from mathematics, we know that these conformal transformations in \mathbb{R}^2 can be described by locally invertible holomorphic or antiholomorphic functions in \mathbb{C} . Thus it is helpful to transform everything into complex coordinates by defining the following:

$$\begin{aligned} z &\equiv x^0 + ix^1, & \partial_z &\equiv \frac{1}{2}(\partial_0 - i\partial_1) \\ \bar{z} &\equiv x^0 - ix^1, & \partial_{\bar{z}} &\equiv \frac{1}{2}(\partial_0 + i\partial_1) \end{aligned} \quad (3.4)$$

where $\partial_i = \partial/\partial x^i$. We can write down the infinitesimal conformal generators as:

$$\ell_n = -z^{n+1}\partial_z, \quad \bar{\ell}_n = -\bar{z}^{n+1}\partial_{\bar{z}}, \quad (3.5)$$

where $n \in \mathbb{Z}$ and the generators with $|n| \leq 1$ correspond to global conformal transformations (they are exactly the 2D version of Eq.(3.3)), the group of which is thus only finite-dimensional. In comparison, the local conformal transformations do not form a group but an infinite-dimensional Lie algebra. The algebra of all the infinitesimal generators in Eq.(3.5) is called the *Witt algebra*, given by:

$$[\ell_n, \ell_m] = (n - m)\ell_{n+m}, \quad [\bar{\ell}_n, \bar{\ell}_m] = (n - m)\bar{\ell}_{n+m}, \quad [\ell_n, \bar{\ell}_m] = 0 \quad (3.6)$$

which is equivalent to the diffeomorphism group on S^1 . But in quantum field theory, we normally need a projective representation. By adding central extension terms to this infinite-dimensional algebra, we can get such a representation of the conformal group, called the *Virasoro algebra*:

$$\begin{aligned} [L_m, L_n] &= (m - n)L_{m+n} + \frac{c}{12}(m^3 - m)\delta_{m+n,0} \\ [\bar{L}_m, \bar{L}_n] &= (m - n)\bar{L}_{m+n} + \frac{c}{12}(m^3 - m)\delta_{m+n,0} \\ [L_m, \bar{L}_n] &= 0 \end{aligned} \quad (3.7)$$

where the *central charge* $c \in \mathbb{C}$. From the physical point of view, the Virasoro algebra is the quantized version of the Witt algebra, because the central extension term comes from the ambiguity of operator ordering, although we only need the Jacobi identity to derive this expression without invoking any physics. Under global conformal transformations $z \rightarrow w$ and $\bar{z} \rightarrow \bar{w}$, a generic field could have a quite complicated form, so an important type of field ϕ is defined as the one with a specific simple behavior:

$$\phi'(w, \bar{w}) = \left(\frac{dw}{dz}\right)^{-h} \left(\frac{d\bar{w}}{d\bar{z}}\right)^{-\bar{h}} \phi(z, \bar{z}) \quad (3.8)$$

and these fields are called *quasi-primary fields*. Here h and \bar{h} are named as *conformal dimensions*, given by the linear combination of the scaling dimension Δ and the spin s :

$$h = \frac{1}{2}(\Delta + s), \quad \bar{h} = \frac{1}{2}(\Delta - s) \quad (3.9)$$

which together with the central charge can determine a unique unitary highest-weight representation of the Virasoro algebra $W(c, h)$ or $\bar{W}(c, \bar{h})$. All the relevant fields in a CFT can be expressed as the linear combination of the quasi-primary fields and their derivatives. Moreover, within the quasi-primary fields, it is possible

to find some of them that transform as in Eq.(3.8) under *any* conformal transformations, and these fields are called *primary fields*. These fields are related to the highest weight representations of the Virasoro algebra, where the highest weight states $|h, \bar{h}\rangle$ are strictly annihilated by the lowering operators $L_{n \geq 1}$:

$$L_0|h, \bar{h}\rangle = h|h, \bar{h}\rangle, \quad \bar{L}_0|h, \bar{h}\rangle = \bar{h}|h, \bar{h}\rangle; \quad \forall n \geq 1, L_n|h, \bar{h}\rangle = 0 \quad (3.10)$$

and these highest-weight states are exactly created by primary fields. Here the generators with $n \leq -1$ are called lowering operators, and one can apply them to $|h, \bar{h}\rangle$ to generate a series of *descendent states* $L_{-n_1} \cdots L_{-n_k} |h, \bar{h}\rangle$. Each primary field together with its descendent states called a *conformal family*, which is apparently closed under conformal transformations as an irreducible representation (irrep) of the Virasoro algebra, and as we shall see in the following section, this important property gives rise to the concept of CHSs.

The conformal families can also lead to the so-called *state-operator correspondence* in radial quantization, where the N -point correlators of descendent states can be written down with the N -point correlators of the corresponding primary states, which can be expanded by the *conformal blocks* given by solving conformal Ward identities, and the critical behaviors of which are depicted by the *operator product expansions* (OPE) encoding the fusion rules of the fields.

3.2 CFT approach to FQHE

The earliest application of CFT in FQHE was carried out by Moore and Read in 1991 [93]. Back then they observed the formal similarities between the model wave functions of FQH states and some correlators (conformal blocks) in 2D CFT. More importantly, based on this observation they predicted a new FQH phase with non-Abelian quasiparticles, which is named the Moore-Read (MR or Pfaffian) state nowadays. The MR state is the candidate of the FQH state at the filling factor with an *even* denominator. This implies that the physics in this phase should be totally different from the Laughlin states. In this section, we would like to introduce the procedure to write down the CFT correlators for FQH states and their applications to both the bulk and the edge of FQH droplets. In particular, we will discuss the seeming paradox, i.e. *why CFT can be used in these incompressible states with a*

length scale set by ℓ_B even if the conformal symmetry requires a scale invariance (given by the dilation generator D as defined in Eq.(3.3)), and whether this CFT description is always valid.

Let us briefly review the equivalence between certain FQH model wave functions and CFT correlators: We can rewrite a wave function, which is a holomorphic polynomial of the electron coordinates z_i , to a conformal block given by the correlation of fields (or vertex operators) $F(z_i)$:

$$\Psi(\{z_i\})_{\text{FQH}} \propto \left\langle \prod_i F(z_i) \right\rangle_{\text{CFT}} \quad (3.11)$$

where $F(z_i)$ is the product of simple currents [25]) and bosonic fields. Apparently, there is a one-to-one correspondence between the electrons and the fields. This can be easily generalized to the states with quasiholes excitations by defining another field H for the quasiholes at h_i (the OPE of which should obey $F(z)H(h) \sim (z - h)^l H'$, $l \geq 0$ to ensure that the braiding between quasiholes and electrons is trivial):

$$\Psi(\{h_i\}, \{z_i\})_{\text{FQH-qh}} \propto \left\langle \prod_i H(h_i) \prod_j F(z_j) \right\rangle_{\text{CFT}} \quad (3.12)$$

The CFT corresponding to different FQH phases can be quite different with respect to their unitarity and rationality, but there is always a $U(1)$ chiral subalgebra corresponding to the electric charge. We can take the simplest case, the Laughlin state at the filling factor $\nu = 1/m$ as our first example:

$$\begin{aligned} \Psi_m(\{z_i\}) &= \prod_{1 \leq i < j \leq N_e} (z_i - z_j)^m \exp \left(- \sum_i \frac{|z_i|^2}{4} \right) \\ &= \left\langle \left(\prod_{i=1}^{N_e} \underbrace{\mathrm{e}^{\mathrm{i}\sqrt{m}\varphi(z_i)}}_{F(z_i)} \right) \exp \left(- \int d^2 z' \sqrt{m} \rho_0 \varphi(z') \right) \right\rangle \end{aligned} \quad (3.13)$$

where $\rho_0 = 1/(2\pi m)$ and the normal ordering notations have been omitted. As we can see, apart from the vertex operators with $U(1)$ charge m , we also need a background charge operator, which reminds us of the plasma analogy [19, 282], and we can understand it from two aspects: (i) Technically speaking, if we only include the vertex operators in the correlator, the final result will just vanish. (ii) Physically speaking, the correlator we consider are with respect to the vacuum, which leads to an important condition called *charge neutrality*, so the background

charge operators are here to balance the electric charge of the electrons to fulfill this condition [283].

Then by properly defining the quasi-hole operator, we can write down the corresponding wave function for quasi-hole states. For clarity, let us add a single quasi-hole to the Laughlin state and write down the wave function with the equivalent CFT correlator by:

$$\begin{aligned}\Psi_m^{\text{qh}}(h; \{z_i\}) &= \prod_{j=1}^{N_e} (z_i - h) \Psi_m(\{z_i\}) \\ &= \underbrace{\left\langle \exp\left(\frac{i}{\sqrt{m}}\varphi(z_0)\right) \left(\prod_{i=1}^{N_e} e^{i\sqrt{m}\varphi(z_i)} \right) \exp\left(-\int d^2 z' \sqrt{m} \rho_0 \varphi(z')\right) \right\rangle}_{H(h)}\end{aligned}\quad (3.14)$$

Note that the ratio between the $U(1)$ charge of the electrons and the quasiholes is m , which indicates that the quasi-hole excitations have *fractional charge* ($U(1)$ charges are proportional to the electric charges), and more H operators can be inserted to the correlator for the FQH states with more quasiholes. This formalism can be generalized to multi-component states and non-abelian states, but we will not explicitly show their wave functions here [284]. Furthermore, the Z_2 simple charge of CFT operators is essential for the single-valuedness of FQH wave functions, and the monodromy charge of the operators is important for braiding or modular property [285–287].

Another important insight from CFT is the understanding of the edge states and especially the relationship between the bulk and the edge of FQH droplets. Obviously, the edge excitations should be described by a $1 + 1$ D theory, and Wen first proposed that they are essentially chiral Luttinger liquids [83]. Later on, people also found that it is naturally possible to use different 2D CFTs (with perturbations) to describe the edge states of different FQH states, and they should share the same counting patterns in the L_z sectors, which also matters for defining CHSs as introduced in the next section [284]. Meanwhile, inspired by the famous holographic principle in high energy physics, the bulk-edge correspondence in condensed matter systems (especially the topological phases) was also found, which allows us to study the bulk via the same CFT model at the edge. More importantly, some relevant quantities can be calculated even in a system without an edge, such as the entanglement entropy [214–218], and the entanglement spectrum [175, 221], which

only requires that the system (thus the Hilbert space and the eigenstates $|\Psi\rangle$) is separated into two parts A and B virtually in the real space or in the guiding center orbitals:

$$|\Psi\rangle = \sum_i e^{-\xi_i/2} |\psi_A^i\rangle \otimes |\psi_B^i\rangle \quad (3.15)$$

where the entanglement spectrum consists of the values of ξ_i , and they can capture exactly the same properties of the corresponding CFT as well. All of these show that the CFT description of the FQH states is not just a coincidence but should be regarded as *a valid description of the physics* in these states.

Now if we look back, the formal similarities between the FQH wave functions and conformal blocks in CFT seem too superficial to explain the reason why CFT can apply so well to the FQH phases. The first point we should make is that, generically speaking, an FQH phase is a *gapless* system (especially in experiments), because of the existence of edge excitations. But to better understand this, we need to mention the relation between CFT and the low-energy effective field theory that describes the FQH states, which has been shown to be a Chern-Simons (CS) theory [77] because the action should be a local one with gauge invariance in bulk (and preferably rotational invariance), but without parity and time reversal symmetry, given by:

$$S_{CS}[A] = \frac{k}{4\pi} \int d^3x \epsilon^{\mu\nu\rho} A_\mu \partial_\nu A_\rho \quad (\text{Laughlin state at } \nu = 1/k) \quad (3.16)$$

where k is the level of this action (which is directly related to the filling factor in this context) and A is *another* gauge field in addition to the one that describes the external magnetic field, which should not change the existing FQH phase of the system [77]. Intuitively speaking, we are discussing the perturbation from some FQH phase or “plateau” by using the CS theory instead of reconstructing the whole system with some quantum field.

The topological feature of this action can be easily found in the lack of a metric tensor because there is only a Levi-Civita pseudotensor $\epsilon^{\mu\nu\rho}$ balancing the indices, which means that it is not sensitive to the geometric properties of the space-time manifold. As a result, the Hamiltonian (or the stress-energy tensor) vanishes, so there are no dynamical degrees of freedom in such a system (but in fact, there can exist dynamics of emergent gauge fields). Although the CS theory has trivial

dynamics, it can successfully predict the robustness of plateaus in the Hall resistivity and describe the anyons with fractional statistics [77]. Furthermore, the gauge invariance will be destroyed at the edge, leading to unconserved currents, the offset of which exactly corresponds to the gapless chiral edge currents in FQH phases. The incompressibility of FQH phases also plays a pivotal role in why CS theory can describe them in the low-energy regime (which we usually care about), which is equivalent to setting the energy scale to either zero or infinity in the system. In this case, only the topological degrees of freedom can influence the system.

Now we have known that CS theory provides the low-energy description of FQH phases. The general relation between CFT and CS theory was noticed by Witten when studying the $2+1$ D Yang-Mills theory (whose action is of the Chern-Simons type) [92]. To canonically quantize the Chern-Simons theory on $\Sigma \times R^1$ and get the corresponding Hilbert space \mathcal{H} , where the (space) surface Σ is oriented and smooth and R^1 represents the time dimension, one can add a complex structure \mathbb{C} on Σ to make it Riemannian. Meanwhile the outcome \mathcal{H}_Σ should not be influenced by the specifically chosen \mathbb{C} but only by Σ , which means that \mathcal{H}_Σ is a *flat* vector bundle on the moduli space of Σ . Such an algebraic structure was found in CFT when Segal was looking for the space of conformal blocks from the Ward identities [288]. Thus Witten was acutely aware of the equivalence between the Hilbert space \mathcal{H}_{CS} of a quantized CS theory and the space of conformal blocks (Moore and Read explained why using CFT to study FQH is reasonable based on this point [93]). So the full relation between the FQH phase, CS theory, and CFT can be illustrated as follows:

$$\begin{array}{ccc} \text{FQH phase} & \xrightarrow[\text{Low-energy}]{\text{Coarse-graining}} & \text{CS action} \\ (\text{Particles}) & & (\text{Sources}) \end{array} \xrightarrow[\mathcal{H}_{\text{CS}}]{\text{Quantized}} \begin{array}{c} \text{Vector space of} \\ \text{conformal blocks} \\ (\text{Fields}) \end{array}$$

This relation reveals *when* we can properly establish a mapping between FQH states and CFTs. In the next section, we will introduce *how* to explicitly make connections between them.

Besides giving the wave functions of FQH states by using CFT, Moore and Read also proposed several conjectures about the relationship between FQHE and CFT, which can serve as a nice wrap-up for the content in this section [284]:

“Representative wave functions for quantum Hall ground states, as well as their quasi-hole excitations, can be expressed in terms of conformal blocks of primary fields in (rational, unitary) CFTs. The holonomies, or statistical braiding matrices, equal the monodromies of these blocks. Furthermore, the same CFTs yield a minimal dynamical theory for the edge of the quantum Hall liquid.”

3.3 Conformal Hilbert spaces

In the last section, we have introduced the nontrivial relationship between FQH states and 2D CFT correlators. Now, let us see how to construct a Virasoro algebra in the Hilbert space of FQH states.

To work in the low-energy regime, a natural way is to set up a Hamiltonian and get the corresponding null space. Based on Chap.2, we know that model Hamiltonians can be defined for some (but not all) FQH states, so here, we can use them to construct the algebra. These null spaces consist of the ground state(s) and all the quasi-hole states, so they can also be regarded as quasi-hole manifolds with the metric induced by the inner product (the case of non-unitary CFT is not considered here for now). Furthermore, if rotational invariance is present, we can use angular momentum to index single particle orbitals, and the null spaces can be automatically separated into different L_z sectors with well-defined ladder operators. Given the electron number N_e and the orbital number N_o , we can construct the representations (of the compact $\mathfrak{su}(2)$ algebra) from the highest weight state. A similar routine can be found in CFT. For example, a Verma module can be derived in the same manner. By using the raising operators on the highest weight state created by the primary field in every possible way, one can generate all the descendent states and thus the whole representation after truncating the null states. The proper way to construct the Virasoro-like generators in the null space \mathcal{H} of rotationally invariant model Hamiltonians has been proposed [139]:

$$\hat{L}_{-n} = \sum_{k=0}^{\infty} g(k+n, k) \cdot \hat{c}_{k+n}^\dagger \hat{c}_k, \quad \hat{L}_n = \sum_{k=0}^{\infty} g(k, k+n) \cdot \hat{c}_k^\dagger \hat{c}_{k+n} \quad (3.17)$$

where the fermionic operators fulfills $\{c_i, c_j^\dagger\} = \delta_{ij}$, $\{c_i, c_j\} = \{c_i^\dagger, c_j^\dagger\} = 0$ and $g(a, b)$ is the normalization factor influenced by the geometry, which leads to different orbital indices. The algebra of these generators is given by:

$$[\hat{L}_m, \hat{L}_{-n}] = (n - m)\hat{L}_{m+n} + \hat{C}_{m,n} \quad (3.18)$$

where the central charge operator is:

$$\hat{C}_{m,n} = \begin{cases} \sum_{k=0}^{m-1} g(k, k + \Delta) \cdot (k - m) \cdot \hat{c}_k^\dagger \hat{c}_{k+\Delta}, & n \geq m \\ \sum_{k=0}^{n-1} g(k + \Delta, k) \cdot (k - n) \cdot \hat{c}_{k+\Delta}^\dagger \hat{c}_k, & n \leq m \end{cases} \quad (3.19)$$

However, the requirements for the primary state ϕ_h , in this case, have to be adjusted a little bit because generically $\hat{L}_n \phi_h$ does not vanish when $n > 0$, which will instead give an excited state outside the null space $\bar{\mathcal{H}}$. As long as we can make sure that (i) all the descendant states are within \mathcal{H} , and (ii) acting $\hat{C}_{m,n}$ or all the lowering operators on the highest weight state will generate a state in $\bar{\mathcal{H}}$, the Virasoro algebra will be strictly obeyed within \mathcal{H} , which means that we do have a conformal symmetry in these sub-Hilbert spaces defined by the model Hamiltonians. Hence we can define these null spaces (or quasi-hole manifolds) as the *conformal Hilbert spaces* (CHSs).

In principle, each model Hamiltonian defines a CHS, which can provide valuable insights into the structure of the full Hilbert space and the relations between different FQH states for us. In the following parts, we shall see that some of the CHSs can be very similar to each other even if they are defined by different model Hamiltonians, which in turn implies that there could exist a mapping between the states within them, so one can discuss almost the same physics in totally different contexts.

3.4 Isomorphism of conformal Hilbert spaces

From the last section, we know that in the full Hilbert space of FQH phases (which could be a single LL), we can find many CHSs defined by different model Hamiltonians. We want to figure out whether some nontrivial relations exist between these spaces, which, in this section, will be shown to be true. We will specifically focus

on describing the *similarities* among these spaces by defining the isomorphism between different CHSs from the generating function of the L_z sector degeneracies. This idea can be extended to the FQH phases with anyonic quasi-hole excitations and even bosonic FQH phases. As the next section explains, the upshot can provide a rigorous reinterpretation of the CF theory.

3.4.1 Partition

We will first review some relevant analytic number theory concepts and try to balance intuition and rigor. Then the application of the essential conclusions to analyzing the L_z sector degeneracy and the corresponding highest-weight (HW) state degeneracy will be given in the following parts.

For any positive integer n , it is always possible to decompose it into several *positive* integers. For example, 3 can be written as $3 = 1 + 2 = 1 + 1 + 1$, so there are 3 different ways to decompose it. Each decomposition of the integer n is called a *partition* of n , and the numbers inside a decomposition are called *parts*. Thus for the former example, we have three partitions for the number 3: $\{3\}$, $\{1, 2\}$, and $\{1, 1, 1\}$. In the partition $\{1, 2\}$, 1 and 2 are both the parts. Normally the partition number of 0 is defined to be one. Then we can give the rigorous definition of partition and partition number as follows:

Definition 3.1 (Partition). A partition of $n \in \mathbb{Z}_+$ is a finite non-increasing sequence including n_1 parts of 1, n_2 parts of 2, n_3 parts of 3, \dots , n_k parts of k such that $\sum_k k \cdot n_k = n$, where $\forall k, n_k \in \mathbb{Z}_+$.

Definition 3.2 (Partition number). The total number of different partitions of a non-zero integer n is called a *partition number*, denoted by $p(n)$ without any restrictions, or $p(n|\mathcal{R})$ with additional restrictions. Here \mathcal{R} denotes the set of all the restrictions to the partitions of k .

One of the core problems in the partition theory is to give the exact value of the partition numbers of an arbitrary integer n , the formula of which has been provided by a convergent infinite series [289, 290]. Nowadays, efficient algorithms have been developed to calculate the partition numbers for a given integer. Moreover, the visualized method can also be used for solving the partition numbers, such as Durfee squares, Ferrers diagrams, and Young diagrams, which are especially useful

k	p(k)	1	2	3	4	5	6	7	8	9	10	11	12	...
0	1	1	0	0	0	0	0	0	0	0	0	0	0	...
1	1	1	0	0	0	0	0	0	0	0	0	0	0	...
2	2	1	1	0	0	0	0	0	0	0	0	0	0	...
3	3	1	1	1	0	0	0	0	0	0	0	0	0	...
4	5	1	2	1	1	0	0	0	0	0	0	0	0	...
5	7	1	2	2	1	1	0	0	0	0	0	0	0	...
6	11	1	3	3	2	1	1	0	0	0	0	0	0	...
7	15	1	3	4	3	2	1	1	0	0	0	0	0	...
8	22	1	4	5	5	3	2	1	1	0	0	0	0	...
9	30	1	4	7	6	5	3	2	1	1	0	0	0	...
10	42	1	5	8	9	7	5	3	2	1	1	0	0	...
11	56	1	5	10	11	10	7	5	3	2	1	1	0	...
12	77	1	6	12	15	13	11	7	5	3	2	1	1	...
:	:	:	:	:	:	:	:	:	:	:	:	:	:	...

TABLE 3.1: **Integer partition numbers $p(k)$ and $p(k|i)$** (denoted by the corresponding integers in the first row for simplicity). Here i means that there are i parts in the partitions of integer k .

in combinatorics [291]. However, it is not hard to imagine that when the integer n gets larger and larger, any method of calculating the partition number of n will be more and more time-consuming and eventually fail to answer within a limited or meaningful time. Moreover, even a simple restriction to the parts (for example, all the parts are required to be different from each other, or there must be i parts in each partition, as Table 3.1 shows) can bring enormous complexity to the derivation of the exact formula for the partition numbers. In fact, studying the degeneracy of the L_z sectors or the highest-weight states in the Hilbert space of an FQH system does have lots of restrictions to the parts of partitions of an incredibly large number (proportional to the number of electrons in the system). The story does not stop here, though, because the main question we are asking is not *how to calculate all the partition numbers* as explained in the following sections, the difficulty of which, however, urges us to use a different idea from directly solving the partition numbers to deal with the partitions.

The methods in analytic number theory can lend us a hand in this case. A standard way to study the partition number sequence is by formally constructing the corresponding power series of a dummy variable $q \in (0, 1)$ (more variables might be needed with additional restrictions):

Definition 3.3 (Generating function). The formal infinite series is defined as the generating function for the sequence $p(1|\mathcal{R}), p(2|\mathcal{R}), p(3|\mathcal{R}), \dots$, etc.

$$\mathcal{G}(q|\mathcal{R}) \equiv \sum_{k \geq 0} p(k|\mathcal{R}) \cdot q^k \quad (3.20)$$

where the set of restrictions is denoted by \mathcal{R} . If the coefficient of each term (the partition number) is not restricted to \mathbb{N} , but some other algebraic structures, for example, a polynomial ring, then we can get the generating function for its elements as well. For example, the generating function of the Laguerre polynomials discussed in Appendix.E can be written as:

$$\mathcal{G}_{\text{Laguerre}}(q) = \sum_{n=0}^{\infty} L_n^{(0)}(x) \cdot q^n = \frac{1}{1-q} \cdot e^{-\frac{qx}{1-q}} \quad (3.21)$$

If we look back into the history of physics, the application of partitions can even be found in the era of Boltzmann, i.e. before the establishment of quantum mechanics, where the partition functions in statistical mechanics are exactly a direct application of generating functions [48]. Furthermore, the generating functional formalism (or path integrals) in quantum field theory is based on the same spirit [292]. Unsurprisingly, this formalism also applies to the counting of conformal families as the last section explains. Intuitively speaking, *the generating function offers a way to describe the distribution of elements in the system based on some pre-defined weight (which could be given by energy, action, etc.) without losing any information*. Specifically, if $\mathcal{R} \neq \emptyset$, then $\mathcal{G}(q|\mathcal{R})$ is called restricted. We have the following corollary:

Corollary 3.1. *The relationship between $\mathcal{G}(q)$ and $p(k)$ can be written as:*

$$p(k) = \frac{1}{k!} \left. \frac{\partial^k \mathcal{G}(q)}{\partial q^k} \right|_{q=0} \equiv \left. \frac{\partial_k \mathcal{G}(q)}{k!} \right|_{q=0} \quad (3.22)$$

However in practice, normally we prefer not to (even if in principle we can) extract an *arbitrary* partition number from the generating function, because of the unavoidable higher-order derivatives. The precious advantage of the generating function is that the number of partitions of n under some particular conditions *often* equals the number of partitions of n under entirely different conditions, so

we can figure out how to write down closed-form expressions for the partition series with restrictions, such that we can compare two partition series $\{p(n|\mathcal{R}_1)\}$ and $\{p(n'|\mathcal{R}_2)\}$ with different restrictions just by looking at their generating functions instead of calculating all the partition numbers. In fact, by doing so we don't need to know about any one of the partition numbers at all, because *all* the information about the partitions has been encoded in the generating function. A physicist-friendly example is that calculating any (thermodynamic) quantity can be eventually related to the operations of the partition function.

3.4.2 Restricted generating functions

As we have explained, what we care about is properly writing down the generating function with given restrictions \mathcal{R} . So in this subsection, all the useful generating functions that we need for discussing physics will be introduced or derived. Let us start with some jargon in number theory for later use. The essence of using series to denote the partitions is that we can literally simulate the binary operation of “taking” or “leaving” by using the following expressions:

Definition 3.4 (q -Pochhammer symbol).

$$\begin{aligned} (a)_n &= (a; q)_n = (1 - a)(1 - aq) \cdots (1 - aq^{n-1}); \\ (a)_\infty &= (a; q)_\infty = \lim_{n \rightarrow \infty} (a; q)_n; \quad (a)_0 = 1 \end{aligned} \tag{3.23}$$

Here each term in the brackets is like a box that we can choose whether we want to take the meaningful term inside $(-aq^i, i \in \{0, 1, \dots, n-1\})$ or not (1), and the variable a serves the role of a counter, which can also be set to be q to make the partition restriction-free. Thus one only needs to look at the coefficient of the term $a^m \cdot q^N$ when looking for the partition number of N with m parts. Another important symbol is the generalization of the binomial coefficient:

Definition 3.5. (q -Gaussian polynomial)

$$\left[\begin{matrix} n \\ m \end{matrix} \right]_q = \begin{cases} (q)_n (q)_m^{-1} (q)_{n-m}^{-1}, & 0 \leq m \leq n \\ 0, & \text{otherwise} \end{cases} \tag{3.24}$$

which has many practical properties that can be used for our following derivations, as shown in Ref.[289]. Then to reflect the restrictions to the parts on the generating function, we have to manipulate the powers of the formal variables as seen in the q -Pochhammer symbols. Hence let us consider a multiple Laurent series of the formal variables λ_i :

$$\sum_{n_1, n_2, \dots, n_m \geq 0} \alpha_{n_1, n_2, \dots, n_m} \lambda_1^{n_1 - n_2} \lambda_2^{n_2 - n_3} \dots \lambda_{m-1}^{n_{m-1} - n_m} \quad (3.25)$$

where α denotes the coefficients irrelevant to λ_i . The behavior of the powers can be used to restrict the parts after defining a useful operator [293]:

Definition 3.6 (Regularization operator). The operator $\hat{\Omega}_\lambda$ is defined to act on a multiple Laurent series of λ_i , annihilate all the terms with negative exponents, and set any remaining coefficients to 1.

The regularization operator can help eliminate all the formal variables because of the following lemma [293]:

Lemma 3.2 (Elimination of coefficients by the regularization operator).

$$\hat{\Omega}_\lambda \frac{\lambda^{-k}}{(1 - \lambda x)(1 - y/\lambda)} = \frac{x^k}{(1 - x)(1 - xy)} \quad (3.26)$$

which can be easily generalized to the case with more than one formal variable, as shown in the following section. Furthermore, to extract the partition number from a partition function, we can formally define the following:

Definition 3.7. (Extraction operator) Define the operator which can extract the coefficient from the series by:

$$\hat{\Lambda}_j^{(q)} \sum_{n=0}^{\infty} a_n q^n = a_j \quad (3.27)$$

Here the exact form of the operator $\hat{\Lambda}_j^{(q)}$ does not matter, and apparently, the operator $\frac{\partial_k}{k!}|_{q=0}$ acting on a generating function can be regarded as a well-defined extraction operator. Now we are all set to give the restricted generating function to be used in the following discussions:

Theorem 3.3 (Generic restricted partitions). *For the number of partitions of n :*

- (i) *into exactly m parts;*
- (ii) *each part (in descending order) differs from the next by at least $k \geq 0$;*
- (iii) *the smallest part $\geq L \geq 0$;*
- (iv) *the largest part $\leq N$;*

The generating function is given by:

$$\mathcal{G}(q|L^{\geq}; N^{\leq}; m^=; k) = q^{\frac{km(m-1)}{2} + Lm} \left[\begin{matrix} N + m - k(m-1) - L \\ m \end{matrix} \right]_q \quad (3.28)$$

where $n, m, k, L, N \in \mathbb{N}$.

Proof. Let us start with some simple partitions without so many restrictions and add the conditions step by step. Firstly consider the generating function of the partition numbers of n into parts $\leq N$ with $N \in \mathbb{Z}_+$:

$$\mathcal{G}(q|; N^{\leq}; ;) = \sum_{n=0}^{\infty} p(n|; N^{\leq}; ;) q^n = \sum_{n_1=0}^{\infty} q^{1 \cdot n_1} \sum_{n_2=0}^{\infty} q^{2 \cdot n_2} \cdots \sum_{n_N=0}^{\infty} q^{N \cdot n_N} = \frac{1}{(q)_N} \quad (3.29)$$

Then we can think about the generating function of the partition numbers of n into $\leq m$ parts:

$$\mathcal{G}(q|; ; m^{\leq}; ;) = \sum_{n=0}^{\infty} p(n|; ; m^{\leq}; ;) q^n = \sum_{n_1 \geq n_2 \geq \cdots \geq n_m \geq 0} q^{n_1 + n_2 + \cdots + n_m} \quad (3.30)$$

which, according to the definition of the regularization operator, is equivalent to:

$$\begin{aligned}
& \mathcal{G}(q|; ; m^{\leq};)) \\
&= \hat{\Omega}_\lambda \sum_{n_1, n_2, \dots, n_m \geq 0} q^{n_1+n_2+\dots+n_m} \lambda_1^{n_1-n_2} \lambda_2^{n_2-n_3} \dots \lambda_{m-1}^{n_{m-1}-n_m} \\
&= \hat{\Omega}_\lambda \sum_{n_1=0}^{\infty} (q\lambda_1)^{n_1} \sum_{n_2=0}^{\infty} (q\lambda_2/\lambda_1)^{n_2} \dots \sum_{n_{m-1}=0}^{\infty} (q\lambda_{m-1}/\lambda_{m-2})^{n_{m-1}} \sum_{n_m=0}^{\infty} (q/\lambda_{m-1})^{n_m} \\
&= \frac{1}{(1-q)(1-q^2)\dots(1-q^m)} = \frac{1}{(q)_m} = \mathcal{G}(q|; m^{\leq}; ;)
\end{aligned} \tag{3.31}$$

Thus *the partition numbers of an integer n into parts $\leq m$ is equal to the partition numbers of n into $\leq m$ parts*. This basic example confirms the possibility of establishing an equivalence between two partitions with entirely different conditions. Now we can figure out how to add all the restrictions by translating them to the requirements of the generating function. The following discussions assume all the parts are in descending order from n_1 to n_m . The unrestricted generating function can be written as:

$$\mathcal{G}(q|; ; ;) = \hat{\Omega}_\lambda \sum_{n_1, n_2, \dots, n_\infty=0}^{\infty} q^{n_1+n_2+\dots+n_\infty} \lambda_1^{n_1-n_2} \lambda_2^{n_2-n_3} \dots \lambda_\infty^{n_\infty} \tag{3.32}$$

Now let us translate and impose the restrictions one by one, and the differences in the generating function from the last step will be colored blue:

$$(i) \text{ Exactly } m \text{ parts} \iff \forall n_i \in \{n_1, n_2, \dots, n_m\}, n_i > 0 \iff n_m \geq 1$$

We can write down the generating function of partitions of n into *exactly m* parts with the help of the regularization operator:

$$\mathcal{G}(q|; ; m^=;)) = \hat{\Omega}_\lambda \sum_{n_1, n_2, \dots, \textcolor{blue}{n_m}=0}^{\infty} q^{n_1+n_2+\dots+\textcolor{blue}{n_m}} \lambda_1^{n_1-n_2} \lambda_2^{n_2-n_3} \dots \lambda_{m-1}^{n_{m-1}-n_m} \lambda_m^{\textcolor{blue}{n_m-1}} \tag{3.33}$$

$$(ii) \text{ Each part differs from the next by at least } k \geq 0 \iff \text{If } i = j - 1, \forall n_i, n_j \in \{n_1, n_2, \dots, n_m\}, n_i - n_j \geq k$$

This means that we have to subtract a specific constant from the powers:

$$\mathcal{G}(q|; ; m^=; k) = \hat{\Omega}_\lambda \sum_{n_1, n_2, \dots, n_m=0}^{\infty} q^{n_1+n_2+\dots+n_m} \lambda_1^{n_1-n_2-k} \lambda_2^{n_2-n_3-k} \dots \lambda_{m-1}^{n_{m-1}-n_m-k} \lambda_m^{n_m-1} \quad (3.34)$$

where we use the powers of the λ_i variables to restrict the differences between the adjacent parts. Also, as long as the difference k is greater than 1, there must be m distinct parts in the partitions.

$$(iii) \text{ The smallest part is } \geq L \geq 0 \iff n_m \geq L \geq 0$$

To restrict the smallest part n_m , we can simply subtract L from the power of λ_m , considering all the terms with $n_m - L < 0$ will be eliminated by the regularization operator:

$$\begin{aligned} & \mathcal{G}(q|L^=; ; m^=; k) \\ &= \hat{\Omega}_\lambda \sum_{n_1, n_2, \dots, n_m=0}^{\infty} q^{n_1+n_2+\dots+n_m} \lambda_1^{n_1-n_2-k} \lambda_2^{n_2-n_3-k} \dots \lambda_{m-1}^{n_{m-1}-n_m-k} \lambda_m^{n_m-L} \end{aligned} \quad (3.35)$$

$$(iv) \text{ The largest part is } \leq N \iff n_1 \leq N$$

Similar to the last step, we can add another formal variable λ_0 :

$$\begin{aligned} & \mathcal{G}(q|L^=; N^=; m^=; k) \\ &= \hat{\Omega}_\lambda \sum_{n_1, n_2, \dots, n_m=0}^{\infty} q^{n_1+n_2+\dots+n_m} \lambda_0^{N-n_1} \lambda_1^{n_1-n_2-k} \lambda_2^{n_2-n_3-k} \dots \lambda_{m-1}^{n_{m-1}-n_m-k} \lambda_m^{n_m-L} \end{aligned} \quad (3.36)$$

However, in this way, the regularization operator cannot simplify the final result. The solution is to introduce another variable $x \in (0, 1)$ to the generating function. Let us consider the case with the largest part equal to j instead:

$$\begin{aligned} & \sum_{j,n=0}^{\infty} p(n|L^=; j^=; m^=; k) x^j q^n \\ &= \hat{\Omega}_\lambda \sum_{n_1, n_2, \dots, n_m=0}^{\infty} x^{n_1} q^{n_1+n_2+\dots+n_m} \lambda_1^{n_1-n_2-k} \lambda_2^{n_2-n_3-k} \dots \lambda_{m-1}^{n_{m-1}-n_m-k} \lambda_m^{n_m-L} \end{aligned} \quad (3.37)$$

Then by using the extraction operator, we can write down the generating function with the largest part $\leq N$ as:

$$\begin{aligned}\mathcal{G}(q|L^{\geq}; N^{\leq}; m^=; k) &= \sum_{s=0}^N \sum_{n=0}^{\infty} p(n|L^{\geq}; s^=; m^=; k) q^n \\ &= \sum_{s=0}^N \hat{\Lambda}_s^{(x)} \left[\sum_{j,n=0}^{\infty} p(n|L^{\geq}; j^=; m^=; k) x^j q^n \right]\end{aligned}\quad (3.38)$$

We can deal with the part inside the bracket (Eq.(3.37)) first, and the trick is to use the regularization operator to eliminate all the formal variables:

$$\begin{aligned}& \sum_{j,n=0}^{\infty} p(n|L^{\geq}; j^=; m^=; k) x^j q^n \\ &= \hat{\Omega}_{\lambda} \sum_{n_1, n_2, \dots, n_m=0}^{\infty} x^{n_1} q^{n_1+n_2+\dots+n_m} \lambda_1^{n_1-n_2-k} \lambda_2^{n_2-n_3-k} \dots \lambda_{m-1}^{n_{m-1}-n_m-k} \lambda_m^{n_m-L} \\ &= \hat{\Omega}_{\lambda} \frac{(xq)^k \cdot (xq^2)^k \cdot (xq^3)^k \cdots (xq^{m-1})^k \lambda_m^{-L}}{(1-xq)(1-xq^2) \cdots (1-xq^{m-1})(1-\lambda_m xq^m)} \\ &= \frac{(xq)^k \cdot (xq^2)^k \cdot (xq^3)^k \cdots (xq^{m-1})^k \cdot (xq^m)^L}{(1-xq)(1-xq^2) \cdots (1-xq^{m-1})(1-xq^m)} \\ &= \frac{q^{\frac{km(m-1)}{2}+Lm}}{(xq;q)_m} x^{(m-1)k+L}\end{aligned}\quad (3.39)$$

Note that the extraction operator does not commute with the summation with respect to the same index, so we can write down the final conclusion by getting rid of the formal variable x :

$$\begin{aligned}& \mathcal{G}(q|L^{\geq}; N^{\leq}; m^=; k) \\ &= \sum_{s=0}^N \hat{\Lambda}_s^{(x)} \left[\frac{q^{\frac{km(m-1)}{2}+Lm}}{(xq;q)_m} x^{k(m-1)+L} \right] = \hat{\Lambda}_N^{(x)} \sum_{s=0}^{\infty} x^s \frac{q^{\frac{km(m-1)}{2}+Lm}}{(xq;q)_m} x^{k(m-1)+L} \\ &= \hat{\Lambda}_N^{(x)} \frac{q^{\frac{km(m-1)}{2}+Lm}}{(x;q)_{m+1}} x^{k(m-1)+L} = q^{\frac{km(m-1)}{2}+Lm} \cdot \hat{\Lambda}_N^{(x)} \left\{ \sum_{i=0}^{\infty} \left[\begin{array}{c} m+i \\ m \end{array} \right]_q x^{i+k(m-1)+L} \right\} \\ &= q^{\frac{km(m-1)}{2}+Lm} \left[\begin{array}{c} N+m-k(m-1)-L \\ m \end{array} \right]_q\end{aligned}\quad (3.40)$$

□

The benefit of this general conclusion is that we can get most of the commonly-used generating functions from it without using specific methods for different restrictions as usually carried out in the textbooks [289]. The regularization operator's application also hints at how to properly manipulate the powers, which could be generalized to other restrictions. Note that the same notation of the generating functions will be used in the following discussions considering they correspond to different physical contexts, such as different statistics or generalized admissible rules (to be explained later). Below are several useful corollaries:

Corollary 3.4 (Bosonic partitions). *The generating function of the partition numbers of integer n into at most m parts, each of which is no greater than N denoted by $G^B(q|N, m)$ can be written as:*

$$\mathcal{G}^B(q|N, m) = \left[\begin{array}{c} N+m \\ m \end{array} \right]_q \quad (3.41)$$

Proof. The key idea here is to observe that the bosonic statistics is equivalent to requiring the partitions to have at most m parts, which gives the condition $L = k = 0$. Thus we have

$$\mathcal{G}^B(q|N, m) = G(q|0; N^{\leq}; m^=; 0) = \left[\begin{array}{c} N+m \\ m \end{array} \right]_q \quad (3.42)$$

□

Corollary 3.5 (Fermionic partitions). *The generating function of the number of partitions into exactly m distinct parts, the maximal one of which = N , denoted by $G^F(q|N, m)$, is given by:*

$$\mathcal{G}^F(q|N, m) = q^{\frac{m(m+1)}{2}} \left[\begin{array}{c} N \\ m \end{array} \right]_q \quad (3.43)$$

Proof. Similarly, requiring the partitions to have m distinct parts is equivalent to the condition $L = k = 1$. Thus we have

$$\mathcal{G}^F(q|N, m) = G(q|1; N^{\leq}; m^=; 1) \quad (3.44)$$

□

It is not hard to notice that if we replace q with the Boltzmann factor $e^{-\frac{E}{kT}}$, these two generating functions are precisely the bosonic and the fermionic partition function. Before relating these mathematical conclusions to CHSs, let us briefly introduce how to generalize the generating function to the case with more restrictions. This can help us understand non-Abelian states such as the Moore-Read state in future research. We shall start with another property of the regularization operator:

Corollary 3.6 (Elimination of coefficients by the regularization operator).

$$\hat{\Omega}_\lambda \frac{\lambda^{-k}}{(1-x)(1-\lambda y)} = \frac{x^k}{(1-\lambda x)(1-\frac{y}{x})} \quad (3.45)$$

Proof.

$$\begin{aligned} \hat{\Omega}_\lambda \frac{\lambda^{-k}}{(1-\lambda x)(1-\lambda y)} &= \hat{\Omega}_\lambda \sum_{n=0}^{\infty} (\lambda x)^n \sum_{m=0}^{\infty} (\lambda y)^m \cdot \lambda^{-k} = \hat{\Omega}_\lambda \sum_{n,m=0}^{\infty} \left(\frac{y}{x}\right)^m (x\lambda)^{n+m-k} \cdot x^k \\ &= x^k \cdot \sum_{s=0}^{\infty} x^s \sum_{m=0}^{\infty} \left(\frac{y}{x}\right)^m = \frac{x^k}{(1-x)(1-\frac{y}{x})} \end{aligned} \quad (3.46)$$

□

Then we would like to get the partition function with two restrictions to the differences between parts. Here, we only consider the partitions with non-repetitive parts corresponding to the fermionic statistics in physics. An important observation of the restrictions can be made:

Proposition 3.1 (Equivalence between partition restrictions). *For the non-negative consecutive integer set \mathcal{S} , denote the set of all the subset of \mathcal{S} with four consecutive integers as \mathcal{S}_4 and the set of all the parts in the partition p as \mathcal{S}_p . Then for $\mathcal{S}_p \in \mathcal{S}$, the following restrictions to the partition p should be equivalent and lead to the same generating function:*

$$\forall s \in \mathcal{S}_4, \text{card}(s \cap \mathcal{S}_p) \leq 2 \iff p_{i+2} - p_i \geq 4, i \leq \text{card}(\mathcal{S}_p) - 2 \quad (3.47)$$

Proof. (\implies) Can be easily proved by using the method of exhaustion.

(\Leftarrow) $\forall i \leq \text{card}(\mathcal{S}_p) - 2$ and $\in \mathbb{N}$, given that $p_{i+2} > p_{i+1} > p_i$, we have $p_{i+1}^{\max} = p_{i+2} - 1 \geq p_i + 4 - 1 = \inf(p_{i+1}^{\max})$, s.t. the smallest set that contains p_{i+1} is $s_{p_i} \setminus \{p_i\}$, where s_n denotes the subset of \mathcal{S}_4 with the minimal element n . Thus $\text{card}(s_{p_i} \cap \mathcal{S}_p) \leq 2$, so $\text{card}(s \cap \mathcal{S}_p) \leq 2$. \square

which naturally leads to the following:

Corollary 3.7 (Equivalence between generalized admissible rule and partition restrictions). *The (fermionic) Moore-Read state can be given by the so-called Jack polynomials (introduced in the next section), with the generalized admissible rule that there can only be at most 2 electrons in every 4 orbital. Based on the proposition above, it is equivalent to the restriction $n_{i+2} - n_i \geq 4$ for any part n_i with a well-defined n_{i+2} in the partition.*

Thus we can derive the following result:

Theorem 3.8 (Moore-Read restricted partitions). *For the number of partitions of n :*

- (i) *into exactly m parts, and m is even;*
- (ii) *each part (in descending order) differs from the next by at least 1;*
- (iii) *each part (in descending order) differs from the second next by at least 4;*
- (iv) *the smallest part ≥ 0 ;*
- (v) *the largest part $\leq N$;*

The generating function is given by:

$$\mathcal{G}(q, x | 0^\geq; N^\leq; m^=; 1; 4) = \frac{x \cdot q^{\frac{m}{2}}}{(q)^{\frac{m}{2}} \cdot (x; q)^{\frac{m}{2}}} \quad (3.48)$$

where $m, N \in \mathbb{N}$ and m is even.

Proof. Consider the generating function given by:

$$\begin{aligned}
& \mathcal{G}(q|0^\geq; N^\leq; m^=; 1; 4) \\
& = \hat{\Omega}_{\lambda, \mu} \sum_{n_1, n_2, \dots, n_m \geq 0} (\lambda_1 \mu_1 x q)^{n_1} \cdot \left(\frac{\lambda_2}{\lambda_1} \mu_2 x q \right)^{n_2} \cdot \left(\frac{\lambda_3 \mu_3}{\lambda_2 \mu_1} q \right)^{n_3} \cdot \left(\frac{\lambda_4 \mu_4}{\lambda_3 \mu_2} q \right)^{n_4} \\
& \quad \cdots \left(\frac{\lambda_{m-2} \mu_{m-2}}{\lambda_{m-3} \mu_{m-4}} q \right)^{n_{m-2}} \cdot \left(\frac{\lambda_{m-1} \mu_{m-1}}{\lambda_{m-2} \mu_{m-3}} q \right)^{n_{m-1}} \cdot \left(\frac{\lambda_m \mu_m}{\lambda_{m-1} \mu_{m-2}} q \right)^{n_m} \\
& \quad \cdot \prod_{i=1}^{m-1} \lambda_i^{-1} \prod_{j=1}^{m-2} \mu_j^{-4} \mu_{m-1}^0 \cdot \mu_m^0
\end{aligned} \tag{3.49}$$

After transforming all the terms in the brackets into simpler forms, with the help of Lemma 3.2, we can eliminate the formal variants λ_i and μ_i term by term. Let us start with λ_i :

$$\begin{aligned}
& \hat{\Omega}_\lambda \frac{\lambda_1^{-1} \cdots}{(1 - \lambda_1 \mu_1 x q) (1 - \frac{\lambda_2}{\lambda_1} \mu_2 q) \cdots} \\
& = \frac{(\mu_1 x q) (\mu_1 \mu_2 x q^2) \cdots (\mu_{m-2} \mu_{m-1} x q^{m-1}) \cdot \prod_{j=1}^{m-2} \mu_j^{-4}}{(1 - \mu_1 x q) (1 - \mu_1 \mu_2 x q^2) \cdots (1 - \mu_{m-2} \mu_{m-1} x q^{m-1}) (1 - \mu_{m-1} \mu_m x q^m)}
\end{aligned} \tag{3.50}$$

Then we can eliminate the μ_j term based on Corollary 3.6:

$$\begin{aligned}
& \hat{\Omega}_\mu \frac{\mu_1 \prod_{i=1}^{m-2} \mu_i \mu_{i+1} \cdot \prod_{j=1}^{m-2} \mu_j^{-4} \cdot \prod_{k=1}^{m-1} x q^k}{(1 - \mu_1 x q) (1 - \mu_1 \mu_2 x q^2) \cdots (1 - \mu_{m-2} \mu_{m-1} x q^{m-1}) (1 - \mu_{m-1} \mu_m x q^m)} \\
& = \frac{\prod_{i=1}^{\frac{m-2}{2}} (x^2 \cdot q^{-4i})}{\prod_{j=1}^{\frac{m}{2}} (1 - q^j) (1 - x q^j)} \cdot \prod_{k=1}^{m-1} x q^k \\
& = \frac{x \cdot q^{\frac{m}{2}}}{(q)^{\frac{m}{2}} \cdot (x; q)^{\frac{m}{2}}}
\end{aligned} \tag{3.51}$$

Note that here we formally define $\prod_{k=1}^n x \equiv x^n$. We can also use the regularization operator to eliminate x in the generating function if we want. \square

In the next part, we shall introduce a nice way to represent the wave functions of many FQH states, which also reveals why the partition theory is relevant.

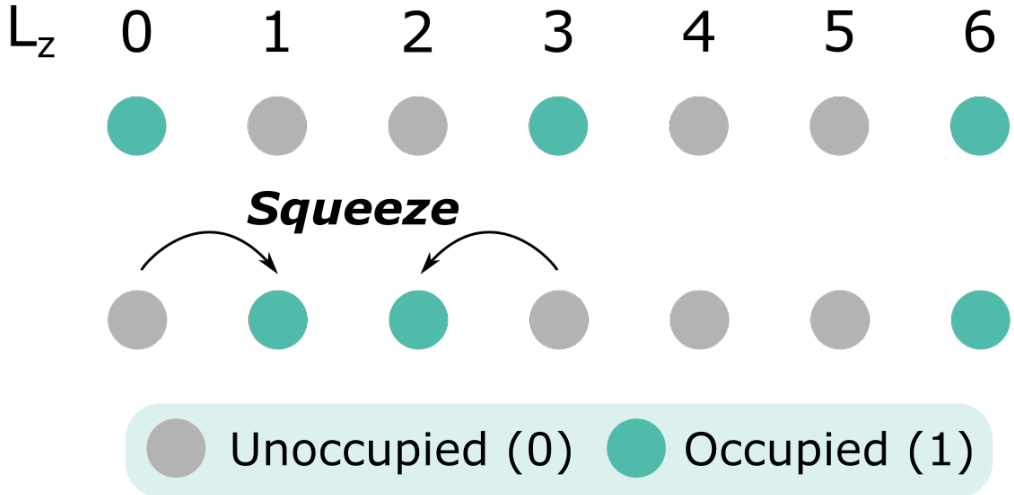


FIGURE 3.1: Jack polynomials and the squeezing operation on the disk.

3.4.3 Jack polynomials and generalized admissible rules

The systematic study of the algebraic properties of the polynomials used to write down the model wave functions (including the initial Laughlin wave functions or the Moore-Read wave functions afterward, etc.) was carried out by Bernevig and Haldane [137, 195, 196]. They found that they can be expressed as a specific type of symmetric polynomials with proper normalization, called the *Jack polynomials* (jacks), which are friendly to numerical realizations and possess many nice mathematical properties. One can also think of the Jack polynomials as one of the mathematical objects connecting FQH to CFT because they are conjectured to be the correlator of $W_k(k+1, k+r)$ CFTs [294–296].

Let us start with a brief introduction of the Jack polynomials. These polynomials are the unique homogeneous polynomial-type eigenfunctions of the Laplace-Beltrami operator. We will stick to rotationally invariant systems in the following part for simplicity. The pseudo-spin structure (coming from an emergent orbital angular momentum) in the quantized LLs enables us to define second-quantized wave functions in an occupation-number-like basis for the many-body wave functions as shown in Fig.3.1. For example, the magnetic field can be introduced by putting a Dirac magnetic monopole at the center of the sphere with a total of $2S$ magnetic fluxes, rendering a spinor structure of the single particle the wave function with total spin $S+N$, where N is the LL index [20]. Without loss of generality, we use the LLL with $N=0$, so the total number of single-particle orbitals in the

LLL is $N_o = 2S + 1$. We can thus express a many-body state with a string of N_o binary numbers, corresponding to the single particle orbitals sequentially from the north pole to the south pole. We use the integer 1 to denote an occupied orbital and 0 for an empty orbital [195]. For example, if $S = 3$ and we have two electrons around the sphere's north pole, this state can be denoted as $|1100000\rangle$, with a total number of seven orbitals.

On the disk geometry, the occupation basis also corresponds to the first-quantized wave functions with the symmetric gauge. Each digit in the occupation basis from left to right corresponds to the orbital from the origin (z_k^0) to the edge ($z_k^{N_o-1}$), where $z_k = x_k + iy_k$ is the holomorphic coordinate of the k^{th} electron. The many-body wave functions for the FQH states are linear combinations of such monomials. For example, the monomial $|1101\rangle$ in the first quantized form is given by:

$$|1101\rangle \sim (z_1 - z_2)z_3^3 + (z_3 - z_1)z_2^3 + (z_2 - z_3)z_1^3 \quad (3.52)$$

One important characteristic of the Jack polynomial states is the existence of a *root configuration*, with all of the occupation bases of the state “squeezed” from the root configuration as shown in Fig.3.1 [137, 195, 196]. For instance, if one considers the Laughlin-1/3 state with 3 electrons, the wave function $(z_1 - z_2)^3(z_1 - z_3)^3(z_2 - z_3)^3$ is a Jack polynomial denoted by $J_{|1001001}^{\alpha=-2}$. Here 1001001 is the root configuration, and $\alpha = -2$ in the superscript is derived from the admission rule of the root configuration. All coefficients of the monomials in the Jack polynomial are determined by α , and these monomials are “squeezed” from the root configuration, so we can unambiguously determine a Jack polynomial by its α and root configuration. Note that the Jacks with the same α but different root configurations (one is squeezed from another) are only *linear independent* rather than orthogonal.

We denote two monomials m_1, m_2 and that m_2 is squeezed from m_1 by $m_1 \succ m_2$. That implies m_2 is obtained from m_1 by repeatedly moving two electrons in the binary string towards each other without changing the total angular momentum of the monomial. Explicitly for the Laughlin-1/3 state with three electrons, we have

the following:

$$\begin{aligned}
 J_{|1001001\rangle}^{-2} \sim & (z_1 - z_2)^3(z_1 - z_3)^3(z_2 - z_3)^3 \\
 = & |1001001\rangle - 3|0110001\rangle - 3|1000110\rangle \\
 & + 6|0101010\rangle - 15|0011100\rangle
 \end{aligned} \tag{3.53}$$

Since all the possible occupation bases are squeezed from the root configurations above, we can figure out how to get those we need to compose the eigenstates. As mentioned at the beginning, the model wave functions for the FQH states on the sphere in many cases are the Jack polynomials characterized by the so-called *generalized admissible rules* (also known as clustering properties or *generalized Pauli principle*), which is normally represented by three numbers (k, r, N) (sometimes N is omitted, so we only use (k, r) to denote the rule). Its physical significance is that there can exist no more than k particles in r consecutive orbitals (in a system with N particles) [20]. Thus, for example, if we have two jacks with the root configurations 10010001 and 01100001 , then the second one will be truncated with the $(1, 3)$ -admissible rule. In practice, these generalized admissible rules can be “read-off” from the (model) Hamiltonian and the particle statistics.

Another efficient method to pick the bases we need is called the local exclusion condition (LEC), firstly proposed in [204, 205]. A LEC is defined by a triple, denoted by $\hat{n} = \{n, n_e, n_h\}$, giving the constraint that there can be no more than n_e electrons or n_h holes in a circular droplet containing n fluxes anywhere in the quantum fluid. For a spherical geometry, one can check the orbitals at the north pole for the *highest weight states*.

3.4.4 Isomorphic conformal Hilbert spaces

Based on the discussion above, the total power of the variables in a monomial is precisely the \hat{L}_z quantum number. Then we can conclude that the dimension of the L_z sectors is determined by the partition number of $L_z \in \mathbb{N}$ with some restrictions from the particle statistics, the geometry, the symmetry, and the model Hamiltonian (represented by some generalized admissible rules). It is possible to write down the generating function of the L_z sector degeneracies despite the difficulty of accurately solving the degeneracy of each L_z sector.

Now that we have learned about how to properly use the generating functions to represent the counting in the L_z sectors within CHSs and how to restrict these generating functions with minimal separations between parts. Furthermore from the discussion on the Jack polynomial formalism of writing down the model wave functions for many FQH states, as Fig.3.2 shows, we can see that these restrictions are exactly corresponding to the generalized admissible rules describing different model Hamiltonians, which define the CHSs.

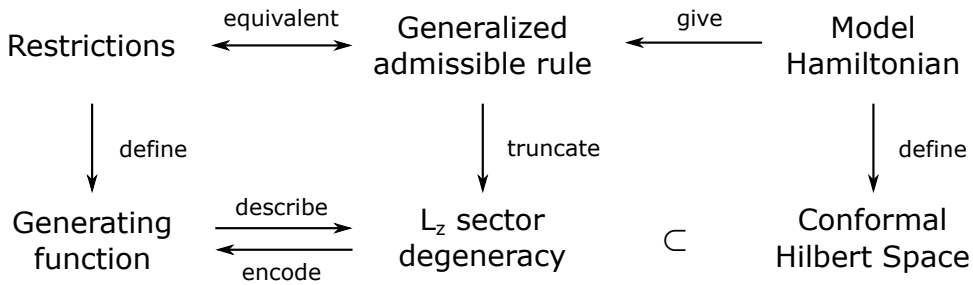


FIGURE 3.2: Relations between the generating function with restrictions and the degeneracy of L_z sectors within some CHS.

Then the next question to be answered is, how to define the equivalence between different CHSs based on the generating functions? Let us firstly list the properties that such a relationship should have:

- *The equivalence depends on some symmetry.* Because symmetry can bring good quantum numbers (such as the L_z due to rotational invariance), which can lead to degeneracies within the CHS. This can provide a corresponding generating function to set up the equivalence. In this thesis, we will only discuss rotational invariance but it can definitely be generalized to other cases, which remains to be studied in the future.
- *The equivalence should be insensitive to the exact range of the angular momenta.* Because we are establishing the equivalence between different CHSs with (possibly) different particle numbers and orbital numbers, the range of the angular momenta is almost certain to differ. So the thing we should care about is the relative position of the L_z sectors within each CHS.

- The equivalence should be well-defined for any system size. Indeed in the context of FQH, theoretical concepts are normally considered in the thermodynamic limit. But we want to define a stronger relation showing that two CHSs are always equivalent, which is also valuable for carrying out the composite fermionization introduced in the next section.

Based on all these points, here we introduce the concept of isomorphism of CHSs:

Definition 3.8. (Isomorphism of CHSs) Given two CHSs \mathcal{H}_1 and \mathcal{H}_2 , the L_z sector degeneracies of which are described by the partition sequence, $p_1(n)$ and $p_2(n')$ correspondingly with the generating functions $\mathcal{G}_1(q)$ and $\mathcal{G}_2(q)$. If the generating functions fulfill the following:

$$\mathcal{G}_1(q) = \mathcal{G}_2(q) \cdot q^n, \quad n \in \mathbb{Z} \quad (3.54)$$

then \mathcal{H}_1 and \mathcal{H}_2 are called *isomorphic* to each other, denoted by $\mathcal{H}_1 \cong \mathcal{H}_2$.

It can be seen that such a definition fulfills all the requirements above. From the mathematical point of view, we believe that it is proper to call such a relation “isomorphism” considering the isomorphism between (finite-dimensional) vector spaces is given by their identical dimensions, which in our case are interpreted as the degeneracies in each L_z sectors. Furthermore, the isomorphism defined here has explicit physical meanings rather than only serving as fancy mathematics. For example, one can study the zeros of these generating functions of polynomial-type in \mathbb{C} and obviously, the only difference between isomorphic ones will be the multiplicity of the zero point at the original point. Recall that Lee and Yang determined the phase transitions based on the zeros of partition functions [297, 298], and we can naturally speculate that the isomorphic CHSs are of the same “universality”. More physical insights about this relation will be provided in the next section.

Given that all the information about the CHS is contained in the generating functions, we are not surprised that it is possible for two CHSs with entirely different physical conditions to be isomorphic. Before introducing more examples in the next section, we can look into one of the simplest examples, which is the isomorphism between the Hilbert spaces with different geometries:

Proposition 3.2. *The Hilbert space of an FQH system on the disk is isomorphic to the one with the same electron number and orbital number on the sphere.*

Proof. The range of the L_z quantum numbers is just shifted from the disk to the sphere. So for a given particle number N_e with N_o orbitals, we have:

$$\mathcal{G}(q| \subset B^2) = \mathcal{G}(q| \subset S^2) \cdot q^{\frac{N_e(N_o-1)}{2}} \quad (3.55)$$

□

Thus in practice, we can adopt a constant g to denote the shift caused by the geometry. Besides defining the isomorphism between CHSs, the generating function formalism can also be used to calculate other physical quantities, considering they are the “prototype” of partition functions. For example, one can calculate the thermal Hall coefficient (related to the central charge) of an FQH phase by differentiating the corresponding generating function [130, 137]. Also, the counting pattern given by the generating function matches the entanglement spectrum (generally in the lower part) [175, 221]. All these properties can be traced to the relation between FQH states and CFT correlators, as explained in the last section.

3.5 Composite fermionization

We have established a well-defined isomorphism between different CHSs, so it is natural to think about the mapping from one CHS to another. In this section, we would like to reinterpret the concept of CFs (the composite particles of electron and magnetic fluxes) as something unambiguously induced by the mapping between isomorphic CHSs. Furthermore, although there is no particle-hole symmetry in the sub-Hilbert spaces of a single LL, one can still get the particle-hole conjugate of a state by mapping it to some CHS of CFs. The same idea can even be generalized to particles with totally different statistics, which will be mentioned at the end of this section.

3.5.1 Brief review on the composite fermion theory

The strong-coupling nature of the FQH phases of electrons is due to the dominance of the Coulomb interaction over other energy scales, which makes the problem hard to solve. However, the CF theory provides an effective and *phenomenological* way to eliminate the strong-coupling interactions between the electrons and make the FQH phases of electrons map into the IQH phases of CFs, but still retain the important topological features. The basis of the CF theory is the intuitive claim of attaching each electron with an even number of magnetic flux quanta (to keep the fermionic statistics), which forms a new bound state and renders the former partially-filled LLs to a fully-filled CF Λ -levels (or simply CF levels) due to the reduced magnetic field as shown in Fig.3.5. Furthermore, the CF theory can also map an electronic FQH state to a CF FQH state [71–76].

According to the founder of the CF theory, it was inspired by the concept of vortices in superconductors. The key idea of flux attachment originated from observing the Hall resistivity plateaus, where one can clearly see those corresponding to the filling factor $1/3$, $2/5$, $3/7$, and so on up to $1/2$, with their corresponding particle-hole conjugate partners [74]. Moreover, these filling factors obey a specific pattern like $\nu = n/(2p \cdot n \pm 1)$, so one can modify an electronic wave function by absorbing the additional $2p$ fluxes into the electrons to get a phase with an integer filling factor $\nu^* = n$. Furthermore, some potential signatures of CFs near specific plateaus were observed in experiments, which to some extent confirms the validity of the flux-attachment argument [299, 300]. But the nature of these emergent CFs remains controversial.

The CF picture can be integrated into different theoretical approaches to FQHE. One choice is to use CFs coupled to a Chern-Simons gauge field with some mean-field approximations when writing down a topological field theory (e.g., in the Lopez–Fradkin theory, etc.) [301, 302]. However, a more commonly used method is to write down the first-quantized ground-state wave explicitly functions $\Psi_{\frac{n}{2pn \pm 1}}$ from a CF trial wave function $\Phi_{\pm n}$ by following some routines [74]. The result can be written as:

$$\Psi_{\frac{n}{2pn \pm 1}} = \mathcal{P}_{\text{LLL}} \Phi_{\pm n} \prod_{j < k} (z_j - z_k)^{2p} \quad (3.56)$$

where \mathcal{P}_{LLL} means that one need to move all the \bar{z} to the left (“normal-order”) and then replace \bar{z} with $\frac{\partial}{\partial z}$, i.e. a projection to the LLL. From this point of view, the

Laughlin wave function can be *derived* from the IQH wave function of the CFs at $\nu = 1$. The same method can also be generalized to some excited states or FQH states with partially polarized spins.

The intuitive flux-attachment picture is definitely one of the advantages of the CF theory. Furthermore, the wave functions given by Eq.(3.56) were proved to have lower energy than those given by the Haldane-Halperin hierarchy formalism [99], which cannot deal with partially-polarized FQH states and the Fermi sea at $\nu = 1/(2p)$ as well. However, there are also several issues to be further cleared out. Here we list some of them: if we start from an IQH state of CFs, with the magnetic field strength increasing, the interaction between the CFs will eventually become significant, and this requires us to consider the FQH states of CFs. So it seems that the CF theory only *postpones* the difficulty of dealing with the strong couplings rather than fully resolves them. Similarly, some FQH states are interpreted as arising from the pairing of the CFs; it is also essential to understand how the pairing emerges and vanishes with a magnetic field. Another concern is about the nature of flux attachment. In principle, phase transitions could occur during this process, leading to significant modifications to the current CF theory. More details about this theory can be found in Ref.[74, 76].

In short, the CF theory is a very effective formalism based on phenomenology to understand FQH phases, which has not been fully understood.

3.5.2 Composite fermionization as the mapping between isomorphic CHSs

In the CF theory, the procedure based on Eq.(3.56) of getting the electronic wave function from the CF trial wave function is called the *composite fermionization*. But from the isomorphism between different CHSs, one can also define a mapping between the states to accomplish the same thing and even more, which is a natural idea from a mathematical point of view. Thus in this section, we will illustrate why this mapping is also physically relevant and introduce how to properly carry out the composite fermionization between CHSs, which can be regarded as the rigorous generalization and reinterpretation of this routine.

Let us start with the Laughlin states, the ground states of the linear combination of two-body Haldane pseudopotentials. The corresponding generating function have been derived as in Theorem 3.3: for the Laughlin state at the filling factor $\nu = 1/m$ with N_e electrons and N_o orbitals, it is given by:

$$\mathcal{G}_{\text{Laughlin}-1/m} = q^{\frac{mN_e(N_e-1)}{2} + N_e + g} \left[\begin{array}{c} N_o - (m-1)(N_e-1) \\ N_e \end{array} \right]_q \quad (3.57)$$

where g is the geometric shift determined by the system's geometry, which will not influence the isomorphism. Note that this expression also applies to the quasi-hole states (i.e., $N_o \geq m \cdot N_e - m + 1$). Our task is to find a dual description of the whole CHS, especially the ground state, which is equivalent to looking for the operations that transform the generating function in Eq.(3.57) to those describing other isomorphic CHSs. One can easily find such operations from the properties of q -Gaussian polynomials (the power function will not influence the isomorphism at all). One of them is to keep the particle number N_e as a constant but change the number of orbitals. If the new generating function is also corresponding to a Laughlin state, one can solve the Diophantine equation to know about the new CHS:

$$(m' - m)(N_e - 1) = N'_o - N_o \quad (3.58)$$

For fermionic states, m can only be odd numbers, which means that $m' - m$ has to be even. Thus in the context of CHS, we are *attaching/detaching an even number of fluxes to/from each electron* to form or decompose the *CFs*, denoted by cf^{2k} , $k \in \mathbb{Z}$, because the total number of fluxes has to be a constant to make sure that we are still describing the same physical system. Meanwhile, as m changes to m' , the restrictions in the new CHS become different as well, corresponding to a new model Hamiltonian. Such a procedure is equivalent to the flux-attachment argument in the CF theory. The difference is that we get this naturally from searching for the isomorphic CHSs of the given one, but in the CF theory, this argument serves as a basic *assumption*, so they cannot be verified or falsified. Note that the quantum states in a CHS can also be regarded as a unitary representation of the Lie algebra \mathfrak{g} of some Lie group G (in our case, the $SU(2)$ group describing the angular momentum) so we will not be surprised by getting the same result with other approaches such as Lie algebra.

After getting an isomorphic CHS \mathcal{H}_2 for the given \mathcal{H}_1 , one can *always* find a proper one-to-one mapping between the states as:

$$\begin{bmatrix} \phi_1 \\ \phi_2 \\ \phi_3 \\ \vdots \\ \phi_i \\ \vdots \end{bmatrix}_{\mathcal{H}_2} = \underbrace{\begin{bmatrix} F_{11} & F_{12} & F_{13} & \cdots & F_{1j} & \cdots \\ F_{21} & F_{22} & F_{23} & \cdots & F_{2j} & \cdots \\ F_{31} & F_{32} & F_{33} & \cdots & F_{3j} & \cdots \\ \vdots & \vdots & \vdots & \ddots & \vdots & \vdots \\ F_{i1} & F_{i2} & F_{i3} & \cdots & F_{ij} & \cdots \\ \vdots & \vdots & \vdots & \vdots & \vdots & \ddots \end{bmatrix}}_{F\text{-matrix}} \begin{bmatrix} \psi_1 \\ \psi_2 \\ \psi_3 \\ \vdots \\ \psi_j \\ \vdots \end{bmatrix}_{\mathcal{H}_1} \quad (3.59)$$

where we call the transformation matrix the F -matrix (inspired by S -matrix but between different and mostly orthogonal Hilbert spaces). Isomorphism ensures that F -matrix is square and thus invertible (the orthonormal states ensure the full rank). In this thesis, by composite fermionization, we mean the process of (completely or partially) *solving the F -matrix* for two isomorphic CHSs. For simple cases like Laughlin states, the ground states in the isomorphic CHSs are the unique highest-weight state in the $L_z = 0$ sector, so one can directly map them to each other. Generically speaking, there could be degeneracy in the eigenstates with the same L_z and L^2 quantum numbers, which implies that the F -matrix is not uniquely determined, and such a redundant degree of freedom can be distinguished as a *gauge*. Meanwhile, from the well-ordering theorem [303], one can always attach an ordered structure to the degenerate states within some L_z sectors. Thus one way to fix the gauge for the mapping is by using a small perturbation of other pseudopotentials, and we will show the details in the following part. Meanwhile, one can choose other gauges according to different requirements; for example, if we want the CF particles from composite fermionization to be more localized, then the density distribution can be adopted to choose from the available gauges.

Consider the Laughlin state at $\nu = 1/5$ of electrons on the sphere, for example, which is the unique ground state of the model Hamiltonian $\hat{H}_{\text{Laughlin-}1/5} = \hat{V}_1^{2\text{bdy}} + \hat{V}_3^{2\text{bdy}}$. The left and the right column in Fig.3.3 shows the whole mapping between all the eigenstates in the electronic CHS with 3 electrons and 11 orbitals defined by $\hat{H}_{\text{Laughlin-}1/5}$ and in the CF's CHS with 3 CFs and 7 orbitals defined by $\hat{H}_{\text{Laughlin-}1/3} = \hat{V}_1^{2\text{bdy}}$. Starting from the highest L_z sector, the whole Hilbert spaces concerning the corresponding model Hamiltonians can be constructed by acting \hat{L}_- successively. and clearly the electronic Laughlin state at $\nu = 1/5$ can be

mapped to the Laughlin- $1/3$ state of cf^2 as discussed above. More examples can be found in Chap.5. Furthermore, composite fermionization also allows determining the degeneracy within each L_z sector as shown in the middle column of Fig.3.3, which is the difference between the degeneracy of neighboring L_z sectors. If the restriction is given by other things rather than the generalized admissible rule (e.g., LEC), then the argument about the highest weight state degeneracy could fail.

This formalism can be generalized to higher CF levels (in analogy to the LLs). As Fig.3.4 shows, combining one electron with two fluxes allows us to write down each CF as “10” in the root configurations. On the electronic side, the vacuum consists of three fluxes; on the CF side, there will be two more fluxes. Then by adding particles (electrons with two fluxes on the left and CFs on the right side), we can find the equivalence between the Laughlin state at $\nu = 1/3$ of electrons and a fully-filled CF level (a CF IQH state). If more particles are added, we can also observe the correspondence between the FQH state at $\nu = 2/5$ of electrons and the CF IQH state at $\nu^* = 2$, etc.

It is worth noticing that this approach does not make any reference to a particular wave function, which therefore could be less useful in evaluating experimentally relevant numbers such as gaps, collective mode energies, etc. because it is hard to do quantitative computations with it for large system sizes. In this case, one can take the wave-function-based CF approach to get a variational wave function, which also works for the states without model Hamiltonians [71, 74]. But for the second LL (SLL) or the longer-range interactions, the CFs end up interacting, and other approaches are needed to understand the states occurring in the SLL.

3.5.3 Particle-hole conjugate within a CHS

By observing Eq.(3.57), we can see that if all the occupied and unoccupied orbitals are exchanged, and the restrictions remain unchanged for the unoccupied ones, the generating function will stay the same, but of course, the CHS will be different. Thus we can also establish a *bijection* between these two CHSS, which can be understood as the particle-hole (PH) conjugate of each other. Note that usually, this is only well-defined within a single LL. Otherwise, there will be no “complete” electrons in a sub-Hilbert space anymore. However, the PH conjugation can be defined for any type of fermions, in particular for CFs and composite fermionization, which

allows us to map an electronic state in a CHS to a CF state in one CF level, where we can get the PH conjugate of the CF state and map it back to the electronic basis. Explicit examples will be discussed in Chap.5. The complete commutative diagram between the electronic FQH and CF states is shown in Fig.3.6.

3.6 Summary

In this chapter, we introduced the essential concept of CHS, which originates from the conformal invariance in the sub-Hilbert spaces defined by model Hamiltonians. Meanwhile, as one of the most promising and intuitive theoretical frameworks, the CF theory can explain and quantitatively give the model wave function for many FQH states. We provide a novel interpretation of the composite fermionization as the unitary mapping between isomorphic CHSs, which leads to equivalent CF descriptions of the same FQH states. The isomorphism between CHSs can be rigorously confirmed from the generating functions of their L_z sector degenerates, which also relates the FQH states to conformal blocks with the same generating function. This new approach does not require a presumed CF model wave function and can formally map *any* given state in one CHS to another.

Furthermore, the concept of the CFs as the fluxes attached to electrons naturally emerges in the bijection between isomorphic CHSs. Thus one can regard this as a generalization to the original CF theory. Furthermore, by mapping an FQH state within some CHS to the fully-filled IQH state of CFs and taking the particle-hole conjugate, one can unambiguously define its particle-hole conjugate within this CHS even without well-defined electrons or holes, which can explain the origin of multiple graviton modes in FQH phases as shown in Chap.5. In the near future, it will be significant to generalize this formalism for those states that cannot be expressed as jacks but still have some clustering properties.

Electron basis	Angular momentum	CF basis
$N_e = 3$	$ L^2, L_z, k\rangle$	$N_{CF} = 3$
$N_o = 10$		$N_o' = 7$
$ 10010010000\rangle$	$ 6, 6, 1 \rangle$	$ 1110000\rangle$
\downarrow	\downarrow	\downarrow
$ 10010001000\rangle$	$ 6, 5, 1 \rangle$	$ 1101000\rangle$
\downarrow	\downarrow	\downarrow
$ 10010000100\rangle$	$ 6, 4, 1 \rangle$	$ 1100100\rangle$
$ 10001001000\rangle$	$ 4, 4, 1 \rangle$	$ 1011000\rangle$
\downarrow	\downarrow	\downarrow
$ 10010000010\rangle$	$ 6, 3, 1 \rangle$	$ 1100010\rangle$
$ 01001001000\rangle$	$ 4, 3, 1 \rangle$	$ 1010100\rangle$
$ 10001000100\rangle$	$ 3, 3, 1 \rangle$	$ 0111000\rangle$
\downarrow	\downarrow	\downarrow
$ 10010000001\rangle$	$ 6, 2, 1 \rangle$	$ 1100001\rangle$
$ 01001000100\rangle$	$ 4, 2, 1 \rangle$	$ 1010010\rangle$
$ 10000100100\rangle$	$ 3, 2, 1 \rangle$	$ 0110100\rangle$
$ 10001000010\rangle$	$ 2, 2, 1 \rangle$	$ 1001100\rangle$
\downarrow	\downarrow	\downarrow
$ 10001000001\rangle$	$ 6, 1, 1 \rangle$	$ 1010001\rangle$
$ 01000100100\rangle$	$ 4, 1, 1 \rangle$	$ 1001010\rangle$
$ 10000100010\rangle$	$ 3, 1, 1 \rangle$	$ 0101100\rangle$
$ 01001000010\rangle$	$ 2, 1, 1 \rangle$	$ 0110010\rangle$
\downarrow	\downarrow	\downarrow
$ 10000100001\rangle$	$ 6, 0, 1 \rangle$	$ 1001001\rangle$
$ 01000100010\rangle$	$ 4, 0, 1 \rangle$	$ 1000110\rangle$
$ 10000010010\rangle$	$ 3, 0, 1 \rangle$	$ 0110001\rangle$
$ 01001000001\rangle$	$ 2, 0, 1 \rangle$	$ 0101010\rangle$
$ 00100100100\rangle$	$ 0, 0, 1 \rangle$	$ 0011100\rangle$

FIGURE 3.3: **Isomorphism between the CHS of electrons and CFs.** The electron CHS (left column) is defined by the model Hamiltonian $\hat{V}^{2\text{bdy}}$ and the CF one (right column) is the lowest CF level. All the eigenstates (k denotes the degeneracy) of the angular momentum operator can be expressed as the linear combination of the states on both sides, from which one can easily see the degeneracy of the highest-weight states.

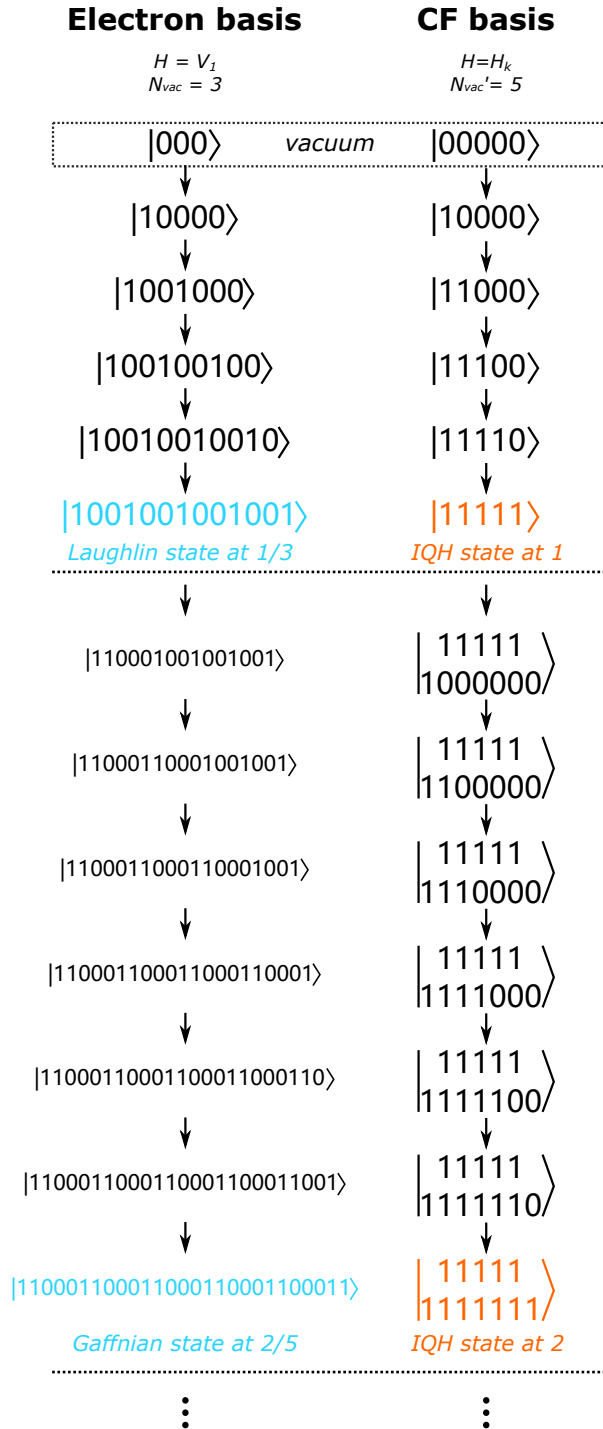


FIGURE 3.4: Composite fermionization between electron and CF basis. On the left column, each state is a jack with the root configuration in the ket and on the right side, a monomial. One can clearly see the correspondence between the electronic Laughlin state at $\nu = 1/3$ /Gaffnian state at $\nu = 2/5$ and the CF IQH states.

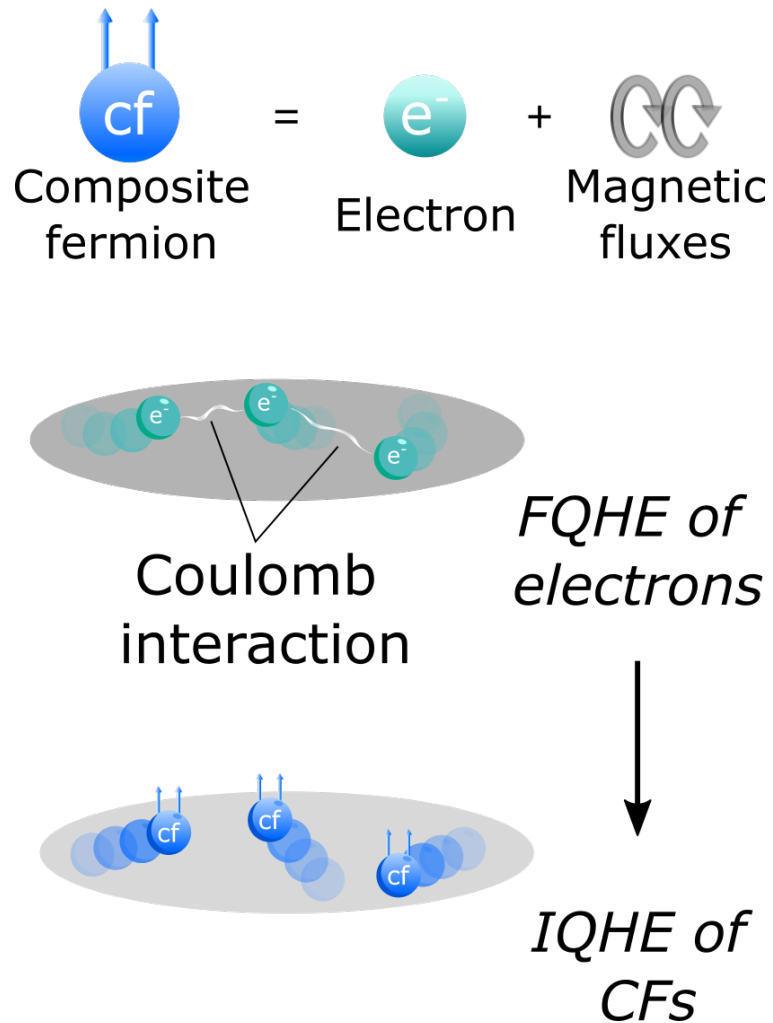


FIGURE 3.5: **The concept of CFs.** A CF is given by attaching one electron with an even number of magnetic flux quanta (which is also called flux attachment). The simplest outcome is that one can eliminate the strong-coupling interactions between the electrons and makes the FQH phases of electrons degenerate into the IQH phases of CFs. Furthermore, one can also relate the FQH states at different filling factors by using the idea of flux attachment.

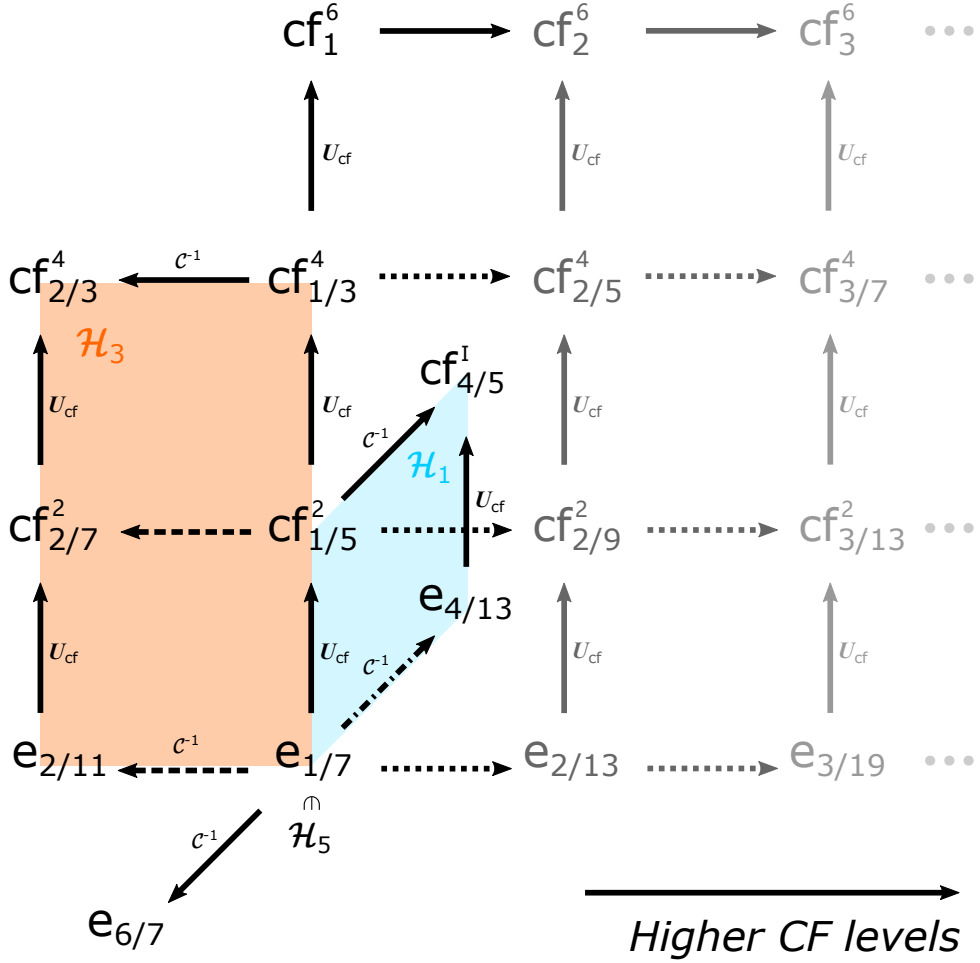


FIGURE 3.6: **Commutative diagram of electronic states and CF states within different CHSs.** Here we use particle filling factor to denote the states and take the Laughlin state at $\nu = 1/7$ as an example, which can be described by three different CF states. U_{cf} denotes the unitary transformation or composite fermionization between isomorphic CHSs. One can find the corresponding particle-hole dual states (denoted by \mathcal{C}^{-1}) within \mathcal{H}_1 (null space of $\hat{V}_1^{2\text{bdy}}$), \mathcal{H}_3 (null space of $\hat{V}_1^{2\text{bdy}} + \hat{V}_3^{2\text{bdy}}$) or the LLL, and map them back to the electron basis. For the fully-filled CF level, we can also increase the LL index to get more Jain states, but the experimental signature could diminish with higher CF levels, as the fading color represents. The same formalism can be generalized to the Laughlin state with an arbitrary filling factor.

Chapter 4

Graviton Modes in Fractional Quantum Hall Liquids

In this section we would like to introduce some quantitative results of the specific low-lying neutral excitations in the FQH phases, called the *graviton modes*. It is not a coincidence that this mode is named after such a highly nontrivial particle, so an introduction to the gravitons will be provided in the first section, where we will focus on the progress of how physicists understand this particle from different approaches and what we expect from the gravitons as specific modes in FQH phases. More interpretations of the FQH gravitons will be introduced in the next chapter. In the second section, we shall see the method to construct the wave function for the graviton modes, which requires a similar approximation as the one Feynman used to study the roton modes in the superfluid. A vital quantity called structure factor will be introduced afterward, with the help of which we can analytically derive the energy of the graviton modes with respect to the three-body and two-body model Hamiltonians. The results can provide many interesting physical insights into the structure of the CHSs and the low-lying excitations, which can be experimentally observed, as introduced in the last section.

4.1 Gravitons as quasiparticles

To understand the differences and, more importantly, the similarities between the FQH graviton modes and the gravitons in space-time, we need to know more about

the concept of gravitons in a more general context, especially the role it plays in physics.

Theoretically speaking, an intuitive way to understand gravitons is to relate them to the gravitational wave, which has been discovered from the merging of black holes [304]. Their relationship is very similar to the one between photons and electromagnetic waves or phonons and acoustic waves. They are the quantization of gravity and carriers of gravitational radiations at the quantum scale. However, as the most intriguing and challenging question in contemporary physics, the quantization of 4D gravity (also known as *quantum gravity*), or more precisely, the attempt to include gravity into a coherent formalism with the other three forces described by quantum field theory, is far from complete, which leads to the incompatibility in the large (governed by general relativity, GR) and the small scales (based on quantum field theory, QFT) in physics [305, 306].

Technically speaking, we tend to understand the QFT as an effective low-energy one, which requires the theory to be irrelevant to the ultraviolet(UV) part, which can be renormalized to get a convergent result that is the same as the complete theory. The main issue of merging gravity into this formalism is that we need infinite terms to cancel out the infinities in the context of QFT (or non-renormalizable). Furthermore, the role of time is different in these two theories, which is equivalent to other dimensions in GR but more like a special parameter in QFT (there are spatial position operators but no time operators).

The deeper reason why QFT and GR cannot be consistent can be found when one tries comparing GR with other successful gauge theories (such as the $U(1)$ theory describing electromagnetic fields) to check their differences: The gauge theories are considering the dynamics of the bundle sections when the geometry is *fixed*, but GR is considering the dynamics of *the geometry (differential structure) itself* [307, 308]. Also, the diffeomorphic invariance in GR ensures that all the observables should be global in a quantum gravity theory, but QFT is instead a theory about local observables [292]. Recently there has been a promising argument called AdS/CFT correspondence that may reconcile this point, which can define a *local* QFT on the asymptotic space-time boundary to describe the *global* quantum gravity in bulk [279]. Of course, this list of contradictions can still be expanded. Still, the main message here is that whether one tries to make the QFT more gravity-like, or the GR more quantum-like, is unlikely to succeed. The introduction of gravitons,

though well defined by all means (one can consider them as the spin-2 or more precisely helicity-2 and massless representations of the Poincaré group without invoking other details), is more or less a *dangerous but understandable* move for unifying the gravity and the quantum, considering it cannot be described by QFT and is not needed in GR.

There have been several novel theories aiming at solving this dilemma, among which the most famous one is the string theory (which is believed to be self-consistent and uses more languages of QFT) [309, 310]. However, the scale that string theory describes is around Planck's length, so it seems hopeless to observe anything to support it in the experiments for now. One of the most important predictions of string theory is the existence of gravitons as *closed strings* [311, 312]. But things are not optimistic for the observation of gravitons either due to the significantly small cross-section as predicted [313]. Another radical attempt called emergent gravity proposed the possibility that gravity could be not a fundamental interaction at all, but only an emergent entropic force from quantum entanglement [314, 315]. So far, none of these arguments have been or even gotten close to being verified.

Thus to study gravitons, there seem to be two choices for the physicists; one is by constructing more powerful detectors than the existing ones (for around 37 orders of magnitude as estimated by Dyson [316]), which might be something we have to make happen in the future to *directly* detect the gravitons; or more realistically, by taking a detour, to see whether it is possible to simulate something similar in specific systems. Condensed matter systems can be regarded as the best candidate for this because of the emergence of abundant quasiparticles that has been observed [317]. In the following sections, we would like to show that one can find the behavior of massive spin-2 gravitons in FQH droplets. The energy of these modes can be rigorously derived from a microscopic picture. On the other hand, the emergence of gravitons in a quantum liquid entirely consisting of electrons also raises a question about the nature of space-time: will there also be some *Planck particles* just like the electrons in FQH liquids, the interaction of which is the origin of the fundamental forces? Maybe they are precisely the strings or something else. But studying the behavior of these FQH graviton modes can help us understand the gravitons better.

The study of the FQH graviton modes also contributes to our understanding of the geometric aspects of FQH phases [230, 318, 319]. As neutral excitations, graviton modes can be experimentally measured with inelastic photon scattering since the

momentum transfer of the photons is small [108, 109, 114, 320–322]. An acoustic crystalline wave is also predicted to act like a gravitational wave, which can interact with the graviton modes as a probe [323]. Furthermore, an optimal-control-based variational quantum algorithm has been designed for realizing the graviton mode in quantum computers [187]. There has also been much interest in the graviton mode due to its spin structure, allowing it to couple selectively to circularly polarized light, making them useful for experimentally distinguishing different topological phases [324]. In addition, it has been recently suggested that coupling the incompressible ground state to the graviton mode from geometric deformation can be responsible for the quench dynamics in FQH [236]. In the context of these experimental proposals and numerical results, a Dirac CF theory conjectures that certain FQH phases may have more than one graviton mode [325, 326]. Thus, from the theoretical and experimental perspectives, analytic results of long-wavelength neutral excitations can help us understand the fundamental nature of the geometric aspects of the FQH topological phases.

4.2 Single mode approximation

It is helpful to get a model wave function for the mode we study in a microscopic formalism. In this section, we shall review how to get the variational wave function describing the FQH graviton modes (which had not been called “graviton modes” when GMP first discovered it) and several concepts relevant to graviton modes that are often mentioned in the literature.

The first-ever single mode approximation (SMA) is believed to be made by Feynman when he was studying the collective modes in superfluid ^4He [48, 49]. A significant feature of the superfluid spectrum is the linear low-lying excitations at small wave numbers (or long wavelengths) followed by a roton minimum [264]. Feynman argued that there must be low-lying phononic collective excitations based on the observation that there can be no nodes in bosonic ground state wave functions. The variational wave function of these low-lying excitations with a specific momentum q can be derived unambiguously from a given (uniform) ground state $|0\rangle$ by using one density operator (that is why it is called “single”) on it:

$$|\mathbf{q}\rangle = \frac{1}{\sqrt{\mathcal{N}}} \cdot \hat{\rho}_{\mathbf{q}} |0\rangle \quad (4.1)$$

which will be orthogonal to the ground state while preserving the intrinsic correlations, and the normalization factor is denoted as \mathcal{N} here. This is similar to how we get the excited state of quantum harmonic oscillators by simply multiplying a displacement operator to the ground state $\psi_0(x)$ to change the parity, i.e., $\psi_1(x) = \hat{x}\psi_0(x)$. It is worth noticing that these modes correspond to *density fluctuations* in the ground state because the probability of a state $\langle \mathbf{q}|\mathbf{q} \rangle \sim \rho_{\mathbf{q}}$, where $\rho_{\mathbf{q}}$ is the density at wave vector \mathbf{q} , which means that those states acting like density waves will have a higher probability than more uniform ones. Furthermore, Feynman also gave the expression for the energy of these modes by observing the similarity between the normalization factor and the static structure factor $S(\mathbf{q})$, which will be introduced at length in the next section [48, 49]:

$$\Delta(\mathbf{q}) = \frac{\mathbf{q}^2}{2m \cdot S(\mathbf{q})} \quad (4.2)$$

where m is the single-particle mass. This expression *qualitatively* agreed well with the experimental results in the long-wavelength limit and successfully predicted the roton minimum.

Unsurprisingly, collective excitations are also observed in the spectra of FQH phases. GMP found that it is possible to use the single mode approximation to describe a species of these modes called the *magneto-roton modes* near the long-wavelength limit as shown in Fig.4.1, even though the underlying particles in FQH phases are fermionic electrons [51, 52]. It seems natural to find low-lying single-particle (thus charged) excitations in generic fermionic systems as well because of the existence of the Fermi surface, but for IQH phases ($\nu \in \mathbb{N}_+$) with a strong magnetic field, the single mode approximation is valid without LL mixing in the long-wavelength limit because of the Kohn's theorem [327]. But for FQH phases ($\nu \in \mathbb{Q}_+$), there will be low-lying intra-LL excitations, and if we directly apply the density operator on the ground state, the resulting state will have quite high energy near the next LL. Thus GMP made a slight modification by replacing the density operator with the guiding-center density operator [51, 52] as introduced in Sec.2.3:

$$|\psi_{\mathbf{q}}\rangle = \frac{1}{\sqrt{\mathcal{N}}} \cdot \delta \hat{\rho}_{\mathbf{q}} |\psi_0\rangle \quad (4.3)$$

where \mathcal{N} is the normalization factor, and we have defined the regularised guiding center density operator as:

$$\delta\hat{\rho}_{\mathbf{q}} = \hat{\rho}_{\mathbf{q}} - \langle \psi_0 | \hat{\rho}_{\mathbf{q}} | \psi_0 \rangle \quad (4.4)$$

so this mode is also called *GMP mode* because GMP first found its model wave function. As a result, all the relevant quantities, such as the static structure factor, will be projected to a single LL. This mode $|\psi_{\mathbf{q}}\rangle$ based on the modified single mode approximation was found to describe the *neutral density mode* with the wave vector up to the one corresponding to the magneto-roton minimum (analogous to the roton minimum in the superfluid spectrum) very well by numerical results, even better than Feynman's original application to ${}^4\text{He}$, because the magnetic field renders the orbitals of electrons to be closed, which automatically fulfills the continuity equation without back-flow corrections:

$$\boldsymbol{\nabla} \cdot \langle \hat{\mathbf{J}}(\mathbf{R}) \rangle = -\frac{1}{2} \boldsymbol{\nabla} \cdot \langle \boldsymbol{\nabla} \times \hat{\rho}_{\mathbf{R}} \cdot \mathbf{e}_z \rangle = 0 \quad (4.5)$$

where \mathbf{e}_z is the unit vector along the orthogonal direction to the surface [52]. Meanwhile, there can still be currents after the LL projection due to the drift along the direction of $\mathbf{E} \times \mathbf{B}$. When the wave vector gets larger than the magneto-roton minimum, the single mode approximation will fail because other modes, such as multi-roton modes, can couple to the density fluctuation as well [112]. As for the leading role in this thesis, the graviton modes are exactly the neutral density modes in the long wavelength limit, so the wave function in Eq.(4.3) is reasonable to be used as their model wave function.

Furthermore, this mode is found to possess a quadrupole moment in the long-wavelength limit, so people also call it a *quadrupole mode*, which becomes a dipole moment near the magneto-roton minimum. This can be easily seen when we numerically construct the SMA wave function, which is found to be equivalent to an angular momentum boosting after LL projection on the sphere [199]:

$$|\psi_{L,M}\rangle = \sum_i \hat{C}_{m_i+M, M, m_i}^{S, L, S} |\psi_0\rangle \quad (4.6)$$

where i is the particle index, L denotes the additional angular momentum added to *each* electrons starting from 2 and $\hat{C}_{m'Mm}^{SLS}|m\rangle = C_{m'Mm}^{SLS}|m'\rangle$ is the operator giving the corresponding Clebsch-Gordan coefficients. It has been verified that the

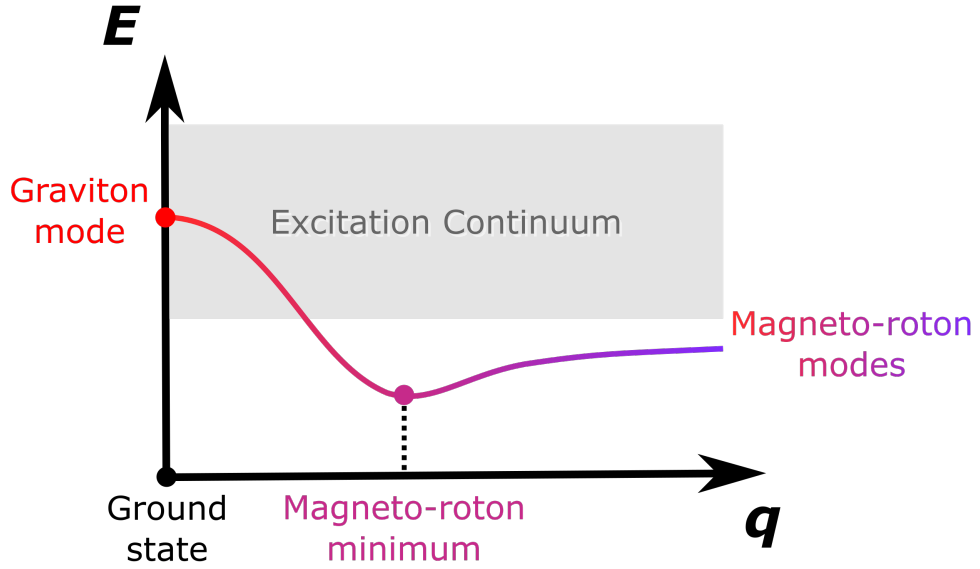


FIGURE 4.1: **Illustration of the excitation spectrum of the Laughlin state.** The graviton mode is the magneto-roton mode in the long-wavelength limit.

single mode approximation is *exact* for the magneto-roton modes in the $L = 2$ and 3 sectors. For graviton modes in a rotationally invariant system, we require $L = M = 2$. Thus the corresponding root configurations of the FQH states can be given by boosting the second electron by 2. For example, the roots of the graviton modes of the first two Laughlin states can be written as:

$$\begin{array}{c} \dots \\ 1 \\ \dots \\ 1 \\ 0 \\ 0 \\ 0 \\ 0 \\ 1 \\ 0 \\ 0 \\ 1 \\ 0 \\ 0 \\ 1 \\ 0 \\ 0 \\ 1 \\ 0 \\ 0 \end{array} \quad (\nu = 1/3) \quad (4.7)$$

$$\begin{array}{c} \dots \\ 1 \\ \dots \\ 1 \\ 0 \\ 0 \\ 1 \\ 0 \\ 0 \\ 0 \\ 0 \\ 0 \\ 1 \\ 0 \\ 0 \\ 0 \\ 0 \\ 1 \\ 0 \\ 0 \\ 0 \\ 0 \\ 1 \end{array} \quad (\nu = 1/5) \quad (4.8)$$

which shows a clear quadrupole structure consisting of two quasiholes (denoted by the dots) and two quasielectrons (denoted by the circles).

To wrap up, the terms we have used can be organized into the relation:

$$\begin{aligned} \text{Graviton mode} &\leftrightarrow \text{GMP mode} \leftrightarrow \text{Quadrupole mode} \\ &\leftrightarrow \text{Magneto-roton/Density mode with } \mathbf{q} \rightarrow 0 \end{aligned}$$

which reveals different aspects of this mode. In the following discussions, we will only call $|\psi_{\mathbf{q}}\rangle$ the graviton mode, defined by:

Definition 4.1. The SMA wave function describing the graviton modes

$$|\psi_{\mathbf{q}}\rangle = \frac{1}{\sqrt{\mathcal{N}}} \cdot \delta \hat{\rho}_{\mathbf{q}} |\psi_0\rangle \quad (4.9)$$

which we believe is the most proper name to reveal the geometric nature of this mode as explained in the next chapter.

4.3 Structure factor

Just like how we can *see* things by receiving and processing the photons with specific frequencies and momenta scattered by the objects, experimentalists use the same idea to probe the internal structure of crystals (indeed we can *directly* observe the structure by using scanning tunneling microscopy(STM) nowadays but let us ignore this technique for now). The difference is that normally the particles they choose are not the photons with the frequency of visible light, but photons with higher frequencies (like X-rays), electrons, or more ideally, neutrons (because they are neutral but not spinless, sensitive to light elements and able to distinguish isotopes). The collision between the probing particles and the lattice could be *elastic*, which means that there will only be momentum transfers (\mathbf{q} changes), or *inelastic*, which is commonly seen in neutron scattering or Raman scattering experiments with both energy and momentum transfers (both ω and \mathbf{q} change) [264]. In the following discussions let us assume that the scattering is coherent, i.e. there will be no spin flipping, and we will introduce the physical significance and properties of an important quantity called the *structure factor*, and its interplay with the SMA state.

The basic idea is that when we calculate the scattering rate by using Fermi's golden rule [328] (now we need to use the quantum mechanical formalism) and Born's approximation [329], it is found to be proportional to the *dynamic structure factor*, defined as:

$$\begin{aligned} S(\mathbf{q}, \omega) &\equiv \frac{1}{N} \int_{-\infty}^{\infty} dt e^{i\omega t} \sum_{j,k=1}^N \langle e^{i\mathbf{q} \cdot \hat{\mathbf{r}}_j(t)} \cdot e^{-i\mathbf{q} \cdot \hat{\mathbf{r}}_k(0)} \rangle_i \\ &= \frac{1}{N} \int_{-\infty}^{\infty} dt e^{i\omega t} \langle \hat{\rho}_{-\mathbf{q}}(t) \hat{\rho}_{\mathbf{q}}(0) \rangle_i \end{aligned} \quad (4.10)$$

Thus from this definition, we can interpret it as the quantitative description of the dynamical density correlations. Here $\langle \dots \rangle_i$ denotes taking the average over all the possible initial states, so we can write down an equivalent expression as:

$$S(\mathbf{q}, \omega) = \frac{2\pi}{N} \sum_i \frac{e^{-\beta E_i}}{Z} |\langle \psi_i | \rho_{\vec{q}} | \psi_f \rangle|^2 \cdot \delta [\omega - (E_f - E_i)] \quad (4.11)$$

where β is the Boltzmann coefficient and Z is the partition function of the initial states. This turns out to be the *spectral function* of the SMA state $|\psi_{\mathbf{q}}\rangle = \hat{\rho}_{\vec{q}}|\psi_f\rangle$ in the Hilbert space consisting of the initial states! As we shall see later, these properties lead to the important role of the structure factor in the calculations about the graviton modes.

Meanwhile as $S(\mathbf{q}, \omega)$ provides a distribution of the frequency ω , we can naturally study the corresponding moments μ_n . The zeroth moment is called a *static structure factor*, given by:

$$S(\mathbf{q}) \equiv \mu_0 [S(\mathbf{q}, \omega)] = \int_{-\infty}^{\infty} \frac{d\omega}{2\pi} S(\mathbf{q}, \omega) = \frac{1}{N} \sum_{j,k} \langle \hat{\rho}_{-\mathbf{q}}(0) \hat{\rho}_{\mathbf{q}}(0) \rangle_i \quad (4.12)$$

Thus if we look at the $S(\mathbf{q})$ in a system in equilibrium, it should be directly related to the two-point density correlator. Also, consider the case with a unique initial state $|\psi_0\rangle$, the static structure factor provides nothing but the normalization factor of the corresponding SMA state constructed from $|\psi_0\rangle$.

The first moment is called a *oscillator strength*:

$$f(\mathbf{q}) \equiv \mu_1 [S(\mathbf{q}, \omega)] = \int_{-\infty}^{\infty} \frac{d\omega}{2\pi} \omega S(\mathbf{q}, \omega) = \frac{1}{2N} \left\langle \left[\hat{\rho}_{-\mathbf{q}}, \left[\hat{H}_s, \hat{\rho}_{\mathbf{q}} \right] \right] \right\rangle_i \quad (4.13)$$

where \hat{H}_s is the Hamiltonian of the probed system. For a generic system with a commutative geometry (so the operators along orthogonal directions commute), the commutator can be derived explicitly [52]:

$$\left\langle \left[\hat{\rho}_{-\mathbf{q}}, \left[\hat{H}_s, \hat{\rho}_{\mathbf{q}} \right] \right] \right\rangle_i = \frac{Nq^2}{m} \quad (4.14)$$

where $q = |\mathbf{q}|$ and m denotes the mass of the particles in the system. The corresponding oscillator strength is $q^2/2m$, also called the *f-sum rule* [264, 330]. The expectation value of the energy of the excitations created in this process is given

by the ratio:

$$\Delta(\mathbf{q}) = \frac{f(\mathbf{q})}{S(\mathbf{q})} \quad (4.15)$$

So the static structure factor serves as the renormalization factor of the energy gained by a single particle from $\hbar\mathbf{q}$ due to the particle configuration in the system, which will be unity if there is no internal structure at all (i.e. a single particle scattering). Moreover, $\Delta(\mathbf{q})$ in a system with commutative geometry will give the Feynman-Bijl formula [49, 331]:

$$\Delta(\mathbf{q}) = \frac{1}{S(\mathbf{q})} \frac{q^2}{2m} \quad (4.16)$$

which will fail when there is a magnetic field present in the system because it will bring non-commutativity to the orthogonal directions. But Eq.(4.15) still holds. In 1985, GMP first transplanted the formalism above to the collective modes in FQH phases as introduced in the last section. The f -sum rule in this case gives the upper bound of the collective-mode dispersion, which reveals the equivalence between the exactness of SMA and how much the density-wave modes saturate the f -sum rule. Furthermore, they define the guiding center static structure factor \bar{S} and the guiding center oscillator strength \bar{f} and found that both quantities have the quartic leading term in the long-wavelength limit. In 2011, Haldane set up the relation between \bar{S} and \bar{f} to the guiding center shear modulus of an FQH droplet, which also showed their geometric nature [230].

The graviton modes are constructed by using the density fluctuations from the ground state, so we can imagine that they should contribute to the static structure factor as well. It is worth noticing that the definition of the static structure factor can be different among literature. For example, it could be defined per magnetic flux or per electron, etc. In the following discussions, we will adopt the convention:

Definition 4.2. Regularised two-body (static) guiding-center structure factor for the unperturbed ground state:

$$S_{\mathbf{q}} = \langle \delta\hat{\rho}_{\mathbf{q}} \delta\hat{\rho}_{-\mathbf{q}} \rangle_0 \quad (4.17)$$

where $\langle \quad \rangle_0$ denotes taking the expectation value with respect to the ground state.

By doing so we can clearly see that the normalization factor \mathcal{N} in the SMA wave function Eq.(4.3) is exactly the two-body structure factor S_q . Haldane derived an

important property of this quantity, called the self-duality, which holds as long as the density matrix is *translationally invariant*, given by:

$$S_{\mathbf{q}} - S_{\infty} = \xi \int \frac{d^2 \mathbf{q}'}{2\pi} e^{i\mathbf{q} \times \mathbf{q}'} (S_{\mathbf{q}'} - S_{\infty}) \quad (4.18)$$

where $\xi = 1$ for bosons and -1 for fermions and we will omit “static” in the following for simplicity. Note that this means that $S_{\mathbf{q}} - S_{\infty}$ is an eigenfunction of the 2D Fourier transform functional. Another important quantity we need is:

Definition 4.3. Reduced three-body guiding-center structure factor for the unperturbed ground state:

$$\bar{S}_{\mathbf{q}_1, \mathbf{q}_2} = \sum_{i \neq j \neq k} \langle \hat{\rho}_{\mathbf{q}_1}^i \hat{\rho}_{\mathbf{q}_2}^j \hat{\rho}_{-\mathbf{q}_1 - \mathbf{q}_2}^k \rangle_0 = \sum_{i \neq j \neq k} \left\langle e^{iq_{1a}\hat{R}_i^a} e^{iq_{2a}\hat{R}_j^a} e^{-i(q_{1a}+q_{2a})\hat{R}_k^a} \right\rangle_0 \quad (4.19)$$

This quantity is defined by guiding center density operators so we call it “reduced”. This definition will not influence the physics but only simplify the derivations. It also has the self-duality property because of its translationally invariant nature.

4.4 Analytic results of the graviton gap

In this section, we will show how to derive the *exact* expression of the energy of graviton modes with respect to two-body and three-body model Hamiltonians, which will help with rigorously determining whether a graviton mode belongs to some specific CHS, and we will focus on the intuition behind each step while trying to keep the mathematical rigor. It is worth noting that although using LEC offers a very simple way of determining if the graviton mode belongs to the null space of some model Hamiltonian, it only applies to the cases where the root configurations are easy to find, and fundamentally the LEC scheme is only “proven” numerically [204, 205].

4.4.1 Assumptions

Firstly let us focus on all the physical assumptions we make, some of which can simplify the question and some of them are necessary to the discussion:

Assumption 1 (Rotational invariance) *The angular momentum quantum numbers are good quantum numbers and the interactions only have radial components.*

This restricts the geometry to the disk or the sphere, and the single-particle wave functions are given by the generalized Laguerre polynomials after picking a symmetric gauge.

Assumption 2 (Long-wavelength limit) *The momentum of the graviton mode should be close to 0.*

This condition is crucial in the whole derivation and directly related to the validity of the next assumption. If somehow we can apply the conclusion to the modes out of this domain, we expect to get the mean value of the energy of all the modes coupling to the density of the ground state, which will not be related to graviton modes anymore.

Assumption 3 (Single-mode approximation) *The graviton mode wave function can be constructed by the regularized density operator acting on the ground state.*

The single-mode approximation is *exact* only in the long-wavelength limit because the corresponding graviton mode will saturate the oscillator-strength sum rule. Normally a hidden condition with this assumption is that the ground state should be homogeneous and isotropic, which is naturally fulfilled in the FQH phases we discuss.

Assumption 4 (Thermodynamic limit) *The particle number in the system is considered as infinity.*

This assumption can be weakened as long as there is no strong edge effect or finite-size effect present in the system. Here we just push everything such as particle number or system size to infinity for simplicity.

Assumption 5 (Single LL) *All the physical quantities will be projected to a single LL.*

This means that only the guiding center coordinates are involved in the dynamics and it is also the origin of effective many-body interactions. Without loss of generality, one can choose the LLL.

Assumption 6 (Fermionic statistics) All the particles are fermions in the system.

The wave functions should be anti-symmetric as a result. We assume the fermionic case considering that strong repulsive interactions are required for stabilizing bosonic IQH or FQH phases because of the condensation behavior near zero temperature, which will be an unnecessary burden to the Hamiltonian. But it does not kill off the possibility of studying graviton modes in bosonic phases (think about the success of SMA in superfluid), which remains to be studied in the future.

Furthermore, the magnetic length l_B is set to be 1. Bold symbols (e.g. \mathbf{q}_i) are used to denote two-dimensional vectors and the scalars will be plain (e.g. q_i). Also, the Einstein summation convention is adopted in the results.

4.4.2 Three-body interactions

As explained in Chap. 2, The generic three-body Hamiltonian in a single LL can be written as:

$$\begin{aligned} \hat{H}_{3\text{bdy}} = & \int \frac{d^2\mathbf{q}_1 d^2\mathbf{q}_2}{(2\pi)^4} V_{\mathbf{q}_1, \mathbf{q}_2} \hat{\rho}_{\mathbf{q}_1} \hat{\rho}_{\mathbf{q}_2} \hat{\rho}_{-\mathbf{q}_1 - \mathbf{q}_2} \\ & - \int \frac{d^2\mathbf{q}_1 d^2\mathbf{q}_2}{(2\pi)^4} V_{\mathbf{q}_1, \mathbf{q}_2} (\hat{\rho}_{\mathbf{q}_1 + \mathbf{q}_2} \hat{\rho}_{-\mathbf{q}_1 - \mathbf{q}_2} + \hat{\rho}_{\mathbf{q}_1} \hat{\rho}_{-\mathbf{q}_1} + \hat{\rho}_{\mathbf{q}_2} \hat{\rho}_{-\mathbf{q}_2}) \\ & - N_e \int \frac{d^2\mathbf{q}_1 d^2\mathbf{q}_2}{(2\pi)^4} V_{\mathbf{q}_1, \mathbf{q}_2} = \sum_{i \neq j \neq k} \int \frac{d^2\mathbf{q}_1 d^2\mathbf{q}_2}{(2\pi)^4} V_{\mathbf{q}_1, \mathbf{q}_2} \hat{\rho}_{\mathbf{q}_1}^i \hat{\rho}_{\mathbf{q}_2}^j \hat{\rho}_{-\mathbf{q}_1 - \mathbf{q}_2}^k \end{aligned} \quad (4.20)$$

where N_e denotes the number of electrons and the summation over particle indices with $i \neq j \neq k$ restricts this interaction to be strictly three-body. Then the ground state energy should be given by:

$$E_0 = \sum_{i \neq j \neq k} \int \frac{d^2\mathbf{q}_1 d^2\mathbf{q}_2}{(2\pi)^4} V_{\mathbf{q}_1, \mathbf{q}_2} \langle \psi_0 | \hat{\rho}_{\mathbf{q}_1}^i \hat{\rho}_{\mathbf{q}_2}^j \hat{\rho}_{-\mathbf{q}_1 - \mathbf{q}_2}^k | \psi_0 \rangle = \int \frac{d^2\mathbf{q}_1 d^2\mathbf{q}_2}{(2\pi)^4} V_{\mathbf{q}_1, \mathbf{q}_2} \bar{S}_{\mathbf{q}_1, \mathbf{q}_2} \quad (4.21)$$

where $\bar{S}_{\mathbf{q}_1, \mathbf{q}_2}$ denotes the reduced three-body structure factor for the unperturbed ground state.

Remember that the graviton mode can be described by the SMA model wave function in the long-wavelength limit:

$$|\psi_{\mathbf{q}}\rangle = \frac{1}{\sqrt{S_q}} \delta\hat{\rho}_{\mathbf{q}} |\psi_0\rangle \quad (4.22)$$

where $\delta\hat{\rho}_{\mathbf{q}}$ denotes the regularised *guiding centre* operator (note that we omit the bar here). The energy of the graviton mode is given by:

$$\begin{aligned} \delta E_{\mathbf{q} \rightarrow 0} &= \lim_{\mathbf{q} \rightarrow 0} \frac{\langle \psi_{\mathbf{q}} | \hat{H}_{3\text{bdy}} | \psi_{\mathbf{q}} \rangle}{\langle \psi_{\mathbf{q}} | \psi_{\mathbf{q}} \rangle} - E_0 = \lim_{\mathbf{q} \rightarrow 0} \frac{\left\langle \psi_0 \left| \left[\delta\hat{\rho}_{-\mathbf{q}}, \left[\hat{H}_{3\text{bdy}}, \delta\hat{\rho}_{\mathbf{q}} \right] \right] \right| \psi_0 \right\rangle}{2S_q} \\ &= \lim_{\mathbf{q} \rightarrow 0} \sum_{i \neq j \neq k} \int \frac{d^2\mathbf{q}_1 d^2\mathbf{q}_2}{(2\pi)^4} V_{\mathbf{q}_1, \mathbf{q}_2} \times \frac{\left\langle \psi_0 \left| \left[\delta\hat{\rho}_{-\mathbf{q}}, \left[\hat{\rho}_{\mathbf{q}_1}^i \hat{\rho}_{\mathbf{q}_2}^j \hat{\rho}_{-\mathbf{q}_1 - \mathbf{q}_2}^k, \delta\hat{\rho}_{\mathbf{q}} \right] \right] \right| \psi_0 \right\rangle}{2S_q} \end{aligned} \quad (4.23)$$

Thus it can be regarded as exactly a special case of Eq.(4.15). Note that *the particle indices have no effect on the commutation rules of the density operators*, so for simplicity we will omit the index i, j, k and the summation symbol $\sum_{i \neq j \neq k}$ in the following derivations. Firstly by considering the GMP algebra:

$$[\hat{\rho}_{\mathbf{q}_1}, \hat{\rho}_{\mathbf{q}_2}] = 2i \sin \frac{\mathbf{q}_1 \wedge \mathbf{q}_2}{2} \hat{\rho}_{\mathbf{q}_1 + \mathbf{q}_2} \quad (4.24)$$

we can write the commutator as:

$$\begin{aligned} & [\hat{\rho}_{-\mathbf{q}}, [\hat{\rho}_{\mathbf{q}_1} \hat{\rho}_{\mathbf{q}_2} \hat{\rho}_{-\mathbf{q}_1 - \mathbf{q}_2}, \hat{\rho}_{\mathbf{q}}]] \\ &= -4 \left[\sin \frac{(\mathbf{q}_1 + \mathbf{q}_2) \wedge \mathbf{q}}{2} \sin \frac{(\mathbf{q}_1 + \mathbf{q}_2 - \mathbf{q}) \wedge \mathbf{q}}{2} + \sin \frac{\mathbf{q}_2 \wedge \mathbf{q}}{2} \sin \frac{(\mathbf{q}_2 + \mathbf{q}) \wedge \mathbf{q}}{2} \right. \\ & \quad \left. + \sin \frac{\mathbf{q}_1 \wedge \mathbf{q}}{2} \sin \frac{(\mathbf{q}_1 + \mathbf{q}) \wedge \mathbf{q}}{2} \right] \bar{S}_{\mathbf{q}_1, \mathbf{q}_2} \\ & \quad - 4 \sin \frac{\mathbf{q} \wedge (\mathbf{q}_1 + \mathbf{q}_2)}{2} \left[\sin \frac{\mathbf{q}_1 \wedge \mathbf{q}}{2} (\bar{S}_{\mathbf{q}_1 - \mathbf{q}, \mathbf{q}_2} + \bar{S}_{\mathbf{q}_1 + \mathbf{q}, \mathbf{q}_2}) \right. \\ & \quad \left. + \sin \frac{\mathbf{q}_2 \wedge \mathbf{q}}{2} (\bar{S}_{\mathbf{q}_1, \mathbf{q}_2 - \mathbf{q}} + \bar{S}_{\mathbf{q}_1, \mathbf{q}_2 + \mathbf{q}}) \right] \\ & \quad - 4 \sin \frac{\mathbf{q}_2 \wedge \mathbf{q}}{2} \sin \frac{\mathbf{q}_1 \wedge \mathbf{q}}{2} (\bar{S}_{\mathbf{q}_1 - \mathbf{q}, \mathbf{q}_2 + \mathbf{q}} + \bar{S}_{\mathbf{q}_1 + \mathbf{q}, \mathbf{q}_2 - \mathbf{q}}) \\ & \equiv \mathcal{S}_1 + \mathcal{S}_2 + \mathcal{S}_3 \end{aligned} \quad (4.25)$$

which can be expanded as:

$$\begin{aligned}\mathcal{S}_1 &= -2[(\mathbf{q}_1 \wedge \mathbf{q}) \cdot (\mathbf{q}_2 \wedge \mathbf{q}) + (\mathbf{q}_2 \wedge \mathbf{q})^2 + (\mathbf{q}_1 \wedge \mathbf{q})^2 + O(\mathbf{q}^3)]\bar{S}_{\mathbf{q}_1, \mathbf{q}_2} \\ \mathcal{S}_2 &= [(\mathbf{q}_1 \wedge \mathbf{q})^2 + (\mathbf{q}_1 \wedge \mathbf{q}) \cdot (\mathbf{q}_2 \wedge \mathbf{q}) + O(\mathbf{q}^3)](\bar{S}_{\mathbf{q}_1 - \mathbf{q}, \mathbf{q}_2} + \bar{S}_{\mathbf{q}_1 + \mathbf{q}, \mathbf{q}_2}) \\ &\quad + [(\mathbf{q}_2 \wedge \mathbf{q})^2 + (\mathbf{q}_1 \wedge \mathbf{q}) \cdot (\mathbf{q}_2 \wedge \mathbf{q}) + O(\mathbf{q}^3)](\bar{S}_{\mathbf{q}_1, \mathbf{q}_2 - \mathbf{q}} + \bar{S}_{\mathbf{q}_1, \mathbf{q}_2 + \mathbf{q}}) \\ \mathcal{S}_3 &= -[(\mathbf{q}_1 \wedge \mathbf{q}) \cdot (\mathbf{q}_2 \wedge \mathbf{q}) + O(\mathbf{q}^3)](\bar{S}_{\mathbf{q}_1 - \mathbf{q}, \mathbf{q}_2 + \mathbf{q}} + \bar{S}_{\mathbf{q}_1 + \mathbf{q}, \mathbf{q}_2 - \mathbf{q}})\end{aligned}\tag{4.26}$$

Then we expand the structure factors to the second order, which gives:

$$\begin{aligned}&\bar{S}_{\mathbf{q}_1 - \mathbf{q}, \mathbf{q}_2} + \bar{S}_{\mathbf{q}_1 + \mathbf{q}, \mathbf{q}_2} \\ &= 2\bar{S}_{\mathbf{q}_1, \mathbf{q}_2} + \left(\mathbf{q}_x \frac{\partial}{\partial \mathbf{q}_{1x}} + \mathbf{q}_y \frac{\partial}{\partial \mathbf{q}_{1y}} \right)^2 \bar{S}_{\mathbf{q}_1, \mathbf{q}_2} + O(\mathbf{q}^3) \sim [2 + (\mathbf{q} \cdot \boldsymbol{\nabla}_1)^2]\bar{S}_{\mathbf{q}_1, \mathbf{q}_2}\end{aligned}\tag{4.27}$$

and

$$\begin{aligned}&\bar{S}_{\mathbf{q}_1, \mathbf{q}_2 - \mathbf{q}} + \bar{S}_{\mathbf{q}_1, \mathbf{q}_2 + \mathbf{q}} \\ &= 2\bar{S}_{\mathbf{q}_1, \mathbf{q}_2} + \left(\mathbf{q}_x \frac{\partial}{\partial \mathbf{q}_{2x}} + \mathbf{q}_y \frac{\partial}{\partial \mathbf{q}_{2y}} \right)^2 \bar{S}_{\mathbf{q}_1, \mathbf{q}_2} + O(\mathbf{q}^3) \sim [2 + (\mathbf{q} \cdot \boldsymbol{\nabla}_2)^2]\bar{S}_{\mathbf{q}_1, \mathbf{q}_2}\end{aligned}\tag{4.28}$$

and

$$\begin{aligned}&\bar{S}_{\mathbf{q}_1 - \mathbf{q}, \mathbf{q}_2 + \mathbf{q}} + \bar{S}_{\mathbf{q}_1 + \mathbf{q}, \mathbf{q}_2 - \mathbf{q}} \\ &= 2\bar{S}_{\mathbf{q}_1, \mathbf{q}_2} + \left(\mathbf{q}_x \frac{\partial}{\partial \mathbf{q}_{1x}} + \mathbf{q}_y \frac{\partial}{\partial \mathbf{q}_{1y}} - \mathbf{q}_x \frac{\partial}{\partial \mathbf{q}_{2x}} - \mathbf{q}_y \frac{\partial}{\partial \mathbf{q}_{2y}} \right)^2 \bar{S}_{\mathbf{q}_1, \mathbf{q}_2} + O(\mathbf{q}^3) \\ &\sim [2 + (\mathbf{q} \cdot (\boldsymbol{\nabla}_1 - \boldsymbol{\nabla}_2))^2]\bar{S}_{\mathbf{q}_1, \mathbf{q}_2}\end{aligned}\tag{4.29}$$

where we use $\boldsymbol{\nabla}_i \equiv \frac{\partial}{\partial q_{ix}} \hat{\mathbf{e}}_x + \frac{\partial}{\partial q_{iy}} \hat{\mathbf{e}}_y$. By taking the three equations above back to Eq.(4.25), we have:

$$\begin{aligned}&\langle \psi_0 | [\hat{\rho}_{-\mathbf{q}}, [\hat{\rho}_{\mathbf{q}_1} \hat{\rho}_{\mathbf{q}_2} \delta \hat{\rho}_{-\mathbf{q}_1 - \mathbf{q}_2}, \delta \hat{\rho}_{\mathbf{q}}]] | \psi_0 \rangle \\ &= [(\mathbf{q}_1 \wedge \mathbf{q})(\mathbf{q} \cdot \boldsymbol{\nabla}_1) + (\mathbf{q}_2 \wedge \mathbf{q})(\mathbf{q} \cdot \boldsymbol{\nabla}_2)]^2 \bar{S}_{\mathbf{q}_1, \mathbf{q}_2} + O(\mathbf{q}^5)\end{aligned}\tag{4.30}$$

In the last section, we have introduced the self-duality of the two-body structure factor, so we can expand them with the generalized Laguerre polynomials based on the following lemma:

Lemma 4.1. *Let the operators \hat{F}^1 and \hat{F}^{-1} denote the two-dimensional Fourier transform and its inverse transform, then the eigenvalue equation for operator \hat{F}^1*

is given by [332]:

$$\hat{F}^1 [\Psi_{sm}(\mathbf{q})] = (-1)^s (i)^m \Psi_{sm}(\mathbf{p}) \quad (4.31)$$

with the two-dimensional Laguerre–Gaussian (LG) function of vector \mathbf{q} defined by:

$$\Psi_{sm}(\mathbf{q}) = \left[\frac{2(s!)}{(s+m)!} \right]^{1/2} \mathbf{q}^m L_s^{(m)}(|\mathbf{q}|^2) \exp\left(-\frac{1}{2}|\mathbf{q}|^2\right) \quad (4.32)$$

Now we will prove that the three-body structure factor also has the same property:

Proposition 4.1. *The reduced structure factor $\bar{S}_{\tilde{\mathbf{q}}_1, \tilde{\mathbf{q}}_2}$ can be expanded with generalized Laguerre-Gaussian functions as:*

$$\begin{aligned} \bar{S}_{\tilde{\mathbf{q}}_1, \tilde{\mathbf{q}}_2} &= \sum_{i; n_1 n_2} d_i^{n_1 n_2} \sqrt{\frac{n_1! \cdot n_2!}{(n_1 + i)! \cdot (n_2 - i)!}} \left(\frac{\tilde{\mathbf{q}}_1}{\tilde{\mathbf{q}}_2} \right)^i \times L_{n_1}^{(i)}\left(\frac{\tilde{Q}_1}{2}\right) L_{n_2}^{(-i)}\left(\frac{\tilde{Q}_2}{2}\right) e^{-\frac{1}{4}(\tilde{Q}_1 + \tilde{Q}_2)} \\ &= \int \frac{d^2 \tilde{\mathbf{p}}_1 d^2 \tilde{\mathbf{p}}_2}{4 \times 4\pi^2} e^{-\frac{i}{2}(\tilde{\mathbf{q}}_1 \times \tilde{\mathbf{p}}_1 + \tilde{\mathbf{q}}_2 \times \tilde{\mathbf{p}}_2)} \bar{S}_{\tilde{\mathbf{p}}_1, \tilde{\mathbf{p}}_2} \end{aligned} \quad (4.33)$$

and the Fourier transform can be written as:

$$\begin{aligned} \bar{S}_{\tilde{\mathbf{p}}_1, \tilde{\mathbf{p}}_2} &= \sum_{i; n_1 n_2} (-1)^{n_1 + n_2} d_i^{n_1 n_2} \sqrt{\frac{n_1! \cdot n_2!}{(n_1 + i)! \cdot (n_2 - i)!}} \left(\frac{\tilde{\mathbf{p}}_1}{\tilde{\mathbf{p}}_2} \right)^i \\ &\quad \times L_{n_1}^{(i)}\left(\frac{\tilde{P}_1}{2}\right) L_{n_2}^{(-i)}\left(\frac{\tilde{P}_2}{2}\right) e^{-\frac{1}{4}(\tilde{P}_1 + \tilde{P}_2)} \end{aligned} \quad (4.34)$$

where we have defined:

$$\tilde{Q}_1 = \tilde{\mathbf{q}}_1^2 = |\tilde{\mathbf{q}}_1|^2, \quad \tilde{Q}_2 = \tilde{\mathbf{q}}_2^2 = |\tilde{\mathbf{q}}_2|^2, \quad \tilde{P}_1 = \tilde{\mathbf{p}}_1^2 = |\tilde{\mathbf{p}}_1|^2, \quad \tilde{P}_2 = \tilde{\mathbf{p}}_2^2 = |\tilde{\mathbf{p}}_2|^2 \quad (4.35)$$

Proof. This is equivalent to proving the *self-duality* of the three-body structure factor. For any three particles indexed by s , j , and k in the system, the conclusions in Eq.(2.64) are always true. So by considering the definition of the reduced structure factor, we can rewrite it as:

$$\bar{S}_{\mathbf{q}_1, \mathbf{q}_2} = \sum_{s \neq j \neq k} \mathcal{N}^{sjk} \cdot \sum_{n_1, n_2} \sum_{n'_1, n'_2} \alpha^{*n_1 n_2} \alpha^{n'_1 n'_2} \left(\left\langle n_1, n_2 \left| e^{i\tilde{q}_{sa}\hat{R}_{sj}^a} e^{i\tilde{q}_{ja}\hat{R}_{sj,k}^a} \right| n'_1, n'_2 \right\rangle \right)_{sjk} \quad (4.36)$$

where $\alpha^{n_1 n_2}$ is defined in Definition.2.63 the tensor \mathcal{N}^{sjk} describes the overall factor related to all the other particles:

$$\mathcal{N}^{sjk} = \mathcal{N}(\mathbf{R}_1, \dots, \mathbf{R}_{s-1}, \mathbf{R}_{s+1}, \dots, \mathbf{R}_{j-1}, \mathbf{R}_{j+1}, \dots, \mathbf{R}_{k-1}, \mathbf{R}_{k+1}, \dots, \mathbf{R}_N) \quad (4.37)$$

Thus by defining:

$$d_i^{n_1 n_2} = \sum_{s \neq j \neq k} \mathcal{N}^{sjk} \alpha^{*n_1 n_2} \alpha^{n'_1 n'_2} = \sum_{s \neq j \neq k} \mathcal{N}^{sjk} \alpha^{*n_1, n_2} \alpha^{n_1+i, n_2-i} \quad (4.38)$$

we can write the reduced structure factor as:

$$\bar{S}_{\tilde{\mathbf{q}}_1, \tilde{\mathbf{q}}_2} = \sum_{i; n_1 n_2} d_i^{n_1 n_2} \sqrt{\frac{n_1! \cdot n_2!}{(n_1 + i)! \cdot (n_2 - i)!}} \left(\frac{\tilde{\mathbf{q}}_1}{\tilde{\mathbf{q}}_2} \right)^i \times L_{n_1}^{(i)} \left(\frac{\tilde{Q}_1}{2} \right) L_{n_2}^{(-i)} \left(\frac{\tilde{Q}_2}{2} \right) e^{-\frac{1}{4}(\tilde{Q}_1 + \tilde{Q}_2)} \quad (4.39)$$

Note that n'_1 and n'_2 have been represented by $i \equiv \Delta n_1$ here. Then according to Lemma.4.1, generalized Laguerre polynomials are the eigenfunctions of two-dimensional Fourier transform, so Eq.(4.34) obviously holds, which gives the self-duality of $\bar{S}_{\mathbf{q}_1, \mathbf{q}_2}$. \square

As we can see, the problem with the definition above is that we need to do lots of numerical calculations to get the values of $d_i^{n_1 n_2}$. However, the ratio between the coefficients $d_i^{n_1 n_2}$ with different i only depends on α^{*n_1, n_2} and α^{n_1+i, n_2-i} , which can be calculated easily and the results are shown in Table.F.1. So one can take a specific $d_i^{n_1 n_2}$ as a reference to efficiently get the other expansion coefficients with the same n_1 and n_2 but different i .

Definition 4.4. The reduced-structure-factor expansion coefficient of the reference

$$\begin{aligned} \bar{d}^{n_1 n_2} &\equiv \int \frac{d^2 \tilde{\mathbf{q}}_1 d^2 \tilde{\mathbf{q}}_2}{(2\pi)^4} \bar{S}_{\tilde{\mathbf{q}}_1, \tilde{\mathbf{q}}_2} L_{n_1}^{(0)} \left(\frac{\tilde{Q}_1}{2} \right) L_{n_2}^{(0)} \left(\frac{\tilde{Q}_2}{2} \right) e^{-\frac{1}{4}(\tilde{Q}_1 + \tilde{Q}_2)} = d_0^{n_1 n_2} \\ &\propto \alpha^{n_1, n_2} = \sum_{n_1, n_2} \langle n_1, n_2 | \psi_3 \rangle \end{aligned} \quad (4.40)$$

Corollary 4.2. Any expansion coefficient can also be expressed as

$$d_i^{n_1 n_2} = \frac{\alpha^{n_1+i, n_2-i}}{\alpha^{n_1, n_2}} \cdot \bar{d}^{n_1 n_2} \quad (4.41)$$

Similarly the rotationally-invariant interaction $V_{\tilde{Q}_1, \tilde{Q}_2}$ can also be expanded with the Laguerre-Gaussian polynomials (or Haldane pseudopotentials) as explained in Chap.2:

$$V_{\tilde{\mathbf{q}}_1, \tilde{\mathbf{q}}_2} = \sum_{m_1 m_2} c^{m_1 m_2} L_{m_1}^{(0)} \left(\frac{\tilde{Q}_1}{2} \right) L_{m_2}^{(0)} \left(\frac{\tilde{Q}_2}{2} \right) e^{-\frac{1}{4}(\tilde{Q}_1 + \tilde{Q}_2)} \quad (4.42)$$

Note that the form of the interactions can be freely chosen as long as it obeys the basic assumptions in the last section. In this thesis, we will not take the more complicated forms involving generalized Laguerre polynomials into account.

Then by differentiating the exponential functions, we have:

$$\begin{aligned} & (\mathbf{q} \cdot \nabla_1)^2 e^{-\frac{i}{2}(\tilde{\mathbf{q}}_1 \wedge \tilde{\mathbf{p}}_1 + \tilde{\mathbf{q}}_2 \wedge \tilde{\mathbf{p}}_2)} \\ &= \left[q_x \left(\frac{\partial \tilde{q}_{1x}}{\partial q_{1x}} \frac{\partial}{\partial \tilde{q}_{1x}} + \frac{\partial \tilde{q}_{2x}}{\partial q_{1x}} \frac{\partial}{\partial \tilde{q}_{2x}} \right) + q_y \left(\frac{\partial \tilde{q}_{1y}}{\partial q_{1y}} \frac{\partial}{\partial \tilde{q}_{1y}} + \frac{\partial \tilde{q}_{2y}}{\partial q_{1y}} \frac{\partial}{\partial \tilde{q}_{2y}} \right) \right]^2 e^{-\frac{i}{2}(\tilde{\mathbf{q}}_1 \wedge \tilde{\mathbf{p}}_1 + \tilde{\mathbf{q}}_2 \wedge \tilde{\mathbf{p}}_2)} \\ &= - \left[\frac{\mathbf{q}}{2} \wedge \left(\frac{1}{\sqrt{2}} \tilde{\mathbf{p}}_1 + \frac{\sqrt{3}}{\sqrt{2}} \tilde{\mathbf{p}}_2 \right) \right]^2 e^{-\frac{i}{2}(\tilde{\mathbf{q}}_1 \wedge \tilde{\mathbf{p}}_1 + \tilde{\mathbf{q}}_2 \wedge \tilde{\mathbf{p}}_2)} \end{aligned} \quad (4.43)$$

and:

$$(\mathbf{q} \cdot \nabla_2)^2 e^{-\frac{i}{2}(\tilde{\mathbf{q}}_1 \wedge \tilde{\mathbf{p}}_1 + \tilde{\mathbf{q}}_2 \wedge \tilde{\mathbf{p}}_2)} = - \left[\frac{\mathbf{q}}{2} \wedge \left(-\frac{1}{\sqrt{2}} \tilde{\mathbf{p}}_1 + \frac{\sqrt{3}}{\sqrt{2}} \tilde{\mathbf{p}}_2 \right) \right]^2 e^{-\frac{i}{2}(\tilde{\mathbf{q}}_1 \wedge \tilde{\mathbf{p}}_1 + \tilde{\mathbf{q}}_2 \wedge \tilde{\mathbf{p}}_2)} \quad (4.44)$$

and also:

$$\begin{aligned} & (\mathbf{q} \cdot \nabla_1)(\mathbf{q} \cdot \nabla_2) e^{-\frac{i}{2}(\tilde{\mathbf{q}}_1 \wedge \tilde{\mathbf{p}}_1 + \tilde{\mathbf{q}}_2 \wedge \tilde{\mathbf{p}}_2)} \\ &= - \left[\frac{\mathbf{q}}{2} \wedge \left(\frac{1}{\sqrt{2}} \tilde{\mathbf{p}}_1 + \frac{\sqrt{3}}{\sqrt{2}} \tilde{\mathbf{p}}_2 \right) \right] \left[\frac{\mathbf{q}}{2} \wedge \left(-\frac{1}{\sqrt{2}} \tilde{\mathbf{p}}_1 + \frac{\sqrt{3}}{\sqrt{2}} \tilde{\mathbf{p}}_2 \right) \right] e^{-\frac{i}{2}(\tilde{\mathbf{q}}_1 \wedge \tilde{\mathbf{p}}_1 + \tilde{\mathbf{q}}_2 \wedge \tilde{\mathbf{p}}_2)} \end{aligned} \quad (4.45)$$

Remember that in the long-wavelength limit, the wave number $\mathbf{q} \rightarrow 0$, and we have the limit of the structure factor as:

$$\lim_{|\mathbf{q}| \rightarrow 0} S_{\mathbf{q}} = \eta \cdot \mathbf{q}^4 = \frac{N_e \kappa}{2} \cdot \mathbf{q}^4 \quad (4.46)$$

where κ is no greater than the Hall viscosity of the ground state $|\psi_0\rangle$ [333]. Thus the graviton mode gap turns out to be:

$$\begin{aligned} \delta\tilde{E}_{\mathbf{q}\rightarrow 0} = & -\frac{1}{6S_{\mathbf{q}}}\int\frac{d^2\tilde{\mathbf{q}}_1 d^2\tilde{\mathbf{q}}_2}{(2\pi)^4}V_{\tilde{\mathbf{q}}_1,\tilde{\mathbf{q}}_2}\int\frac{d^2\tilde{\mathbf{p}}_1 d^2\tilde{\mathbf{p}}_2}{2^4\times 4\pi^2}e^{-\frac{i}{2}(\tilde{\mathbf{q}}_1\wedge\tilde{\mathbf{p}}_1+\tilde{\mathbf{q}}_2\wedge\tilde{\mathbf{p}}_2)}\bar{S}_{\tilde{\mathbf{p}}_1,\tilde{\mathbf{p}}_2} \\ & \times \left\{ \left[\left(\frac{1}{\sqrt{2}}\tilde{\mathbf{q}}_1 + \frac{1}{\sqrt{6}}\tilde{\mathbf{q}}_2 \right) \wedge \mathbf{q} \right] \left[\left(\frac{1}{\sqrt{2}}\tilde{\mathbf{p}}_1 + \frac{\sqrt{3}}{\sqrt{2}}\tilde{\mathbf{p}}_2 \right) \wedge \mathbf{q} \right] \right. \\ & \left. + \left[\left(-\frac{1}{\sqrt{2}}\tilde{\mathbf{q}}_1 + \frac{1}{\sqrt{6}}\tilde{\mathbf{q}}_2 \right) \wedge \mathbf{q} \right] \left[\left(-\frac{1}{\sqrt{2}}\tilde{\mathbf{p}}_1 + \frac{\sqrt{3}}{\sqrt{2}}\tilde{\mathbf{p}}_2 \right) \wedge \mathbf{q} \right] \right\}^2 \end{aligned} \quad (4.47)$$

We can set $\theta_q = \frac{\pi}{2}$ without losing any generality and get:

$$\begin{aligned} \delta\tilde{E}_{\mathbf{q}} = & -\frac{1}{6\eta}\int\frac{2|\tilde{\mathbf{q}}_1|d|\tilde{\mathbf{q}}_1|\times 2|\tilde{\mathbf{q}}_2|d|\tilde{\mathbf{q}}_2|}{4\times(2\pi)^4}V_{\tilde{\mathbf{q}}_1,\tilde{\mathbf{q}}_2}\int\frac{2|\tilde{\mathbf{p}}_1|d|\tilde{\mathbf{p}}_1|\times 2|\tilde{\mathbf{p}}_2|d|\tilde{\mathbf{p}}_2|}{4\times 2^4\times 4\pi^2} \\ & \times \sum_{\Delta n_1} \left| \bar{S}_{\tilde{\mathbf{p}}_1,\tilde{\mathbf{p}}_2}^{(\Delta n_1)} \right| \Theta^{(\Delta n_1)}(\tilde{\mathbf{q}}_1, \tilde{\mathbf{q}}_2, \tilde{\mathbf{p}}_1, \tilde{\mathbf{p}}_2) \end{aligned} \quad (4.48)$$

where $\left| \bar{S}_{\tilde{\mathbf{p}}_1,\tilde{\mathbf{p}}_2}^{(\Delta n_1)} \right|$ denotes the radial part of each term in the structure factor expansion. Moreover the angular integral is defined by

$$\begin{aligned} \Theta^{(\Delta n_1)}(\tilde{\mathbf{q}}_1, \tilde{\mathbf{q}}_2, \tilde{\mathbf{p}}_1, \tilde{\mathbf{p}}_2) = & \iiint_{-\pi}^{\pi} d\theta_{\tilde{\mathbf{q}}_1} d\theta_{\tilde{\mathbf{q}}_2} d\theta_{\tilde{\mathbf{p}}_1} d\theta_{\tilde{\mathbf{p}}_2} e^{i\Delta n_1(\theta_{\tilde{\mathbf{p}}_1}-\theta_{\tilde{\mathbf{p}}_2})} \\ & \times e^{-\frac{i}{2}[|\tilde{\mathbf{q}}_1||\tilde{\mathbf{p}}_1|\sin(\theta_{\tilde{\mathbf{q}}_1}-\theta_{\tilde{\mathbf{p}}_1})+|\tilde{\mathbf{q}}_2||\tilde{\mathbf{p}}_2|\sin(\theta_{\tilde{\mathbf{q}}_2}-\theta_{\tilde{\mathbf{p}}_2})]} \\ & \times [|\tilde{\mathbf{q}}_1||\tilde{\mathbf{p}}_1|\cos(\theta_{\tilde{\mathbf{q}}_1})\cos(\theta_{\tilde{\mathbf{p}}_1}) + |\tilde{\mathbf{q}}_2||\tilde{\mathbf{p}}_2|\cos(\theta_{\tilde{\mathbf{q}}_2})\cos(\theta_{\tilde{\mathbf{p}}_2})]^2 \end{aligned} \quad (4.49)$$

The integral with \sin function in the exponential function reminds us of the Bessel function:

$$\int_{-\pi}^{\pi} \int_{-\pi}^{\pi} d\theta_1 d\theta_2 e^{i[x\sin(\theta_1-\theta_2)-\alpha(\theta_1-\theta_2)+\beta\theta_2]} = 4\pi^2 J_\alpha(x)\delta(\beta) \quad (4.50)$$

This can save us from dealing with infinite terms in the Laguerre-Gaussian expansion as follows. The integrand in $\Theta^{(\Delta n_1)}(\tilde{\mathbf{q}}_1, \tilde{\mathbf{q}}_2, \tilde{\mathbf{p}}_1, \tilde{\mathbf{p}}_2)$ can be reorganized:

$$\begin{aligned} & \left[e^{-\frac{i}{2}[|\tilde{\mathbf{q}}_1||\tilde{\mathbf{p}}_1|\sin(\theta_{\tilde{\mathbf{q}}_1}-\theta_{\tilde{\mathbf{p}}_1})+|\tilde{\mathbf{q}}_2||\tilde{\mathbf{p}}_2|\sin(\theta_{\tilde{\mathbf{q}}_2}-\theta_{\tilde{\mathbf{p}}_2})]} |\tilde{\mathbf{q}}_i||\tilde{\mathbf{p}}_i||\tilde{\mathbf{q}}_j||\tilde{\mathbf{p}}_j| \right] \\ & \times e^{i\Delta n_1(\theta_{\tilde{\mathbf{p}}_1}-\theta_{\tilde{\mathbf{p}}_2})} \cos(\theta_{\tilde{\mathbf{q}}_i})\cos(\theta_{\tilde{\mathbf{p}}_i})\cos(\theta_{\tilde{\mathbf{q}}_j})\cos(\theta_{\tilde{\mathbf{p}}_j}) \\ = & \frac{[\dots]}{2^4} \left(e^{i\theta_{\tilde{\mathbf{q}}_i}} + e^{-i\theta_{\tilde{\mathbf{q}}_i}} \right) \left(e^{i\theta_{\tilde{\mathbf{q}}_j}} + e^{-i\theta_{\tilde{\mathbf{q}}_j}} \right) \left[e^{i\Delta n_1\theta_{\tilde{\mathbf{p}}_1}} e^{-i\Delta n_1\theta_{\tilde{\mathbf{p}}_2}} \left(e^{i\theta_{\tilde{\mathbf{p}}_i}} + e^{-i\theta_{\tilde{\mathbf{p}}_i}} \right) \left(e^{i\theta_{\tilde{\mathbf{p}}_j}} + e^{-i\theta_{\tilde{\mathbf{p}}_j}} \right) \right] \end{aligned} \quad (4.51)$$

where $i, j \in \{1, 2\}$. Thus according to Theorem 4.50, when $i = j$, Δn must vanish for getting a non-zero term in $\Theta^{(\Delta n_1)}(\tilde{\mathbf{q}}_1, \tilde{\mathbf{q}}_2, \tilde{\mathbf{p}}_1, \tilde{\mathbf{p}}_2)$ otherwise integrating either $\theta_{\tilde{\mathbf{q}}_1}$

or $\theta_{\tilde{q}_2}$ will give a zero. As for $i \neq j$, only when

$$1 \pm \Delta n_1 = \pm 1 \quad (4.52)$$

can we have a non-zero term in $\Theta^{(\Delta n_1)}(\tilde{q}_1, \tilde{q}_2, \tilde{p}_1, \tilde{p}_2)$. Hence Δn_1 can only be ± 2 or 0. In short, we have made sure that:

Proposition 4.2. *The domain of the quantum number differences is given by*

$$\Delta n_1 = -\Delta n_2 \in \{\pm 2, 0\} \quad (4.53)$$

Then we can discuss each case one by one:

- When $i = j$ and $\Delta n_1 = 0$

Based on Theorem 4.50, when $i = j$, $\Theta^{(0)}(\tilde{q}_1, \tilde{q}_2, \tilde{p}_1, \tilde{p}_2)$ can be written as:

$$\begin{aligned} & \frac{1}{2^4} \iiint_{-\pi}^{\pi} d\theta_{\tilde{q}_1} d\theta_{\tilde{q}_2} d\theta_{\tilde{p}_1} d\theta_{\tilde{p}_2} e^{-\frac{i}{2} [|\tilde{q}_1||\tilde{p}_1| \sin(\theta_{\tilde{q}_1} - \theta_{\tilde{p}_1}) + |\tilde{q}_2||\tilde{p}_2| \sin(\theta_{\tilde{q}_2} - \theta_{\tilde{p}_2})]} \\ & \times \tilde{Q}_i \tilde{P}_i [4 + e^{i2(\theta_{\tilde{q}_i} - \theta_{\tilde{p}_i})} + e^{-i2(\theta_{\tilde{q}_i} - \theta_{\tilde{p}_i})}] \\ & = 4\pi^4 \tilde{Q}_i \tilde{P}_i \times \left[J_0\left(\frac{|\tilde{q}_1||\tilde{p}_1|}{2}\right) J_0\left(\frac{|\tilde{q}_2||\tilde{p}_2|}{2}\right) + \frac{1}{2} J_2\left(\frac{|\tilde{q}_i||\tilde{p}_i|}{2}\right) J_0\left(\frac{|\tilde{q}_{3-i}||\tilde{p}_{3-i}|}{2}\right) \right] \end{aligned} \quad (4.54)$$

Finally, we can transform the Bessel functions to the generalized Laguerre polynomials based on Eq.(2.35):

$$\begin{aligned} & \Theta^{(0)}(\tilde{Q}_1, \tilde{Q}_2, \tilde{P}_1, \tilde{P}_2) \\ & = 4 \times 4\pi^4 e^{-\frac{1}{4}(\tilde{Q}_1 + \tilde{Q}_2 + \tilde{P}_1 + \tilde{P}_2)} \sum_{a,b=0}^{\infty} (-1)^{a+b} \left[\frac{\tilde{Q}_1 \tilde{P}_1 + \tilde{Q}_2 \tilde{P}_2}{2} \right. \\ & \times L_a^{(0)}\left(\frac{\tilde{Q}_1}{2}\right) L_a^{(0)}\left(\frac{\tilde{P}_1}{2}\right) L_b^{(0)}\left(\frac{\tilde{Q}_2}{2}\right) L_b^{(0)}\left(\frac{\tilde{P}_2}{2}\right) \\ & + \frac{\tilde{Q}_1 \tilde{P}_1}{a+1} L_a^{(1)}\left(\frac{\tilde{Q}_1}{2}\right) L_a^{(1)}\left(\frac{\tilde{P}_1}{2}\right) L_b^{(0)}\left(\frac{\tilde{Q}_2}{2}\right) L_b^{(0)}\left(\frac{\tilde{P}_2}{2}\right) \\ & \left. \times + \frac{\tilde{Q}_2 \tilde{P}_2}{b+1} L_a^{(0)}\left(\frac{\tilde{Q}_1}{2}\right) L_a^{(0)}\left(\frac{\tilde{P}_1}{2}\right) L_b^{(1)}\left(\frac{\tilde{Q}_2}{2}\right) L_b^{(1)}\left(\frac{\tilde{P}_2}{2}\right) \right] \end{aligned} \quad (4.55)$$

Now we can calculate the integral by considering the completeness and orthogonality of the generalized Laguerre polynomials [334], which can help derive two quantities that we need:

Definition 4.5 (Linear combination of Kronecker-delta symbols).

$$\begin{aligned}\Delta_{ij} &\equiv \int_0^\infty xe^{-x} L_i^{(0)}(x) L_j^{(1)}(x) dx = \int_0^\infty xe^{-x} \left[L_i^{(1)}(x) - L_{i-1}^{(1)}(x) \right] L_j^{(1)}(x) dx \\ &= (i+1)\delta_{i,j} - i\delta_{i-1,j}\end{aligned}\quad (4.56)$$

and:

$$\begin{aligned}\Delta_{ij}^* &\equiv \int_0^\infty xe^{-x} L_i^{(0)}(x) L_j^{(0)}(x) dx \\ &= \int_0^\infty xe^{-x} \left[L_i^{(1)}(x) - L_{i-1}^{(1)}(x) \right] \left[L_j^{(1)}(x) - L_{j-1}^{(1)}(x) \right] dx \\ &= (i+1)\delta_{i,j} - (i+1)\delta_{i,j-1} - i\delta_{i-1,j} + i\delta_{i-1,j-1}\end{aligned}\quad (4.57)$$

Furthermore for simpliity we denote the constant factor in $\bar{S}_{\tilde{\mathbf{p}}_1, \tilde{\mathbf{p}}_2}$ as

$$\omega_i^{n_1 n_2} = \sqrt{\frac{n_1! \cdot n_2!}{(n_1+i)! \cdot (n_2-i)!}} \quad (4.58)$$

Now we are all set to get the final result. By using the orthogonality of the generalized Laguerre polynomials, we can see that the contribution to the energy gap turns out to be the combination of delta functions. So we can expect that the only input of the final expression will be $c^{m_1 m_2}$ and $d_0^{n_1 n_2}$ and try to absorb all the other coefficients into an independent quantity:

$$\begin{aligned}\delta \tilde{E}_{\mathbf{q}}^{(0)} &= -\frac{1}{2^6 \times 3\eta\pi^2} \sum_{m_1 m_2} \sum_{n_1 n_2} c^{m_1 m_2} d_0^{n_1 n_2} \sum_{a,b} (-1)^{m_1+m_2+a+b} \\ &\quad \left(\frac{2}{a+1} \Delta_{n_1 a} \Delta_{m_1 a} \delta_{n_2, b} \delta_{m_2, b} + \Delta_{n_1 a}^* \Delta_{m_1 a}^* \delta_{n_2, b} \delta_{m_2, b} \right. \\ &\quad \left. + \frac{2}{b+1} \Delta_{n_2 b} \Delta_{m_2 b} \delta_{n_1 a} \delta_{m_1 a} + \Delta_{n_2, b}^* \Delta_{m_2, b}^* \delta_{n_1 a} \delta_{m_1 a} \right) \\ &\equiv -\frac{1}{2^6 \times 3\eta\pi^2} \Gamma_{m_1 m_2 n_1 n_2}^0 c^{m_1 m_2} d_0^{n_1 n_2}\end{aligned}\quad (4.59)$$

By considering Definition 4.5, we have:

$$\begin{aligned}
& \sum_{a,b} (-1)^{m_1+m_2+a+b} \frac{1}{a+1} \Delta_{n_1 a} \Delta_{m_1 a} \delta_{n_2, b} \delta_{m_2, b} \\
& \quad - m_1 \delta_{m_1-1, a} \delta_{n_1, a} - m_1 \delta_{m_1-1, a} \delta_{n_1-1, a}] (-1)^{m_2} \delta_{n_2, m_2} \\
& = [(-1)^{2n_1} (n_1 + 1) \delta_{n_1, m_1} + (-1)^{2n_1-1} n_1 \delta_{n_1-1, m_1} \\
& \quad - (-1)^{2n_1+1} (n_1 + 1) \delta_{m_1-1, n_1} - (-1)^{2n_1} n_1 \delta_{m_1, n_1}] \delta_{n_2, m_2} \\
& = [\delta_{n_1, m_1} + (n_1 + 1) \delta_{n_1, m_1-1} - n_1 \delta_{n_1, m_1+1}] \delta_{n_2, m_2}
\end{aligned} \tag{4.60}$$

The symmetric operation of $m_1, m_2 \leftrightarrow n_1, n_2$ and $a \leftrightarrow b$ gives all the other terms. Then by combining them, one can easily get the independent quantity for the case with $i = j$ and $\Delta n_1 = 0$:

Proposition 4.3. *The tensor describing the contribution to δE_q from the diagonal terms is given by*

$$\begin{aligned}
\Gamma_{m_1 m_2 n_1 n_2}^0 &= 2(n_1^2 + n_2^2 + n_1 + n_2 + 2) \delta_{n_1, m_1} \delta_{n_2, m_2} \\
& \quad - n_1(n_1 - 1) \delta_{n_1, m_1+2} \delta_{n_2, m_2} (n_1 + 1)(n_1 + 2) \delta_{n_1, m_1-2} \delta_{n_2, m_2} \\
& \quad - n_2(n_2 - 1) \delta_{n_1, m_1} \delta_{n_2, m_2+2} - (n_2 + 1)(n_2 + 2) \delta_{n_1, m_1} \delta_{n_2, m_2-2}
\end{aligned} \tag{4.61}$$

- When $i \neq j$ and $\Delta n_1 = 0$

First, we need a special property of the Bessel functions (of the first kind) with integer indices [334]:

Lemma 4.3 (Index Parity of Bessel functions).

$$J_{-n}(x) = (-1)^n J_n(x), \quad n \in \mathbb{N} \tag{4.62}$$

which means that these Bessel functions are “odd” with respect to their indices. Thus it is not surprising to have the following conclusion:

Proposition 4.4. *There is no contribution to δE_q from the terms with $i \neq j$ and $\Delta n_1 = 0$.*

Proof. The angular integral can be written as:

$$\begin{aligned}
& \iiint_{-\pi}^{\pi} d\theta_{\tilde{q}_1} d\theta_{\tilde{q}_2} d\theta_{\tilde{p}_1} d\theta_{\tilde{p}_2} e^{-\frac{i}{2} [|\tilde{q}_1||\tilde{p}_1| \sin(\theta_{\tilde{q}_1} - \theta_{\tilde{p}_1}) + |\tilde{q}_2||\tilde{p}_2| \sin(\theta_{\tilde{q}_2} - \theta_{\tilde{p}_2})]} \\
& \times \frac{1}{2^4} |\tilde{\mathbf{q}}_1| |\tilde{\mathbf{p}}_1| |\tilde{\mathbf{q}}_2| |\tilde{\mathbf{p}}_2| \left(e^{i\theta_{\tilde{q}_1}} + e^{-i\theta_{\tilde{q}_1}} \right) \left(e^{i\theta_{\tilde{p}_1}} + e^{-i\theta_{\tilde{p}_1}} \right) \left(e^{i\theta_{\tilde{q}_2}} + e^{-i\theta_{\tilde{q}_2}} \right) \left(e^{i\theta_{\tilde{p}_2}} + e^{-i\theta_{\tilde{p}_2}} \right) \\
& = \pi^4 |\tilde{\mathbf{q}}_1| |\tilde{\mathbf{p}}_1| |\tilde{\mathbf{q}}_2| |\tilde{\mathbf{p}}_2| \times \left[J_1 \left(\frac{|\tilde{\mathbf{q}}_1| |\tilde{\mathbf{p}}_1|}{2} \right) J_1 \left(\frac{|\tilde{\mathbf{q}}_2| |\tilde{\mathbf{p}}_2|}{2} \right) + J_1 \left(\frac{|\tilde{\mathbf{q}}_1| |\tilde{\mathbf{p}}_1|}{2} \right) J_{-1} \left(\frac{|\tilde{\mathbf{q}}_2| |\tilde{\mathbf{p}}_2|}{2} \right) \right. \\
& \left. + J_{-1} \left(\frac{|\tilde{\mathbf{q}}_1| |\tilde{\mathbf{p}}_1|}{2} \right) J_1 \left(\frac{|\tilde{\mathbf{q}}_2| |\tilde{\mathbf{p}}_2|}{2} \right) + J_{-1} \left(\frac{|\tilde{\mathbf{q}}_1| |\tilde{\mathbf{p}}_1|}{2} \right) J_{-1} \left(\frac{|\tilde{\mathbf{q}}_2| |\tilde{\mathbf{p}}_2|}{2} \right) \right] = 0
\end{aligned} \tag{4.63}$$

□

- When $i \neq j$ and $\Delta n_1 = \pm 2$

By observing the integral one can easily find that the case with $\Delta n_1 = -2$ and the one with $\Delta n_1 = 2$ are completely symmetric. So after one of them is solved, the other one can be derived by exchanging the indices. Without losing generality, we can calculate the angular integral $\Theta^{(-2)}(\tilde{Q}_1, \tilde{Q}_2, \tilde{P}_1, \tilde{P}_2)$ with $i \neq j$ and $\Delta n_1 = -2$ first, given by:

$$\begin{aligned}
& \iiint_{-\pi}^{\pi} d\theta_{\tilde{q}_1} d\theta_{\tilde{q}_2} d\theta_{\tilde{p}_1} d\theta_{\tilde{p}_2} e^{-\frac{i}{2} [|\tilde{q}_1||\tilde{p}_1| \sin(\theta_{\tilde{q}_1} - \theta_{\tilde{p}_1}) + |\tilde{q}_2||\tilde{p}_2| \sin(\theta_{\tilde{q}_2} - \theta_{\tilde{p}_2})]} \times \frac{1}{2^4} \times e^{-2i(\theta_{\tilde{p}_1} - \theta_{\tilde{p}_2})} \\
& \times 2 |\tilde{\mathbf{q}}_1| |\tilde{\mathbf{p}}_1| |\tilde{\mathbf{q}}_2| |\tilde{\mathbf{p}}_2| \left(e^{i\theta_{\tilde{q}_1}} + e^{-i\theta_{\tilde{q}_1}} \right) \left(e^{i\theta_{\tilde{p}_1}} + e^{-i\theta_{\tilde{p}_1}} \right) \left(e^{i\theta_{\tilde{q}_2}} + e^{-i\theta_{\tilde{q}_2}} \right) \left(e^{i\theta_{\tilde{p}_2}} + e^{-i\theta_{\tilde{p}_2}} \right) \\
& = 2\pi^4 \times |\tilde{\mathbf{q}}_1| |\tilde{\mathbf{p}}_1| |\tilde{\mathbf{q}}_2| |\tilde{\mathbf{p}}_2| \times J_1 \left(\frac{|\tilde{\mathbf{q}}_1| |\tilde{\mathbf{p}}_1|}{2} \right) J_1 \left(\frac{|\tilde{\mathbf{q}}_2| |\tilde{\mathbf{p}}_2|}{2} \right)
\end{aligned} \tag{4.64}$$

Now we introduce another formula to be used:

Lemma 4.4 (Generalized Laguerre polynomial integral).

$$\int_0^\infty \frac{d\tilde{P}_1}{2} \left[L_a^{(1)} \left(\frac{\tilde{P}_1}{2} \right) L_{n_1}^{(-2)} \left(\frac{\tilde{P}_1}{2} \right) e^{-\frac{1}{2}\tilde{P}_1} \right] = \delta_{n_1,0} - \delta_{n_1,1} + \delta_{n_1-2,a} - \delta_{n_1-1,a} \tag{4.65}$$

which helps to calculate the contribution to the graviton mode gap in this case by:

$$\delta \tilde{E}_{\mathbf{q}}^{(-2)} = -\frac{1}{6\eta} \int \frac{d\tilde{Q}_1 d\tilde{Q}_2}{4 \times (2\pi)^4} \int \frac{d\tilde{P}_1 d\tilde{P}_2}{4 \times 2^4 \times 4\pi^2} \underbrace{\Theta^{(-2)}(\tilde{Q}_1, \tilde{Q}_2, \tilde{P}_1, \tilde{P}_2) \cdot V_{\tilde{Q}_1, \tilde{Q}_2} \cdot |\bar{S}_{\tilde{\mathbf{p}}_1, \tilde{\mathbf{p}}_2}|}_{\text{Expanded by generalized L-G polynomials}}$$

(4.66)

where these three functions can all be expanded by generalized Laguerre-Gaussian polynomials. Then we can combine the equations above and get the contribution

to the energy as:

$$\begin{aligned}
& - \frac{1}{2^6 \times 3\eta\pi^2} \sum_{a=0}^{\infty} \sum_{m_1, m_2=0}^{\infty} \sum_{b=0}^{\infty} \sum_{n_1, n_2=0}^{\infty} c^{m_1 m_2} d_{-2}^{n_1 n_2} (-1)^{a+b+n_1+n_2} \omega_{-2}^{n_1 n_2} \frac{1}{a+1} \frac{1}{b+1} \\
& \quad \times [(m_1 + 1)\delta_{m_1, a} - m_1 \delta_{m_1-1, a}] \times [(m_2 + 1)\delta_{m_2, b} - m_2 \delta_{m_2-1, b}] \\
& \quad \times [\delta_{n_1, 0} - \delta_{n_1, 1} + \delta_{n_1-2, a} - \delta_{n_1-1, a}] \times [(n_2 + 1)(n_2 + 2)(\delta_{n_2, b} - \delta_{n_2+1, b})] \\
& = - \frac{1}{2^6 \times 3\eta\pi^2} \Gamma_{m_1 m_2 n_1 n_2}^- c^{m_1 m_2} d_{-2}^{n_1 n_2}
\end{aligned} \tag{4.67}$$

where we have:

$$\Gamma_{m_1 m_2 n_1 n_2}^- = \omega_{-2}^{n_1 n_2} \times (n_2 + 1)(n_2 + 2)(\delta_{m_2, n_2} - \delta_{m_2, n_2+2}) \times (\delta_{m_1, n_1} - \delta_{m_1, n_1-2}) \tag{4.68}$$

Then for $\Delta n_1 = +2$ everything is totally symmetric by substituting $n_1 \leftrightarrow n_2$ and $m_1 \leftrightarrow m_2$. So we can directly write down the result:

$$\Gamma_{m_1 m_2 n_1 n_2}^+ = \omega_{+2}^{n_1 n_2} \times (n_1 + 1)(n_1 + 2)(\delta_{m_1, n_1} - \delta_{m_1, n_1+2}) \times (\delta_{m_2, n_2} - \delta_{m_2, n_2-2}) \tag{4.69}$$

Thus by defining:

Definition 4.6 (Characteristic tensor).

$$\tilde{\Gamma}_{m_1 m_2 n_1 n_2}^{\text{3bdy}} = \mathcal{C} \times \left(\Gamma_{m_1 m_2 n_1 n_2}^0 + \frac{\alpha_{n_1+2, n_2-2}}{\alpha_{n_1, n_2}} \times \Gamma_{m_1 m_2 n_1 n_2}^+ + \frac{\alpha_{n_1-2, n_2+2}}{\alpha_{n_1, n_2}} \times \Gamma_{m_1 m_2 n_1 n_2}^- \right) \tag{4.70}$$

where the constant coefficient $\mathcal{C} = -\frac{1}{2^6 \times 3\eta\pi^2}$.

we can get the graviton mode gap with respect to the three-body interaction given by

$$\delta \tilde{E}_{\mathbf{q} \rightarrow 0} = \tilde{\Gamma}_{m_1 m_2 n_1 n_2}^{\text{3bdy}} c^{m_1 m_2} \bar{d}^{n_1 n_2} \tag{4.71}$$

From the last three subsections, we know that the graviton mode gap can be written as:

$$\delta \tilde{E}_{\mathbf{q} \rightarrow 0} = \mathcal{C} \times \left(\Gamma_{m_1 m_2 n_1 n_2}^0 c^{m_1 m_2} d_0^{n_1 n_2} + \Gamma_{m_1 m_2 n_1 n_2}^- c^{m_1 m_2} d_{-2}^{n_1 n_2} + \Gamma_{m_1 m_2 n_1 n_2}^+ c^{m_1 m_2} d_2^{n_1 n_2} \right) \tag{4.72}$$

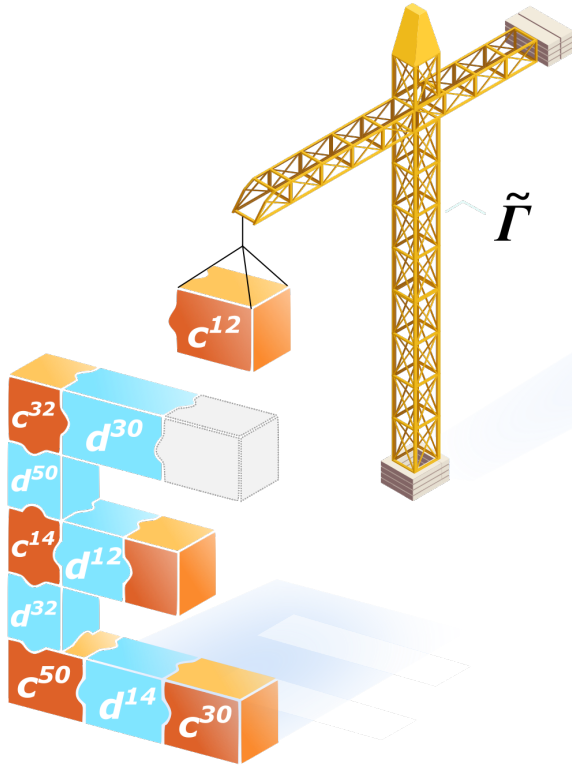


FIGURE 4.2: **Illustration of the characteristic tensor $\tilde{\Gamma}$.** This universal tensor can assemble the coefficients from the model Hamiltonian and the structure factor of the ground state to give the energy of the corresponding graviton mode.

Then according to Corollary 4.2, we can use $\bar{d}^{n_1 n_2}$ to express all the expansion coefficients $d_{\Delta n_1}^{n_1 n_2}$:

$$\begin{aligned}
 \delta \tilde{E}_{q \rightarrow 0} &= \left[\mathcal{C} \times \left(\Gamma_{m_1 m_2 n_1 n_2}^0 + \frac{\alpha_{n_1+2, n_2-2}}{\alpha_{n_1, n_2}} \times \Gamma_{m_1 m_2 n_1 n_2}^+ + \frac{\alpha_{n_1-2, n_2+2}}{\alpha_{n_1, n_2}} \times \Gamma_{m_1 m_2 n_1 n_2}^- \right) \right] \\
 &\quad \times c^{m_1 m_2} \bar{d}^{n_1 n_2} \\
 &= \left(\tilde{\Gamma}_{m_1 m_2 n_1 n_2}^0 + \tilde{\Gamma}_{m_1 m_2 n_1 n_2}^+ + \tilde{\Gamma}_{m_1 m_2 n_1 n_2}^- \right) c^{m_1 m_2} \bar{d}^{n_1 n_2} \\
 &\equiv \tilde{\Gamma}_{m_1 m_2 n_1 n_2}^{\text{3bdy}} c^{m_1 m_2} \bar{d}^{n_1 n_2}
 \end{aligned} \tag{4.73}$$

If the Hamiltonian is defined with a different coefficient in the first place because of different Fourier transform conventions, then the constant coefficient \mathcal{C} here might also change. But this will not change the gaplessness of a state and the characteristic tensor $\tilde{\Gamma}_{m_1 m_2 n_1 n_2}^{\text{3bdy}}$ is always well defined so all that one needs to calculate $\delta \tilde{E}_{q \rightarrow 0}$

is to input the corresponding $c^{m_1 m_2}$ and $\bar{d}^{n_1 n_2}$ as shown in Fig.4.2. The most powerful advantage of this formalism is that the structure of the characteristic tensor $\tilde{\Gamma}_{m_1 m_2 n_1 n_2}^{\text{3bdy}}$ allows us to predict the graviton mode energy of some states with respect to a Hamiltonian without knowing the exact values of $c^{m_1 m_2}$ and $\bar{d}^{n_1 n_2}$. Actually, we only need to know whether these coefficients vanish or not, as explained later. Also, it is definitely possible to generalize this formalism to the interaction with more particles, and we expect to see a rank- $2n$ characteristic tensor for a n -body effective Hamiltonian, which can be studied in the future.

4.4.3 Two-body interactions

Here we will show the characteristic matrix formalism of the graviton mode gap with respect to two-body interactions, which is basically a simplified version of the three-body case. The FQH states with the two-body model Hamiltonian are the Laughlin states, which are not very interesting (considering they are Abelian) but the results can still provide us some insights about this formalism.

The generic two-body Hamiltonian in a single LL as introduced in Chap.2 can be written as:

$$\hat{H}_{\text{2bdy}} = \int \frac{d^2 \mathbf{q}}{(2\pi)^2} V_{\mathbf{q}} \sum_{i \neq j} e^{iq_a(\hat{R}_i^a - \hat{R}_j^a)} = \int \frac{d^2 \mathbf{q}}{(2\pi)^2} V_{\mathbf{q}} \hat{\rho}_{\mathbf{q}} \hat{\rho}_{-\mathbf{q}} - N_e \int \frac{d^2 \mathbf{q}}{(2\pi)^2} V_{\mathbf{q}}$$

where N_e is the number of electrons and the form factor (which is a Gaussian factor in the lowest LL) has been absorbed into $V_{\mathbf{q}}$. We will denote the ground state of \hat{H}_{2bdy} as $|\psi_0\rangle$ with the energy E_0 . Thus to derive the energy of the graviton mode given by the SMA wave function:

$$|\psi_{\mathbf{q}}\rangle = \frac{1}{\sqrt{S_{\mathbf{q}}}} \cdot \delta \hat{\rho}_{\mathbf{q}} |\psi_0\rangle \quad (4.74)$$

with respect to \hat{H}_{2bdy} , we only need to calculate:

$$\begin{aligned} \delta \tilde{E}_{\mathbf{q} \rightarrow 0} &= \lim_{\mathbf{q} \rightarrow 0} \frac{\left\langle \psi_0 \left| \left[\delta \rho_{-\mathbf{q}}, \left[\hat{H}_{\text{2bdy}}, \delta \rho_{\mathbf{q}} \right] \right] \right| \psi_0 \right\rangle}{2S_{\mathbf{q}}} \\ &= \lim_{\mathbf{q} \rightarrow 0} \frac{1}{2S_{\mathbf{q}}} \int \frac{d^2 q'}{(2\pi)^2} V_{\mathbf{q}'} \left[2 \sin \left(\frac{1}{2} \mathbf{q}' \wedge \mathbf{q} \right) \right]^2 \times (\mathbf{q} \cdot \nabla')^2 s_{\mathbf{q}'} \end{aligned} \quad (4.75)$$

where the higher-order terms have been dropped. This is a commonly-seen result that can be found in the literature about neutral modes because it only involves the GMP algebra, and normally people will stop here because it seems that nothing meaningful can be further derived without the input of potential and structure factor. However, we will show that based on the assumptions we have made, it is possible to get a compact formula of $\delta\tilde{E}_{\mathbf{q}\rightarrow 0}$, which can give us lots of information but requires *no* numerical input at all [333].

By defining $q_1 = |\mathbf{q}'|^2$ and $q_2 = |\mathbf{q}''|^2$, the direct transformation of $V_{\mathbf{q}'}$ and $s_{\mathbf{q}''}$ is because both of them are the function of q_1 and q_2 , expanded as:

$$V_{\mathbf{q}_1} = \sum_m c^m L_m(q_1) e^{-\frac{q_1}{2}}, \quad s_{\mathbf{q}_2} = \sum_n d^n L_n(q_2) e^{-\frac{q_2}{2}} \quad (4.76)$$

where m and n are both odd and positive integers because of the fermionic statistics.

Thus the graviton mode gap with respect to the two-body interaction is given by:

$$\delta\tilde{E}_{\mathbf{q}\rightarrow 0} = \frac{1}{2^8 \eta \pi} \Gamma_{mn}^{2\text{bdy}} c^m d^n \quad (4.77)$$

where the characteristic matrix is given by [333]:

$$\Gamma_{mn}^{2\text{bdy}} = (-1)^m \cdot [2(m^2 + m + 1)\delta_{m,n} - (m + 1)(m + 2)\delta_{m,n-2} - m(m - 1)\delta_{m,n+2}] \quad (4.78)$$

Apparently, the calculation for two-body interactions is relatively smooth because it reminds us of many details that can be found in the usual calculations with symmetric gauge, and there are few new concepts involved, unlike in the last section where things can get quite tricky with lots of subtleties arising with three-body interactions.

4.5 Model Hamiltonian of graviton modes

The analytic result we just derived paves the way for calculating the energy of graviton modes with respect to any interaction that can be written as a linear combination of two-body and three-body pseudopotentials. The direct application

is to construct the model Hamiltonians for the gravitons (note that they are not the unique highest-density zero modes of these model-Hamiltonians but live within the corresponding null space), as shown in the example of the gravitons of the Laughlin state at $\nu = 1/3$, the Moore-Read Pfaffian state at $\nu = 1/4$ and the Gaffnian state at $\nu = 2/5$ in this section, which also leads to the insight toward the intrinsic hierarchical structure of the CHSs within a single LL. Note that for some of the FQH states, one can also find the model Hamiltonian of the graviton mode by looking into the wave function. For example, the wave function for the graviton of the Laughlin state at $\nu = 1/5$ is the Laughlin-1/3 graviton \times a 1/2 bosonic Laughlin state, which is within the null-space of two-body pseudopotential $\hat{V}_1^{2\text{bdy}}$ [335].

4.5.1 Laughlin-1/3 graviton mode

The graviton mode of the Laughlin state at $\nu = 1/3$ is the most special one among all the Laughlin states, because it is out of the largest CHS defined by two-body pseudopotentials, i.e. \mathcal{H}_1 defined by $\hat{V}_1^{2\text{bdy}}$, which contains the graviton modes of all the other Laughlin states. Now by using the three-body characteristic tensor formalism, the behavior of the Laughlin-1/3 graviton mode can be analytically discussed, which was suggested to live within the Haffnian CHS (defined below) by numerics. From Eq.(4.40) and Eq.(4.38), we can decompose \bar{d}^{n_1, n_2} as follows:

$$\bar{d}^{n_1, n_2} = \sum_{i=1}^{k_{n_1+n_2}} \lambda_{n_1+n_2, i} A_i^{n_1, n_2} \quad (4.79)$$

where $k_{n_1+n_2}$ denotes the degeneracy of three-body pseudopotentials (or the highest-weight three-body eigenstates of \hat{L}^2) with total relative angular momentum n_1+n_2 ; $\lambda_{n_1+n_2, i}$ depends on the ground state wave function, and $A_i^{n_1, n_2}$ are well-defined as shown in Ref.[203]. When there is no degeneracy in the highest weight state wave function (i.e. $k_{n_1+n_2} = 1$, which is true for $n_1 + n_2 < 9$), \bar{d}^{n_1, n_2} can be considered to be proportional to $A_1^{n_1, n_2} = |\alpha^{n_1, n_2}|^2$. Thus from the ground state energy in

Eq.(4.21), considering that $d^1 = 0$ gives $d^{1,n_2} = 0$ for this state, we can write down:

$$\begin{aligned}\lambda_{1+n_2,1} &= 0, \quad \text{for } n_2 = 2, 4, 5, 6, 7 \\ \Rightarrow \lambda_{a,1} &= 0, \quad \text{for } a = 3, 5, 6, 7, 8 \\ \Rightarrow \bar{d}^{n_1 n_2} &= 0, \quad \text{for } n_1 + n_2 = 3, 5, 6, 7, 8\end{aligned}\tag{4.80}$$

We have thus proved that the graviton mode of the Laughlin-1/3 state lives in the null space of the following three-body Hamiltonian:

$$\hat{H}^{\text{3bdy}} = \sum_{i=3}^6 \tilde{c}_i \hat{V}_i^{\text{3bdy}}\tag{4.81}$$

where $\tilde{c}_4 = 0$ and $\tilde{c}_i > 0$ otherwise. In other words, the graviton mode is in the CHS $\mathcal{H}_{\text{Haffnian}}$, the null space of the *Haffnian* model Hamiltonian $\hat{H}_{\text{Haffnian}} = \hat{V}_3^{\text{3bdy}} + \hat{V}_5^{\text{3bdy}} + \hat{V}_6^{\text{3bdy}}$ (the ground state of which is the Haffnian state) as Fig.4.4 shows. This Hamiltonian provides us with non-vanishing coefficients of c_{m_1, m_2} with $m_1 + m_2 = 3, 5$ and 6 . Thus based on Eq.(4.73), the energy of the graviton mode of the Laughlin-1/3 state is given by:

$$\delta \tilde{E}_{\mathbf{q}} = \tilde{\Gamma}_{m_1 m_2 n_1 n_2}^{\text{3bdy}} c^{m_1 m_2} \bar{d}^{n_1 n_2} = 0\tag{4.82}$$

where the algebraic structure of $\tilde{\Gamma}_{m_1 m_2 n_1 n_2}^{\text{3bdy}}$ ensures that only the coefficients $\bar{d}^{n_1 n_2}$ with $n_1 + n_2 \leq 8$ are involved.

We also illustrate the behaviors of \bar{d}^{n_1, n_2} in Fig.4.3, all the bold coefficients are zero given by the ground state energy of the corresponding model Hamiltonian denoted by different colors:

$$E_0 = \delta_{m_1, n_1} \delta_{m_2, n_2} c^{m_1 m_2} d_0^{n_1 n_2}\tag{4.83}$$

Meanwhile, the fermionic statistics ensure that all the gray coefficients have to vanish. Although the black coefficients are generally not zero, none are involved in the expression. Thus one can *rigorously* prove that the graviton mode energy of the Laughlin-1/3 state with respect to the Haffnian Hamiltonian is zero, i.e., the Haffnian Hamiltonian is the model Hamiltonian of the Laughlin-1/3 graviton mode.

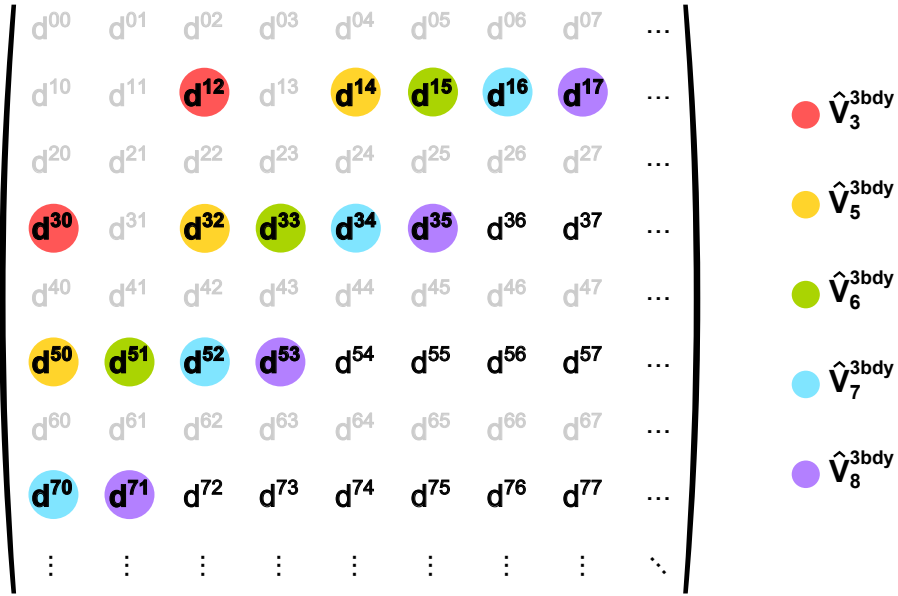


FIGURE 4.3: **Structure of the $\bar{d}_{n_1 n_2}$ coefficients of the Laughlin-1/3 state.** Here, gray coefficients vanish due to the fermionic statistics. Bold coefficients are zero because of the vanishing ground state energy (different colors denote contributions from different three-body model Hamiltonians). Black coefficients are unknown and not necessarily zero. Note that here we omit the bars over the $\bar{d}_{n_1 n_2}$ coefficients for simplicity.

4.5.2 Moore-Read graviton mode

Based on the same idea, only two coefficients \bar{d}^{30} and \bar{d}^{12} of the Moore-Read state vanish as Eq.(4.83), so the energy gap of the corresponding graviton mode with respect to the Hamiltonian $\hat{H}_{\text{MR}} = \hat{V}_3^{\text{3bdy}}$ is given by:

$$\begin{aligned}
 \delta \tilde{E}_{\mathbf{q}} &= \tilde{\Gamma}_{m_1 m_2 n_1 n_2}^{\text{3bdy}} c^{m_1 m_2} \bar{d}^{n_1 n_2} \\
 &= c^{30} (\tilde{\Gamma}_{3032}^{\text{3bdy}} \bar{d}^{32} + \tilde{\Gamma}_{3050}^{\text{3bdy}} \bar{d}^{50}) + c^{12} (\tilde{\Gamma}_{1232}^{\text{3bdy}} \bar{d}^{32} + \tilde{\Gamma}_{1214}^{\text{3bdy}} \bar{d}^{14}) \\
 &= -\frac{1}{2^8 \times 3\eta\pi^2} \times [c^{30} (8\bar{d}^{32} - 16\bar{d}^{50}) + c^{12} (-24\bar{d}^{32} - 16\bar{d}^{14})] \\
 &\propto \lambda_{5,1} \times (c^{30} + 3c^{12})
 \end{aligned} \tag{4.84}$$

where $\lambda_{5,1}$ is the coefficient of the structure factor of the states with the total angular momentum quantum number $n_1 + n_2 = 5$ as in Eq.(4.79), which is proportional to the expectation value of the Moore-Read state with respect to \hat{V}_5^{3bdy} and we

have used the ratio between the coefficients given in Ref.[203]:

$$\alpha^{50} : \alpha^{32} : \alpha^{14} = -\frac{\sqrt{5}}{4} : \frac{1}{2\sqrt{2}} : \frac{3}{4} \quad (4.85)$$

Thus the graviton mode energy of the Moore-Read state can be determined by tuning c^{30} and c^{12} . Furthermore, similar to the Laughlin-1/3 state, the graviton mode of the Moore-Read state will be living within the CHS determined by four-body pseudopotentials, which will not be discussed in detail here.

4.5.3 Gaffnian graviton mode

The case of the Gaffnian state is unsurprisingly a similar case of the Moore-Read state, as the coefficients \bar{d}^{30} , \bar{d}^{12} , \bar{d}^{50} , \bar{d}^{32} and \bar{d}^{14} vanish ensured by its model Hamiltonian $\hat{H}_{\text{Gaffnian}} = \hat{V}_3^{3\text{bdy}} + \hat{V}_5^{3\text{bdy}}$ (only c_{m_1, m_2} with $m_1 + m_2 = 3$ and 5 can be non-zero, so the coefficients d_{m_1, m_2} with the same indices have to vanish to make the ground state energy zero as Eq.(4.83) shows). Then one can write down the energy of the corresponding graviton mode as:

$$\begin{aligned} \delta\tilde{E}_q &= c_{50}(\tilde{\Gamma}_{5052}^{3\text{bdy}}\bar{d}^{52} + \tilde{\Gamma}_{5070}^{3\text{bdy}}\bar{d}^{70}) + c^{32}(\tilde{\Gamma}_{3234}^{3\text{bdy}}\bar{d}^{34} + \tilde{\Gamma}_{3252}^{3\text{bdy}}\bar{d}^{52}) \\ &\quad + c^{14}(\tilde{\Gamma}_{1416}^{3\text{bdy}}\bar{d}^{16} + \tilde{\Gamma}_{1434}^{3\text{bdy}}\bar{d}^{34}) \\ &= -\frac{1}{2^8 \times 3\eta\pi^2} \times [c^{50}(40\bar{d}^{52} - 40\bar{d}^{70}) + c^{32}(-16\bar{d}^{34} - 80\bar{d}^{52}) \\ &\quad + c^{14}(-40\bar{d}^{16} - 24\bar{d}^{34})] \\ &\propto \lambda_{7,1} \times (5c^{50} + 2c^{32} + 9c^{14}) \end{aligned} \quad (4.86)$$

where $\lambda_{7,1}$ is the coefficient of the structure factor of the states with the total angular momentum quantum number $n_1 + n_2 = 7$, which is proportional to the expectation value of the Gaffnian state with respect to $\hat{V}_7^{3\text{bdy}}$, and Ref.[203] offers the ratio between the coefficients:

$$\alpha^{70} : \alpha^{52} : \alpha^{34} : \alpha^{16} = -\frac{\sqrt{21}}{8} : \frac{1}{8} : \frac{\sqrt{15}}{8} : \frac{3\sqrt{3}}{8} \quad (4.87)$$

Thus the graviton mode energy of the Gaffnian state can be determined by tuning c^{50} , c^{32} , and c^{14} . Furthermore, there exist no c^{30} or c^{12} terms in Eq.(4.86), which means that the graviton mode of the Gaffnian state should live in the null space

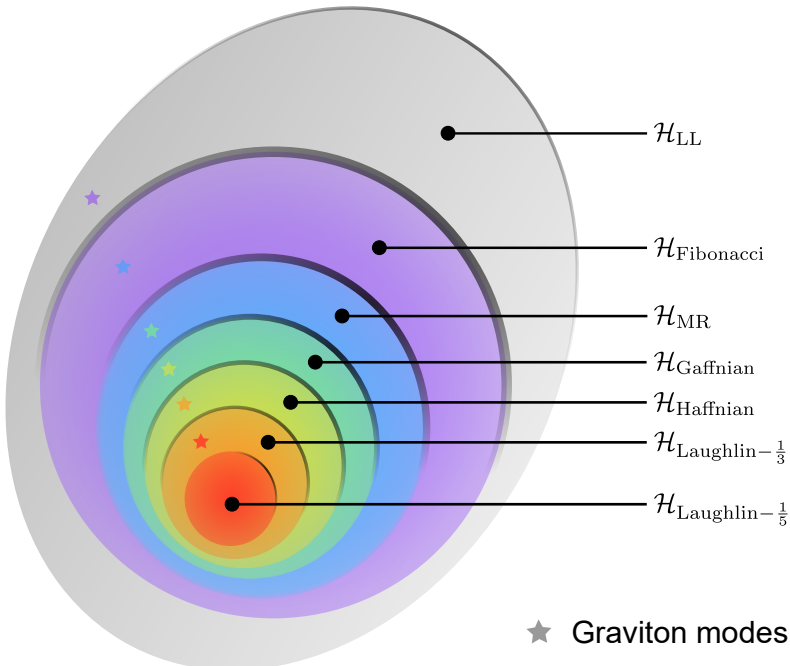


FIGURE 4.4: **Hierarchy of the null spaces of different FQH states.** The null space of different model Hamiltonians can be organized as a hierarchical structure in the full Hilbert space. Meanwhile, the density modes or, more precisely, the graviton modes (denoted by the stars with the corresponding colors) constructed from model ground states live in the next larger null space. For example, the graviton modes of the Laughlin-1/3 phase (orange star) live in the Haffnian null space (green circle), which contains the ground state and all the quasiholes of the Haffnian model Hamiltonian. It is efficient to verify this structure with the characteristic tensor formalism proposed in this thesis.

of the Moore-Read model Hamiltonian $\hat{V}_3^{3\text{bdy}}$, which indicates that the variational energy of the Gaffnian graviton mode is independent of the strength of $\hat{V}_3^{3\text{bdy}}$ in the Hamiltonian.

4.6 Hierarchies within conformal Hilbert spaces

The procedure we have carried out in the last section can be generalized to any graviton modes constructed from the ground state of some well-defined CHS, which, as defined in the last chapter, are spanned by degenerate zero-energy many-body states of special local Hamiltonians, including the well-known generalized pseudopotentials, that physically project into the angular momentum sectors of a cluster of electrons [20, 189]. These states within a CHS are the ground states and quasiholes of a particular FQH phase (though some are believed to be gapless

CHS	Model Hamiltonian
$\mathcal{H}_{\text{Fibonacci}}$	\hat{V}_6^{4bdy}
\mathcal{H}_{MR}	\hat{V}_3^{3bdy}
$\mathcal{H}_{\text{Gaffnian}}$	$\lambda_1 \hat{V}_3^{\text{3bdy}} + \lambda_2 \hat{V}_5^{\text{3bdy}}$
$\mathcal{H}_{\text{Haffnian}}$	$\lambda_1 \hat{V}_3^{\text{3bdy}} + \lambda_2 \hat{V}_5^{\text{3bdy}} + \lambda_3 \hat{V}_6^{\text{3bdy}}$
$\mathcal{H}_{\text{Laughlin-1/(2k+1)}}, k \geq 1$	$\sum_{i=1}^k \lambda_i \hat{V}_{2k-1}^{\text{2bdy}}$

TABLE 4.1: **The CHSs and their model Hamiltonians.** The CHSs are defined as the null spaces of the corresponding model Hamiltonians. Here λ_i can be any constant coefficient.

phases) [190, 336]. Thus like the Hilbert space of the LLL (or any other single LL), such CHSs are built up with *quasiparticles*, which are emergent particles from LL projection and strong interaction. In the LLL, the quasiparticles are simply electrons projected into a single LL, while in other CHSs, they can be abelian or non-abelian anyons [28, 137, 173, 179, 337, 338, 338, 339].

The definition of some commonly-used CHS is shown in Table 4.1. One can observe the relation between the CHSs just by looking at the corresponding model Hamiltonian. Firstly for the CHS defined by model Hamiltonians with the same number of interacting particles (e.g., 2-body for the Laughlin states, 3-body for the Moore-Read, the Gaffnian, and the Haffnian state), they will naturally form a hierarchical structure because the restriction set by the pseudopotentials are getting stronger. Then the tricky things occur at the largest CHS \mathcal{H} defined by n -body model Hamiltonian because one has to find the smallest CHS defined by a $n+1$ -body model Hamiltonian and meanwhile containing \mathcal{H} as its subspace. We have analytically proved that the CHS defined by \hat{V}_1^{2bdy} is within the one defined by $\sum_{i=3}^8 \lambda_i \hat{V}_i^{\text{2bdy}}, \lambda_4 = 0$ as in Eq.(4.80). For the largest CHS \mathcal{H}_{MR} defined by three-body model Hamiltonians, it is within the CHS defined by \hat{V}_6^{4bdy} , which we will not provide a proof for here. The same idea can also be applied to the graviton modes because now we have figured out how to get their model Hamiltonians rigorously. Fig.4.4 shows the complete hierarchical structure of the CHSs with the graviton modes in the LLL.

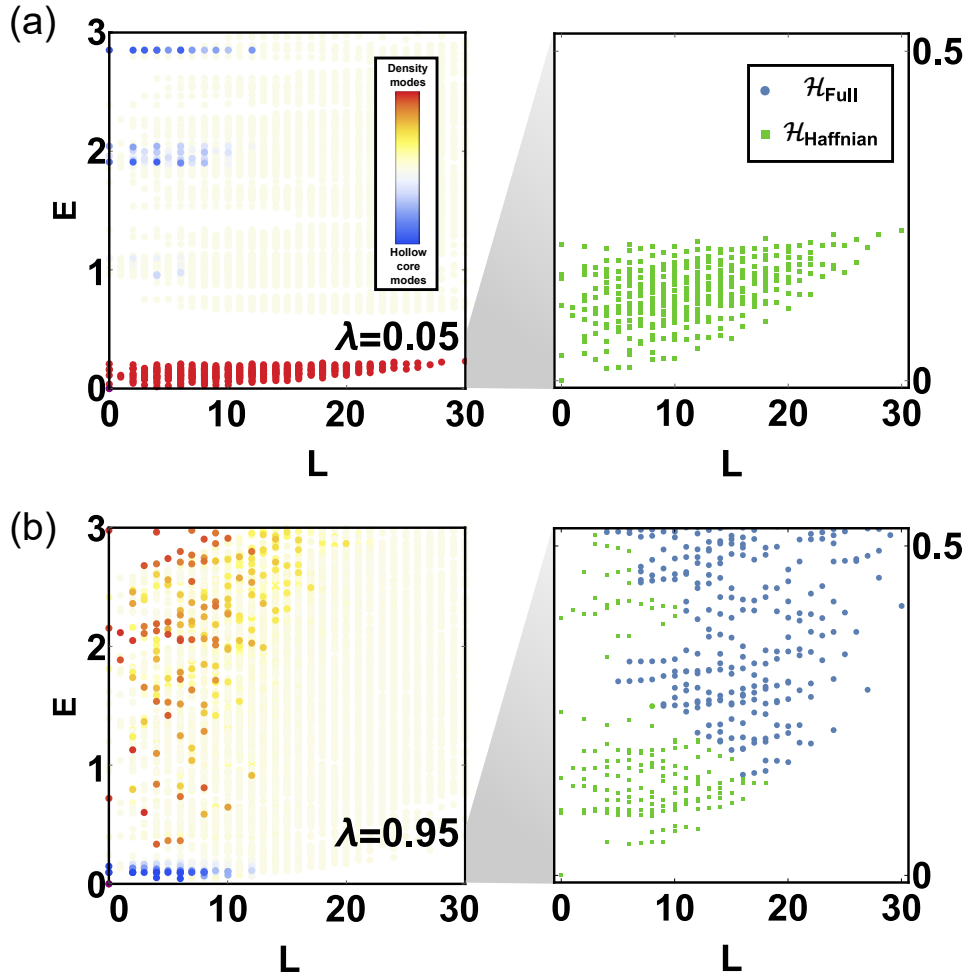


FIGURE 4.5: Spectra of the toy Hamiltonian \hat{H}_L diagonalized in different Hilbert spaces. The case with $\lambda = 0.05$ is shown in (a) and $\lambda = 0.95$ in (b). In the left panel, one can clearly observe the transition of the low-lying states when λ increases from 0.05 to 0.95. These states have different natures, as explained in Fig.4.7. In the right panel, we zoom in on the spectra to the range $E \in [0, 0.5]$ and mark the states living in the Haffnian null space with green squares and other states with blue dots. As expected, the CF picture shows that both the density and the hollow-core modes live in the Haffnian null space. Note that the lowest angular momentum of the hollow-core modes is $L_{\min} = 4$, as can be seen in (b). Furthermore, the quantized energy of the hollow-core modes (especially when $\lambda \rightarrow 0$) can be understood using the root configurations in Eq.(4.89).

4.7 Transitions in low-lying excitations while the ground state is invariant

We have seen that the theoretical derivations reveal the well-organized hierarchical structure of the null space of multiple model Hamiltonians, in which the graviton modes of different FQH states reside. However, for the graviton modes to be experimentally relevant, they must be low-lying in the excitation spectrum. For fully-gapped FQH phases, the graviton modes are also gapped, as shown in Fig.4.4, as they can never live within the same CHS as the ground state. Moreover, given they are neutral excitations, for realistic interactions, they may also become gapless without affecting the robustness of the Hall conductivity plateau [139, 192, 193]. In this section, we proceed to perform numerical calculations for the dynamical properties of the graviton modes using the theoretical tools developed in the previous sections. We focus, in particular, on the Laughlin-1/5 state and the Gaffnian state and discuss possible theoretical and experimental consequences.

4.7.1 Laughlin-1/5 graviton mode

We have shown that the graviton mode of Laughlin-1/5 state lives within the null space of $\hat{V}_1^{2\text{bdy}}$, and thus it is a quantum fluid of Laughlin-1/3 quasiholes. If we look at a short-range interaction with model Hamiltonians involving only $\hat{V}_1^{2\text{bdy}}$ and $\hat{V}_3^{2\text{bdy}}$, the dynamics of the graviton modes is entirely controlled by $\hat{V}_3^{2\text{bdy}}$ (in principle we can also use other two-body pseudopotentials). Then it is helpful to understand the low-lying excitations of the following toy model:

$$\hat{H}_L = (1 - \lambda)\hat{V}_1^{2\text{bdy}} + \lambda\hat{V}_3^{2\text{bdy}} \quad (4.88)$$

The ground state stays invariant as the Laughlin-1/5 state when the value of λ is tuned. In contrast, the low-lying excitations can be qualitatively different. In particular, when λ is close to zero, the graviton mode and the magneto-roton modes should be the low-lying excitations. On the contrary, if there exist states that are punished by $\hat{V}_1^{2\text{bdy}}$ but not $\hat{V}_3^{2\text{bdy}}$, then they will become the low-lying states when λ is close to unity because the energy of the graviton modes is proportional to λ . Thus one can expect the transition of the low-lying states when λ is continuously increased from 0 to 1.

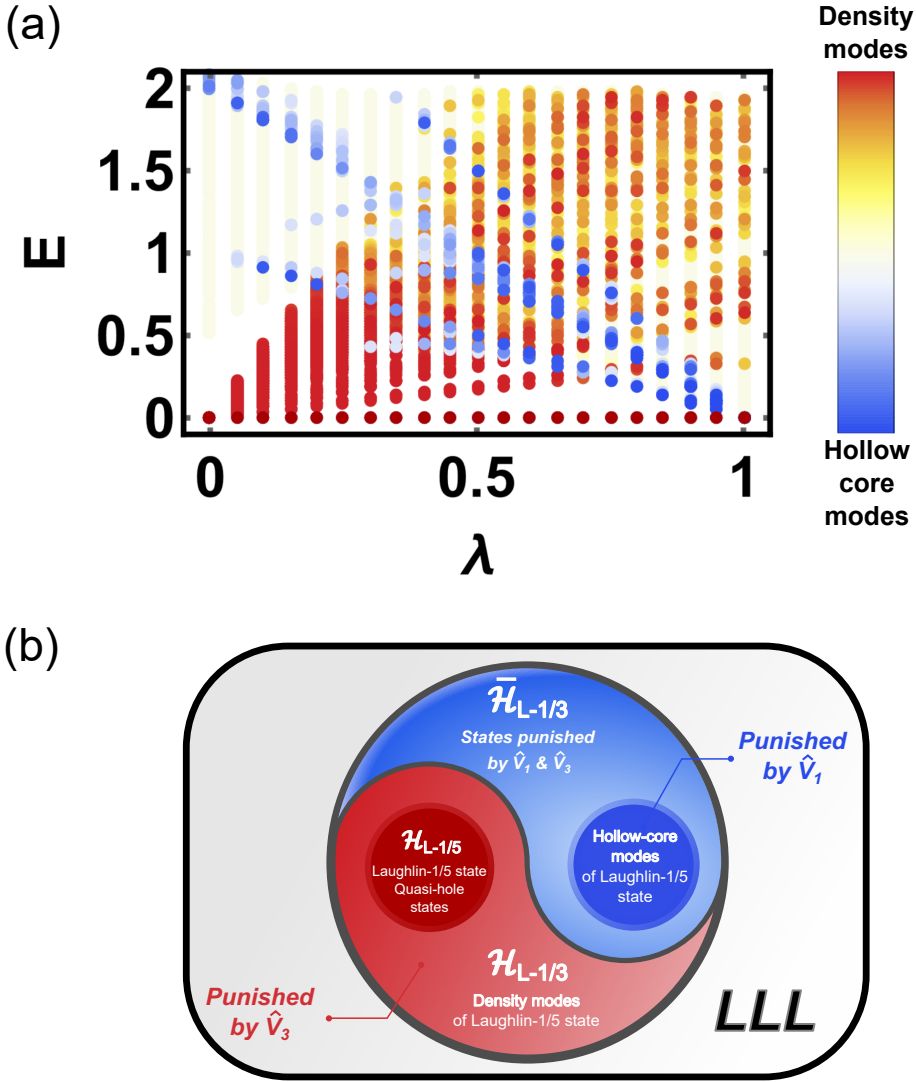


FIGURE 4.6: **Spectrum of the toy Hamiltonian \hat{H}_L with respect to 6 electrons and 26 orbitals.** (a) As the color bar shows, the red dots depict the spectrum of the density modes, and the blue dots denote the hollow-core modes. The color of each dot is determined by calculating their collective overlap with all the density modes in the Laughlin-1/3 null space $\mathcal{H}_{L-1/3}$, or all the hollow-core modes in the complementary space $\bar{\mathcal{H}}_{L-1/3}$. As λ increases, though the ground state (denoted by dark red) stays invariant, the low-lying states show a clear cross-over behavior and transform from density modes to hollow-core modes. (b) illustrates the structure of the Hilbert space and the relationship between the states and the model Hamiltonians. The Laughlin-1/5 null space $\mathcal{H}_{L-1/5}$ (dark red circle) punished by neither $\hat{V}_1^{2\text{bdy}}$ nor $\hat{V}_3^{2\text{bdy}}$ is the sub-space of $\mathcal{H}_{L-1/3}$ (only punished by $\hat{V}_3^{2\text{bdy}}$). Meanwhile, there exist the hollow-core modes (blue circle) only punished by $\hat{V}_1^{2\text{bdy}}$ in $\bar{\mathcal{H}}_{L-1/3}$. All of the other states are punished by both $\hat{V}_1^{2\text{bdy}}$ and $\hat{V}_3^{2\text{bdy}}$, living in the remaining part of $\bar{\mathcal{H}}_{L-1/3}$.

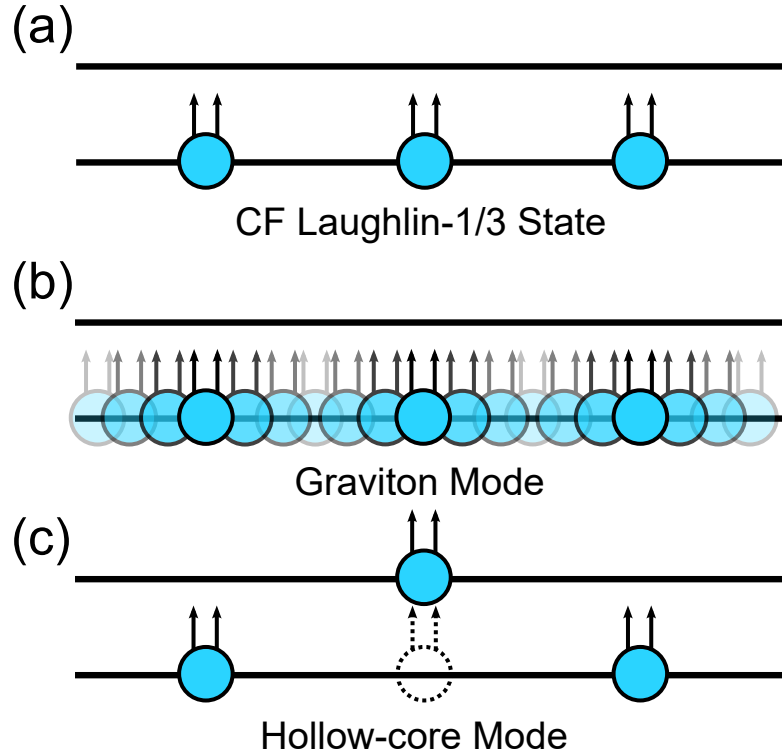


FIGURE 4.7: Nature of the low-lying states with different model Hamiltonian in the CF picture. (a) The Laughlin-1/5 state of the electrons can be reinterpreted as the Laughlin-1/3 state of CFs consisting of one electron and two fluxes, which also follows from the Jain construction. (b) The graviton modes can be understood as the excitations of CFs in the lowest CF level. (c) The hollow-core modes are created by exciting CFs to the second CF level, which still live in the Gaffnian null space.

The results of the Laughlin states with 6 electrons are shown in Fig.4.6. While the ground state is invariant (i.e., the Laughlin-1/5 state, denoted by dark red color in Fig.4.6), the low-lying excitations show an apparent cross-over behavior. When $\lambda \rightarrow 1$, the density modes, including the graviton modes and the multi-magneto-roton modes, indicated by red spectrum in Fig.4.6 (a), are no longer low-lying excitations. The structure of the Hilbert space in the LLL is illustrated in Fig.4.6(b). The null space of the Laughlin-1/5 model Hamiltonian (Laughlin-1/5 null space for short) denoted by the red circle is a proper subspace of the Laughlin-1/3 null space (light-red part), the complement space of which contains the states either only penalized by $\hat{V}_1^{2\text{bdy}}$ (blue circle), or penalized by both $\hat{V}_1^{2\text{bdy}}$ and $\hat{V}_3^{2\text{bdy}}$ (light-blue part). We can refer to the blue states as the “hollow-core” modes since they live within the null space of $\hat{V}_3^{2\text{bdy}}$, but out of the null space of $\hat{V}_1^{2\text{bdy}}$ [340–342].

It is helpful to look more closely at the spectra of \mathcal{H}_L with $\lambda = 0.05$ and $\lambda = 0.95$ as shown in the left panel of Fig.4.5, where the density modes including the graviton modes occupy the low-lying states when λ is close to 0. In contrast, when λ is close to 1, the energy of these states significantly increases as expected, so the hollow-core modes occupy the low-lying excitations. To understand better the nature of the low-lying states, one can also diagonalize \hat{H}_L in different sub-Hilbert spaces instead of the full Hilbert space of a single LL and to check if the truncation of the Hilbert space affects the low-lying excitations. In the right panel of Fig.4.5, the spectra of the Hamiltonian diagonalized in the full Hilbert space are shown, where green squares denote the states that live almost entirely within the Haffnian null space. For both cases, \hat{H}_L with $\lambda = 0.05$ (low-lying excitations consisted of density modes) and $\lambda = 0.95$ (low-lying excitations consisted of hollow-core modes), numerical studies show strong evidence that all the low-lying states live in the Haffnian null space. On the other hand, the graviton and the magneto-roton modes live within the null space of $\hat{V}_1^{2\text{bdy}}$ (which itself is a subspace of Haffnian null space), while the hollow-core modes live outside of the $\hat{V}_1^{2\text{bdy}}$ null space.

We can also understand the differences between these two types of low-lying states, by appealing to the intuitive picture from the CF theory [71, 74]. Fig.4.7 illustrates the physical distinctions between the graviton modes (low-lying states when $\lambda = 0.05$) and the hollow-core modes (low-lying states when $\lambda = 0.95$), where the Laughlin-1/5 state of electrons is reinterpreted as the Laughlin-1/3 state of CFs as Fig.4.7 (a) shows because each CF contains one electron and two fluxes so the filling factor becomes $\nu^* = 1/(5 - 2) = 1/3$. The Laughlin-1/3 null space only contains the states in the first CF level. The graviton and the magneto-roton modes are thus excitations within the partially-filled first CF level, which are low-lying excitations for small λ . In contrast, when λ approaches one, the hollow-core modes come from the excitations of the CFs into the second CF level, in some sense similar to the graviton modes of the Laughlin-1/3 state. Some of the root configurations containing one or more of the “hollow-core” modes can be written as:

$$\begin{aligned} 11000000001000010000100001 \dots & \quad L = 4 \\ 11000000001100000000100001 \dots & \quad L = 8 \\ 11000000001100000000110000 \dots & \quad L = 12 \end{aligned} \tag{4.89}$$

with the lowest angular momentum $L = 4$, agreeing well with Fig.4.5 (b). From these root configurations, one can also understand the quantized energy of the

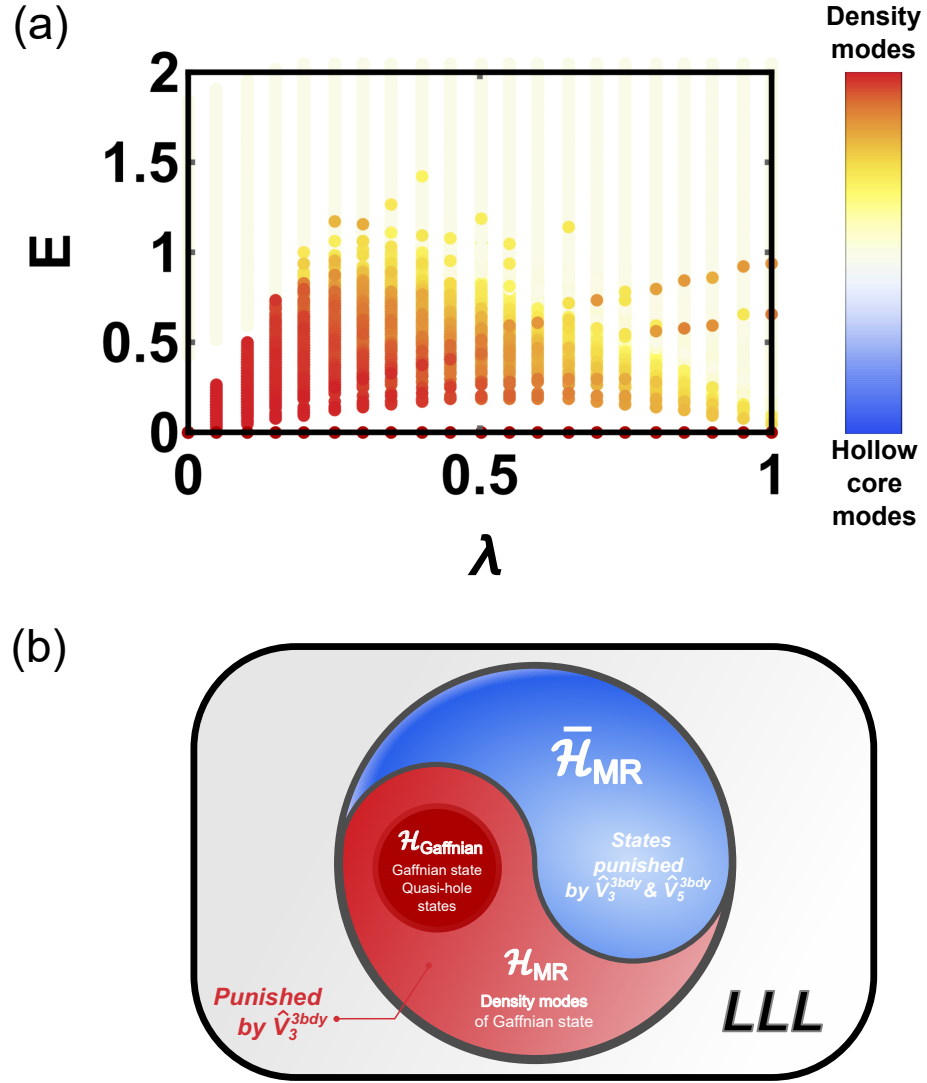


FIGURE 4.8: **Spectrum of the toy Hamiltonian \hat{H}_G with respect to 10 electrons and 22 orbitals.** (a) shows the spectra of the model Hamiltonian \hat{H}_G in Eq.(4.90). The low-lying states are density modes even when λ is quite large, and the absence of hollow-core modes is different from the Laughlin-1/5 state in Fig.4.6. (b) illustrates the structure of the Hilbert space and the relationship between the states and the model Hamiltonians. All the states in the complementary space of the Moore-Read null space are punished by both \hat{V}_3^{3body} and \hat{V}_5^{3body} .

hollow-core modes: each pair of electrons in the root configuration (corresponding to a CF in the second CF level) contributes a unit of energy. Thus for six electrons, the highest energy should be ~ 3 as shown in Fig.4.5(a).

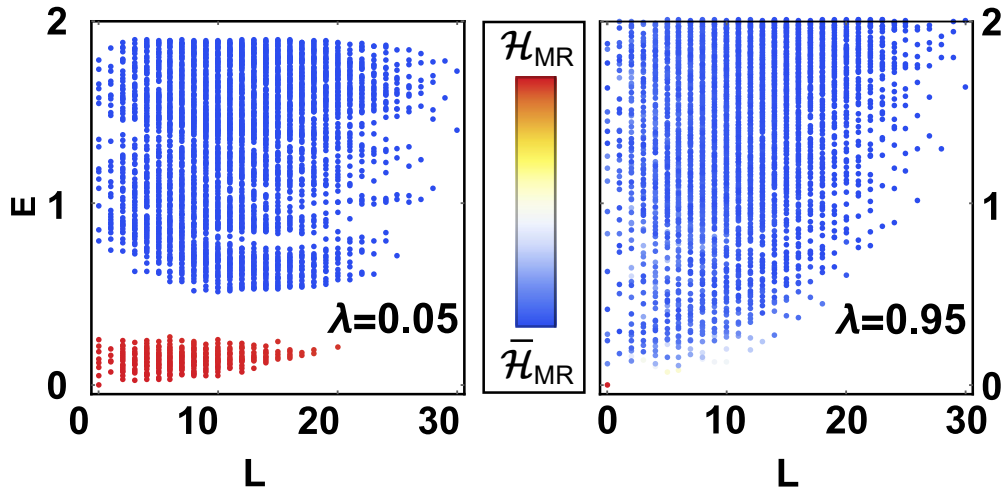


FIGURE 4.9: **Spectra of the toy Hamiltonian \hat{H}_G diagonalized in the full Hilbert spaces.** The spectrum with $\lambda = 0.05$ is shown in the left panel and $\lambda = 0.95$ in the right panel. As expected, when $\lambda = 0.05$, all the low-lying states (density modes) live within the Moore-Read null space \mathcal{H}_{MR} . Meanwhile, when $\lambda = 0.95$, all the states except the ground state are in the complement of \mathcal{H}_{MR} within the LLL, denoted by $\bar{\mathcal{H}}_{\text{MR}}$.

4.7.2 Gaffnian graviton mode

The behaviors of the Gaffnian graviton modes at $\nu = 2/5$ are not entirely the same as the Laughlin-1/5 case, which can be seen in the spectrum of the following toy Hamiltonian:

$$\hat{H}_G = (1 - \lambda)\hat{V}_3^{\text{3bdy}} + \lambda\hat{V}_5^{\text{3bdy}} \quad (4.90)$$

shown in Fig.4.8. The density modes are still behaving as predicted by the theoretical derivations, i.e., occupying the low-lying states of \mathcal{H}_G with $\lambda \rightarrow 0$. However, as shown in Fig.4.8, when $\lambda \rightarrow 1$, there exists no state in the Hilbert space that is only punished by \hat{V}_3^{3bdy} , so the null space of \hat{V}_5^{3bdy} lies entirely within the Gaffnian null space (also see Fig.4.9). Thus there are no hollow-core modes here in contrast to the case for the Laughlin-1/5 phase. It would be interesting to see if this is related to the conjecture that the model Hamiltonian of Eq.4.90 is gapless in the thermodynamic limit at $\nu = 2/5$, while the Laughlin-1/5 phase is gapped.

From Eq.(4.86), we know the graviton mode gap of the Gaffnian state at $\nu = 2/5$ is determined by the expectation value of the ground state with respect to only \hat{V}_7^{3bdy} , denoted by d_{3bdy}^7 to be consistent with the two-body case in Fig.4.10, where the finite size scaling of the structure factor coefficients of different states is shown.

Previous numerical calculations showed evidence that in the thermodynamic limit, the gap of Eq.(4.90) at $\lambda = 0.5$ closes in the $L = 2$ sector [192]. This is indeed the sector of the graviton mode, and we have shown it is in the null space of $\hat{V}_3^{3\text{bdy}}$ with its energy entirely determined by $\hat{V}_5^{3\text{bdy}}$. Our numerical calculation is thus valid for a family of model Hamiltonian of Eq.(4.90) parametrized by λ . Moreover, it shows that the graviton mode of the Gaffnian phase will likely go soft in the thermodynamic limit, as its variational energy is an order of magnitude smaller than the graviton modes in the Moore-Read phase. It is, however, essential to note that the graviton mode energy gap of the Laughlin-1/5 phase is also an order of magnitude lower than that of the Laughlin-1/3 phase, as shown in Fig. 4.10a.

While the Gaffnian model Hamiltonian is a theoretical model that is conjectured to be gapless and thus describes a possibly critical point, it is also closely related to the gapped Jain $\nu = 2/5$ phase from short-range two-body interactions [190, 242, 343]. It would be interesting to see how the graviton modes at $\nu = 2/5$ behave when we approach the critical point from the gapped Jain phase at $\nu = 2/5$. The finite numerical analysis seems to suggest that both the charge gap and the neutral gap will close, but with realistic interactions, we can also entertain the possibility that the graviton modes of the Jain $\nu = 2/5$ phase can close first while the charge gap remains open, in analogy to the nematic FQH phase that has been observed in experiments at $\nu = 2 + 1/3$ [344–346].

4.8 Experimental significance

While we analyze the graviton modes above with only toy models, they can offer insights into the experimental measurements of low-lying neutral excitations in FQH phases, using, for example, Raman scattering or inelastic photon scattering [109, 114, 320, 347]. For the Laughlin phase at $\nu = 1/5$, a short-range realistic interaction (e.g., in the LLL, or with the Coulomb interaction renormalized by sample thickness or screening [55, 348, 349]), the graviton mode as well as the magneto-roton modes will be more prominent. However, since the realistic interaction cannot completely project out the complement of the null space of $\hat{V}_1^{2\text{bdy}}$, the graviton modes will always mix with the hollow-core modes, so their experimental signals will not be as clean as those from, for example, the Laughlin-1/3 phase.

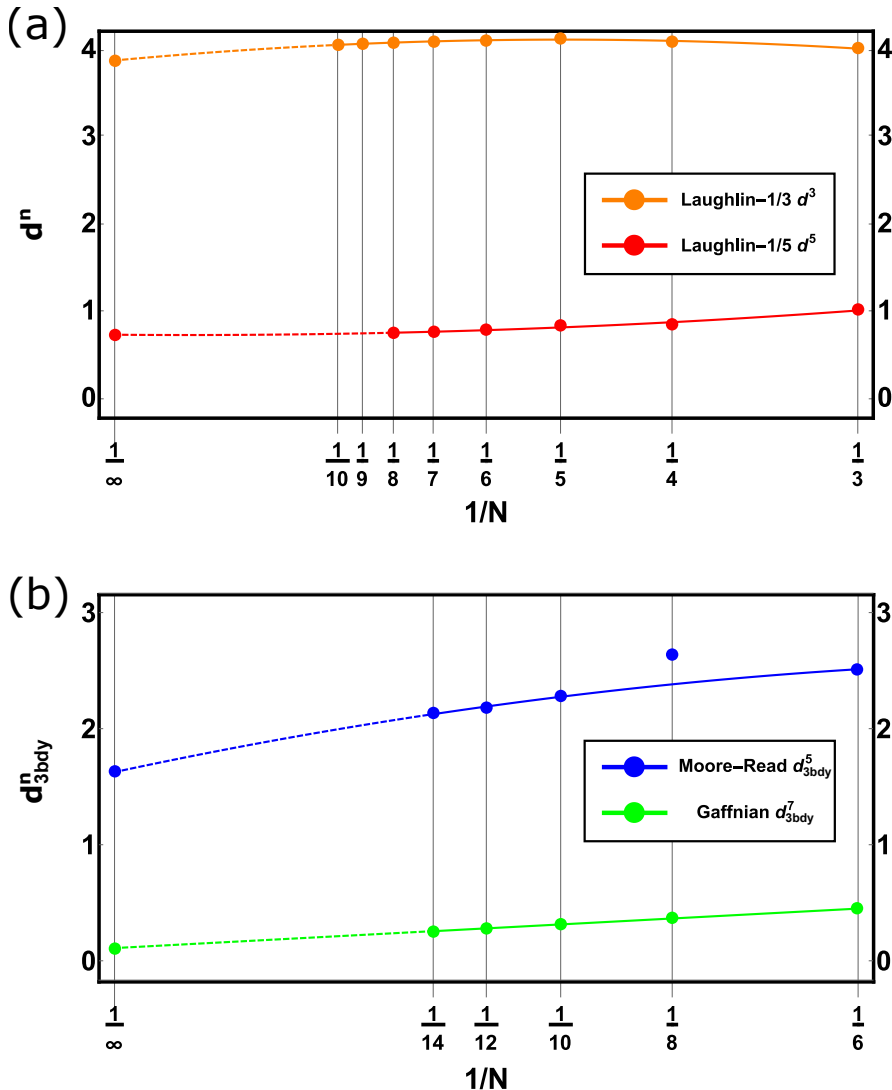


FIGURE 4.10: Finite size scaling of the structure factor coefficients of different states. (a) The structure factor expansion coefficients of the Laughlin- $1/3$ and the Laughlin- $1/5$ state. According to the orthogonality of Laguerre polynomials, d^m of the Laughlin- $1/m$ state is equal to the expectation value of the model Hamiltonian $\hat{V}_m^{2\text{bdy}}$ (thus $c^m = 1$) acting on this state. Thus the numerical results shown here provide the value of the corresponding dimensionless coefficients despite the dimension of energy, which is true for Fig.(b) as well. (b) The expectation value of $\hat{V}_7^{3\text{bdy}}$ with respect to the Gaffnian state (≈ 0.04 in the thermodynamic limit), denoted by $d_{3\text{bdy}}^7$, is significantly smaller than other coefficients in the plot, where the expectation value of $\hat{V}_5^{3\text{bdy}}$ with respect to the Moore-Read state is denoted by $d_{3\text{bdy}}^5$ (≈ 1.6 in the thermodynamic limit).

With longer-range interactions (e.g., in higher LLs), it is still possible for the Laughlin-1/5 state to be robust in the sense that the plateau of the Hall conductivity can be observed [350]. However, we do not expect clear experimental signals of the graviton modes for such interactions due to the strong mixing with the hollow-core modes. If the realistic interaction is short-ranged but dominated by $\hat{V}_3^{3\text{bdy}}$, there will be no graviton modes (or quadruple excitations) at low energy. Instead, the low-lying excitations are in the complement of the null space of $\hat{V}_1^{2\text{bdy}}$, and in particular, the quasiholes excitations can be fractionalized and carry the charge of $e/10$. This is analogous to the nematic FQH phase at $\nu = 1/3$ observed in the experiments and the fractionalization of the Laughlin-1/3 quasiholes near the phase transition [140]. It would thus be exciting if the hollow-core modes, characterized by fractionalized Laughlin-1/5 quasiholes, could be observed in experiments.

4.9 Summary

In this chapter, we have introduced the construction of the model wave function for the graviton modes and presented a number of analytical results for their variational energies in FQH phases. These results are rigorous in the thermodynamic limit for the FQH states concerning any arbitrary two-body or three-body interactions. In particular, we show that the ground state wave function entirely determines the variational energies of the graviton modes. In addition, for short-range interactions, only the leading terms of the ground state structure factor, when expanded in the proper Laguerre-Gaussian basis, are involved in the computation of the graviton mode energy. These analytical results can help construct model Hamiltonians for the graviton modes, which are the exact zero-energy states of these Hamiltonians. We can thus determine analytically if the graviton mode lives entirely within a specific CHS, or if they have finite overlaps in different CHSs. The latter gives a microscopic understanding of the multiple graviton modes proposed in the effective field theory descriptions, as discussed in the next chapter.

There are several proposals for the graviton modes to be detected in experiments, but in general, it is a difficult task because of the high energy of such excitations. For many FQH phases with Coulomb interactions in simple experimental settings, the long-wavelength excitations are not the lowest energy ones. The graviton modes

thus have to compete with multi-roton and other neutral excitations. The analytical results we have derived can help us understand how the graviton energy can be affected by realistic interactions, and how we can tune such interactions to lower their variational energies. This thesis's generalization to three-body interactions also allows us to treat LL mixing in realistic systems [188, 252, 351–353], which can be significant in higher LLs. Detailed studies of the graviton modes in the context of actual experimental parameters will be carried out in the next chapter. The softening of the graviton modes can also allow us to understand potential “phase transitions” in topological systems even when the ground state topological properties are invariant, as we explored numerically with the Laughlin-1/5 state and the Gaffnian state with toy Hamiltonians.

Even with the methodology and the analytical tools developed in this chapter, the quantitative values of the graviton energy in the thermodynamic limit cannot be determined without numerical computations and finite-size scaling. It is, however, a much simpler procedure requiring only the ground state and partial information about its static structure factor, in contrast to the conventional methods requiring the computation of many low-lying states. The universal characteristic tensor shows that the Hilbert space of the FQH states is highly structured. This formalism can, in principle, be generalized to interactions involving more than three particles. The dispersion of the graviton mode can also be computed analytically by expanding the single mode approximation to higher orders in momentum. At this stage, both cases are algebraically very involved. It would be helpful in the future to carry out a more general and systematic calculation of the graviton energy and its dispersion for any arbitrary Hamiltonians. This, combined with a numerically more efficient way to obtain information from the ground state static structure factor (or the density correlation functions), can lead to a much better understanding of the collective neutral excitations in non-abelian FQH phases.

Chapter 5

Microscopic Theory of Multiple Graviton Modes

We have introduced the microscopic theory about the collective neutral excitations with spin-2 in FQH phases, called the graviton modes as a typical manifestation of the interplay between topology and geometry. While Lorentz invariance is absent in this $(2+1)$ -dimensional space-time, these 2D graviton modes encode topological information about their respective FQH phases, and their dynamics lead to rich physics ranging from ground state incompressibility to the dynamical phase transitions of the low-lying excitations [140, 354]. The effective field theory studying the graviton modes has been proposed by using the Newton-Cartan metric, and various experimental proposals for the observation of these modes have been put forward [187, 236, 238, 318, 321, 322, 324–326, 355]. In this chapter, we will reveal the origin of the graviton modes from the metric fluctuations within CHSs [52, 199, 230]. Furthermore, we will discuss more the experimental techniques in probing neutral excitations such as inelastic polarised photon scattering, which can provide valuable information about the chiralities of graviton modes [108, 109, 114, 320, 347].

Meanwhile, with the microscopic theory of the graviton modes established in the last chapter, one can construct model Hamiltonians for these modes in the FQH fluids at different filling factors [333, 354]. Recently numerical results have implied the signature of multiple graviton modes in FQH states [335, 356]. Given that most of the research so far on graviton modes is based on effective field-theoretical

descriptions and numerical analysis with model wave functions [335], we will provide a more detailed microscopic theory for a more complete characterization of the emergence and interaction between different graviton modes by *analytically* showing that multiple graviton modes (gravitons for brevity) are a generic feature for FQH fluids, from the splitting of the long wavelength limit of the GMP mode in different subspaces in a single LL [52]. Using the analytic tools we developed earlier [354], we demonstrate that the number of gravitons is dynamical in nature, and is only meaningful when referring to specific interaction Hamiltonians. Each graviton can be interpreted as the metric fluctuation of a CHS within a single LL. For *short-range two-body interactions*, we show all non-Laughlin FQH states around $\nu = 1/(2n)$ with $n > 1$ (e.g. within the null space of $\hat{\mathcal{V}}_n^{2\text{bdy}} = \sum_{k=1}^n \hat{V}_{2k-1}^{2\text{bdy}}$ Haldane pseudopotential interaction), including the interacting CF states, have at least two gravitons. In particular, the Jain states at $\nu = N/(2nN \pm 1)$ and the Pfaffian states at $\nu = 1/(2n)$ all have two gravitons if $n, N > 1$. The Laughlin states ($N = 1$) and the Jain states with $n = 1$ all have a single graviton. This agrees with the cases studied numerically in both Ref.[335, 356] at $\nu = 2/7, 2/9, 1/4$, at the same time providing an analytic explanation and geometric interpretation to their numerical observations.

5.1 Gravitons as metric fluctuations

To fully understand the geometric features of the graviton modes, let us recall the model wave function of graviton modes given by the SMA in the long wavelength limit:

$$|\psi_g\rangle = \lim_{\mathbf{q} \rightarrow 0} \frac{1}{\sqrt{S_q}} \delta \hat{\rho}_q |\psi_0\rangle \quad (5.1)$$

where S_q is the regularised guiding center structure factor with $\lim_{\mathbf{q} \rightarrow 0} S_q \sim \eta_s |\mathbf{q}|^4$, which is fully determined by $|\psi_0\rangle$. The Haldane bound dictates that the value of η_s gives the upper bound to the topological shift of $|\psi_0\rangle$ [357]. Generically speaking, the regularised (guiding-center) density operator $\delta \hat{\rho}_q$ is the linear combination of

magnetic translational operators. But if we expand $\delta\hat{\rho}_q$ around $q = 0$, the expression can be written as:

$$\begin{aligned} \lim_{q \rightarrow 0} \delta\hat{\rho}_q &= \lim_{q \rightarrow 0} \sum_{n=1}^{\infty} \sum_{i=1}^{N_e} \frac{i^n}{n!} q_{a_1} q_{a_2} \cdots q_{a_n} \partial_{q_{a_1}} \partial_{q_{a_2}} \cdots \partial_{q_{a_n}} e^{iq_a \hat{R}_i^a} \\ &\equiv \sum_{n=1}^{\infty} \sum_{i=1}^{N_e} \frac{i^n}{n!} q_{a_1} q_{a_2} \cdots q_{a_n} \bar{\Lambda}_i^{a_1 a_2 \cdots a_n} \end{aligned} \quad (5.2)$$

which contains infinite infinitesimal generators $\bar{\Lambda}_i^{a_1 a_2 \cdots a_n}$ with i as the particle index, but the discussion to most of them is actually moot because we are working near the zero point, and more importantly not all of them can form sub-algebras. Thus we will focus on the first two orders: one is the sub-algebra given by the regularised translation generator of the center of mass $\hat{P}_a = \epsilon_{ab} \sum_i \bar{\Lambda}_i^b$:

$$[\hat{P}_a, \hat{P}_b] = 0 \quad (5.3)$$

Thus when acting on a uniform ground state, this generator simply gives zero as only the interactions between the internal particles are considered. This is also ensured by the generic inversion symmetry in the Hamiltonian that forces all the odd-ordered generators acting on the ground state to vanish.

For the second order, one can write down the sub-algebra as follows:

$$[\Lambda^{ab}, \Lambda^{cd}] = -i \cdot (\epsilon^{ac} \Lambda^{bd} + \epsilon^{ad} \Lambda^{bc} + \epsilon^{bd} \Lambda^{ac} + \epsilon^{bc} \Lambda^{ad}) \quad (5.4)$$

which is the $\mathfrak{sl}(2, \mathbb{R})$ Lie algebra as the largest finite-dimensional sub-algebra of W^∞ -algebra, so Λ^{mn} are the three generators of area-preserving diffeomorphism in k -space. So one can construct the unitary operator [230, 357]:

$$\hat{U}(\chi) = e^{i\chi_{ab} \Lambda^{ab}} \quad (5.5)$$

where χ_{ab} is a real and symmetric matrix, the determinant of which corresponds to different linear transformations to the space:

$$\det(\chi_{ab}) \begin{cases} < 0, & \text{squeezing} \\ = 0, & \text{shear} \\ > 0, & \text{rotation} \\ = 1, & \text{inversion} \end{cases} \quad (5.6)$$

These generators preserve the algebra of the guiding center coordinates when acting on them:

$$\hat{R}'^a_i = \hat{U}(\chi) \hat{R}_i^a \hat{U}(-\chi) = X_b^a(\alpha) R_i^b \implies [\hat{R}'^a_i, \hat{R}'^b_j] = -i\epsilon^{ab}\delta_{ij} \quad (5.7)$$

where $X_b^a = e^{-2\epsilon^{ac}\chi_{cb}}$. If there is rotational invariance in the system, one can also define the angular momentum operator as the generator in the Cartan sub-algebra of Eq.(5.4):

$$\hat{L}_g = g^{ab}\Lambda_{ab} \quad (5.8)$$

where g^{ab} denotes the corresponding metric. Thus to wrap up, in the long wavelength limit, the regularised density operator acting on the ground state is equivalent to a unitary operator of area-preserving deformation in momentum space:

$$\lim_{\mathbf{q} \rightarrow 0} \delta\hat{\rho}_{\mathbf{q}} |\psi_0\rangle \sim \hat{U}(\chi) |\psi_0\rangle \quad (5.9)$$

This clearly exposes the geometric nature of the graviton mode as the excitation induced by *metric fluctuations* and provides the physical reason for calling these modes “gravitons”. Note that this does not mean that $\delta\hat{\rho}_{\mathbf{q}}$ in the GMP wave function depends on some tunable χ . Instead, the effect of the deformation is entirely determined by the corresponding metric.

5.1.1 The cyclotron and guiding center metrics

From the discussion above, one can see that the metric figures prominently in the discussion of gravitons. It is useful to first consider the simple case of the integer quantum Hall effect (IQHE), which are topological phases coming from fully filled

LLs with the following full Hamiltonian:

$$\hat{H} = \sum_{i=1}^{N_e} \frac{1}{2m} \tilde{g}^{ab} \hat{\pi}_{ia} \hat{\pi}_{ib} + \hat{V}_{\text{int}} \quad (5.10)$$

Here as introduced in Chap.2, $\hat{\pi}_{ia} = \hat{p}_{ia} + e\hat{A}_{ia}$ denotes the dynamical momentum operator of the i -th electron (\hat{p}_i is the canonical momentum and \hat{A}_i is the external vector potential), with the commutation rules $[\hat{\pi}_{ia}, \hat{\pi}_{jb}] = i\delta_{ij}\epsilon_{ab}$. The magnetic field is $B = \epsilon^{ab}\partial_a \hat{A}_{ib}$. The cyclotron energy is assumed to be the dominant energy scale, so any LL mixing induced by electron-electron interaction can be perturbatively captured by few-body interaction of the second term \hat{V}_{int} , which now describes the dynamics only within a single LL [203, 269, 351–353]. The important point here is that the Hilbert space of a single LL, which we will refer to as the LLL without loss of generality, is parametrized by the unimodular metric \tilde{g}^{ab} in Eq.(5.10), which is physically the effective mass tensor. Quantum fluctuations around this metric thus lead to graviton modes in higher LLs, which we can term “cyclotron gravitons”. This graviton has very high energy in a large magnetic field as the only graviton for the IQHE since the LLL is fully filled.

For FQHE in a partially filled LL, the dynamics is determined entirely by the guiding center coordinates $\hat{\bar{R}}^a = \hat{r}^a - \epsilon^{ab}\hat{\pi}_b$. This implies the interaction energy \hat{V}_{int} is a functional of \bar{R}_i only and commutes with the kinetic energy. It can be explicitly expressed as:

$$\hat{V}_{\text{int}} = \int d^2q V_{|\mathbf{q}|} \hat{\rho}_{\mathbf{q}} \hat{\rho}_{-\mathbf{q}} \quad (5.11)$$

where $\hat{\rho}_{\mathbf{q}} = \sum_i e^{i\mathbf{q} \cdot \bar{R}_i}$ is the guiding center density operator. For rotationally invariant systems, we have a new unimodular metric \bar{g}^{ab} defining distance in the momentum space $|\mathbf{q}| = \sqrt{\bar{g}^{ab}q_a q_b}$, which is physically independent of \tilde{g}^{ab} . We illustrate a complete analogy to the “cyclotron graviton” in the IQHE by using the simple example of $\hat{V}_{\text{int}} = \hat{V}_1^{\text{2bdy}}$, or the model Hamiltonian for the Laughlin $\nu = 1/3$ state. Just like the LLL, which is the null space of the kinetic energy parameterized by \tilde{g}^{ab} , the CHS \mathcal{H}_1 defined by \hat{V}_1^{2bdy} (spanned by the Laughlin ground state and quasiholes) is parametrized by \bar{g}^{ab} . The quantum fluctuation around \tilde{g}^{ab} gives the “cyclotron graviton” outside LLL. In contrast, that of \bar{g}^{ab} gives the well-known graviton or quadrupole mode (the long wavelength limit of the GMP mode) outside of \mathcal{H}_1 [230].

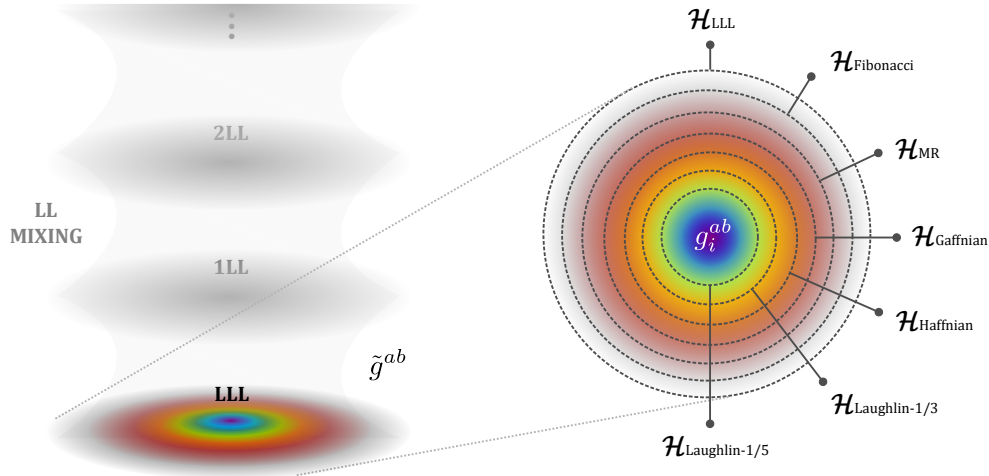


FIGURE 5.1: Intrinsic metrics in FQH states. The left panel shows that the fluctuations of the cyclotron metric \tilde{g}_{ab} originate from the LL mixing. The right panel shows the hierarchical structure of the CHSs (null spaces) of the corresponding model Hamiltonians (more details can be found in Table 4.1) in the LLL. Each of these spaces can have its own metric g_i^{ab} , the fluctuation around which can potentially lead to multiple graviton modes in a single LL.

We want to emphasize the arguments above apply to any \hat{V}_{int} with an incompressible ground state (or even a compressible ground state such as the CF liquid at the filling factor 1/4 [356]). Thus, generally speaking, all FQH states have at least two gravitons due to the structure of the full Hamiltonian: the cyclotron graviton residing in higher LLs at very high energy due to the large magnetic field, and at least one guiding center graviton within the LLL. For the rest of this chapter, we will ignore the cyclotron graviton and focus on the dynamics within the LLL. Still, we will borrow the same concept when understanding the emergence of multiple guiding center gravitons from \hat{V}_{int} .

5.1.2 Metrics within conformal Hilbert spaces

We have found the hierarchical structure of the CHSs within a single LL, which are defined by different model Hamiltonians so generically they can have independent metrics. Let \mathcal{H}_α be one of these CHSs, and the null space of the corresponding model Hamiltonian \hat{V}_α . Just like in Eq.(5.11), \hat{V}_α contains a guiding center metric g_α^{ab} , and \mathcal{H}_α continuously depends on it. This is the geometric aspect we would like to introduce to the CHSs, and each of them can be completely characterized by a triplet of $\{\mathcal{H}_\alpha, \hat{V}_\alpha, g_\alpha^{ab}\}$. For the special case where $\mathcal{H}_\alpha = \mathcal{H}_{\text{LLL}}$, the entire

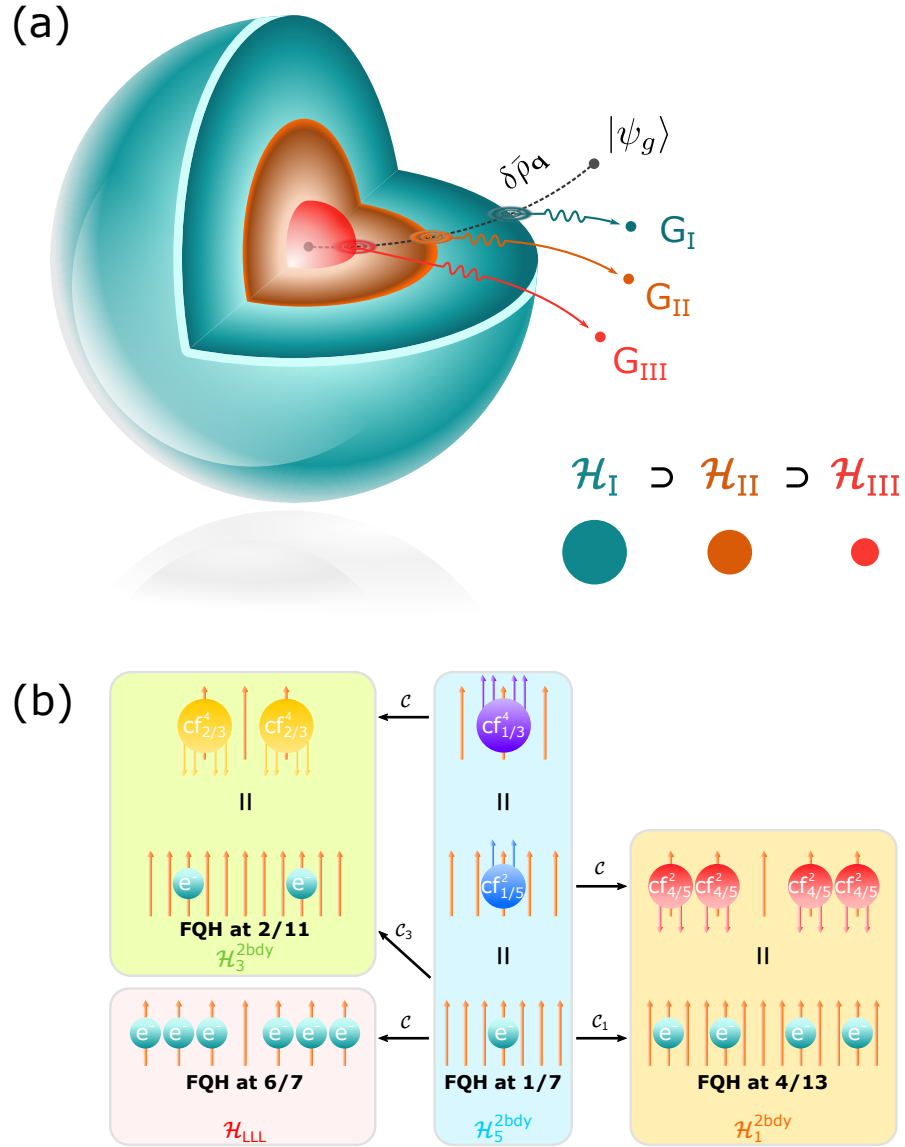


FIGURE 5.2: (a) **Illustration of the hierarchical structure of three CHSs and the ground state $|\psi_0\rangle$ within \mathcal{H}_{III} (red sphere) in the Hilbert space.** The corresponding GMP mode $|\psi_g\rangle$ is outside \mathcal{H}_{I} so one can imagine the regularised guiding center density operator acting on the ground state goes through three CHSs, leading to three emergent gravitons because of the fluctuation around the metric of each of the CHSs. (b) **PH conjugate of Laughlin states within different CHSs.** Here \mathcal{C}_i denotes the PH conjugate within $\mathcal{H}_i^{2\text{bdy}}$, and \mathcal{C} denotes the PH conjugate within a single LL or a single CF level. Arrows represent magnetic fluxes, and the CFs denoted by $\text{cf}_{\nu^*}^n$, consist of one electron and n fluxes, form a CF FQH state at ν^* . Note that the red ($\text{cf}_{4/5}^2$) and the yellow ($\text{cf}_{2/3}^4$) CFs are anti-CFs with the fluxes opposite to the external field.

Hilbert space of the LLL, \hat{V}_α is the kinetic energy Hamiltonian and $g_\alpha^{ab} = \tilde{g}^{ab}$ is the cyclotron metric or the effective mass tensor. All other CHSs are subspaces of \mathcal{H}_{LLL} .

In Fig. (5.1), we illustrate a hierarchical structure of different \mathcal{H}_α in the LLL [354]. For a given \mathcal{H}_α , finding another $\mathcal{H}_\beta \subset \mathcal{H}_\alpha$ is possible. If we fix g_α^{ab} , we can still define a \mathcal{H}_β freely parametrized by g_β^{ab} that is entirely within \mathcal{H}_α . This is straightforward for $\mathcal{H}_\alpha = \mathcal{H}_{\text{LLL}}$ since the cyclotron coordinates and guiding center coordinates commute. For other pairs of CHSs, such geometric tuning can only be realized with the following Hamiltonian:

$$\hat{V}_{\text{int}} = \lambda_\alpha \hat{V}_\alpha + \lambda_\beta \hat{V}_\beta \quad (5.12)$$

with $\lambda_\alpha \gg \lambda_\beta > 0$ (the metric dependence of $\hat{V}_{\alpha,\beta}$ is implicit). For any ground state $|\psi_0\rangle \in \mathcal{H}_\beta$ of Eq.(5.12) we can thus define two types of area-preserving deformation:

$$|\psi_1^\chi\rangle \sim \lim_{|\chi| \rightarrow 0} \hat{P}_\alpha \hat{U}(\chi) |\psi_0\rangle \sim \lim_{|\mathbf{q}| \rightarrow 0} \hat{P}_\alpha \delta \hat{\rho}_{\mathbf{q}} |\psi_0\rangle \quad (5.13)$$

$$|\psi_2^\chi\rangle = \left(\hat{\mathbb{I}} - \hat{P}_\alpha \hat{U}(\chi) \right) |\psi_0\rangle \quad (5.14)$$

where $\hat{U}(\chi) = e^{i\chi_{ab}\hat{\Lambda}^{ab}}$ is the unitary operator inducing the squeezing and rotation of the guiding center metric, with $\hat{\Lambda}^{ab} = \frac{1}{4l_B^2} \sum_i \{\bar{R}_i^a, \bar{R}_i^b\}$; $\delta \hat{\rho}_{\mathbf{q}} = \hat{\rho}_{\mathbf{q}} - \langle \psi_0 | \hat{\rho}_{\mathbf{q}} | \psi_0 \rangle$ is the regularised guiding center density operator, and Eq.(5.13) has been established in [199]. Here \hat{P}_α is the projection into \mathcal{H}_α so that $\hat{V}_\alpha |\psi_1^\chi\rangle = 0$, and $|\psi_1^\chi\rangle$ is associated with the geometric deformation of \mathcal{H}_β . Eq.(5.14) is entirely outside of \mathcal{H}_α ; in some cases, it will vanish, as we will see later. If it is non-vanishing, then $|\psi_2^\chi\rangle$ is associated with the geometric deformation of \mathcal{H}_α . This geometric description forms the microscopic basis of possible multiple gravitons in different FQH phases, dictated by model Hamiltonians in the form of Eq.(5.12). We shall see that they can be resolved by realistic Hamiltonians close to those model Hamiltonians in the following part.

5.2 Emergence of multiple gravitons

Within this framework, let us start with a collection of CHSs $\{\mathcal{H}_k, \hat{V}_k, g_k^{ab}\}$. We will ignore the cyclotron graviton, so all these are subspaces of the LLL, and also with

a hierarchical structure $\mathcal{H}_{k+1} \subset \mathcal{H}_k$. The model Hamiltonian for understanding the gravitons is given by:

$$\hat{V}_{\text{int}} = \sum_{k=1}^m \lambda_k \hat{V}_k, \quad \lambda_k \gg \lambda_{k+1} \quad (5.15)$$

All metrics g_k^{ab} in the Hamiltonian are arbitrary. Without loss of generality, we can set them as $g_k^{ab} = \mathbb{I}_2$ since the gravitons are quantum fluctuations around these fixed metrics. Let the ground state of Eq.(5.15) be $|\psi_0\rangle \in \mathcal{H}_m$, so the quadrupole excitation is obtained from the long wavelength limit of the GMP mode or single mode approximation defined as $|\psi_q\rangle$ in Eq.(5.1) [52, 199]. Note that $|\psi_g\rangle$ and $|\psi_0\rangle$ are orthogonal due to the vanishing expectation value of $\delta\hat{\rho}_q$.

The important question here is which CHS $|\psi_g\rangle$ resides in. If $|\psi_g\rangle \in \mathcal{H}_k$ and $|\psi_g\rangle \notin \mathcal{H}_{k+1}$, then obviously there is no graviton associated with the quantum fluctuation around g_k^{ab} since such fluctuation will bring us out of \mathcal{H}_k . However, $|\psi_g\rangle$ can be decomposed into multiple modes, each within $\mathcal{H}_{k'>k}$ but outside of the $\mathcal{H}_{k'+1}$, associated with the quantum fluctuation around $g_{k'+1}^{ab}$, as long as $|\psi_0\rangle \in \mathcal{H}_{k'+1}$. This is most easily seen by computing the spectral function defined below:

$$I(E) = \sum_n |\langle \psi_n | \psi_g \rangle|^2 \delta(E - E_n) \quad (5.16)$$

where $|\psi_n\rangle$, E_n are the eigenstates and the eigen-energies of Eq.(5.15). Given that $\lambda_k \gg \lambda_{k+1}$, we expect to see $m - k$ distinct peaks well separated in energy, corresponding to $m - k$ gravitons, each with transparent geometric interpretation as illustrated in Fig.5.2(a). The spectral sum rule for the guiding center structure factor will clearly be satisfied from all the contributions of these gravitons, as long as $|\psi_g\rangle$ lives completely within \mathcal{H}_k .

5.2.1 Short-range two-body interaction

A number of analytical results have been derived in the last chapter, which are rigorous in the thermodynamic limit and useful in determining which CHS $|\psi_g\rangle$ resides in [354]. Let us first take \hat{V}_{int} in Eq.(5.15) as a sum of short-range two-body

2/7(8e)	4/13(8e)	2/11(6e)	2/9(8e)	1/4(8e)
0.953[5.3a]	0.986[5.3b]	0.957[5.3c]	0.993[5.4a]; 0.989[5.4b]	0.908[5.7]

TABLE 5.1: **The overlap between the ground states with different filling factors (first row) of the corresponding model Hamiltonian and the Coulomb interaction.** The corresponding electron numbers and the figure indices have been included.

interactions as follows:

$$\hat{V}_{\text{int}} = \sum_{i=1}^n \lambda_i \hat{V}_{2i-1}^{\text{2bdy}} \quad (5.17)$$

with $\hat{V}_{2i-1}^{\text{2bdy}}$ as the $(2i-1)^{\text{th}}$ Haldane pseudopotentials, where fermionic statistics has been considered. Thus the corresponding null spaces $\mathcal{H}_n^{\text{2bdy}}$ is spanned by the Laughlin ground state and quasiholes at $\nu = 1/(2n+1)$. We have proved analytically that $|\psi_g\rangle$ of the Laughlin phase at $\nu = 1/(2n+1)$ resides within $\mathcal{H}_{n-1}^{\text{2bdy}}$, but completely outside of $\mathcal{H}_n^{\text{2bdy}}$ [354] (we take $\mathcal{H}_0^{\text{2bdy}} = \mathcal{H}_{\text{LLL}}$), which is saturated by the ground state and quasiholes. Thus there can only be one graviton and one peak in the spectral function associated with the metric fluctuation of g_n^{ab} . There are, however, many other FQH states that are incompressible with respect to Eq.(5.15) but not in $\mathcal{H}_n^{\text{2bdy}}$. These include the Jain states at $\nu = N/(2nN+1)$, $N > 1$ and their PH conjugate states (within $\mathcal{H}_{n-1}^{\text{2bdy}}$ as defined in Chap.3) at $\nu = N/(2nN-1)$, $N > 1$. Note that all these states still reside within $\mathcal{H}_{n-1}^{\text{2bdy}}$, though the ground state and quasiholes do not saturate $\mathcal{H}_{n-1}^{\text{2bdy}}$, because almost for all Jain states except the Laughlin states, there is no model Hamiltonian for which the Jain states are the exact zero energy state. One can prove analytically that their corresponding $|\psi_g\rangle$ all satisfies $|\psi_g\rangle \in \mathcal{H}_{n-2}^{\text{2bdy}}$. While they are again completely outside of $\mathcal{H}_n^{\text{2bdy}}$, now they have spectral weights within $\mathcal{H}_{n-1}^{\text{2bdy}}$. Thus each of those states will have two gravitons concerning Eq.(5.15), a generic result agreeing with some special cases studied before [335, 356]. These two gravitons are associated with the fluctuation of the metrics g_n^{ab} and g_{n-1}^{ab} , which can also be understood via clustering properties in parton constructions [335].

5.2.2 Effective few-body interactions

Non-abelian FQH states are fascinating in strongly correlated topological systems, and many of them are stabilized by few-body interactions. Their gravitons can also be predicted similarly, assuming they can be stabilized by realistic interactions adiabatically connected to Eq.(5.15). For example, the Pfaffian state at $\nu = 1/(2n)$ can be understood as a condensate of paired CFs, each with one electron attached to $2n$ magnetic fluxes [358, 359]. The model states of these FQH phases all live within $\mathcal{H}_{n-1}^{2\text{bdy}}$. For short-range two-body interactions, they will also all have two gravitons, one within $\mathcal{H}_{n-1}^{2\text{bdy}}$, and the other within $\mathcal{H}_{n-2}^{2\text{bdy}}$.

We now illustrate that the number of gravitons is a *dynamical property* strongly dependent on the interaction. Let us first look at an Abelian case, which is the Jain state at $\nu = 2/9$, corresponding to the $\nu^* = 2$ state of the CFs with each electron bound to four magnetic fluxes, or the $\nu^* = 2/5$ state of the CFs with each electron bound to two magnetic fluxes. We have argued before that with short-range two-body interactions; this FQH state has two gravitons. It is important to note, however, while the CHS of this FQH state is well-defined from the CF construction, such construction does not allow an exact model Hamiltonian within the LLL. The two-body interaction only defines its CHS approximately, though to a very good level of accuracy. A better microscopic Hamiltonian is given as follows:

$$\hat{V}_{\text{int}} = \hat{\mathcal{V}}_n^{3\text{bdy}} \equiv \sum_{i=3}^n \hat{V}_i^{3\text{bdy}} \quad (5.18)$$

where $\hat{V}_i^{3\text{bdy}}$ are the three-body PPs [189]. Note there is no $\hat{V}_4^{3\text{bdy}}$ due to fermionic statistics, and $\hat{V}_9^{2\text{bdy}}, \hat{V}_{11}^{3\text{bdy}}$ are doubly degenerate, so here we take them as an arbitrary linear combination (the CHS is invariant). The unique highest density ground state of Eq.(5.18) with $n = 11$ has a very high overlap with the Jain $\nu = 2/9$ state (> 0.99 for eight electrons). While its quasi-hole counting is non-Abelian, one could conjecture that the ground state is topologically equivalent to the Jain state, in analogy to the Gaffnian state and the Jain $\nu = 2/5$ state that has been studied before [139, 194].

Such subtleties, while important by themselves, do not really affect our discussions about gravitons, which are gapped excitations. The main message here is that the null spaces of $\hat{\mathcal{V}}_n^{3\text{bdy}}$ give a family of CHSs beyond the Laughlin CHSs discussed

before. The Moore-Read, Gaffnian, and Haffnian CHSs are illustrated in Fig.5.1, corresponding to the case of $n = 3, 5, 6$, respectively. Let the null space of $\hat{\mathcal{V}}_n^{3\text{bdy}}$ be $\mathcal{H}_n^{3\text{bdy}}$, and it is easy to check that $\mathcal{H}_{11}^{3\text{bdy}} \subset \mathcal{H}_9^{3\text{bdy}} \subset \mathcal{H}_1^{2\text{bdy}}$. Note that the ground state of $\nu = 2/9$ resides in $\mathcal{H}_{11}^{3\text{bdy}}$, and it has very high overlap with the ground state of $\hat{V}_3^{2\text{bdy}}$. We can thus construct the following Hamiltonian:

$$\hat{V}_{\text{int}} = \lambda_1 \hat{V}_1^{2\text{bdy}} + \lambda_2 \hat{V}_9^{3\text{bdy}} + \hat{V}_3^{2\text{bdy}} \quad (5.19)$$

with $\lambda_1 \gg \lambda_2 \gg 1$. In addition to the original two gravitons (one from the metric fluctuation of $\mathcal{H}_{11}^{3\text{bdy}}$, or the CHS of the $\nu = 2/9$ phase, and the other from the metric fluctuation of $\mathcal{H}_1^{2\text{bdy}}$), there will be a third graviton from the metric fluctuation of $\mathcal{H}_9^{3\text{bdy}}$, easily observable from the spectral function. If we tune λ_2 to zero. In that case, the two peaks corresponding to the gravitons of the lower energies will gradually merge to become a single peak within $\mathcal{H}_1^{2\text{bdy}}$, accounting only for the metric fluctuation of the CHS of the $\nu = 2/9$ as shown in Fig.5.4. Such dynamical behaviors physically correspond to the *energies* of the gravitons in the spectral function. Thus the merging and splitting of resonance peaks in the inelastic photon scattering measurements [108, 112, 360, 361]. Furthermore, merging and splitting gravitons can also be expected for the non-Abelian Pfaffian state at $\nu = 1/4$, which similarly has an exact three-body model Hamiltonian [362–364].

5.3 Chirality of gravitons

The microscopic theory can easily predict the chirality of the gravitons without numerical computations [326] by defining the PH conjugate of CFs within $\mathcal{H}_k^{2\text{bdy}}$ at the CF filling factor of $\nu^* = 2(n-k)/(2(n-k)+1)$, corresponding to the interacting CF states at electron filling factor $\nu = 2(n-k)/(2(n-k)(2k+1)+1)$. Each Laughlin state at $\nu = 1/(2n+1)$ thus have n PH conjugate state with $k = 0, 2, \dots, n-1$, with $k=0$ the usual PH conjugate state in the LLL at $\nu = 2n/(2n+1)$. Since the $\nu = 2(n-k)/(2(n-k)(2k+1)+1)$ state lives entirely within $\mathcal{H}_k^{2\text{bdy}}$ and entirely outside of $\mathcal{H}_{k+1}^{2\text{bdy}}$, one can rigorously show that its graviton mode lives entirely within $\mathcal{H}_{k-1}^{2\text{bdy}}$ for $k > 0$, leading to two gravitons [354]. These two gravitons emerge from the fluctuation of g_k^{ab} , as well as the fluctuation of the metric defining the CHS of $\nu = 2(n-k)/(2(n-k)(2k+1)+1)$. Since we are taking the PH conjugate

within $\mathcal{H}_k^{2\text{bdy}}$, the graviton within $\mathcal{H}_k^{2\text{bdy}}$ will also have the opposite chirality to the one outside of it. For $k = 0$, the anti-Laughlin state at $\nu = 2n/(2n + 1)$ only has one graviton since there is no additional CHS defined by the two-body interaction within the LLL that also contains the CHS of $\nu = 2n/(2n + 1)$.

Thus with short-range two-body interactions, all FQH states related to the Laughlin states by particle-hole (PH) conjugation will have at most two gravitons. Meanwhile, there can be multiple well-defined PH conjugations for each Laughlin state in different Laughlin CHSs, not just within the LLL (where PH conjugation relates the state at ν to $1 - \nu$). This is because the Laughlin state at $\nu = 1/(2n + 1)$ can also be reinterpreted as a Laughlin state of CF with each electron attached to $2k$ magnetic fluxes ($k < n$) at the CF fractional filling factor $\nu^* = 1/(2(n - k) + 1)$ [74, 242] as Fig.5.2(b) shows. For example, the Laughlin-1/7 state of electrons can be reinterpreted as a $\nu = 1/5$ state of cf^2 (one electron bound with two fluxes) within $\mathcal{H}_1^{2\text{bdy}}$. We can then take the PH conjugation within $\mathcal{H}_1^{2\text{bdy}}$, which gives the $\nu = 4/5$ state of cf^2 , corresponding to the $\nu = 4/13$ Jain state of the electron filling, in CF theory it is an interacting CF state (the observed FQH state at $\nu = 4/13$ is unlikely to be a Jain state though [365]). Another example is the FQH state at $\nu = 2/7$ (a $\nu = 2/3$ state of cf^2), which is the PH conjugate of the Laughlin-1/5 state (a $\nu = 1/3$ state of cf^2) within $\mathcal{H}_1^{2\text{bdy}}$. Due to the PH conjugation, we know immediately that these two states have two graviton modes with opposite chiralities. On the other hand, FQH states with one PH conjugation (which is the one within the full LL, e.g., $\nu = 2/9$) will give all graviton modes of the same chirality. The chirality of the graviton modes can thus be predicted without involving numerical calculations (Another way is to look into the wave functions [356]). It is also consistent with Ref.[366], since with PH conjugation, the corresponding FQH ground state will not be annihilated by any local Hamiltonians. Relevant numerical evidence will be shown in the next section.

Note that as an additional degree of freedom, the chirality has to be considered in the “merging” behavior of gravitons. For those with the same chirality, there is no ambiguity here. When two gravitons merge into one, they are physically indistinguishable from a system with a single graviton at the same energy. Microscopically, a hand-waving way of understanding this is that the “stiffness” of the quantum fluctuations of the two metrics are the same, so it is indistinguishable from the fluctuation of a single metric.

However, the graviton modes are not just characterized by energy. Even when only one resonance peak is observed using unpolarized light, it is still possible to observe two resonance peaks at the same energy by using the circularly polarized light, each for one polarization [321, 322, 325]. This is qualitatively different from merging two graviton energies with the same chirality. As a result, only in some cases are the model Hamiltonians for multiple gravitons helpful in understanding why realistic (Coulomb-based) interactions can efficiently resolve multiple gravitons. In contrast, in other cases, realistic interactions can be quite different from model Hamiltonians, so one can consider them as the model Hamiltonians plus perturbations. These perturbations will induce interactions and mixing of the gravitons, especially if their energies are very close. This should also apply to gravitons of opposite chiralities. Nevertheless, both resonance peaks should still be observable for small perturbations with properly polarized light. Beyond small perturbation, we think it remains an open question since gravitons, in principle, can scatter into other states (e.g., multi-roton states with the same quantum number) [112], so that even gravitons with opposite chiralities may mix due to the scattering of other rottons carrying away angular momenta. In this case, additional tuning (e.g., LL mixing) may be required for detecting them in experiments, and we need further research to understand these points.

5.4 Spectral functions from exact diagonalization

While the main concepts and predictions of the gravitons have been formulated analytically above, it is also helpful to further illustrate the formalism with examples of numerical calculations. The spectral functions for the Jain states at $\nu = 2/7, 2/9, 1/4$ with Coulomb interaction have been computed [335, 356]. Here we compute the spectral functions of these and additional FQH states with model Hamiltonians on the sphere to show that two or even more peaks can be unambiguously resolved and far separated compared to the realistic interactions. In all cases we have studied, the ground states of the model Hamiltonians and the realistic Hamiltonians at the same filling factor have very high overlaps (as shown in Table 5.1), showing strong evidence that they are in the same topological phases.

The first two examples are the Jain state at $\nu = 2/7$ (the PH conjugate of the Laughlin $\nu = 1/5$ state within $\mathcal{H}_1^{2\text{bdy}}$) and the interacting CF state at $\nu = 4/13$

(the PH conjugate of the Laughlin $\nu = 1/7$ state within $\mathcal{H}_1^{2\text{bdy}}$, with some experimental evidence [367]). In both cases, the PH conjugate is defined for CFs, each with one electron attached to two fluxes. The CHS of both phases are proper subspaces of $\mathcal{H}_1^{2\text{bdy}}$, but outside of $\mathcal{H}_3^{2\text{bdy}}$. Thus there will be a non-zero component of the graviton outside of $\mathcal{H}_1^{2\text{bdy}}$. A short-range two-body interaction with a very dominant $\hat{V}_1^{2\text{bdy}}$ can thus easily resolve the two gravitons as previously predicted (see Fig.(5.3a,b)). The two gravitons can also be clearly resolved with \hat{V}_{LLL} since it is dominated by $\hat{V}_1^{2\text{bdy}}$.

The Jain state at $\nu = 2/7$ also provides an example for us to further understand the merging of gravitons with different chiralities. Since the PH conjugation reverses the sign of all physical quantities that are odd in time-reversal operations, the two gravitons of this state should have opposite chiralities. By computing the spectral function with respect to the Coulomb interaction in the second LL, where $\hat{V}_1^{2\text{bdy}}$ is much less dominant than in the LLL, but the overlap between the ground states is around 0.982 with the topological gap remaining robust with 8 electrons, one can clearly see the merging behaviors from the overlaps with the gravitons of different chiralities shown in Fig.5.5. Thus in inelastic circularly polarised light scattering experiments, we expect to observe two resonance peaks at almost the same frequency when using lights with both left and right polarizations, corresponding to two gravitons with different chiralities but indistinguishable energy. The anti-Pfaffian state at $\nu = 1/4$ (the particle-hole dual state of the Pfaffian state at $\nu = 1/4$) shows precisely the same behavior as Fig.5.6 shows.

The Jain state at $\nu = 2/7$ also provides an example to understand gravitons' dynamics with realistic interactions further. Since the PH conjugation reverses the sign of all physical quantities that are odd in time-reversal operations, the two gravitons of this state should have opposite chiralities. We compute the spectral function with respect to the Coulomb interaction in the second LL, where $\hat{V}_1^{2\text{bdy}}$ is much less dominant than in the LLL. The overlap between the ground states is around 0.982, with the incompressibility gap remaining robust with 8 electrons. One can clearly see the merging of the energies of the gravitons shown in Fig.5.5, which should be highly relevant in experiments. Thus in the inelastic unpolarised light scattering experiments, we expect to observe two resonance peaks in the LLL but only one resonance peak in the SLL. However, with the circularly polarised

light, one (potentially broadened due to mixing) peak will be observed at almost the same frequency for each polarization in the SLL.

For the Jain state at $\nu = 2/9$, any $\hat{V}_1^{2\text{bdy}}$ dominated interaction (e.g., \hat{V}_{LLL}) will give two gravitons, as can be analytically proven. From numerical studies with eight electrons, the spectral weight of the graviton outside $\mathcal{H}_1^{2\text{bdy}}$ is small compared to other Jain states. It is also another example where a single graviton (here within $\mathcal{H}_1^{2\text{bdy}}$) can be split into two gravitons, this time with the introduction of the three-body interactions. We can analytically show that within $\mathcal{H}_1^{2\text{bdy}}$, there is non-zero graviton spectral weight both within and outside of $\mathcal{H}_9^{3\text{bdy}}$. Thus an introduction of $\hat{V}_9^{3\text{bdy}}$ to the microscopic Hamiltonian can lead to the splitting of the two gravitons in total to three gravitons, as shown in Fig.5.4. It is worth noting that the graviton within $\mathcal{H}_9^{3\text{bdy}}$ dominates, and both the second and the third graviton have spectral weights that are more than one order of magnitude smaller. This could be a finite-size effect since we can analytically show that the spectral weights of all three gravitons are non-zero for any finite systems. It is still possible, however, that in the thermodynamic limit, the weights of the second and/or third graviton vanish. We cannot access system sizes with more than eight electrons numerically and will leave more detailed discussions to future works. Moreover, in experiments, there can be two separated peaks with respect to the Coulomb interaction with a properly tuned $\hat{V}_1^{2\text{bdy}}$ as shown in Fig.5.4(c). Note that the Jain states at $\nu = 2/7$ and $2/9$ are predicted to be stable in the SLL [368, 369].

The non-Abelian Pfaffian state at $\nu = 1/4$ is the exact ground state of $\hat{\mathcal{V}}_{10}^{3\text{bdy}}$. Just like the Pfaffian state at $\nu = 1/2$ (believed to be stabilized by second LL Coulomb interaction) [93, 370], this state can also be stabilized by a slightly modified \hat{V}_{LLL} , with an overlap of 0.91 for eight electrons. While this small perturbation may not be easily realized in experiments, with this Hamiltonian, we have the clear understanding that there will be two gravitons (one inside, and the other outside of $\mathcal{H}_1^{2\text{bdy}}$). It is interesting to note that we have the hierarchical relationship that $\mathcal{H}_9^{3\text{bdy}} \subset \mathcal{H}_1^{2\text{bdy}} \subset \mathcal{H}_8^{3\text{bdy}}$, and both gravitons are within $\mathcal{H}_8^{3\text{bdy}}$ and at the same time outside of $\mathcal{H}_9^{3\text{bdy}}$. Thus with the model Hamiltonian consisting of only three-body PPs, these two gravitons will again merge to become a single graviton, in the absence of $\hat{V}_1^{2\text{bdy}}$, as reflected in Fig.5.7. As a comparison, the anti-Pfaffian state at $\nu = 1/4$ (as the particle-hole conjugate partner of the Pfaffian-1/4 state within \mathcal{H}_1)

has two peaks with opposite chiralities. With a slightly modified Coulomb interaction when the energies of the two gravitons merge, we can see only one resonance peak from the inelastic scattering of the unpolarised light but one resonant peak each for the two circularly polarised light with the opposite chirality. Furthermore, properly tuning $\hat{V}_1^{2\text{bdy}}$ in realistic interactions can lead to a better resolution of the peaks, as shown in Fig.5.7(C). For non-Abelian states, there are additional neutral modes, e.g., the “gravitino” modes at spin $s = 3/2$ for Pfaffian [199, 371] can be considered super-partners of the gravitons. We expect multiple gravitons will also lead to multiple gravitino modes and will leave detailed discussions elsewhere.

5.5 Experimental relevance

The experimental detection of the multiple GMs in FQH systems and their interaction is exciting because of both the topological and geometric aspects of such neutral excitations. Inelastic scattering experiments can be carried out in the FQH state with phonons or photons of proper frequency to check the existence of the GMs and find their energies. To further detect the chiralities of GMs, one needs to use circularly polarised light corresponding to the photons with $+2$ or -2 spin angular momenta transferred to the system [187, 236, 321–323, 325, 326]. With realistic interactions, different GMs can interact and mix strongly if their energies are similar, and for GMs of the same chirality, multiple GMs can merge into one. For GMs of opposite chiralities, even if their energies are close, they may still be resolved with circularly polarised light, so the resonance peaks could be broadened due to mixing and scattering between the GMs and the multi-roton continuum. The microscopic picture we developed points to the crucial role of the hierarchy of energy scales associated with different CHSs, which realistic interaction must imitate to resolve multiple GMs. Thus, realizing a robust Hall plateau may not be enough to detect GMs. The experimental system may need to be flexible enough to tune the effective electron-electron interactions, to control the dynamics of low-lying gapped excitations.

For systems when the LL mixing is negligible (e.g., with a strong magnetic field), our calculation shows that short-range interaction (e.g., the Coulomb interaction in the LLL) can at most resolve two gravitons both for abelian and non-Abelian FQH phases, and we have not found any exceptions. The universality of such

results is due to the algebraic structure of the Laughlin CHSs. To resolve the two gravitons clearly, we prefer to make the effective interaction as short-range as possible. Formally if we expand the realistic two-body interaction in the Haldane PP basis, we should aim to have the ratio consecutive PP coefficients (i.e., the ratio of the coefficient of $\hat{V}_i^{2\text{bdy}}$ over that of $\hat{V}_{i+1}^{2\text{bdy}}$) to be large. This can be achieved by screening electron-electron interaction or by increasing the sample thickness in experiments. In particular, Jain states at $\nu = N/(2nN + 1)$ with $N > 1$, as well as PH conjugate states at $\nu = 2(n - k)/(2(n - k)(2k + 1) + 1)$ with $k > 0$, will all have two gravitons. Numerical calculations also show that short-range interactions favor the incompressibility of these FQH states compared to the bare Coulomb interaction.

The most easily observed second graviton in experiments would be the one outside of the \hat{V}_1 null space (i.e., \mathcal{H}_1), which requires a dominant \hat{V}_1 interaction and can be realized with the Coulomb interaction within the LLL for FQH states around $\nu = 1/4$ as discussed in previous works [354]. For FQH states in the SLL, however, the graviton outside of \mathcal{H}_1 will mix strongly with the ones inside \mathcal{H}_1 because of the significantly stronger \hat{V}_3 as compared to the LLL Coulomb interaction. It is also important to note while the FQH states around $\nu = 1/6$ (e.g., the $\nu = 2/11$ state) all in principle have at least two gravitons (except for the Laughlin state at $\nu = 1/7$), they will be hard to observe even with the LLL Coulomb interaction. This is because such gravitons have to be resolved by a dominant $\hat{V}_3^{2\text{bdy}}$ (as compared to $\hat{V}_{k>3}^{2\text{bdy}}$), which is not the case for the LLL Coulomb interaction. Thus in general, the observation of multiple gravitons, even for simple two-body interactions, will necessarily require careful tuning of experimental parameters with Coulomb-based interaction.

The short-range two-body interactions do not favor non-Abelian FQH states, as the compressible composite Fermi liquid (CFL) states are generally more competitive, for example, at $\nu = 1/(2n)$ [203, 205, 246, 247, 254, 372, 373]. For non-Abelian FQH states, we generally require longer-range interactions (e.g., Coulomb interaction in the second LL) or few-body interactions from LL mixing [139, 203, 364]. While it is hard to predict from finite-size numerical calculations how realistic interactions can stabilize these exotic states, these additional ingredients are necessary if we want to observe more than two gravitons. A possible candidate for three gravitons seems to be the Jain state at $\nu = 2/9$, where we have shown that the proper introduction of

three-body interactions can lead to three peaks in the spectral function. However, we expect one of the peaks resolved by the three-body interaction to be relatively weak, and the dominant peak resides at low energies. Our numerical results so far are inconclusive for this state due to the small system sizes accessible, and more work is needed to establish its behavior from finite size scaling.

5.6 Microscopic basis for the effective field theory

The theoretical formalism also serves as the basis for effective field theory, where we show the necessity of additional modes (called the Haldane modes) depending on properly identifying the base space of such theories. For the effective field theory construction, the number of gravitational fields needed (i.e., the Haldane modes) for a complete description of the response to the metric fluctuation should be determined by the underlying microscopic theory. It is important first to identify the physical Hilbert space on which the effective field theory is based. For example, for the Jain states near $\nu = 1/(2n)$, the elementary particles are CFs with each electron bound to $2n$ magnetic fluxes (and their PH conjugates, or CF holes). CF levels thus span the Hilbert space (the fully filled ones give the Jain $\nu = N/(2nN + 1)$ states) and their PH conjugates (giving Jain states with $\nu = N/(2nN - 1)$). We can denote it as the *base space* of the effective field theory. In particular, it is the full Hilbert space of the LLL for $n = 1$. For $n > 1$, the base space is $\mathcal{H}_{n-1}^{2\text{bdy}}$.

To determine if and how many Haldane modes need to be added to effective field theory, it all depends on if the long wavelength limit of the GMP mode lives entirely within the base space. For $n = 1$, this is definitely the case since the GMP mode lives entirely within the LLL, as illustrated in Fig.5.8(a). In particular, the regularised density operator $\delta\hat{\rho}_q$ is PH symmetric. For $n > 1$, the GMP modes for all the Laughlin states live entirely within the base space, but $\delta\hat{\rho}_q$ is no longer PH symmetric *within the base space*. One can also show rigorously from the microscopic point of view that all Jain states at $\nu = N/(2nN \pm 1)$ with $N > 1$ have GMP modes partially outside of the base space, thus requiring at least one additional Haldane mode to be added to the effective field theory as illustrated in Fig.5.8(b).

In principle, we can have multiple CHSs containing the base space with the hierarchical structure $\mathcal{H}_{\text{base}} \subset \mathcal{H}_1 \subset \dots \subset \mathcal{H}_k$ with $k > 1$, and the GMP mode resides in \mathcal{H}_k having non-zero weights in all $\mathcal{H}_{k' < k}$. We have not found such cases for Jain states with CHSs defined by two-body and three-body PPs, but it may be possible for other FQH states or CHSs defined by few-body PPs involving clusters of more than three electrons. These cases are illustrated by Fig.5.8(c), where more than one Haldane mode is needed for the effective field theory to agree with microscopic Hamiltonians that can resolve those CHSs in terms of energy.

Numerical calculations are essential in verifying effective field theory predictions. Still, it is important to note that the number of Haldane modes needed for the effective field theory does not necessarily correspond to the number of peaks in the graviton spectral function since the latter depends on the microscopic details of the Hamiltonian. Fig.5.8(d) is another example that even within the base space, there can be multiple CHSs, which can be resolved by proper model Hamiltonians. With such interactions, the graviton within the base space (which is the conventional graviton, not the Haldane modes) can lead to multiple spectral weight peaks well separated in energy. However, coupling the composite particles with the Hall manifold metric in the effective theory captures the total weight.

In fact, from an effective theory point of view, we can always use a single Haldane mode to capture all the graviton weights outside of the base space. In contrast, the usual composite particle action can capture all the graviton weights within the base space. While the known Dirac CF description for the Haldane mode strictly speaking only applies to the FQH states very close to $\nu = 1/(2n)$ (i.e., for Jain states $\nu = N/(2nN \pm 1)$ with $N \rightarrow \infty$, and definitely does not apply for Laughlin states at $N = 1$), the general arguments here with the relationship between the GMP modes and the base space should apply to all effective field theory description, with or without particle-hole symmetry.

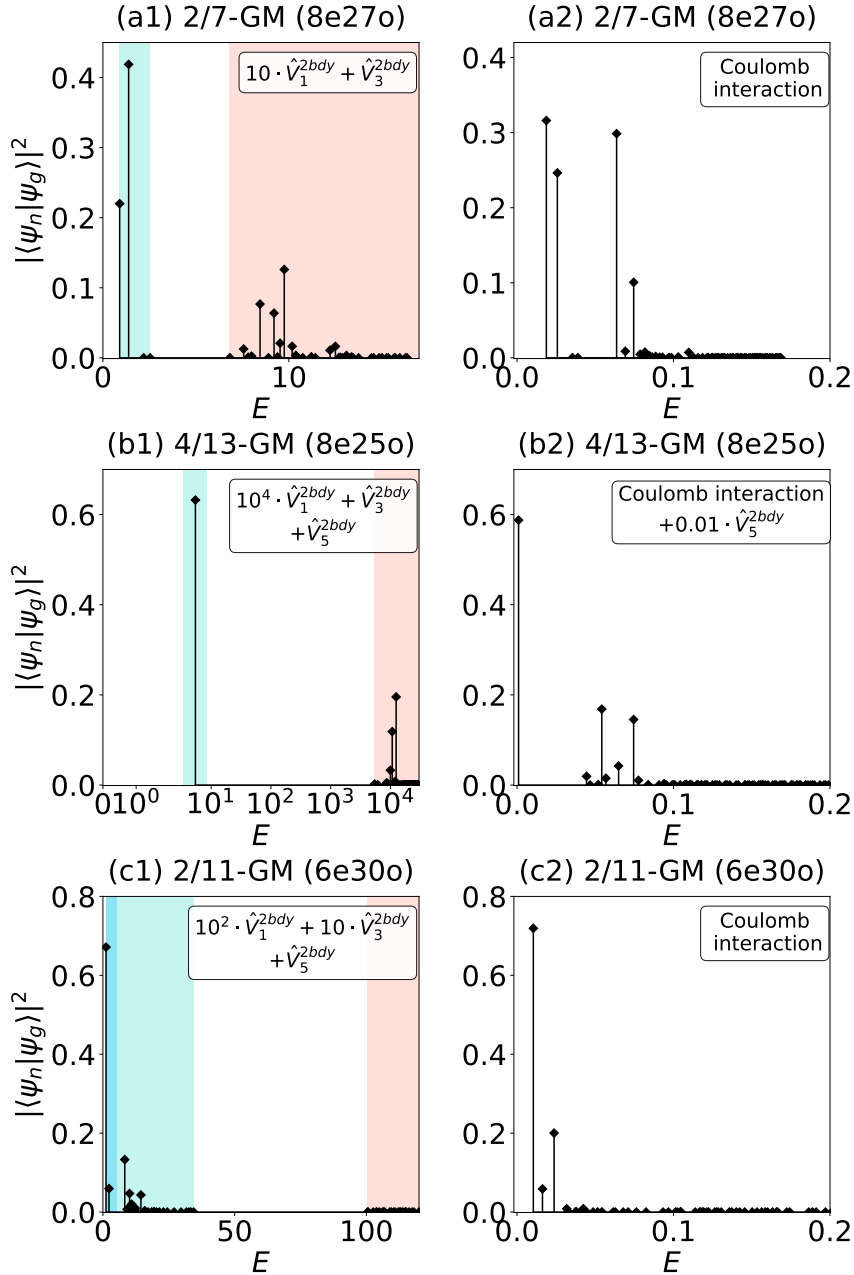


FIGURE 5.3: Spectral functions of the FQH states with the filling factor $\nu = 2/7, 4/13$ and $2/11$. The graviton mode of the FQH state with filling factor ν is called ν -graviton for simplicity. The blue, the turquoise, and the red region denote $\mathcal{H}_3^{2\text{bdy}}$, $\mathcal{H}_1^{2\text{bdy}}$ and its complement correspondingly, from which one can clearly see the gaps between different sectors. For the FQH states with $\nu = 2/7$ and $4/13$, model Hamiltonians show similar signatures of two peaks in the spectral functions as coulomb interactions (a small $\hat{V}_5^{2\text{bdy}}$ is added in (b2) for stabilizing the proper ground state). The corresponding overlap between the model and ground states of the Coulomb interaction can be found in Table 5.1.

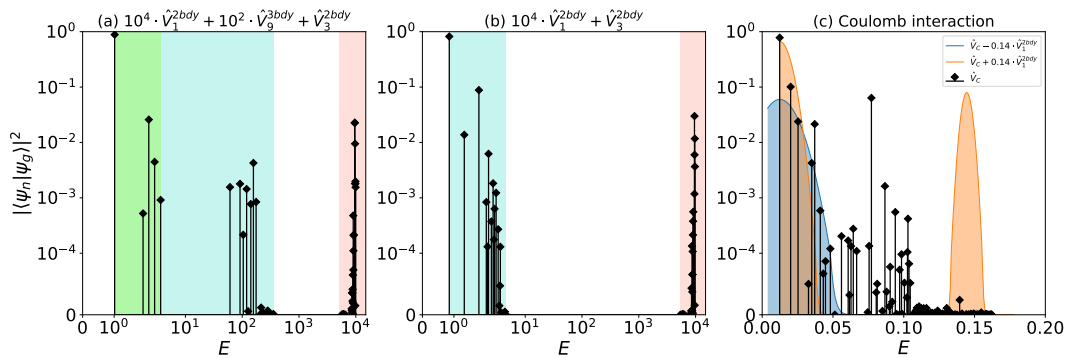


FIGURE 5.4: Spectral functions of FQH states at $\nu = 2/9$ with 8 electrons. (a) shows two peaks within $\mathcal{H}_1^{2\text{bdy}}$ in the spectral function with respect to the model Hamiltonian, where the green sector denotes the null space of $\hat{V}_9^{3\text{bdy}}$. These peaks will merge after $\hat{V}_9^{3\text{bdy}}$ is removed from the Hamiltonian as (b) shows. A slightly exaggerated ratio between different PPs is adopted to clearly show the signature of different CHSs. (c) shows the spectral function of Coulomb interaction, where two peaks can also be clearly observed. In experiments, one can tune $\hat{V}_1^{2\text{bdy}}$ to increase (orange area) or decrease (blue area) the separation to get peaks resolved better. Note that the peaks with modified $\hat{V}_1^{2\text{bdy}}$ have been smoothed by Gaussians.

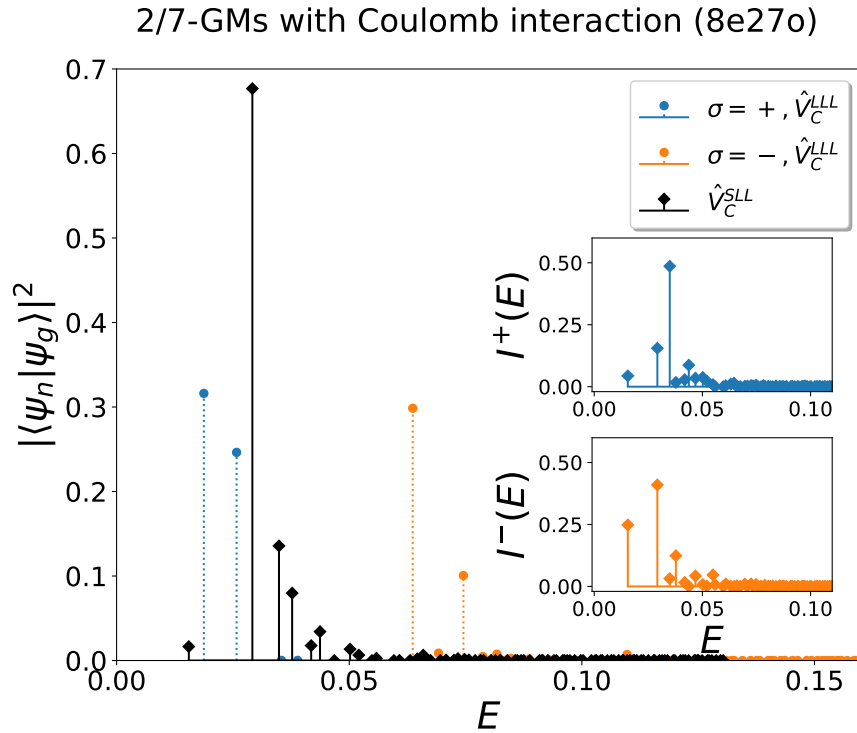


FIGURE 5.5: Spectral functions of the Jain state at $\nu = 2/7$ with 8 electrons with respect to the Coulomb interaction on the LLL and the SLL is shown in the main figure, where we use different colors to distinguish the LLL gravitons with different chiralities, denoted as $\sigma = +$ or $-$. The overlap between the gravitons with respect to the coulomb interaction on the SLL (black peaks in the main plot) and those with different chiralities on the LLL can be found in the subplots, from which one can clearly observe that some of the peaks can be regarded as two gravitons of opposite chiralities at almost the same energy.

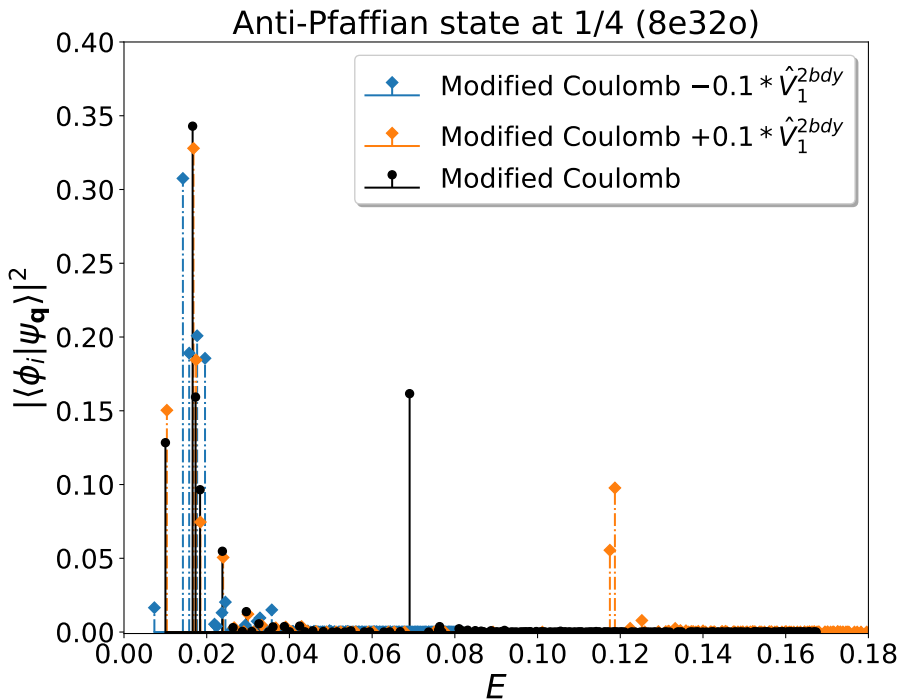


FIGURE 5.6: Spectral functions of the Anti-Pfaffian state at $\nu = 1/4$ with 8 electrons with respect to the Coulomb interaction on the LLL and the SLL is shown in the main figure, where we use different colors to distinguish the LLL gravitons with different chiralities, denoted as $\sigma = +$ or $-$. The overlap between the gravitons with respect to the coulomb interaction on the SLL (black peaks in the main plot) and those with different chiralities on the LLL can be found in the subplots, from which one can clearly observe a similar feature to the case of the Jain state at $2/7$.

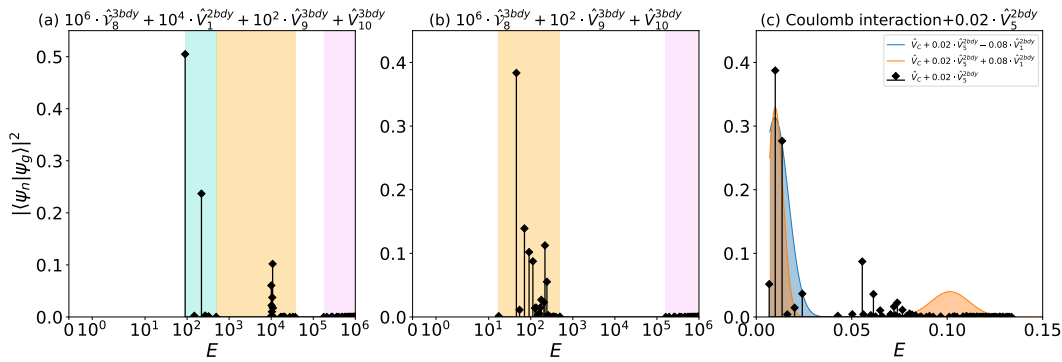


FIGURE 5.7: Spectral functions of the Pfaffian state at $\nu = 1/4$ with 8 electrons. The turquoise, the orange and the pink region denote $\mathcal{H}_1^{2\text{bdy}}$, the null space of $\hat{\mathcal{V}}_8^{3\text{bdy}}$ and its complement correspondingly. When there is no two-body PP $\hat{V}_1^{2\text{bdy}}$ in the Hamiltonian, one can clearly observe the merging of peaks from (a) to (b). Considering the coulomb interaction is $\hat{V}_1^{2\text{bdy}}$ -dominated, we can also observe two peaks in (c), which also shows that one can significantly increase (orange area) or decrease (blue area, and both smoothed by using Gaussians) the separation between the peaks by properly tuning $\hat{V}_1^{2\text{bdy}}$ in experiments. A slightly exaggerated ratio between different PPs is adopted to clearly show the signature of different CHSs. A small $\hat{V}_5^{2\text{bdy}}$ is added in (c) for stabilizing the non-Abelian Pfaffian state.

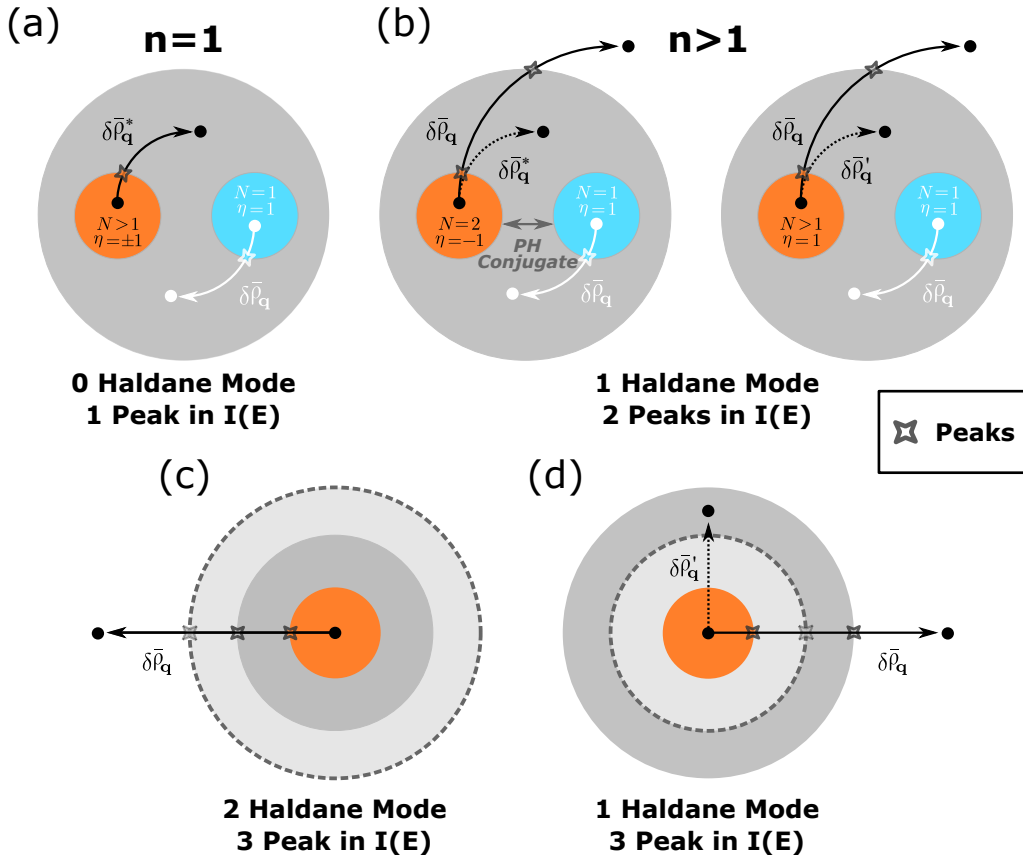


FIGURE 5.8: Number of Haldane modes with different structures of CHSs. Laughlin states ($N = 1, \eta = 1$) are denoted by the white point in the corresponding CHS (blue circle). For the Jain states at $N/(2nN + \eta)$, (a) with $n = 1, N > 1, \eta = \pm 1$, (e.g., the FQH state at $2/3$ and $2/5$, etc.), because $\delta\hat{\rho}_q = \delta\hat{\rho}_q^*$, these states will show the same behavior as the Laughlin state at $1/3$, i.e., one peak with no Haldane mode required. When $n > 1$, (b) shows that a single Haldane mode is needed in the effective field theory despite two peaks observed in the spectral function, among which, given n , the states with $N = 2, \eta = -1$ can be regarded as the particle-hole conjugate partner of the corresponding Laughlin state within some specific CHS, and the states with $N > 1, \eta = 1$ are the states in higher CF levels as shown in Fig.5.2(b). (c) and (d) show more possibilities and conclude that the number of Haldane modes added to the effective theory cannot be easily reckoned from the number of peaks in the spectral function $I(E)$, which is closely related to the microscopic Hamiltonian used.

Chapter 6

Conclusions

There exists a natural geometric degree of freedom in FQH phases, which manifests itself with the anisotropy of the system or the nonuniform dielectric media [230]. It has been hidden in the algebra - when we separate the cyclotron and guiding center coordinates and define the ladder operators, the single irreducible representation of the Heisenberg algebra allows us to define a metric tensor for each coordinate [374]. These two coordinates do not have to be the same. In fact, they are normally independent of each other, and the guiding center metric is determined by a compromise between the effective mass tensor and the Coulomb metric, the values of which should be determined to minimize the ground state energy [230].

The metric tensor can also be defined in specific sub-Hilbert space within a single LL. These subspaces are defined by model Hamiltonians, which can contain effective many-body interactions due to LL mixing [189, 351–353]. Virasoro algebra can be constructed in these subspaces, so an emergent conformal symmetry exists, and thus they are named conformal Hilbert spaces (CHS) [139]. As the null space of the corresponding model Hamiltonian, a CHS contains the densest ground state with all the quasi-hole states, which can be separated into different L_z sectors if there is a rotational invariance. The counting of L_z sectors within a CHS can be analytically given by a generating function, restricted by the generalized clustering rule set by the model Hamiltonian. By comparing the generating functions, one can unambiguously define an isomorphism between CHSs. For any system size, there always exists a unitary mapping from one CHS to another isomorphic one. The process of looking for such a transformation is termed as a composite fermionization

[375] because understanding the same system with isomorphic CHSs is equivalent to the flux-attachment operation proposed in traditional composite fermion theory [71–76]. The particle-hole conjugate is well-defined within the CHSs, which can also form a hierarchical structure within a single LL reminiscent of a fractal structure.

To better understand the geometric aspects in FQH phases, a specific species of excitations is found to be the key. They can be understood as density fluctuations from the ground state and thus a neutral excitation, based on which one can write down the model wave function for them with the single mode approximation (SMA) [51, 52]. Such a wave function is constructed directly from the ground state using a regularised density operator, so the intrinsic correlations are still reserved. There is a quadrupole structure in these modes, which can be understood as the long wavelength limit of the magneto-roton mode as well [199]. More importantly, because the density operator in the long wavelength limit is equivalent to an area-preserving deformation operator [230], these modes are essentially generated by the metric fluctuations within the Hilbert space, so they are named graviton modes considering their spin-2 feature. As a result, a gravitational field theory can be used to describe these massive graviton modes.

Based on the SMA wave function of graviton modes, one can rigorously calculate the expectation value of its energy with respect to microscopic model Hamiltonians by expanding the structure factor in the same Laguerre-Gaussian basis as the pseudopotentials. The result is governed by a universal and well-defined characteristic tensor (characteristic metric for two-body Hamiltonians), the structure of which allows us to calculate or prove many useful properties of FQH states without any numerical input. For example, one can include the graviton modes into the hierarchical structure of CHSs, giving the corresponding model Hamiltonian for the gravitons constructed from different FQH ground states.

Furthermore, by using toy models, one can predict a transition in the low-lying spectrum with an invariant ground state. By tuning the pseudopotential, one can observe the density modes gradually replaced by the hollow-core modes in some cases, which reveals a finer structure in the Hilbert space. Using a CF picture, one can understand the different natures of these two modes. In particular, because these neutral modes define the incompressibility gap in the FQH phase, the gaplessness of the Gaffnian state could be determined by calculating its energy with

respect to the three-body pseudopotential \hat{V}_7^{3bdy} . But a concrete result requires enough data to do the finite-size scaling.

Because each CHS can hold its own metric, it is possible to generate multiple gravitons if the model Hamiltonian is appropriately assigned. To observe such a phenomenon, one can compute the spectral function of the graviton modes and count the number of peaks. But for the commonly seen FQH states, such as the Laughlin and the Moore-Read states, there can only be one graviton for them, as proved by the characteristic tensor formalism. Thus one can look at their particle-hole conjugate within some specific CHSs. The gravitons can be merged or split by tuning the model Hamiltonian, which could be realized using higher LLs. And to distinguish different gravitons, the energy spectrum is insufficient because the chirality has to be considered with the particle-hole conjugate operation. To observe the gravitons with opposite chiralities, one can use polarised photon scattering experiments [108, 112, 360, 361]. The deterministic effect of the model Hamiltonian implies that the number of gravitons is a dynamical property, which can also help with the field-theoretical approach with the number of additional Haldane modes to satisfy the Haldane bound.

Appendix A

Heisenberg algebra

In this section, we would like to briefly introduce the Heisenberg algebra, which can be regarded as the rigorous description of the fundamental algebraic structure of canonical quantization [265]. Then, after showing the mathematician's definition of this algebra, we will discuss its role in quantum mechanics, especially in understanding IQHE.

A.1 Generic Heisenberg algebra

Definition A.1 (Heisenberg Lie algebra). The Heisenberg Lie algebra \mathfrak{h}_{2d+1} is the vector space $\mathbb{R}_{2d+1} = \mathbb{R}_{2d} \oplus \mathbb{R}$ with the Lie bracket defined by its values on a basis $X_j, Y_j, Z (j = 1, \dots, d)$ by

$$[X_j, Y_k] = \delta_{jk}Z, \quad [X_j, Z] = [Y_j, Z] = 0 \quad (\text{A.1})$$

and any element $h \in \mathfrak{h}_{2d+1}$ can be written as:

$$h = \sum_{j=1}^d x_j X_j + \sum_{k=1}^d y_k Y_k + zZ \quad (\text{A.2})$$

Then one can also find the corresponding *Heisenberg group* H_{2d+1} (which is called the Weyl group by mathematicians) by using the Baker-Campbell-Hausdorff formula. More importantly, the representations of H_{2d+1} can be easily found, which

turns out to be quite remarkable because *there is only a single irreducible representation(irrep) for this algebra*, derived from the Stone-von Neumann theorem.

A.2 Physical implications

The single irrep of Heisenberg algebra enables physicists to conveniently discuss the commutation between canonical variables after choosing $\pi'(Z) = -i \cdot \hat{\mathbb{I}}$. As good students of quantum mechanics, we know that the canonical commutation rule, proposed by Born and his student Jordan, lies right at the center of quantum mechanics as one of the most basic assumptions(we have tentatively put back the Planck's constant in the equations below):

$$[\hat{Q}_i, \hat{P}_j] = i\hbar\delta_{ij} \cdot \hat{\mathbb{I}} \quad (\text{A.3})$$

which directly leads to the canonical quantization formalism of quantum field theory by noticing the obvious isomorphism between \mathfrak{h}_{2d+1} and the algebra of Poisson brackets with $2d$ canonical variables:

$$\{A, B\} \longmapsto \frac{1}{i\hbar} [\hat{A}, \hat{B}] \quad (\text{A.4})$$

The most commonly-seen application of Eq.(A.3) is in the quantum harmonic oscillators. The Heisenberg algebra serves as the algebra of the corresponding phase space (which is also relevant in the procedure of geometric quantization, but we will skip this part here) and can help define the creation and the annihilation operators that work for many-particle systems, which is essentially another representation of the Heisenberg group:

$$\begin{aligned} \hat{a}_i &= \sqrt{\frac{m\omega}{2\hbar}} \hat{Q}_i + i\sqrt{\frac{1}{2m\omega\hbar}} \hat{P}_i, & \hat{a}_i^\dagger &= \sqrt{\frac{m\omega}{2\hbar}} \hat{Q}_i - i\sqrt{\frac{1}{2m\omega\hbar}} \hat{P}_i \\ \left[a_i, a_j^\dagger \right] &= \delta_{ij} \cdot \hat{\mathbb{I}} \end{aligned} \quad (\text{A.5})$$

and one can find this representation in the Hilbert space of holomorphic functions with the inner product defined with a Gaussian measure as:

$$(F, G) \equiv \pi^{-n} \int_{\mathbb{C}^n} dz \bar{F}(z) \cdot G(z) \cdot e^{-|z|^2} \quad (\text{A.6})$$

Such a space is named as *Segal–Bargmann space* or *Bargmann–Fock space*.

In the context of IQHE, the electrons are moving in an external field, which correlates with the orthogonal spatial dimensions, and a slightly hand-waving understanding of this is that it looks like the phase-space of 1D quantum Harmonic oscillator transferred to the real space because of the non-commutativity between momentum components as shown in the algebra of covariant momenta:

$$[\hat{\pi}_{ia}, \hat{\pi}_{jb}] = i \cdot \hbar e B \cdot \delta_{ij} \epsilon_{ab} \quad (\text{A.7})$$

Hence from this point of view, many things about the real-space dynamics of IQH states can be mapped to the phase space of a quantum harmonic oscillator with one of the coordinates playing the role of canonical momentum and thus the Heisenberg group/algebra, such as the discrete Landau levels, the holomorphic coordinates and wave functions in the lowest Landau level, etc.

Appendix B

W_∞ -algebra and GMP algebra

As explained in the main text, one can define two groups of creation and annihilation operators corresponding to the inter-LL(\hat{a}^\dagger and \hat{a}) and intra-LL(\hat{b}^\dagger and \hat{b}) degrees of freedom. With only the kinetic term considered, \hat{b}^\dagger and \hat{b} commute with the Hamiltonian, which implies that they are the generators of magnetic translations. Note that although the exact form of the operators does depend on the gauge choice, the Heisenberg algebra of \hat{b}^\dagger and \hat{b} is gauge invariant. In this appendix, we would like to introduce another vital algebra in QH Hilbert spaces, called the W_∞ -algebra, which reveals that there are more (actually infinite) commutative operators with the kinetic Hamiltonian. Furthermore, it is isomorphic to the GMP algebra, which offers a geometric interpretation of density operators.

B.1 w -algebra and W -algebra

The notations could be confusing among different literature. So firstly, we would like to introduce the meaning of w -algebra and W -algebra we will adopt in this appendix. The w -algebras are extended conformal algebras, and based on the spin N ; these algebras are denoted as w_N -algebras. Meanwhile, N can be pushed to infinity, and the corresponding algebra is called a w_∞ -algebra, the commutator of which is of the form [376]:

$$[w_s, w_{s'}] \sim w_{s+s'-2} \tag{B.1}$$

where we use w_s to denote the generator with spin s . By generalizing the commutation of w_∞ -algebra to the summation of generators W_s with more spins one can construct the so-called W_∞ -algebra:

$$[W_s, W_{s'}] \sim \sum_{m=2}^{s+s'-2} W_m \quad (\text{B.2})$$

These algebras can also be finite, called the W_N -algebras, which can be regarded as the generalization of the Virasoro algebra to generators with higher spins. (The Virasoro algebra is naturally equivalent to a W_2 algebra). But here, we will restrict our discussion to the two infinity algebras.

B.2 $SDiff(\mathbb{R}^2)$ in phase spaces and QH systems

The w_∞ -algebra and the W_∞ -algebra are both deeply connected to $SDiff(\mathbb{R}^2)$, the area-preserving diffeomorphisms of 2-planes [377]. Thus they are instrumental in studying the dynamics of strings, 2D gravity theories, and the phase space of 1D harmonic oscillators (both classical and quantum), which will be briefly explained as an example to illustrate these two algebras [376, 378].

In the phase space of a 1D classical harmonic oscillator, the symplectic structure $\omega = dq \wedge dp$ is preserved by the canonical transformation defined by a generating function $F(q, p)$, which exactly corresponds to $SDiff(\mathbb{R}^2)$ from (q, p) to (Q, P) (also known as the Liouville's theorem):

$$Q = q + \frac{\partial F}{\partial p} = \{q, F\}; \quad P = p - \frac{\partial F}{\partial q} = \{p, F\} \quad (\text{B.3})$$

where $\{ \}$ denotes the Poisson brackets. Then each term in the expansion of $F(q, p)$, denoted by $F_{n,m} = -q^{n+1}p^{m+1}$, is a generator and their algebra is the w_∞ -algebra:

$$\{F_{n,m}, F_{k,l}\} = [(m+1)(k+1) - (n+1)(l+1)]F_{n+k, m+l} \quad (\text{B.4})$$

We can generalize the same idea to the QH systems. By combining the magnetic translation generators(or the intra-LL orbital ladder operators) into:

$$\hat{\mathcal{B}}_{n,m} \equiv \left(\hat{b}^\dagger \right)^{n+1} \hat{b}^{m+1}, \quad n, m \geq -1 \quad (\text{B.5})$$

One can easily see that all these operators commute with the Hamiltonian, which corresponds to an infinite symmetry. The commutation between them is given by:

$$\left[\hat{\mathcal{B}}_{n,m}, \hat{\mathcal{B}}_{k,l} \right] = \sum_{s=0}^{\min(m,k)} \frac{(m+1)!(k+1)!}{(m-s)!(k-s)!(s+1)!} \hat{\mathcal{B}}_{n+k-s, m+l-s} - (m \leftrightarrow l, n \leftrightarrow k) \quad (\text{B.6})$$

This is exactly the full form of the w_∞ -algebra. Note that one can take the classical limit by truncating all the higher order terms of \hbar :

$$\left[\hat{\mathcal{B}}_{n,m}, \hat{\mathcal{B}}_{k,l} \right] = \hbar((m+1)(k+1) - (n+1)(l+1)) \hat{\mathcal{B}}_{n+k, m+l} + O(\hbar^2) \quad (\text{B.7})$$

which shows that they are related by quantization in physics after replacing the commutators with Poisson brackets, i.e.

The W_∞ -algebra is the quantum deformation of the w_∞ -algebra.

One can apply for central extension within any spin sectors for the W_∞ -algebra but only within the spin-2 sector for the w_∞ -algebra.

Considering the duality between the two sets of ladder operators in QH systems, one can also construct another W_∞ -algebra of \hat{a} and \hat{a}^\dagger in precisely the same way. The complete algebra of the generators in the whole Hilbert space will be the direct product $W_\infty^A \otimes W_\infty^B$.

B.3 GMP algebra and FFZ algebra

Suppose one essential intrinsic algebra of QH states concerning the kinetic energy is the Heisenberg algebra (apart from the ubiquitous C^* -algebras of observables). In that case, the Girvin-MacDonald-Platzman(GMP) algebra should be considered the other primarily for the FQH states (including fractional Chern insulators) because it describes the algebraic structure of the interaction Hamiltonian. Moreover,

a significant feature of the GMP algebra is that it is isomorphic to the W_∞ -algebra we introduced above:

$$\left[\hat{\tilde{\rho}}_{\mathbf{q}_1}, \hat{\tilde{\rho}}_{\mathbf{q}_2} \right] = -2i \sin \left(\frac{1}{2} \mathbf{q}_1 \wedge \mathbf{q}_2 \right) \hat{\tilde{\rho}}_{\mathbf{q}_1 + \mathbf{q}_2}; \quad \left[\hat{\tilde{\rho}}_{\mathbf{q}_1}, \hat{\tilde{\rho}}_{\mathbf{q}_2} \right] = 2i \sin \left(\frac{1}{2} \mathbf{q}_1 \wedge \mathbf{q}_2 \right) \hat{\tilde{\rho}}_{\mathbf{q}_1 + \mathbf{q}_2} \quad (\text{B.8})$$

because here, the magnetic translation operators play the role of the generating function $F(q, p)$ in the phase space of harmonic oscillators. One can expand it to work out the algebra of the generators of different order based on the same recipe.

Very similar behavior can also be found in a topologically massive gauge theory with Chern-Simons terms on the torus, where one can get the Fairlie-Fletcher-Zachos (FFZ) algebra of generators [379]:

$$\left[\tilde{\mathcal{W}}_{n, \bar{n}}, \tilde{\mathcal{W}}_{m, \bar{m}} \right] = -2i \sin \frac{2\pi}{k} (n_1 m_2 - n_2 m_1) \tilde{\mathcal{W}}_{n+m, \overline{n+m}} \quad (\text{B.9})$$

where $m_1, m_2, n_1, n_2 \in \mathbb{Z}$ and $\tilde{\mathcal{W}}_{n, \bar{n}}$ is equivalent to a magnetic translation operator. Thus one can regard it as the discretized version of the GMP algebra.

Appendix C

Schrieffer-Wolff transformation

Schrieffer-Wolff(SW) transformation is a degenerate perturbation method that can generate an effective Hamiltonian in a low-energy subspace within the whole Hilbert space. Hence, it is naturally suitable for the system with discrete subspaces such as FQH problems considering we normally project everything to a single LL (especially the LLL) [272]. In this appendix, we will intuitively introduce the assumptions, the expression, and the physical ideas behind this method.

The first thing one should notice is that the statement of projecting everything to a “low-energy” subspace is technically not accurate. In fact, one can do the SW transformation to *any subspace* within the Hilbert space. But the requirement is that the spectrum of the subspace we would like to project onto must be isolated from the other parts in the full spectrum, as Fig. shows. After the perturbation, the gap remains open, which determines the errors in the result. So, in other words, the subspace we are considering is *closed* under the effect of the perturbation so we can treat them as a whole and consider the change of its spectrum, which will not mix with the other parts either. The SW transformation can be understood as a slight rotation to all the quantum states within this subspace, as Fig. shows, which is typically called a *direct rotation*, and one can observe this from the expression:

$$\hat{H}_{\text{eff}} = e^{\hat{S}} \hat{H} e^{-\hat{S}} = \hat{H} + [\hat{S}, \hat{H}] + \frac{1}{2} [\hat{S}, [\hat{S}, \hat{H}]] + \dots \quad (\text{C.1})$$

where \hat{S} is an anti-Hermitian operator that can be solved perturbatively. In the context of FQH states, the perturbation originates from LL mixings as derived in the main text.

Appendix D

Jacobi coordinates

Jacobi coordinates are used to rearrange the degrees of freedom of different particles, commonly used in dealing with many-body systems like polyatomic molecules or celestial mechanics [380]. The key of this method is to transform the separated coordinate of each particle to the center of mass of their combinations. In some cases, the dynamic equations can be simplified to some extent by this procedure. However, note that for a generic N -body problem with $N \geq 3$, such a coordinate transformation cannot help reduce the complicity of solving the equations. So it only works very efficiently when there are other constraints in the system, in other words, in those essentially low-dimensional problems.

The procedure of transforming to Jacobi coordinates is quite organized, as illustrated below:

- Index all the N particles in the system;
- Define the first Jacobi position vector \mathbf{R}_1 as the relative position between the second and the first particle at \mathbf{r}_2 and \mathbf{r}_1 , pointing to the first one;
- Define the second Jacobi position vector \mathbf{R}_2 as the relative position between the center of mass of the first two particles c_{12} and the third particle at \mathbf{r}_3 , pointing to the center of mass of the first two particles
- ...

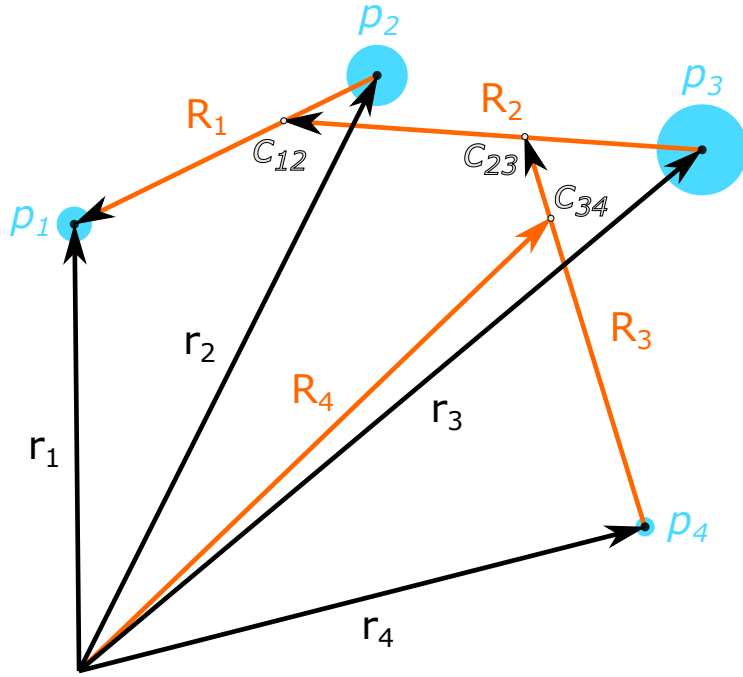


FIGURE D.1: Jacobi coordinates.

- Define the k -th Jacobi position vector \mathbf{R}_k as the relative position between the center of mass of the first k particles $c_{k-1,k}$ and the $k+1$ -th particle at \mathbf{r}_{k+1} , pointing to the center of mass of the first k particles;
- ...

which can be formally written as:

$$\begin{aligned} \mathbf{R}_j &= \frac{1}{m_{0j}} \sum_{k=1}^j m_k \mathbf{r}_k - \mathbf{r}_{j+1}, \\ \mathbf{R}_N &= \frac{1}{m_{0N}} \sum_{k=1}^N m_k \mathbf{r}_k, \quad m_{0j} = \sum_{k=1}^j m_k \end{aligned} \tag{D.1}$$

where j is an integer within $[1, N - 1]$.

In our discussions on the effective many-body interactions in a single Landau level, these Jacobi coordinate operators commute with each other so one can construct ladder operators for them and simplifies the problem by noticing that the center of mass of all the particles does not affect the dynamics because it does not exist in the Hamiltonian.

Appendix E

Generalized Laguerre polynomials

In this section, we will introduce a group of important polynomials in the discussion to FQH wave functions, especially in a rotationally invariant system, called generalized Laguerre polynomials $L_n^{(\alpha)}(x)$, which can be defined in several equivalent ways. Here we will only list some of them:

- the solution of the generalized Laguerre's equations: $xy'' + (\alpha + 1 - x)y' + ny = 0$;
- the contour integral $\frac{1}{2\pi i} \oint_C \frac{e^{-xt/(1-t)}}{(1-t)^{\alpha+1} t^{n+1}} dt$ with C circles the origin without enclosing the essential singularity at 1
- the series $\sum_{i=0}^n (-1)^i \binom{n+\alpha}{n-i} \frac{x^i}{i!}$
- the recursive polynomials given by $L_{k+1}^{(\alpha)}(x) = \frac{(2k+1+\alpha-x)L_k^{(\alpha)}(x)-(k+\alpha)L_{k-1}^{(\alpha)}(x)}{k+1}$ with $L_0^{(\alpha)}(x) = 1$ and $L_1^{(\alpha)}(x) = 1 + \alpha - x$;
- ...

One can write down the corresponding generating function as:

$$\frac{1}{(1-t)^{\alpha+1}} e^{-tx/(1-t)} = \sum_{n=0}^{\infty} t^n L_n^{(\alpha)}(x) \quad (\text{E.1})$$

These polynomials make up a *complete and orthogonal* basis (concerning a Gaussian measure) for the Segal–Bargmann space (as discussed in Appendix A):

$$\int_0^\infty x^\alpha e^{-x} L_n^{(\alpha)}(x) L_m^{(\alpha)}(x) dx = \frac{\Gamma(n + \alpha + 1)}{n!} \delta_{n,m} \quad (\text{E.2})$$

This is also why they act as the wave functions of orbitals within a single Landau level. Furthermore, there is a recurrence relation given by:

$$L_n^{(\alpha)}(x) = L_n^{(\alpha+1)}(x) - L_{n-1}^{(\alpha+1)}(x) = \sum_{j=0}^k \binom{k}{j} L_{n-j}^{(\alpha+k)}(x) \quad (\text{E.3})$$

It has been rigorously proved that the generalized Laguerre polynomials with Gaussian measures are the eigenfunctions of 2D Fourier transform, denoted by the functional operator \hat{F} [332]:

$$\hat{F} [\Psi_{n\alpha}(\mathbf{q})] = (-1)^n (i)^\alpha \cdot \Psi_{n\alpha}(\mathbf{p}) \quad (\text{E.4})$$

with the eigenfunction of the vector \mathbf{q} defined by:

$$\Psi_{n\alpha}(\mathbf{q}) = \left[\frac{2(n!)}{(n + \alpha)!} \right]^{1/2} \mathbf{q}^\alpha \cdot L_n^{(\alpha)}(|\mathbf{q}|^2) e^{-\frac{1}{2}|\mathbf{q}|^2} \quad (\text{E.5})$$

which can thus be used to expand any eigenfunctions of \hat{F} , such as the (static) structure factors of FQH states.

The first kind of Bessel functions are closely related to the generalized Laguerre polynomials:

$$\frac{J_\alpha(x)}{\left(\frac{x}{2}\right)^\alpha} = \frac{e^{-t}}{\Gamma(\alpha + 1)} \sum_{k=0}^{\infty} \frac{L_k^{(\alpha)}\left(\frac{x^2}{4t}\right)}{\binom{k + \alpha}{k}} \frac{t^k}{k!} \quad (\text{E.6})$$

which can help calculate the matrix element of the δ -potential. Furthermore, the Hardy-Hille formula also relates the hyper-geometric functions to the generalized Laguerre polynomials by:

$$\sum_{n=0}^{\infty} \frac{n! \Gamma(\alpha + 1)}{\Gamma(n + \alpha + 1)} L_n^{(\alpha)}(x) L_n^{(\alpha)}(y) t^n = \frac{1}{(1-t)^{\alpha+1}} e^{-(x+y)t/(1-t)} {}_0F_1 \left(; \alpha + 1; \frac{xyt}{(1-t)^2} \right) \quad (\text{E.7})$$

Appendix F

Three-electron wave functions in a magnetic field

In this section, we will closely follow Laughlin's solution to the Schrödinger equation of three 2D electrons moving in a magnetic field:

$$H_{\text{internal}} = \frac{1}{2m} \left[\frac{\hbar}{i} \nabla_a - \frac{e}{c} \mathbf{A}_a \right]^2 + \frac{1}{2m} \left[\frac{\hbar}{i} \nabla_b - \frac{e}{c} \mathbf{A}_b \right]^2 + \frac{e^2}{\sqrt{2}} \left[\frac{1}{|z_b|} + \frac{1}{\left| -\frac{1}{2}z_b + \frac{\sqrt{3}}{2}z_a \right|} + \frac{1}{\left| -\frac{1}{2}z_b - \frac{\sqrt{3}}{2}z_a \right|} \right] \quad (\text{F.1})$$

where we have used the Jacobi coordinates (the center of mass is not present in the Hamiltonian):

$$\begin{aligned} z_a &= \left(\frac{2}{3} \right)^{1/2} \left[\left(\frac{z_1 + z_2}{2} \right) - z_3 \right] \\ z_b &= \frac{1}{\sqrt{2}} (z_1 - z_2) \end{aligned} \quad (\text{F.2})$$

The complete orthonormal basis states of the anti-symmetric FQH three-body wave functions provided in Ref.[18] are written as:

$$|\Psi_{kl}\rangle = \frac{1}{[2^{6l+4k+1}(3l+k)!k!\pi^2]^{1/2}} \left[\frac{(z_a + iz_b)^{3l} - (z_a - iz_b)^{3l}}{2i} \right] \cdot (z_a^2 + z_b^2)^k e^{-(1/4) \cdot (|z_a|^2 + |z_b|^2)} \quad (\text{F.3})$$

the expansion of which in the n_1, n_2 basis can be found in Table F.1 [203].

(k, l)	$\alpha = 2k + 3l$	$ \Psi_{kl}\rangle = \sum_{n_1, n_2} \alpha^{n_1, n_2} n_1, n_2\rangle$
(0,1)	3	$\frac{1}{2} 3, 0\rangle - \frac{\sqrt{3}}{2} 1, 2\rangle$
(1,1)	4	$-\frac{\sqrt{5}}{4} 5, 0\rangle + \frac{1}{2\sqrt{2}} 3, 2\rangle + \frac{3}{4} 1, 4\rangle$
(0,2)	6	$\frac{\sqrt{3}}{4} 5, 1\rangle - \frac{1}{2}\sqrt{\frac{5}{2}} 3, 3\rangle + \frac{\sqrt{3}}{4} 1, 5\rangle$
(2,1)	7	$-\frac{\sqrt{21}}{8} 7, 0\rangle + \frac{1}{8} 5, 2\rangle + \frac{\sqrt{15}}{8} 3, 4\rangle + \frac{3\sqrt{3}}{8} 1, 6\rangle$
(1,2)	8	$\frac{3}{4\sqrt{2}} 7, 1\rangle - \frac{\sqrt{7}}{4\sqrt{2}} 5, 3\rangle - \frac{\sqrt{7}}{4\sqrt{2}} 3, 5\rangle + \frac{3}{4\sqrt{2}} 1, 7\rangle$
(0,3)	9	$\frac{1}{16} 9, 0\rangle - \frac{3}{8} 7, 2\rangle + \frac{3\sqrt{7}}{8\sqrt{2}} 5, 4\rangle - \frac{\sqrt{21}}{8} 3, 6\rangle + \frac{3}{16} 1, 8\rangle$
(3,1)	9	$-\frac{\sqrt{21}}{8} 9, 0\rangle + \frac{\sqrt{3}}{4\sqrt{2}} 5, 4\rangle + \frac{1}{2} 3, 6\rangle + \frac{\sqrt{21}}{8} 1, 8\rangle$

TABLE F.1: **The anti-symmetric three-body wave functions expanded in the basis of $|n_1, n_2\rangle$.** The values of α^{n_1, n_2} can be found easily by looking at the coefficient of the corresponding basis. For example, $\alpha^{5,0}$ is the coefficient of $|5, 1\rangle$, i.e. $-\frac{\sqrt{5}}{4}$.

List of Author's Awards and Publications¹

Awards

- Best Poster Award in 50 Years of Physics in Singapore Symposium, IAS, Nanyang Technological University. Feb 2023.
- SPMS PAP Best Laboratory Teaching Assistant Award, SPMS, Nanyang Technological University. Jan 2022.
- SPMS Outstanding Contribution Award, SPMS, Nanyang Technological University. Jul 2021.

Journal Articles

- Wang, Y., Yang, B.(2022). Analytic exposition of the graviton modes in fractional quantum Hall effects and its physical implications. *Physical Review B*, 105, 035144.
- Liu, Y., Wang, Y., Hu, N. C., Lin, J. Y., Lee, C. H., & Zhang, X. (2020). Topological corner modes in a brick lattice with nonsymmorphic symmetry. *Physical Review B*, 102(3), 035142. (Co-first author)
- Zhang, X., Chen, Y., Wang, Y., Liu, Y., Lin, J. Y., Hu, N. C., ... & Lee, C. H. (2019). Entangled four-dimensional multicomponent topological states from photonic crystal defects. *Physical Review B*, 100(4), 041110.

¹The superscript * indicates joint first authors

- Lee, C. H., **Wang, Y.**, Chen, Y., & Zhang, X. (2018). Electromagnetic response of quantum Hall systems in dimensions five and six and beyond. *Physical Review B*, 98(9), 094434. (Co-first author)

Preprints

- **Wang, Y.**, Yang, B.(2022). Geometric Fluctuation of Conformal Hilbert Spaces and Multiple Graviton Modes in Fractional Quantum Hall Effect. arXiv:2201.00020.
- H. Q., Trung, **Wang, Y.**, and Yang, B.(2022). Spin-statistics relation and robustness of braiding phase for anyons in fractional quantum Hall effect. arXiv:2208.13786.

Conferences

- **Wang, Y.**, Graviton modes in fractional quantum Hall droplets. *50 Years of Physics in Singapore: A Symposium in Celebration of Professor K K Phua*. (Poster session)
- **Wang, Y.**, Analytic exposition of the graviton modes in fractional quantum Hall effects and its physical implications. Solid State Physics II T18.74, *IPS Meeting 2022*. (Oral contributed)
- **Wang, Y.**, Analytic exposition of the graviton modes in fractional quantum Hall effects and its physical implications. N65 Fractional Quantum Hall Effect: Theory and Numerics, *APS March Meeting 2022*. (Oral contributed)

Bibliography

- [1] E. H. Hall et al. On a new action of the magnet on electric currents. *American Journal of Mathematics*, 2(3):287–292, 1879. [1](#)
- [2] J. D. Jackson. Classical electrodynamics, 1999. [1](#)
- [3] K. v. Klitzing, G. Dorda, and M. Pepper. New method for high-accuracy determination of the fine-structure constant based on quantized hall resistance. *Phys. Rev. Lett.*, 45(6):494, 1980. [1](#), [2](#), [21](#), [22](#)
- [4] L. D. Landau. Diamagnetismus der metalle. *Zeitschrift für Physik*, 64:629–637, 1930. [1](#)
- [5] V. Fock. Konfigurationsraum und zweite quantelung. *Zeitschrift für Physik*, 75(9-10):622–647, 1932. [1](#)
- [6] W. J. De Haas and P. M. Van Alphen. The dependence of the susceptibility of diamagnetic metals upon the field. *Proc. Netherlands Roy. Acad. Sci.*, 33 (1106):170, 1930. [1](#)
- [7] M. Suzuki and I. S. Suzuki. Lecture note on solid state physics de haas-van alphen effect, 2006. [1](#)
- [8] E. M. Lifshits and A. M. Kosevich. Theory of the shubnikov—de haas effect. *Journal of Physics and Chemistry of Solids*, 4(1-2):1–10, 1958. [1](#)
- [9] D. E. Soule, J. W. McClure, and L. B. Smith. Study of the shubnikov-de haas effect. determination of the fermi surfaces in graphite. *Physical Review*, 134(2A):A453, 1964. [1](#)
- [10] D. Tong. Lectures on the quantum hall effect. *arXiv preprint arXiv:1606.06687*, 2016. [1](#)
- [11] D. C. Tsui, H. L. Stormer, and A. C. Gossard. Two-dimensional magneto-transport in the extreme quantum limit. *Phys. Rev. Lett.*, 48(22):1559, 1982. [2](#)
- [12] B. I. Halperin. Quantized hall conductance, current-carrying edge states, and the existence of extended states in a two-dimensional disordered potential. *Phys. Rev. B*, 25:2185–2190, Feb 1982. [3](#)

- [13] D. J. Thouless, M. Kohmoto, M. P. Nightingale, and M. den Nijs. Quantized hall conductance in a two-dimensional periodic potential. *Physical review letters*, 49(6):405, 1982. [3](#)
- [14] P. Streda. Theory of quantised hall conductivity in two dimensions. *Journal of Physics C: Solid State Physics*, 15(22):L717, 1982.
- [15] R. B. Laughlin. Quantized hall conductivity in two dimensions. *Phys. Rev. B*, 23(10):5632, 1981. [5](#)
- [16] D. Thouless. Quantization of particle transport. *Phys. Rev. B*, 27(10):6083, 1983.
- [17] Q. Niu, D. J. Thouless, and Y.-S. Wu. Quantized hall conductance as a topological invariant. *Phys. Rev. B*, 31:3372–3377, Mar 1985. [3](#)
- [18] R. B. Laughlin. Quantized motion of three two-dimensional electrons in a strong magnetic field. *Phys. Rev. B*, 27(6):3383, 1983. [4, 164](#)
- [19] R. B. Laughlin. Anomalous quantum hall effect: an incompressible quantum fluid with fractionally charged excitations. *Phys. Rev. Lett.*, 50(18):1395, 1983. [4, 44](#)
- [20] F. D. M. Haldane. Fractional quantization of the hall effect: A hierarchy of incompressible quantum fluid states. *Phys. Rev. Lett.*, 51:605–608, Aug 1983. [4, 34, 63, 65, 110](#)
- [21] F. D. M. Haldane and E. H. Rezayi. Finite-size studies of the incompressible state of the fractionally quantized hall effect and its excitations. *Phys. Rev. Lett.*, 54:237–240, Jan 1985. [4](#)
- [22] F. D. M. Haldane and E. H. Rezayi. Periodic laughlin-jastrow wave functions for the fractional quantized hall effect. *Phys. Rev. B*, 31:2529–2531, Feb 1985. [4](#)
- [23] R. Tao and D. J. Thouless. Fractional quantization of hall conductance. *Phys. Rev. B*, 28:1142–1144, Jul 1983. [4, 5](#)
- [24] E. J. Bergholtz and A. Karlhede. Quantum hall system in tao-thouless limit. *Phys. Rev. B*, 77:155308, Apr 2008.
- [25] E. J. Bergholtz, T. H. Hansson, M. Hermanns, A. Karlhede, and S. Viefers. Quantum hall hierarchy wave functions: From conformal correlators to tao-thouless states. *Phys. Rev. B*, 77:165325, Apr 2008. [4, 40, 44](#)
- [26] S. M. Girvin and T. Jach. Interacting electrons in two-dimensional landau levels: Results for small clusters. *Phys. Rev. B*, 28:4506–4509, Oct 1983. [4](#)
- [27] S. A. Trugman and S. Kivelson. Exact results for the fractional quantum hall effect with general interactions. *Physical Review B*, 31(8):5280, 1985. [4](#)

- [28] D. Arovas, J. R. Schrieffer, and F. Wilczek. Fractional statistics and the quantum hall effect. *Phys. Rev. Lett.*, 53(7):722, 1984. [4](#), [111](#)
- [29] A. Stern. Anyons and the quantum hall effect—a pedagogical review. *Annals of Physics*, 323(1):204–249, 2008. [4](#)
- [30] B. I. Halperin. Statistics of quasiparticles and the hierarchy of fractional quantized hall states. *Phys. Rev. Lett.*, 52:1583–1586, Apr 1984. [4](#)
- [31] R. Tao and Y.-S. Wu. Gauge invariance and fractional quantized hall effect. Technical report, Washington Univ., Seattle (USA). Dept. of Physics, 1984. [5](#)
- [32] D. Yoshioka. Ground state of the two-dimensional charged particles in a strong magnetic field and the fractional quantum hall effect. *Phys. Rev. B*, 29:6833–6839, Jun 1984. [5](#)
- [33] L. Bonsall and A. A. Maradudin. Some static and dynamical properties of a two-dimensional wigner crystal. *Phys. Rev. B*, 15:1959–1973, Feb 1977. [5](#)
- [34] V. J. Goldman, M. Santos, M. Shayegan, and J. E. Cunningham. Evidence for two-dimentional quantum wigner crystal. *Phys. Rev. Lett.*, 65:2189–2192, Oct 1990.
- [35] D. Levesque, J. J. Weis, and A. H. MacDonald. Crystallization of the incompressible quantum-fluid state of a two-dimensional electron gas in a strong magnetic field. *Phys. Rev. B*, 30:1056–1058, Jul 1984. [5](#)
- [36] D. J. Thouless. Long-range order and the fractional quantum hall effect. *Phys. Rev. B*, 31:8305–8307, Jun 1985. [5](#)
- [37] Pui K. Lam and S. M. Girvin. Liquid-solid transition and the fractional quantum-hall effect. *Phys. Rev. B*, 30:473–475, Jul 1984. [5](#)
- [38] V. J. Goldman, M. Shayegan, and D. C. Tsui. Evidence for the fractional quantum hall state at $\nu = \frac{1}{7}$. *Phys. Rev. Lett.*, 61:881–884, Aug 1988.
- [39] W. Pan, H. L. Stormer, D. C. Tsui, L. N. Pfeiffer, K. W. Baldwin, and K. W. West. Transition from an electron solid to the sequence of fractional quantum hall states at very low landau level filling factor. *Phys. Rev. Lett.*, 88:176802, Apr 2002.
- [40] A. C. Archer, K. Park, and J. K. Jain. Competing crystal phases in the lowest landau level. *Phys. Rev. Lett.*, 111:146804, Oct 2013.
- [41] Z.-W. Zuo, A. C. Balram, S. Pu, J. Zhao, T. Jolicoeur, A. Wójs, and J. K. Jain. Interplay between fractional quantum hall liquid and crystal phases at low filling. *Phys. Rev. B*, 102:075307, Aug 2020.

- [42] Y. J. Chung, D. Graf, L. W. Engel, K. A. V. Rosales, P. T. Madathil, K. W. Baldwin, K. W. West, L. N. Pfeiffer, and M. Shayegan. Correlated states of 2d electrons near the landau level filling $\nu = 1/7$. *Phys. Rev. Lett.*, 128: 026802, Jan 2022. [5](#)
- [43] M. A. Paalanen, D. C. Tsui, A. C. Gossard, and J. C. M. Hwang. Disorder and the fractional quantum hall effect. *Solid state communications*, 50(9): 841–844, 1984. [5](#)
- [44] B. J. F. Lin, M. A. Paalanen, A. C. Gossard, and D. C. Tsui. Weak localization of two-dimensional electrons in $\text{GaAs-Al}_x\text{Ga}_{1-x}\text{As}$ heterostructures. *Physical Review B*, 29(2):927, 1984.
- [45] B. J. F. Lin, D. C. Tsui, M. A. Paalanen, and A. C. Gossard. Mobility of the two-dimensional electron gas in $\text{GaAs-Al}_x\text{Ga}_{1-x}\text{As}$ heterostructures. *Applied physics letters*, 45(6):695–697, 1984.
- [46] H. P. Wei, D. C. Tsui, M. A. Paalanen, and A. M. M. Pruisken. Experiments on delocalization and universality in the integral quantum hall effect. *Physical review letters*, 61(11):1294, 1988.
- [47] P. W. Adams and M. A. Paalanen. Localization in a nondegenerate two-dimensional electron gas. *Physical review letters*, 58(20):2106, 1987. [5](#)
- [48] R. P. Feynman. *Statistical mechanics: a set of lectures*. CRC press, 2018. [6](#), [52](#), [82](#), [83](#)
- [49] R. P. Feynman. Atomic theory of the λ transition in helium. *Physical Review*, 91(6):1291, 1953. [82](#), [83](#), [88](#)
- [50] G. D. Mahan. *Many-particle physics*. Springer Science & Business Media, 2013. [6](#)
- [51] S. M. Girvin, A. H. MacDonald, and P. M. Platzman. Collective-excitation gap in the fractional quantum hall effect. *Phys. Rev. Lett.*, 54:581–583, Feb 1985. [6](#), [27](#), [83](#), [150](#)
- [52] S. M. Girvin, A. H. MacDonald, and P. M. Platzman. Magneto-roton theory of collective excitations in the fractional quantum hall effect. *Phys. Rev. B*, 33(4):2481, 1986. [6](#), [27](#), [83](#), [84](#), [87](#), [123](#), [124](#), [131](#), [150](#)
- [53] D. Yoshioka. Excitation energies of the fractional quantum hall effect. *Journal of the Physical Society of Japan*, 55(3):885–896, 1986. [6](#)
- [54] G. Fano, F. Ortolani, and E. Colombo. Configuration-interaction calculations on the fractional quantum hall effect. *Phys. Rev. B*, 34:2670–2680, Aug 1986. [6](#)
- [55] F. C. Zhang and S. Das Sarma. Excitation gap in the fractional quantum hall effect: Finite layer thickness corrections. *Phys. Rev. B*, 33(4):2903–2905, Feb 1986. [6](#), [119](#)

- [56] T. Chakraborty, P. Pietiläinen, and F. C. Zhang. Elementary excitations in the fractional quantum hall effect and the spin-reversed quasiparticles. *Phys. Rev. Lett.*, 57:130–133, Jul 1986. [6](#)
- [57] T. Chakraborty and P. Pietiläinen. Fractional quantum hall effect at half-filled landau level in a multiple-layer electron system. *Phys. Rev. Lett.*, 59: 2784–2787, Dec 1987. [6](#)
- [58] M. Rasolt and A. H. MacDonald. Collective excitations in the fractional quantum hall effect of a multicomponent fermion system. *Phys. Rev. B*, 34: 5530–5539, Oct 1986.
- [59] C. R. Dean, A. F. Young, P. Cadden-Zimansky, L. Wang, H. Ren, K. Watanabe, T. Taniguchi, P. Kim, J. Hone, and K. L. Shepard. Multicomponent fractional quantum hall effect in graphene. *Nature Physics*, 7(9):693–696, 2011. [6](#)
- [60] R. Prange and S. M. Girvin. *The quantum Hall effect*. Springer US, 1987. [6, 12](#)
- [61] R. Willett, J. P. Eisenstein, H. L. Störmer, D. C. Tsui, A. C. Gossard, and J. H. English. Observation of an even-denominator quantum number in the fractional quantum hall effect. *Phys. Rev. Lett.*, 59:1776–1779, Oct 1987. [7](#)
- [62] K. K. W. Ma, M. R. Peterson, V. W. Scarola, and K. Yang. Fractional quantum hall effect at the filling factor $\nu = 5/2$, 2022. [7](#)
- [63] C. N. Yang. Concept of off-diagonal long-range order and the quantum phases of liquid he and of superconductors. *Rev. Mod. Phys.*, 34:694–704, Oct 1962. [7](#)
- [64] S. M. Girvin and A. H. MacDonald. Off-diagonal long-range order, oblique confinement, and the fractional quantum hall effect. *Phys. Rev. Lett.*, 58 (12):1252–1255, Mar 1987. [9](#)
- [65] E. H. Rezayi and F. D. M. Haldane. Off-diagonal long-range order in fractional quantum-hall-effect states. *Phys. Rev. Lett.*, 61:1985–1988, Oct 1988. [7](#)
- [66] F. D. M. Haldane. Model for a quantum hall effect without landau levels: Condensed-matter realization of the "parity anomaly". *Phys. Rev. Lett.*, 61: 2015–2018, Oct 1988. [7, 22](#)
- [67] A. K. Geim. Graphene: status and prospects. *science*, 324(5934):1530–1534, 2009. [7](#)
- [68] A. K. Geim and K. S. Novoselov. The rise of graphene. In *Nanoscience and technology: a collection of reviews from nature journals*, pages 11–19. World Scientific, 2010. [7](#)

- [69] B. E. Kane, D. C. Tsui, and G. Weimann. Evidence for edge currents in the integral quantum hall effect. *Phys. Rev. Lett.*, 59:1353–1356, Sep 1987. [7](#)
- [70] M. Büttiker. Absence of backscattering in the quantum hall effect in multi-probe conductors. *Phys. Rev. B*, 38:9375–9389, Nov 1988. [7](#)
- [71] J. K. Jain. Composite-fermion approach for the fractional quantum hall effect. *Phys. Rev. Lett.*, 63(2):199, 1989. [8](#), [69](#), [73](#), [116](#), [150](#)
- [72] J. K. Jain. A unified theory of the integer and the fractional quantum hall effects. *Journal of Physics and Chemistry of Solids*, 51(8):889–899, 1990.
- [73] J. K. Jain. Microscopic theory of the fractional quantum hall effect. *Advances in Physics*, 41(2):105–146, 1992.
- [74] J. K. Jain. *Composite fermions*. Cambridge University Press, 2007. [69](#), [70](#), [73](#), [116](#), [135](#)
- [75] J. K. Jain. Composite fermion theory of exotic fractional quantum hall effect. *Annu. Rev. Condens. Matter Phys.*, 6(1):39–62, 2015.
- [76] J. K. Jain. *Thirty Years of Composite Fermions and Beyond*, chapter 1 in *Fractional Quantum Hall Effects*, pages 1–78. World Scientific, 2020. [8](#), [69](#), [70](#), [150](#)
- [77] S. C. Zhang, T. Hansson, and S. Kivelson. Effective-field-theory model for the fractional quantum hall effect. *Phys. Rev. Lett.*, 62(1):82, 1989. [9](#), [46](#), [47](#)
- [78] S. C. Zhang. The chern–simons–landau–ginzburg theory of the fractional quantum hall effect. *International Journal of Modern Physics B*, 6(01):25–58, 1992. [9](#)
- [79] G. V. Dunne. Aspects of chern-simons theory. In *Aspects topologiques de la physique en basse dimension. Topological aspects of low dimensional systems*, pages 177–263, Berlin, Heidelberg, 1999. Springer Berlin Heidelberg. ISBN 978-3-540-46637-6. [9](#)
- [80] B. Blok and X.-G. Wen. Effective theories of the fractional quantum hall effect at generic filling fractions. *Phys. Rev. B*, 42:8133–8144, Nov 1990. [9](#)
- [81] X.-G. Wen and Q. Niu. Ground-state degeneracy of the fractional quantum hall states in the presence of a random potential and on high-genus riemann surfaces. *Phys. Rev. B*, 41:9377–9396, May 1990. [9](#)
- [82] F. D. M. Haldane. Many-particle translational symmetries of two-dimensional electrons at rational landau-level filling. *Phys. Rev. Lett.*, 55:2095–2098, Nov 1985. [9](#)
- [83] X.-G. Wen. Chiral luttinger liquid and the edge excitations in the fractional quantum hall states. *Phys. Rev. B*, 41:12838–12844, Jun 1990. [10](#), [45](#)

- [84] X.-G. Wen. Edge excitations in the fractional quantum hall states at general filling fractions. *Modern Physics Letters B*, 05(01):39–46, 1991.
- [85] X.-G. Wen. Gapless boundary excitations in the quantum hall states and in the chiral spin states. *Phys. Rev. B*, 43:11025–11036, May 1991.
- [86] X.-G. Wen. Edge transport properties of the fractional quantum hall states and weak-impurity scattering of a one-dimensional charge-density wave. *Phys. Rev. B*, 44:5708–5719, Sep 1991.
- [87] X.-G. Wen. Theory of the edge states in fractional quantum hall effects. *International Journal of Modern Physics B*, 06(10):1711–1762, 1992. [10](#)
- [88] X.-G. Wen, Y.-S. Wu, and Y. Hatsugai. Chiral operator product algebra and edge excitations of a fractional quantum hall droplet. *Nuclear Physics B*, 422 (3):476–494, 1994.
- [89] B. Yan, R. R. Biswas, and C. H. Greene. Bulk-edge correspondence in fractional quantum hall states. *Phys. Rev. B*, 99:035153, Jan 2019. [10](#), [17](#)
- [90] B. A. Bernevig. Topological insulators and topological superconductors. In *Topological Insulators and Topological Superconductors*. Princeton university press, 2013. [10](#), [13](#)
- [91] X.-G. Wen and A. Zee. Classification of abelian quantum hall states and matrix formulation of topological fluids. *Phys. Rev. B*, 46:2290–2301, Jul 1992. [10](#)
- [92] E. Witten. Quantum field theory and the jones polynomial. *Communications in Mathematical Physics*, 121:351–399, 1989. [10](#), [47](#)
- [93] G. Moore and N. Read. Nonabelions in the fractional quantum hall effect. *Nucl. Phys. B*, 360(2-3):362–396, 1991. [10](#), [20](#), [43](#), [47](#), [138](#)
- [94] N. Read and Dmitry Green. Paired states of fermions in two dimensions with breaking of parity and time-reversal symmetries and the fractional quantum hall effect. *Phys. Rev. B*, 61:10267–10297, Apr 2000. [10](#), [12](#), [20](#)
- [95] M. Ibañez, J. Links, G. Sierra, and S.-Y. Zhao. Exactly solvable pairing model for superconductors with $p_x + ip_y$ -wave symmetry. *Phys. Rev. B*, 79: 180501, May 2009. [10](#), [12](#)
- [96] M. Greiter, X.-G. Wen, and F. Wilczek. Paired hall state at half filling. *Phys. Rev. Lett.*, 66:3205–3208, Jun 1991. [10](#)
- [97] Y. W. Suen, L. W. Engel, M. B. Santos, M. Shayegan, and D. C. Tsui. Observation of a $\nu=1/2$ fractional quantum hall state in a double-layer electron system. *Phys. Rev. Lett.*, 68:1379–1382, Mar 1992. [10](#)

- [98] J. P. Eisenstein, G. S. Boebinger, L. N. Pfeiffer, K. W. West, and Song He. New fractional quantum hall state in double-layer two-dimensional electron systems. *Phys. Rev. Lett.*, 68:1383–1386, Mar 1992. [10](#)
- [99] B. I. Halperin. Theory of the quantized hall conductance. *Helvetica Physica Acta*, 56(1-3):75–102, 1983. [10](#), [70](#)
- [100] S. He, S. Das Sarma, and X. C. Xie. Quantized hall effect and quantum phase transitions in coupled two-layer electron systems. *Phys. Rev. B*, 47: 4394–4412, Feb 1993.
- [101] M. R. Peterson and S. Das Sarma. Quantum hall phase diagram of half-filled bilayers in the lowest and the second orbital landau levels: Abelian versus non-abelian incompressible fractional quantum hall states. *Phys. Rev. B*, 81: 165304, Apr 2010.
- [102] Z. Papić, M. O. Goerbig, N. Regnault, and M. V. Milovanović. Tunneling-driven breakdown of the 331 state and the emergent pfaffian and composite fermi liquid phases. *Phys. Rev. B*, 82:075302, Aug 2010. [10](#)
- [103] A. Cappelli, C. A. Trugenberger, and G. R. Zemba. Infinite symmetry in the quantum hall effect. *Nuclear Physics B*, 396(2-3):465–490, 1993. [11](#)
- [104] H. Azuma. w_∞ algebra in the integer quantum hall effects. *Progress of Theoretical Physics*, 92(2):293–307, 1994.
- [105] D. Karabali. Algebraic aspects of the fractional quantum hall effect. *Nuclear Physics B*, 419(3):437–454, 1994.
- [106] M. Flohr and R. Varnhagen. Infinite symmetry in the fractional quantum hall effect. *Journal of Physics A: Mathematical and General*, 27(11):3999, 1994.
- [107] A. Cappelli and L. Maffi. W-infinity symmetry in the quantum hall effect beyond the edge. *Journal of High Energy Physics*, 2021(5):1–39, 2021. [11](#)
- [108] A. Pinczuk, B. S. Dennis, L. N. Pfeiffer, and K. West. Observation of collective excitations in the fractional quantum hall effect. *Phys. Rev. Lett.*, 70 (25):3983, 1993. [11](#), [82](#), [123](#), [134](#), [151](#)
- [109] A. Pinczuk, B. S. Dennis, L. N. Pfeiffer, and K. W. West. Light scattering by collective excitations in the fractional quantum hall regime. *Phys. B: Condens. Matter*, 249:40–43, 1998. [11](#), [82](#), [119](#), [123](#)
- [110] M. A. Eriksson, A. Pinczuk, B. S. Dennis, S. H. Simon, L. N. Pfeiffer, and K. W. West. Collective excitations in the dilute 2d electron system. *Phys. Rev. Lett.*, 82:2163–2166, Mar 1999.
- [111] M. Kang, A. Pinczuk, B. S. Dennis, M. A. Eriksson, L. N. Pfeiffer, and K. W. West. Inelastic light scattering by gap excitations of fractional quantum hall states at $1/3 \leq \nu \leq 2/3$. *Phys. Rev. Lett.*, 84:546–549, Jan 2000.

- [112] M. Kang, A. Pinczuk, B. S. Dennis, L. N. Pfeiffer, and K. W. West. Observation of multiple magnetorotons in the fractional quantum hall effect. *Phys. Rev. Lett.*, 86(12):2637–2640, Mar 2001. [84](#), [134](#), [136](#), [151](#)
- [113] C. F. Hirjibehedin, Irene Dujovne, A. Pinczuk, B. S. Dennis, L. N. Pfeiffer, and K. W. West. Splitting of long-wavelength modes of the fractional quantum hall liquid at $\nu = 1/3$. *Phys. Rev. Lett.*, 95:066803, Aug 2005.
- [114] U. Wurstbauer, K. W. West, L. N. Pfeiffer, and A. Pinczuk. Resonant inelastic light scattering investigation of low-lying gapped excitations in the quantum fluid at $\nu = 5/2$. *Phys. Rev. Lett.*, 110(2):026801, 2013. [11](#), [82](#), [119](#), [123](#)
- [115] R. G. Clark, J. R. Mallett, S. R. Haynes, J. J. Harris, and C. T. Foxon. Experimental determination of fractional charge e/q for quasiparticle excitations in the fractional quantum hall effect. *Phys. Rev. Lett.*, 60(17):1747–1750, Apr 1988. [11](#)
- [116] C. L. Kane and M. P. A. Fisher. Nonequilibrium noise and fractional charge in the quantum hall effect. *Physical review letters*, 72(5):724, 1994.
- [117] V. J. Goldman and B. Su. Resonant tunneling in the quantum hall regime: measurement of fractional charge. *Science*, 267(5200):1010–1012, 1995.
- [118] J. D. F. Franklin, I. Zailer, C. J. B. Ford, P. J. Simpson, J. E. F. Frost, D. A. Ritchie, M. Y. Simmons, and M. Pepper. The aharonov-bohm effect in the fractional quantum hall regime. *Surface science*, 361:17–21, 1996.
- [119] E.-A. Kim, M. J. Lawler, S. Vishveshwara, and E. Fradkin. Measuring fractional charge and statistics in fractional quantum hall fluids through noise experiments. *Physical Review B*, 74(15):155324, 2006.
- [120] D. E. Feldman and B. I. Halperin. Fractional charge and fractional statistics in the quantum hall effects. *Reports on Progress in Physics*, 84(7):076501, 2021. [11](#), [12](#)
- [121] R. De-Picciotto, M. Reznikov, M. Heiblum, V. Umansky, G. Bunin, and D. Mahalu. Direct observation of a fractional charge. *Physica B: Condensed Matter*, 249:395–400, 1998. [11](#)
- [122] L. Saminadayar, D. C. Glattli, Y. Jin, and B. c.-m. Etienne. Observation of the $e/3$ fractionally charged Laughlin quasiparticle. *Physical Review Letters*, 79(13):2526, 1997. [11](#)
- [123] A. M. Chang, L. N. Pfeiffer, and K. W. West. Observation of chiral Luttinger behavior in electron tunneling into fractional quantum hall edges. *Phys. Rev. Lett.*, 77:2538–2541, Sep 1996. [12](#)
- [124] F. P. Milliken, C. P. Umbach, and R. A. Webb. Indications of a Luttinger liquid in the fractional quantum hall regime. *Solid State Communications*, 97(4):309–313, 1996. [12](#)

- [125] R. L. Willett, L. N. Pfeiffer, and K. W. West. Measurement of filling factor $5/2$ quasiparticle interference with observation of charge $e/4$ and $e/2$ period oscillations. *Proceedings of the National Academy of Sciences*, 106(22):8853–8858, 2009. [12](#)
- [126] R. Sabo, I. Gurman, A. Rosenblatt, F. Lafont, D. Banitt, J. Park, M. Heiblum, Y. Gefen, V. Umansky, and D. Mahalu. Edge reconstruction in fractional quantum hall states. *Nature Physics*, 13(5):491–496, 2017.
- [127] H. Bartolomei, M. Kumar, R. Bisognin, A. Marguerite, J.-M. Berroir, E. Bocquillon, B. Placais, A. Cavanna, Q. Dong, U. Gennser, et al. Fractional statistics in anyon collisions. *Science*, 368(6487):173–177, 2020.
- [128] R. O. Umucalar, E. Macaluso, T. Compartin, and I. Carusotto. Time-of-flight measurements as a possible method to observe anyonic statistics. *Phys. Rev. Lett.*, 120:230403, Jun 2018. [14](#)
- [129] B. Yang. Anyons in conformal hilbert spaces: Statistics and dynamics of gapless excitations in fractional quantum hall systems. *International Journal of Modern Physics B*, 36(21):2230003, 2022. [12](#)
- [130] C. L. Kane and M. P.A. Fisher. Quantized thermal transport in the fractional quantum hall effect. *Phys. Rev. B*, 55(23):15832, 1997. [12, 68](#)
- [131] B. Lian and J. Wang. Theory of the disordered $\nu = \frac{5}{2}$ quantum thermal hall state: Emergent symmetry and phase diagram. *Phys. Rev. B*, 97:165124, Apr 2018. [12](#)
- [132] A. Sharma, S. Pu, and J. K. Jain. Bardeen-cooper-schrieffer pairing of composite fermions. *Phys. Rev. B*, 104:205303, Nov 2021. [12](#)
- [133] A. Stern. Non-abelian states of matter. *Nature*, 464(7286):187–193, 2010. [12](#)
- [134] B. Dutta, W. Yang, R. Melcer, H. K. Kundu, M. Heiblum, V. Umansky, Y. Oreg, A. Stern, and D. Mross. Distinguishing between non-abelian topological orders in a quantum hall system. *Science*, 375(6577):193–197, 2022. [12, 13, 20](#)
- [135] M. Banerjee, M. Heiblum, A. Rosenblatt, Y. Oreg, D. E. Feldman, A. Stern, and V. Umansky. Observed quantization of anyonic heat flow. *Nature*, 545(7652):75–79, 2017. [12](#)
- [136] M. Banerjee, M. Heiblum, V. Umansky, D. E. Feldman, Y. Oreg, and A. Stern. Observation of half-integer thermal hall conductance. *Nature*, 559(7713):205–210, 2018. [12, 20](#)
- [137] B. A. Bernevig and F. D. M. Haldane. Properties of non-abelian fractional quantum hall states at filling $\nu = k/r$. *Phys. Rev. Lett.*, 101:246806, Dec 2008. [12, 13, 63, 64, 68, 111](#)

- [138] M. Hermanns, N. Regnault, B. A. Bernevig, and E. Ardonne. From irrational to nonunitary: Haffnian and haldane-rezayi wave functions. *Phys. Rev. B*, 83:241302, Jun 2011. [12](#)
- [139] B. Yang. Gaffnian and haffnian: Physical relevance of nonunitary conformal field theory for the incompressible fractional quantum hall effect. *Physical Review B*, 103(11):115102, 2021. [14](#), [48](#), [113](#), [133](#), [140](#), [149](#)
- [140] Trung Q. Ha and B. Yang. Fractionalization and dynamics of anyons and their experimental signatures in the $\nu = n + 1/3$ fractional quantum hall state. *Phys. Rev. Lett.*, 127:046402, Jul 2021. [12](#), [121](#), [123](#)
- [141] A. A. Koulakov, M. M. Fogler, and B. I. Shklovskii. Charge density wave in two-dimensional electron liquid in weak magnetic field. *Phys. Rev. Lett.*, 76: 499–502, Jan 1996. [12](#)
- [142] M. M. Fogler, A. A. Koulakov, and B. I. Shklovskii. Ground state of a two-dimensional electron liquid in a weak magnetic field. *Phys. Rev. B*, 54: 1853–1871, Jul 1996.
- [143] R. R. Du, D. C. Tsui, H. L. Stormer, L. N. Pfeiffer, K. W. Baldwin, and K. W. West. Strongly anisotropic transport in higher two-dimensional landau levels. *Solid State Communications*, 109(6):389–394, 1999. ISSN 0038-1098.
- [144] M. P. Lilly, K. B. Cooper, J. P. Eisenstein, L. N. Pfeiffer, and K. W. West. Evidence for an anisotropic state of two-dimensional electrons in high landau levels. *Phys. Rev. Lett.*, 82:394–397, Jan 1999.
- [145] J. P. Eisenstein, K. B. Cooper, L. N. Pfeiffer, and K. W. West. Insulating and fractional quantum hall states in the first excited landau level. *Phys. Rev. Lett.*, 88:076801, Jan 2002. [12](#)
- [146] A. Kitaev. Unpaired majorana fermions in quantum wires. *Physics-uspekhi*, 44(10S):131, 2001. [13](#)
- [147] A. Kitaev. Fault-tolerant quantum computation by anyons. *Annals of Physics*, 303(1):2–30, 2003. [13](#)
- [148] A. Kitaev. Anyons in an exactly solved model and beyond. *Annals of Physics*, 321(1):2–111, 2006. [13](#)
- [149] A. Altland and M. R. Zirnbauer. Nonstandard symmetry classes in mesoscopic normal-superconducting hybrid structures. *Phys. Rev. B*, 55:1142–1161, Jan 1997. [13](#)
- [150] X. Chen, Z.-C. Gu, and X.-G. Wen. Local unitary transformation, long-range quantum entanglement, wave function renormalization, and topological order. *Physical review b*, 82(15):155138, 2010. [13](#)

- [151] X. Chen, Z.-C. Gu, and X.-G. Wen. Complete classification of one-dimensional gapped quantum phases in interacting spin systems. *Physical review b*, 84(23):235128, 2011.
- [152] X. Chen, Z.-C. Gu, Z.-X. Liu, and X.-G. Wen. Symmetry protected topological orders and the group cohomology of their symmetry group. *Physical Review B*, 87(15):155114, 2013.
- [153] T. Lan, L. Kong, and X.-G. Wen. Modular extensions of unitary braided fusion categories and 2+1d topological/spt orders with symmetries. *Communications in Mathematical Physics*, 351(2):709–739, 2017. [13](#)
- [154] C. L. Kane, R. Mukhopadhyay, and T. C. Lubensky. Fractional quantum hall effect in an array of quantum wires. *Phys. Rev. Lett.*, 88:036401, Jan 2002. [13](#)
- [155] H. Ma, E. Lake, X. Chen, and M. Hermele. Fracton topological order via coupled layers. *Phys. Rev. B*, 95:245126, Jun 2017.
- [156] Y. Fuji and A. Furusaki. Quantum hall hierarchy from coupled wires. *Phys. Rev. B*, 99:035130, Jan 2019. [13](#)
- [157] X.-L. Qi and S.-C. Zhang. Topological insulators and superconductors. *Rev. Mod. Phys.*, 83:1057–1110, Oct 2011. [13](#)
- [158] M. Z. Hasan and C. L. Kane. Colloquium: Topological insulators. *Rev. Mod. Phys.*, 82:3045–3067, Nov 2010.
- [159] S.-Q. Shen. *Topological insulators*, volume 174. Springer, 2012. [13](#)
- [160] K. I. Bolotin, F. Ghahari, M. D. Shulman, H. L. Stormer, and P. Kim. Observation of the fractional quantum hall effect in graphene. *Nature*, 462(7270):196–199, 2009. [13, 21](#)
- [161] X. Du, I. Skachko, F. Duerr, A. Luican, and E. Y. Andrei. Fractional quantum hall effect and insulating phase of dirac electrons in graphene. *Nature*, 462(7270):192–195, 2009.
- [162] B. E. Feldman, B. Krauss, J. H. Smet, and A. Yacoby. Unconventional sequence of fractional quantum hall states in suspended graphene. *Science*, 337(6099):1196–1199, 2012.
- [163] B. E. Feldman, A. J. Levin, B. Krauss, D. A. Abanin, B. I. Halperin, J. H. Smet, and A. Yacoby. Fractional quantum hall phase transitions and four-flux states in graphene. *Physical Review Letters*, 111(7):076802, 2013.
- [164] J. Li, C. Tan, S. Chen, Y. Zeng, T. Taniguchi, K. Watanabe, J. Hone, and C. R. Dean. Even-denominator fractional quantum hall states in bilayer graphene. *Science*, 358(6363):648–652, 2017. [13](#)

- [165] A. S. Sørensen, E. Demler, and M. D. Lukin. Fractional quantum hall states of atoms in optical lattices. *Phys. Rev. Lett.*, 94:086803, Mar 2005. [13](#)
- [166] M. Hafezi, A. S. Sørensen, E. Demler, and M. D. Lukin. Fractional quantum hall effect in optical lattices. *Phys. Rev. A*, 76:023613, Aug 2007.
- [167] N. R. Cooper and J. Dalibard. Reaching fractional quantum hall states with optical flux lattices. *Phys. Rev. Lett.*, 110:185301, Apr 2013. [13](#), [22](#)
- [168] Y.-J. Lin, R. L. Compton, K. Jiménez-García, J. V. Porto, and I. B. Spielman. Synthetic magnetic fields for ultracold neutral atoms. *Nature*, 462(7273):628–632, 2009. [13](#)
- [169] G. Jotzu, M. Messer, R. Desbuquois, M. Lebrat, T. Uehlinger, D. Greif, and T. Esslinger. Experimental realization of the topological haldane model with ultracold fermions. *Nature*, 515(7526):237–240, 2014.
- [170] M. E. Tai, A. Lukin, M. Rispoli, R. Schittko, T. Menke, D. Borgnia, P. M. Preiss, F. Grusdt, A. M. Kaufman, and M. Greiner. Microscopy of the interacting harper–hofstadter model in the two-body limit. *Nature*, 546(7659):519–523, 2017. [13](#)
- [171] C. Nayak, S. H. Simon, A. Stern, M. Freedman, and S. Das Sarma. Non-abelian anyons and topological quantum computation. *Rev. Mod. Phys.*, 80:1083–1159, Sep 2008. [13](#)
- [172] X.-G. Wen. Non-abelian statistics in the fractional quantum hall states. *Phys. Rev. Lett.*, 66:802–805, Feb 1991. [13](#)
- [173] N. Read and E. Rezayi. Quasiholes and fermionic zero modes of paired fractional quantum hall states: The mechanism for non-abelian statistics. *Phys. Rev. B*, 54(23):16864, 1996. [111](#)
- [174] E. Grosfeld, S. H. Simon, and A. Stern. Switching noise as a probe of statistics in the fractional quantum hall effect. *Phys. Rev. Lett.*, 96:226803, Jun 2006.
- [175] R. Thomale, A. Sterdyniak, N. Regnault, and B. A. Bernevig. Entanglement gap and a new principle of adiabatic continuity. *Phys. Rev. Lett.*, 104:180502, May 2010. [13](#), [17](#), [45](#), [68](#)
- [176] S. Das Sarma, M. Freedman, and C. Nayak. Topologically protected qubits from a possible non-abelian fractional quantum hall state. *Phys. Rev. Lett.*, 94:166802, Apr 2005. [13](#)
- [177] P. Bonderson, A. Kitaev, and K. Shtengel. Detecting non-abelian statistics in the $\nu = 5/2$ fractional quantum hall state. *Phys. Rev. Lett.*, 96:016803, Jan 2006. [13](#)
- [178] M. Dolev, M. Heiblum, V. Umansky, A. Stern, and D. Mahalu. Observation of a quarter of an electron charge at the $\nu = 5/2$ quantum hall state. *Nature*, 452(7189):829–834, 2008. [14](#)

- [179] R. L. Willett, L. N. Pfeiffer, and K. W. West. Alternation and interchange of e/4 and e/2 period interference oscillations consistent with filling factor 5/2 non-abelian quasiparticles. *Phys. Rev. B*, 82(20):205301, 2010. [14](#), [111](#)
- [180] A. E. Feiguin, E. Rezayi, C. Nayak, and S. Das Sarma. Density matrix renormalization group study of incompressible fractional quantum hall states. *Phys. Rev. Lett.*, 100:166803, Apr 2008. [14](#)
- [181] J. Zhao, D. N. Sheng, and F. D. M. Haldane. Fractional quantum hall states at $\frac{1}{3}$ and $\frac{5}{2}$ filling: Density-matrix renormalization group calculations. *Phys. Rev. B*, 83:195135, May 2011.
- [182] T. Ito and N. Shibata. Density matrix renormalization group study of the $\nu = 1/3$ edge states in fractional quantum hall systems. *Phys. Rev. B*, 103: 115107, Mar 2021. [14](#)
- [183] R. Morf and B. I. Halperin. Monte carlo evaluation of trial wavefunctions for the fractional quantized hall effect: Spherical geometry. *Zeitschrift für Physik B Condensed Matter*, 68(2):391–406, 1987. [14](#)
- [184] R. Morf and B. I. Halperin. Monte carlo evaluation of trial wave functions for the fractional quantized hall effect: Disk geometry. *Phys. Rev. B*, 33: 2221–2246, Feb 1986.
- [185] J. Wang, S. D. Geraedts, E. H. Rezayi, and F. D. M. Haldane. Lattice monte carlo for quantum hall states on a torus. *Phys. Rev. B*, 99:125123, Mar 2019. [14](#)
- [186] A. Rahmani, K. J. Sung, H. Puterman, P. Roushan, P. Ghaemi, and Z. Jiang. Creating and manipulating a Laughlin-type $\nu = 1/3$ fractional quantum hall state on a quantum computer with linear depth circuits. *PRX Quantum*, 1: 020309, Nov 2020. [14](#)
- [187] A. Kirmani, K. Bull, C.-Y. Hou, V. Saravanan, S. M. Saeed, Z. Papić, A. Rahmani, and P. Ghaemi. Probing geometric excitations of fractional quantum hall states on quantum computers. *Phys. Rev. Lett.*, 129:056801, Jul 2022. [14](#), [82](#), [123](#), [139](#)
- [188] W. Bishara and C. Nayak. Effect of landau level mixing on the effective interaction between electrons in the fractional quantum hall regime. *Phys. Rev. B*, 80(12):121302, Sep 2009. [14](#), [122](#)
- [189] S. H. Simon, E. H. Rezayi, and N. R. Cooper. Generalized quantum hall projection hamiltonians. *Phys. Rev. B*, 75:075318, Feb 2007. [14](#), [110](#), [133](#), [149](#)
- [190] S. H. Simon, E. H. Rezayi, N. R. Cooper, and I. Berdnikov. Construction of a paired wave function for spinless electrons at filling fraction $\nu = 2/5$. *Phys. Rev. B*, 75:075317, Feb 2007. [14](#), [111](#), [119](#)

- [191] S. C. Davenport, E. Ardonne, N. Regnault, and S. H. Simon. Spin-singlet gaffnian wave function for fractional quantum hall systems. *Phys. Rev. B*, 87:045310, Jan 2013.
- [192] T. Jolicoeur and P. Mizusaki, T. and Lecheminant. Absence of a gap in the gaffnian state. *Phys. Rev. B*, 90(7):075116, 2014. [113](#), [119](#)
- [193] B. Kang and J. E. Moore. Neutral excitations in the gaffnian state. *Phys. Rev. B*, 95(24):245117, 2017. [113](#)
- [194] B. Yang, Y.-H. Wu, and Z. Papić. Effective abelian theory from a non-abelian topological order in the $\nu = 2/5$ fractional quantum hall effect. *Phys. Rev. B*, 100(24):245303, 2019. [14](#), [133](#)
- [195] B. A. Bernevig and F. D. M. Haldane. Model fractional quantum hall states and jack polynomials. *Phys. Rev. Lett.*, 100:246802, Jun 2008. [16](#), [63](#), [64](#)
- [196] B. A. Bernevig and F. D. M. Haldane. Generalized clustering conditions of jack polynomials at negative jack parameter α . *Phys. Rev. B*, 77(18):184502, 2008. [63](#), [64](#)
- [197] B. A. Bernevig and N. Regnault. Anatomy of abelian and non-abelian fractional quantum hall states. *Phys. Rev. Lett.*, 103:206801, Nov 2009.
- [198] R. Thomale, B. Estienne, N. Regnault, and B. A. Bernevig. Decomposition of fractional quantum hall model states: Product rule symmetries and approximations. *Phys. Rev. B*, 84:045127, Jul 2011. [16](#)
- [199] B. Yang, Z.-X. Hu, Z. Papić, and F. D. M. Haldane. Model wave functions for the collective modes and the magnetoroton theory of the fractional quantum hall effect. *Phys. Rev. Lett.*, 108:256807, Jun 2012. [16](#), [84](#), [123](#), [130](#), [131](#), [139](#), [150](#)
- [200] H. Wang, R. Narayanan, X. Wan, and F. Zhang. Fractional quantum hall states in two-dimensional electron systems with anisotropic interactions. *Phys. Rev. B*, 86:035122, Jul 2012. [16](#)
- [201] B. Yang, Z. Papić, E. H. Rezayi, R. N. Bhatt, and F. D. M. Haldane. Band mass anisotropy and the intrinsic metric of fractional quantum hall systems. *Phys. Rev. B*, 85:165318, Apr 2012.
- [202] B. Yang, Z.-X. Hu, C. H. Lee, and Z. Papić. Generalized pseudopotentials for the anisotropic fractional quantum hall effect. *Phys. Rev. Lett.*, 118:146403, Apr 2017. [16](#)
- [203] B. Yang. Three-body interactions in generic fractional quantum hall systems and impact of galilean invariance breaking. *Phys. Rev. B*, 98:201101, Nov 2018. [16](#), [32](#), [36](#), [106](#), [109](#), [127](#), [140](#), [164](#)

- [204] B. Yang. Emergent commensurability from hilbert space truncation in fractional quantum hall fluids. *Phys. Rev. B*, 100:241302, Dec 2019. [16](#), [65](#), [89](#)
- [205] B. Yang and A. C. Balram. Elementary excitations in fractional quantum hall effect from classical constraints. *New J. Phys.*, 23(1):013001, 2021. [16](#), [65](#), [89](#), [140](#)
- [206] N. Regnault and B. A. Bernevig. Fractional chern insulator. *Phys. Rev. X*, 1:021014, Dec 2011. [17](#), [22](#)
- [207] Y.-L. Wu, B. A. Bernevig, and N. Regnault. Zoology of fractional chern insulators. *Phys. Rev. B*, 85:075116, Feb 2012. [17](#)
- [208] C. H. Lee, R. Thomale, and X.-L. Qi. Pseudopotential formalism for fractional chern insulators. *Phys. Rev. B*, 88:035101, Jul 2013.
- [209] C. Liu, T. Repellin, B. A. Bernevig, and N. Regnault. Fractional chern insulators beyond Laughlin states. *Phys. Rev. B*, 87:205136, May 2013.
- [210] A. G. Grushin, Á. Gómez-León, and T. Neupert. Floquet fractional chern insulators. *Phys. Rev. Lett.*, 112:156801, Apr 2014. [17](#)
- [211] E. M. Spanton, A. A. Zibrov, H. Zhou, T. Taniguchi, K. Watanabe, M. P. Zaletel, and A. F. Young. Observation of fractional chern insulators in a van der waals heterostructure. *Science*, 360(6384):62–66, 2018. [17](#)
- [212] P. J. Ledwith, G. Tarnopolsky, E. Khalaf, and A. Vishwanath. Fractional chern insulator states in twisted bilayer graphene: An analytical approach. *Phys. Rev. Research*, 2:023237, May 2020. [17](#)
- [213] H.-C. Jiang, Z. Wang, and L. Balents. Identifying topological order by entanglement entropy. *Nature Physics*, 8(12):902–905, 2012. [17](#)
- [214] B. Zeng, H. Zhai, and Z. Xu. Entanglement properties of some fractional quantum hall liquids. *Phys. Rev. A*, 66:042324, Oct 2002. [17](#), [45](#)
- [215] A. Kitaev and J. Preskill. Topological entanglement entropy. *Phys. Rev. Lett.*, 96:110404, Mar 2006.
- [216] O. S. Zozulya, M. Haque, K. Schoutens, and E. H. Rezayi. Bipartite entanglement entropy in fractional quantum hall states. *Phys. Rev. B*, 76:125310, Sep 2007.
- [217] M. Haque, O. Zozulya, and K. Schoutens. Entanglement entropy in fermionic Laughlin states. *Phys. Rev. Lett.*, 98:060401, Feb 2007.
- [218] M. B. Hastings. Entropy and entanglement in quantum ground states. *Phys. Rev. B*, 76:035114, Jul 2007. [45](#)

- [219] X.-L. Qi, H. Katsura, and A. W. W. Ludwig. General relationship between the entanglement spectrum and the edge state spectrum of topological quantum states. *Phys. Rev. Lett.*, 108:196402, May 2012.
- [220] D. Das and S. Datta. Universal features of left-right entanglement entropy. *Phys. Rev. Lett.*, 115:131602, Sep 2015. [17](#)
- [221] H. Li and F. D. M. Haldane. Entanglement spectrum as a generalization of entanglement entropy: Identification of topological order in non-abelian fractional quantum hall effect states. *Phys. Rev. Lett.*, 101(1):010504, 2008. [17, 45, 68](#)
- [222] J. Dubail, N. Read, and E. H. Rezayi. Real-space entanglement spectrum of quantum hall systems. *Phys. Rev. B*, 85:115321, Mar 2012. [17](#)
- [223] Z. Liu and R. N. Bhatt. Quantum entanglement as a diagnostic of phase transitions in disordered fractional quantum hall liquids. *Phys. Rev. Lett.*, 117:206801, Nov 2016.
- [224] Z. Liu and R. N. Bhatt. Evolution of quantum entanglement with disorder in fractional quantum hall liquids. *Phys. Rev. B*, 96:115111, Sep 2017.
- [225] L.-X. Wei, N. Jiang, Q. Li, and Z.-X. Hu. Entanglement spectrum edge reconstruction and correlation hole of fractional quantum hall liquids. *Phys. Rev. B*, 101:075137, Feb 2020.
- [226] G. J. Henderson, G. J. Sreejith, and S. H. Simon. Entanglement action for the real-space entanglement spectra of chiral abelian quantum hall wave functions. *Phys. Rev. B*, 104:195434, Nov 2021. [17](#)
- [227] M. P. Zaletel and R. S. K. Mong. Exact matrix product states for quantum hall wave functions. *Phys. Rev. B*, 86:245305, Dec 2012. [18](#)
- [228] B. Estienne, Z. Papić, N. Regnault, and B. A. Bernevig. Matrix product states for trial quantum hall states. *Phys. Rev. B*, 87:161112, Apr 2013.
- [229] M. Schossler, S. Bandyopadhyay, and A. Seidel. Inner workings of fractional quantum hall parent hamiltonians: A matrix product state point of view. *Phys. Rev. B*, 105:155124, Apr 2022. [18](#)
- [230] F. D. M. Haldane. Geometrical description of the fractional quantum hall effect. *Phys. Rev. Lett.*, 107, 9 2011. ISSN 00319007. [18, 26, 81, 88, 123, 125, 127, 149, 150](#)
- [231] I. V. Tokatly and G. Vignale. Lorentz shear modulus of fractional quantum hall states. *Journal of Physics: Condensed Matter*, 21(27):275603, 2009. [18](#)
- [232] N. Read and E. H. Rezayi. Hall viscosity, orbital spin, and geometry: Paired superfluids and quantum hall systems. *Phys. Rev. B*, 84:085316, Aug 2011.

- [233] B. Bradlyn, M. Goldstein, and N. Read. Kubo formulas for viscosity: Hall viscosity, ward identities, and the relation with conductivity. *Phys. Rev. B*, 86:245309, Dec 2012.
- [234] T. Scaffidi, N. Nandi, B. Schmidt, A. P. Mackenzie, and J. E. Moore. Hydrodynamic electron flow and hall viscosity. *Phys. Rev. Lett.*, 118:226601, Jun 2017.
- [235] C. Hoyos and D. T. Son. Hall viscosity and electromagnetic response. *Phys. Rev. Lett.*, 108:066805, Feb 2012.
- [236] Z. Liu, A. C. Balram, Z. Papić, and A. Gromov. Quench dynamics of collective modes in fractional quantum hall bilayers. *Phys. Rev. Lett.*, 126:076604, Feb 2021. [18](#), [82](#), [123](#), [139](#)
- [237] G. Y. Cho, Y. You, and E. Fradkin. Geometry of fractional quantum hall fluids. *Phys. Rev. B*, 90:115139, Sep 2014. [18](#)
- [238] A. Gromov and D. T. Son. Bimetric theory of fractional quantum hall states. *Phys. Rev. X*, 7, 11 2017. ISSN 21603308. [18](#), [123](#)
- [239] D. R. Hofstadter. Energy levels and wave functions of bloch electrons in rational and irrational magnetic fields. *Phys. Rev. B*, 14:2239–2249, Sep 1976. [19](#)
- [240] R. G. Mani and K. Von Klitzing. Fractional quantum hall effects as an example of fractal geometry in nature. *Zeitschrift für Physik B Condensed Matter*, 100(4):635–642, 1996.
- [241] L. Wang, Y. Gao, B. Wen, Z. Han, T. Taniguchi, K. Watanabe, M. Koshino, J. Hone, and C. R. Dean. Evidence for a fractional fractal quantum hall effect in graphene superlattices. *Science*, 350(6265):1231–1234, 2015. [19](#)
- [242] J. K. Jain and V. J. Goldman. Hierarchy of states in the fractional quantum hall effect. *Phys. Rev. B*, 45(3):1255, 1992. [19](#), [119](#), [135](#)
- [243] N. Regnault, B. A. Bernevig, and F.D.M. Haldane. Topological entanglement and clustering of jain hierarchy states. *Phys. Rev. Lett.*, 103(1):016801, Jun 2009. [19](#)
- [244] A. C. Balram, C. Tőke, and J. K. Jain. Luttinger theorem for the strongly correlated fermi liquid of composite fermions. *Physical review letters*, 115(18):186805, 2015. [19](#)
- [245] K. Lee, J. Shao, E.-A. Kim, F. D. M. Haldane, and E. H. Rezayi. Pomeranchuk instability of composite fermi liquids. *Physical review letters*, 121(14):147601, 2018. [19](#)
- [246] M. Levin, B. I. Halperin, and B. Rosenow. Particle-hole symmetry and the pfaffian state. *Phys. Rev. Lett.*, 99(23):236806, 2007. [20](#), [140](#)

- [247] S.-S. Lee, S. Ryu, C. Nayak, and M. P.A. Fisher. Particle-hole symmetry and the $\nu = 5/2$ quantum hall state. *Phys. Rev. Lett.*, 99(23):236807, 2007. [20](#), [140](#)
- [248] D. T. Son. Is the composite fermion a dirac particle? *Phys. Rev. X*, 5:031027, Sep 2015. [20](#)
- [249] D. T. Son. The dirac composite fermion of the fractional quantum hall effect. *Annual Review of Condensed Matter Physics*, 9:397–411, 2018.
- [250] E. H. Rezayi, K. Pakrouski, and F. D. M. Haldane. Stability of the particle-hole pfaffian state and the 5 2-fractional quantum hall effect. *Phys. Rev. B*, 104(8):L081407, 2021. [20](#)
- [251] X. Wan, Z.-X. Hu, E. H. Rezayi, and K. Yang. Fractional quantum hall effect at $\nu = 5/2$: Ground states, non-abelian quasiholes, and edge modes in a microscopic model. *Phys. Rev. B*, 77:165316, Apr 2008. [20](#)
- [252] A. Wójs, C. Tőke, and J. K. Jain. Landau-level mixing and the emergence of pfaffian excitations for the 5/2 fractional quantum hall effect. *Phys. Rev. Lett.*, 105(9):096802, Aug 2010. [122](#)
- [253] Y.-F. Wang, Z.-C. Gu, C.-D. Gong, and D. N. Sheng. Fractional quantum hall effect of hard-core bosons in topological flat bands. *Phys. Rev. Lett.*, 107:146803, Sep 2011.
- [254] E. H. Rezayi. Landau level mixing and the ground state of the $\nu = 5/2$ quantum hall effect. *Phys. Rev. Lett.*, 119:026801, Jul 2017. [20](#), [140](#)
- [255] S. H. Simon, M. Ippoliti, M. P. Zaletel, and E. H. Rezayi. Energetics of pfaffian–anti-pfaffian domains. *Phys. Rev. B*, 101:041302, Jan 2020. [20](#)
- [256] W. Zhu, D. N. Sheng, and K. Yang. Topological interface between pfaffian and anti-pfaffian order in $\nu = 5/2$ quantum hall effect. *Phys. Rev. Lett.*, 125: 146802, Sep 2020. [20](#)
- [257] Z. F. Ezawa. *Quantum Hall effects: Field theoretical approach and related topics*. World Scientific Publishing Company, 2008. [21](#), [25](#)
- [258] C. Repellin, T. Yefsah, and A. Sterdyniak. Creating a bosonic fractional quantum hall state by pairing fermions. *Phys. Rev. B*, 96:161111, Oct 2017. [22](#)
- [259] P. Rosson, M. Lubasch, M. Kiffner, and D. Jaksch. Bosonic fractional quantum hall states on a finite cylinder. *Phys. Rev. A*, 99:033603, Mar 2019.
- [260] A. Hudomal, N. Regnault, and I. Vasić. Bosonic fractional quantum hall states in driven optical lattices. *Phys. Rev. A*, 100:053624, Nov 2019. [22](#)
- [261] V. Pasquier. Quantum hall effect and non-commutative geometry. In *Quantum Spaces*, pages 1–17. Springer, 2007. [22](#)

- [262] P. W. Anderson. Absence of diffusion in certain random lattices. *Phys. Rev.*, 109:1492–1505, Mar 1958. [22](#)
- [263] S. Pu, G. J. Sreejith, and J. K. Jain. Anderson localization in the fractional quantum hall effect. *Phys. Rev. Lett.*, 128:116801, Mar 2022. [22](#)
- [264] S. M. Girvin and K. Yang. *Modern condensed matter physics*. Cambridge University Press, 2019. [23](#), [82](#), [86](#), [87](#)
- [265] P. Woit. *Quantum theory, groups and representations*. Springer, 2017. [27](#), [152](#)
- [266] D. C. Brody and L. P. Hughston. Geometric quantum mechanics. *Journal of geometry and physics*, 38(1):19–53, 2001. [27](#)
- [267] Ha Q. Trung, Y. Wang, and B. Yang. Spin-statistics relation and robustness of braiding phase for anyons in fractional quantum hall effect. *arXiv preprint arXiv:2208.13786*, 2022. [29](#)
- [268] G. Szegö. *Orthogonal polynomials*, volume 23. American Mathematical Soc., 1939. [34](#)
- [269] M. R. Peterson and C. Nayak. More realistic hamiltonians for the fractional quantum hall regime in gaas and graphene. *Phys. Rev. B*, 87:245129, Jun 2013. [35](#), [127](#)
- [270] S. Das Sarma, S. Adam, E. H. Hwang, and E. Rossi. Electronic transport in two-dimensional graphene. *Rev. Mod. Phys.*, 83:407–470, May 2011. [35](#)
- [271] J. R. Schrieffer and P. A. Wolff. Relation between the anderson and kondo hamiltonians. *Physical Review*, 149(2):491, 1966. [36](#)
- [272] S. Bravyi, D. P. Di Vincenzo, and D. Loss. Schrieffer–wolff transformation for quantum many-body systems. *Annals of physics*, 326(10):2793–2826, 2011. [36](#), [159](#)
- [273] S. M. Girvin and T. Jach. Formalism for the quantum hall effect: Hilbert space of analytic functions. *Phys. Rev. B*, 29:5617–5625, May 1984. [38](#)
- [274] P. Ginsparg. Applied conformal field theory. *arXiv preprint hep-th/9108028*, 1988. [40](#), [41](#)
- [275] J. Fuchs. Lectures on conformal field theory and kac-moody algebras. In *Conformal Field Theories and Integrable Models*, pages 1–54. Springer, 1997.
- [276] P. Francesco, P. Mathieu, and D. Sénéchal. *Conformal field theory*. Springer Science & Business Media, 2012. [40](#)
- [277] L. Onsager. Crystal statistics. i. a two-dimensional model with an order-disorder transition. *Physical Review*, 65(3-4):117, 1944. [41](#)

- [278] A. M. Polyakov. Quantum geometry of bosonic strings. *Physics Letters B*, 103(3):207–210, 1981. [41](#)
- [279] J. Maldacena. The large-n limit of superconformal field theories and supergravity. *International journal of theoretical physics*, 38(4):1113–1133, 1999. [41](#), [80](#)
- [280] Z. Merali. String theory finds a bench mate. *Nature*, 478(7369):302, 2011. [41](#)
- [281] S. Sachdev. Condensed matter and ads/cft. In *From gravity to thermal gauge theories: the AdS/CFT correspondence*, pages 273–311. Springer, 2011. [41](#)
- [282] M. Fremling. Success and failure of the plasma analogy for Laughlin states on a torus. *Journal of Physics A: Mathematical and Theoretical*, 50(1):015201, 2016. [44](#)
- [283] Y. Tournois. *Abelian and non-abelian quantum Hall hierarchies*. PhD thesis, Department of Physics, Stockholm University, 2020. [45](#)
- [284] T. H. Hansson, M. Hermanns, S. H. Simon, and S. F. Viefers. Quantum hall physics: Hierarchies and conformal field theory techniques. *Reviews of Modern Physics*, 89(2):025005, 2017. [45](#), [47](#)
- [285] R. Blumenhagen and E. Plauschinn. *Introduction to conformal field theory: with applications to string theory*, volume 779. Springer Science & Business Media, 2009. [45](#)
- [286] K. Schoutens and X.-G. Wen. Simple-current algebra constructions of 2+1-dimensional topological orders. *Phys. Rev. B*, 93:045109, Jan 2016.
- [287] Y. Fukusumi and O. S. Barićić. Kubo’s response theory and bosonization with a background gauge field and irrelevant perturbations. *Phys. Rev. B*, 104:235145, Dec 2021. [45](#)
- [288] G. B. Segal. The definition of conformal field theory. In *Differential geometrical methods in theoretical physics*, pages 165–171. Springer, 1988. [47](#)
- [289] G. E. Andrews. *The theory of partitions*. Cambridge university press, 1998. [50](#), [54](#), [59](#)
- [290] J.-F. Fortin, P. Jacob, and P. Mathieu. Generating function for k-restricted jagged partitions. *arXiv preprint math-ph/0305055*, 2003. [50](#)
- [291] J. H. Van Lint and R. M. Wilson. *A course in combinatorics*. Cambridge university press, 2001. [51](#)
- [292] S. Weinberg. *The quantum theory of fields*, volume 2. Cambridge university press, 1995. [52](#), [80](#)

- [293] P. A. MacMahon. Combinatory Analysis, Volumes I and II, volume 137. American Mathematical Soc., 2001. [54](#)
- [294] A. B. Zamolodchikov and V. A. Fateev. Nonlocal (parafermion) currents in two-dimensional conformal quantum field theory and self-dual critical points in zn -symmetric statistical systems. Sov. Phys. JETP, 62(2):215–225, 1985. [63](#)
- [295] B. Feigin, M. Jimbo, T. Miwa, and E. Mukhin. A differential ideal of symmetric polynomials spanned by jack polynomials at $r\beta=-(r=1)/(k+1)$. International Mathematics Research Notices, 2002(23):1223–1237, 2002.
- [296] B. Estienne, N. Regnault, and R. Santachiara. Clustering properties, jack polynomials and unitary conformal field theories. Nuclear physics B, 824(3):539–562, 2010. [63](#)
- [297] C. N. Yang and T. D. Lee. Statistical theory of equations of state and phase transitions. i. theory of condensation. Phys. Rev., 87:404–409, Aug 1952. [67](#)
- [298] T. D. Lee and C. N. Yang. Statistical theory of equations of state and phase transitions. ii. lattice gas and ising model. Phys. Rev., 87:410–419, Aug 1952. [67](#)
- [299] V. J. Goldman, B. Su, and J. K. Jain. Detection of composite fermions by magnetic focusing. Phys. Rev. Lett., 72:2065–2068, Mar 1994. [69](#)
- [300] M. S. Hossain, M. K. Ma, M. A. Mueed, L. N. Pfeiffer, K. W. West, K. W. Baldwin, and M. Shayegan. Direct observation of composite fermions and their fully-spin-polarized fermi sea near $\nu = 5/2$. Phys. Rev. Lett., 120:256601, Jun 2018. [69](#)
- [301] T. H. Hansson, C.-C. Chang, J. K. Jain, and S. Viefers. Composite-fermion wave functions as correlators in conformal field theory. Phys. Rev. B, 76:075347, Aug 2007. [69](#)
- [302] Z. Dong and T. Senthil. Noncommutative field theory and composite fermi liquids in some quantum hall systems. Phys. Rev. B, 102:205126, Nov 2020. [69](#)
- [303] E. Zermelo. Beweis, daß jede menge wohlgeordnet werden kann. Mathematische Annalen, 59(4):514–516, 1904. [72](#)
- [304] B. P. et al. Abbott. Observation of gravitational waves from a binary black hole merger. Phys. Rev. Lett., 116:061102, Feb 2016. [80](#)
- [305] C. Rovelli. Quantum gravity. Cambridge university press, 2004. [80](#)
- [306] C. Kiefer. Why quantum gravity? In Approaches to fundamental physics, pages 123–130. Springer, 2007. [80](#)

- [307] S. Weinberg. Effective gauge theories. *Physics Letters B*, 91(1):51–55, 1980. [80](#)
- [308] T. Eguchi, P. B. Gilkey, and A. J. Hanson. Gravitation, gauge theories and differential geometry. *Physics reports*, 66(6):213–393, 1980. [80](#)
- [309] B. Zwiebach. *A first course in string theory*. Cambridge university press, 2004. [81](#)
- [310] J. Polchinski. *String theory*. Cambridge university press, 2005. [81](#)
- [311] H. Kawai, D. C. Lewellen, and S. H. H. Tye. A relation between tree amplitudes of closed and open strings. *Nuclear Physics B*, 269(1):1–23, 1986. [81](#)
- [312] Z. Bern. Perturbative quantum gravity and its relation to gauge theory. *Living Reviews in Relativity*, 5(1):1–57, 2002. [81](#)
- [313] B. R. Holstein. Graviton physics. *American Journal of physics*, 74(11):1002–1011, 2006. [81](#)
- [314] T. Jacobson. Thermodynamics of spacetime: the einstein equation of state. *Physical Review Letters*, 75(7):1260, 1995. [81](#)
- [315] T. Padmanabhan. Thermodynamical aspects of gravity: new insights. *Reports on Progress in Physics*, 73(4):046901, 2010. [81](#)
- [316] F. Dyson. Is a graviton detectable? In *XVIIth International Congress on Mathematical Physics*, pages 670–682. World Scientific, 2014. [81](#)
- [317] G. E. Volovik. *The universe in a helium droplet*, volume 117. OUP Oxford, 2003. [81](#)
- [318] D. T. Son. Newton-cartan geometry and the quantum hall effect. *arXiv preprint arXiv:1306.0638*, 6 2013. URL <http://arxiv.org/abs/1306.0638>. [81](#), [123](#)
- [319] K. Yang. Geometry of compressible and incompressible quantum hall states: Application to anisotropic composite-fermion liquids. *Phys. Rev. B*, 88, 12 2013. ISSN 10980121. [81](#)
- [320] A. Pinczuk, B. S. Dennis, L. N. Pfeiffer, and K. W. West. Inelastic light scattering in the regimes of the integer and fractional quantum hall effects. *Semicond. Sci. Technol.*, 9(11S):1865, 1994. [82](#), [119](#), [123](#)
- [321] S. F. Liou, F. D. M. Haldane, Yang K., and E. H. Rezayi. Chiral gravitons in fractional quantum hall liquids. *Phys. Rev. Lett.*, 123, 9 2019. ISSN 10797114. [123](#), [136](#), [139](#)
- [322] D. X. Nguyen and D. T. Son. Probing the spin structure of the fractional quantum hall magnetoroton with polarized raman scattering. *Phys. Rev. Research*, 3:023040, Apr 2021. [82](#), [123](#), [136](#)

- [323] K. Yang. Acoustic wave absorption as a probe of dynamical geometrical response of fractional quantum hall liquids. *Phys. Rev. B*, 93:161302, Apr 2016. ISSN 24699969. [82](#), [139](#)
- [324] S. Golkar, D. X. Nguyen, and D. T. Son. Spectral sum rules and magneto-roton as emergent graviton in fractional quantum hall effect. *J. High Energy Phys.*, 2016:1–15, 1 2016. ISSN 10298479. [82](#), [123](#)
- [325] F. D. M. Haldane, E. H. Rezayi, and K. Yang. Graviton chirality and topological order in the half-filled landau level. *Phys. Rev. B*, 104:L121106, Sep 2021. [82](#), [136](#), [139](#)
- [326] D. X. Nguyen and D. T. Son. Dirac composite fermion theory of general jain sequences. *Phys. Rev. Research*, 3:033217, Sep 2021. [82](#), [123](#), [134](#), [139](#)
- [327] W. Kohn. Cyclotron resonance and de haas-van alphen oscillations of an interacting electron gas. *Phys. Rev.*, 123:1242–1244, Aug 1961. [83](#)
- [328] P. A. M. Dirac. The quantum theory of the emission and absorption of radiation. *Proceedings of the Royal Society of London. Series A, Containing Papers of a Mathematical and Physical Character*, 114(767):243–265, 1927. [86](#)
- [329] M. Born. Quantenmechanik der stoßvorgänge. *Zeitschrift für physik*, 38(11): 803–827, 1926. [86](#)
- [330] M. Kohmoto. Topological invariant and the quantization of the hall conductance. *Annals of Physics*, 160(2):343–354, 1985. [87](#)
- [331] A. Bijl, J. De Boer, and A. Michels. Properties of liquid helium ii. *Physica*, 8(7):655–675, 1941. [88](#)
- [332] L. Yu, W. Huang, M. Huang, Z. Zhu, X. Zeng, and W. Ji. The laguerre-gaussian series representation of two-dimensional fractional fourier transform. *Journal of Physics A: Mathematical and General*, 31(46):9353, 1998. [94](#), [163](#)
- [333] B. Yang. Microscopic theory for nematic fractional quantum hall effect. *Phys. Rev. Research*, 2:033362, Sep 2020. [97](#), [105](#), [123](#)
- [334] M. Abramowitz and I. A. Stegun. *Handbook of mathematical functions with formulas, graphs, and mathematical tables*, volume 55. US Government printing office, 1948. [99](#), [100](#)
- [335] A. C. Balram, Z. Liu, A. Gromov, and Z. Papić. Very-high-energy collective states of partons in fractional quantum hall liquids. *Phys. Rev. X*, 12:021008, Apr 2022. [106](#), [123](#), [124](#), [132](#), [136](#)
- [336] G. Cristofano, G. Maiella, R. Musto, and F. Nicodemi. Topological order in quantum hall effect and two-dimensional conformal field theory. *Nucl. Phys. B*, 33(3):119–133, 1993. [111](#)

- [337] K. T. Law. Probing non-abelian statistics in $\nu = 12/5$ quantum hall state. *Phys. Rev. B*, 77:205310, May 2008. [111](#)
- [338] B. Parsa, V. Gurarie, and C. Nayak. Plasma analogy and non-abelian statistics for ising-type quantum hall states. *Phys. Rev. B*, 83:075303, Feb 2011. [111](#)
- [339] B. A. Bernevig and F. D. M. Haldane. Clustering properties and model wave functions for non-abelian fractional quantum hall quasielectrons. *Phys. Rev. Lett.*, 102:066802, Feb 2009. [111](#)
- [340] F. D. M. Haldane and E. H. Rezayi. Spin-singlet wave function for the half-integral quantum hall effect. *Phys. Rev. Lett.*, 60:956–959, Mar 1988. [115](#)
- [341] D. Yoshioka, A. H. MacDonald, and S. M. Girvin. Connection between spin-singlet and hierarchical wave functions in the fractional quantum hall effect. *Phys. Rev. B*, 38:3636–3639, Aug 1988.
- [342] G. Misguich, T. Jolicoeur, and T. Mizusaki. Bubble phase at $\nu = \frac{1}{3}$ for spinless hollow-core interaction. *Phys. Rev. B*, 102:245107, Dec 2020. [115](#)
- [343] M. H. Freedman, J. Gukelberger, M. B. Hastings, S. Trebst, M. Troyer, and Z. Wang. Galois conjugates of topological phases. *Phys. Rev. B*, 85:045414, Jan 2012. [119](#)
- [344] N. Regnault, J. Maciejko, S. A. Kivelson, and S. L. Sondhi. Evidence of a fractional quantum hall nematic phase in a microscopic model. *Phys. Rev. B*, 96(3):035150, 2017. [119](#)
- [345] J. Maciejko, B. Hsu, Y. J. Kivelson, S. A .and Park, and S. L. Sondhi. Field theory of the quantum hall nematic transition. *Phys. Rev. B*, 88(12):125137, 2013.
- [346] B. E. Feldman, M. T. Randeria, A. Gynis, F. Wu, H. Ji, R. J. Cava, A. H. MacDonald, and A. Yazdani. Observation of a nematic quantum hall liquid on the surface of bismuth. *Science*, 354(6310):316–321, 2016. [119](#)
- [347] U. Wurstbauer, A. L. Levy, A. Pinczuk, K. W. West, L. N. Pfeiffer, M. J. Manfra, G. C. Gardner, and J. D. Watson. Gapped excitations of unconventional fractional quantum hall effect states in the second landau level. *Phys. Rev. B*, 92(24):241407, 2015. [119, 123](#)
- [348] K. Park, N. Meskini, and J. K. Jain. Activation gaps for the fractional quantum hall effect: realistic treatment of transverse thickness. *J. Condens. Matter Phys.*, 11(38):7283, 1999. [119](#)
- [349] M. R. Peterson, T. Jolicoeur, and S. D. Sarma. Finite-layer thickness stabilizes the pfaffian state for the 5/2 fractional quantum hall effect: wave function overlap and topological degeneracy. *Phys. Rev. Lett.*, 101(1):016807, 2008. [119](#)

- [350] A. C. Balram and S. Pu. Positions of the magnetoroton minima in the fractional quantum hall effect. *Eur. Phys. J. B*, 90(6), Jun 2017. ISSN 1434-6036. [121](#)
- [351] F. D. M. Haldane and K. Yang. Landau level mixing and levitation of extended states in two dimensions. *Phys. Rev. Lett.*, 78(2):298, 1997. [122](#), [127](#), [149](#)
- [352] I. Sodemann and A. H. MacDonald. Landau level mixing and the fractional quantum hall effect. *Phys. Rev. B*, 87(24):245425, 2013.
- [353] S. H. Simon and E. H. Rezayi. Landau level mixing in the perturbative limit. *Phys. Rev. B*, 87(15):155426, 2013. [122](#), [127](#), [149](#)
- [354] Y. Wang and B. Yang. Analytic exposition of the graviton modes in fractional quantum hall effects and its physical implications. *Phys. Rev. B*, 105:035144, Jan 2022. [123](#), [124](#), [130](#), [131](#), [132](#), [134](#), [140](#)
- [355] Luo X., Y. S. Wu, and Yu Y. Noncommutative chern-simons theory and exotic geometry emerging from the lowest landau level. *Phys. Rev. D*, 93, 6 2016. ISSN 24700029. [123](#)
- [356] D. X. Nguyen, F. D. M. Haldane, E. H. Rezayi, D. T. Son, and K. Yang. Multiple magnetorotons and spectral sum rules in fractional quantum hall systems. *Phys. Rev. Lett.*, 128:246402, Jun 2022. [123](#), [124](#), [128](#), [132](#), [135](#), [136](#)
- [357] F. D. M. Haldane. "hall viscosity" and intrinsic metric of incompressible fractional hall fluids. *arXiv preprint arXiv:0906.1854*, 2009. [124](#), [125](#)
- [358] B. I. Halperin, P. A. Lee, and N. Read. Theory of the half-filled landau level. *Phys. Rev. B*, 47:7312–7343, Mar 1993. [133](#)
- [359] G. Möller and S. H. Simon. Paired composite-fermion wave functions. *Phys. Rev. B*, 77:075319, Feb 2008. [133](#)
- [360] P. M. Platzman and S. He. Resonant raman scattering from magneto rotons in the fractional quantum hall liquid. *Physica Scripta*, 1996(T66):167, 1996. [134](#), [151](#)
- [361] I. V. Kukushkin, J. H. Smet, V. W. Scarola, V. Umansky, and K. von Klitzing. Dispersion of the excitations of fractional quantum hall states. *Science*, 324(5930):1044–1047, 2009. [134](#), [151](#)
- [362] E. Fradkin, C. Nayak, A. Tsvelik, and F. Wilczek. A chern-simons effective field theory for the pfaffian quantum hall state. *Nucl. Phys. B*, 516(3):704–718, 1998. [134](#)
- [363] N. Read and E. Rezayi. Beyond paired quantum hall states: Parafermions and incompressible states in the first excited landau level. *Phys. Rev. B*, 59 (12):8084, 1999.

- [364] B. Yang. Fractional quantum hall effect from frustration-free hamiltonians. *Phys. Rev. Lett.*, 125:176402, Oct 2020. [134](#), [140](#)
- [365] R. K. Dora and A. C. Balram. Nature of the anomalous 4/13 fractional quantum hall effect in graphene. *Phys. Rev. B*, 105:L241403, Jun 2022. [135](#)
- [366] D. X. Nguyen, D. T. Son, and C. Wu. Lowest landau level stress tensor and structure factor of trial quantum hall wave functions. *arXiv preprint arXiv:1411.3316*, 2014. [135](#)
- [367] W. Pan, H. L. Stormer, D. C. Tsui, L. N. Pfeiffer, K. W. Baldwin, and K. W. West. Fractional quantum hall effect of composite fermions. *Phys. Rev. Lett.*, 90:016801, Jan 2003. [137](#)
- [368] A. C. Balram. A non-Abelian parton state for the $\nu = 2 + 3/8$ fractional quantum Hall effect. *SciPost Phys.*, 10:083, 2021. [138](#)
- [369] A. Kumar, G. A. Csáthy, M. J. Manfra, L. N. Pfeiffer, and K. W. West. Non-conventional odd-denominator fractional quantum hall states in the second landau level. *Phys. Rev. Lett.*, 105:246808, Dec 2010. [138](#)
- [370] R. H. Morf. Transition from quantum hall to compressible states in the second landau level: New light on the $\nu = 5/2$ enigma. *Phys. Rev. Lett.*, 80: 1505–1508, Feb 1998. [138](#)
- [371] A. Gromov, E. J. Martinec, and S. Ryu. Collective excitations at filling factor 5/2: The view from superspace. *Phys. Rev. Lett.*, 125:077601, Aug 2020. [139](#)
- [372] A. C. Balram, Csaba Tóke, A. Wójs, and J. K. Jain. Spontaneous polarization of composite fermions in the $n = 1$ landau level of graphene. *Phys. Rev. B*, 92:205120, Nov 2015. [140](#)
- [373] W. N. Faugno, A. C. Balram, M. Barkeshli, and J. K. Jain. Prediction of a non-abelian fractional quantum hall state with f -wave pairing of composite fermions in wide quantum wells. *Phys. Rev. Lett.*, 123:016802, Jul 2019. [140](#)
- [374] F. D. M. Haldane and Y. Shen. Geometry of landau orbits in the absence of rotational symmetry. *arXiv preprint arXiv:1512.04502*, 2015. [149](#)
- [375] B. Yang. The composite fermion theory revisited: a microscopic derivation without landau level projection. *arXiv preprint arXiv:2207.12418*, 2022. [150](#)
- [376] C. N. Pope. Lectures on w algebras and w gravity. *arXiv preprint hep-th/9112076*, 1991. [155](#), [156](#)
- [377] E. Sezgin. Area-preserving diffeomorphisms, w_{infty} algebras and w_{infty} gravity. *arXiv preprint hep-th/9202086*, 1992. [156](#)
- [378] X. Shen. W-infinity and string theory. *arXiv preprint hep-th/9202072*, 1992. [156](#)

- [379] I. I. Kogan. Area preserving diffeomorphisms and *w_{infinity}* symmetry in a 2+1 chern-simons theory. *Modern Physics Letters A*, 7(40):3717–3730, 1992.
[158](#)
- [380] H. Cabral and F. Diacu. Classical and celestial mechanics: the Recife lectures. Princeton University Press, 2002. [160](#)